ISSN 1007-9327 (print)
ISSN 2219-2840 (online)

World Journal of *Gastroenterology*

World J Gastroenterol 2020 August 28; 26(32): 4729-4888

Published by Baishideng Publishing Group Inc

World Journal of Gastroenterology

Contents

Weekly Volume 26 Number 32 August 28, 2020

MINIREVIEWS

ORIGINAL ARTICLE

Basic Study

Case Control Study

Retrospective Study

Observational Study

Prospective Study

World Journal of Gastroenterology

Weekly Volume 26 Number 32 August 28, 2020

Contents

ABOUT COVER

Editorial Board of *World Journal of Gastroenterology*, Dr. Conrado M Fernandez-Rodriguez is Chief of the Gastroenterology Unit at Alcorcon Foundation University Hospital and Associate Professor of Medicine at University Rey Juan Carlos. His main research interest is chronic liver diseases, for which he has authored more than 140 peer-reviewed publications, including in top gastroenterology and hepatology journals. He serves as Director of the Scientific Committee of the Spanish Society of Digestive Diseases, Associate Editor of Hepatology for *Spanish Journal of Gastroenterology*. He is also a member of the Spanish Steering Committee of Alcohol-Related Liver Disease National Registry (ReHalc) and Scientific Advisor of the Spanish Committee for Hepatitis C virus Elimination, and direct participant in several multicenter international clinical trials (Respond-2, REGENERATE, STELLAR-4) and national trials and registries (TRIC-1, HEPAMet, Hepa-C, ColHai). (L-Editor: Filipodia)

AIMS AND SCOPE

The primary aim of *World Journal of Gastroenterology* (*WJG*, *World J Gastroenterol*) is to provide scholars and readers from various fields of gastroenterology and hepatology with a platform to publish high-quality basic and clinical research articles and communicate their research findings online. *WJG* mainly publishes articles reporting research results and findings obtained in the field of gastroenterology and hepatology and covering a wide range of topics including gastroenterology, hepatology, gastrointestinal endoscopy, gastrointestinal surgery, gastrointestinal oncology, and pediatric gastroenterology.

INDEXING/ABSTRACTING

The *WJG* is now indexed in Current Contents®/Clinical Medicine, Science Citation Index Expanded (also known as SciSearch®), Journal Citation Reports®, Index Medicus, MEDLINE, PubMed, PubMed Central, and Scopus. The 2020 edition of Journal Citation Report® cites the 2019 impact factor (IF) for *WJG* as 3.665; IF without journal self cites: 3.534; 5-year IF: 4.048; Ranking: 35 among 88 journals in gastroenterology and hepatology; and Quartile category: Q2.

RESPONSIBLE EDITORS FOR THIS ISSUE

NAME OF JOURNAL
World Journal of Gastroenterology

ISSN
ISSN 1007-9327 (print) ISSN 2219-2840 (online)

LAUNCH DATE
October 1, 1995

FREQUENCY
Weekly

EDITORS-IN-CHIEF
Andrzej S Tarnawski, Subrata Ghosh

EDITORIAL BOARD MEMBERS
http://www.wjgnet.com/1007-9327/editorialboard.htm

PUBLICATION DATE
August 28, 2020

INSTRUCTIONS TO AUTHORS
https://www.wjgnet.com/bpg/gerinfo/204

GUIDELINES FOR ETHICS DOCUMENTS
https://www.wjgnet.com/bpg/GerInfo/287

GUIDELINES FOR NON-NATIVE SPEAKERS OF ENGLISH
https://www.wjgnet.com/bpg/gerinfo/240

PUBLICATION ETHICS
https://www.wjgnet.com/bpg/GerInfo/288

PUBLICATION MISCONDUCT
https://www.wjgnet.com/bpg/gerinfo/208

ARTICLE PROCESSING CHARGE
https://www.wjgnet.com/bpg/gerinfo/242

STEPS FOR SUBMITTING MANUSCRIPTS
https://www.wjgnet.com/bpg/GerInfo/239

ONLINE SUBMISSION
https://www.f6publishing.com

World Journal of Gastroenterology

Submit a Manuscript: https://www.f6publishing.com

World J Gastroenterol 2020 August 28; 26(32): 4729-4738

DOI: 10.3748/wjg.v26.i32.4729

ISSN 1007-9327 (print) ISSN 2219-2840 (online)

MINIREVIEWS

New advances in radiomics of gastrointestinal stromal tumors

Roberto Cannella, Ludovico La Grutta, Massimo Midiri, Tommaso Vincenzo Bartolotta

ORCID number: Roberto Cannella 0000-0002-3808-0785; Ludovico La Grutta 0000-0002-3557-0084; Massimo Midiri 0000-0003-1824-7549; Tommaso Vincenzo Bartolotta 0000-0002-8808-379X.

Author contributions: Cannella R and Bartolotta TV wrote and revised the manuscript for important intellectual content; La Grutta L and Midiri M made critical revisions related to important intellectual content of the manuscript; all the Authors approved the final version of the article.

Conflict-of-interest statement: All authors have no any conflict of interests.

Manuscript source: Invited Manuscript

Roberto Cannella, Ludovico La Grutta, Massimo Midiri, Tommaso Vincenzo Bartolotta, Section of Radiology - BiND, University Hospital "Paolo Giaccone", Palermo 90127, Italy

Tommaso Vincenzo Bartolotta, Department of Radiology, Fondazione Istituto Giuseppe Giglio, Ct.da Pietrapollastra, Cefalù (Palermo) 90015, Italy

Corresponding author: Tommaso Vincenzo Bartolotta, MD, PhD, Assistant Professor, Section of Radiology - BiND, University Hospital "Paolo Giaccone", Via del Vespro 129, Palermo 90127, Italy. tv_bartolotta@yahoo.com

Abstract

Gastrointestinal stromal tumors (GISTs) are uncommon neoplasms of the gastrointestinal tract with peculiar clinical, genetic, and imaging characteristics. Preoperative knowledge of risk stratification and mutational status is crucial to guide the appropriate patients' treatment. Predicting the clinical behavior and biological aggressiveness of GISTs based on conventional computed tomography (CT) and magnetic resonance imaging (MRI) evaluation is challenging, unless the lesions have already metastasized at the time of diagnosis. Radiomics is emerging as a promising tool for the quantification of lesion heterogeneity on radiological images, extracting additional data that cannot be assessed by visual analysis. Radiomics applications have been explored for the differential diagnosis of GISTs from other gastrointestinal neoplasms, risk stratification and prediction of prognosis after surgical resection, and evaluation of mutational status in GISTs. The published researches on GISTs radiomics have obtained excellent performance of derived radiomics models on CT and MRI. However, lack of standardization and differences in study methodology challenge the application of radiomics in clinical practice. The purpose of this review is to describe the new advances of radiomics applied to CT and MRI for the evaluation of gastrointestinal stromal tumors, discuss the potential clinical applications that may impact patients' management, report limitations of current radiomics studies, and future directions.

Key words: Gastrointestinal stromal tumors; Radiomics; Texture analysis; Computed tomography; Magnetic resonance imaging; Clinical applications

Core tip: Radiomics researches have demonstrated promising results for the differential

Received: May 28, 2020
Peer-review started: May 28, 2020
First decision: June 4, 2020
Revised: June 16, 2020
Accepted: August 1, 2020
Article in press: August 1, 2020
Published online: August 28, 2020

P-Reviewer: Akai H
S-Editor: Ma YJ
L-Editor: A
P-Editor: Ma YJ

diagnosis of gastrointestinal stromal tumors (GISTs) with other gastrointestinal neoplasms in the stomach and duodenum. Excellent performances have been reported for the evaluation of risk status, the preoperative identification of high-risk tumors, and the prediction of prognosis after target therapies. Radiogenomics studies are still lacking, with only initial evidences describing the potential of radiomics for the diagnosis of GISTs without KIT mutations. In this work we review the new advances in radiomics applied to the computed tomography and magnetic resonance imaging of GISTs.

Citation: Cannella R, La Grutta L, Midiri M, Bartolotta TV. New advances in radiomics of gastrointestinal stromal tumors. *World J Gastroenterol* 2020; 26(32): 4729-4738
URL: https://www.wjgnet.com/1007-9327/full/v26/i32/4729.htm
DOI: https://dx.doi.org/10.3748/wjg.v26.i32.4729

INTRODUCTION

Gastrointestinal stromal tumors (GISTs) are uncommon mesenchymal neoplasms of the gastrointestinal tract, originating from the interstitial cells of Cajal[1]. GISTs may arise anywhere along all the gastrointestinal tract, being more commonly encountered in the stomach (50%-60% of cases) or small intestine (30%-40%), while they are rarely observed in the esophagus and colorectum[1,2]. All GISTs have malignant potential with varying degree of biological aggressiveness. Liver and peritoneum are the most common sites of metastatic disease or recurrence after curative resection, which occurs in about 40% of patients[3-5]. GISTs are also characterized by peculiar genetic alterations, with 85% of tumors presenting with activating mutations in the KIT proto-oncogene, while a minority of lesions show mutations of platelet-derived growth factor α (PDGFRα), or occasionally may lack of known mutations (wild type GISTs)[6]. The advent of imatinib mesylate, a selective tyrosine kinase inhibitor of the KIT and PDGFα receptors, has revolutionized the treatment of GISTs, significantly improving the patients' survival even in advanced stages.

Contrast-enhanced computed tomography (CT) is the imaging modality of choice for preoperative diagnosis, staging, as well as postoperative follow-up and assessment of treatment response in patients with GISTs[7,8]. On contrast-enhanced CT, GISTs usually present with peculiar imaging features, most often with large (> 5 cm) abdominal mass, heterogeneous enhancement, and variable amount of necrosis[9-12]. Other imaging findings include presence of calcifications, ulceration or cystic degeneration[11,12]. Magnetic resonance imaging (MRI) may provide additional information for the evaluation of primary tumors in peculiar location (*i.e.*, rectum) and may be preferred for the differential diagnosis of liver metastasis from other benign hepatic lesions[13,14]. In clinical practice, predicting the behavior of GISTs is challenging, unless the lesions have already metastasized at the time of diagnosis. Although some imaging predictors of malignant potential have been identified (size, location, margins, enhancement pattern) and variably correlated with prognosis and survival of GISTs, small tumors lacking of concerning imaging features may still metastasize, making difficult to predict aggressive tumors.

Radiomics is emerging as a promising tool that allows to quantify lesion heterogeneity, extracting additional quantitative data from radiological imaging that cannot be evaluated by human eyes[15,16]. In recent years, multiple researches have explored the performance of radiomics models in abdominal oncologic applications, with significant results for lesions characterization, evaluation of therapeutic response and prediction of patients' survival after surgical or systemic treatments[17-22]. The application of radiomics in GISTs could be used to further improve the patients' management and provide new advances in quantitative lesion evaluation due to the unique clinical, genetic, and imaging characteristics of these tumors.

With this review, we aim to describe the new advances of radiomics applied to CT and MR imaging for the evaluation of gastrointestinal stromal tumors, discuss the potential clinical applications that may impact patients' management, report limitations of current radiomics studies, and future directions.

WORKFLOW OF RADIOMICS ANALYSIS

Radiomics is based on the mathematical quantification of images heterogeneity, through the analysis of distribution and relationships of pixel intensities within a region of interest (ROI)[15,16]. Radiomics analysis requires a multistep process, starting from imaging acquisition, and including lesion segmentation, features extraction, features selection and reduction, predictive model building, and finally validation and clinical interpretation of the results[19,20,23].

Radiomics can be potentially applied to any type of radiological images, including ultrasound, CT, MRI and positron emission tomography/CT, but most of studies are nowadays based on CT or MRI examinations[19]. Image acquisition is one of the most critical steps for radiomics, since scanning and technical parameters may influence the reproducibility of radiomics features. Particularly, reconstruction algorithm and slice thickness had demonstrated to largely impact on the reproducibility of radiomics features on CT[24-26]. The heterogeneous imaging acquisition may be problematic for evaluation of retrospective data acquired with different CT or MRI scanners, while prospective study should ensure that all patients will be imaged using standardized parameters[27]. It is also important to select the optimal phase/sequence for image analysis. Pre-contrast images are not affected by the contrast administration, but lesion segmentation is more difficult, especially for smaller tumors that are difficult to distinguish on non-contrast CT. Contrast-enhanced images may provide better assessment of lesion heterogeneity, but type and non-standardized timing of contrast agent administration may represent additional confounding factors, especially for images acquired on arterial phase.

Lesion segmentation is the most critical step of radiomics process. Segmentation may be performed manually by expert radiologists, using semi-automatic, or automatic software[27]. Although manual segmentation is time consuming and it is subject to intra- and inter-reader variability, it is still considered as the gold standard for most of radiomics studies[18,19,23]. The segmentation is usually realized by drawing a ROI within the tumor margins (Figure 1), avoiding the inclusion of any extra-tumoral tissues such as bowel mucosa, intestinal content, or peritumoral vessels. The ROI can be placed on a single slide (2D ROI) on the largest tumor cross section or include the whole lesion (3D ROI). Although the latter may capture more tissue heterogeneity, its clinical advantage remains debated.

Several in-house build or commercially available radiomics research software are nowadays used for extract a large number of radiomics features. These features may be divided into semantic (qualitative features usually reported by radiologists such as size, margins, enhancement pattern) or agnostic (which are mathematical and quantitative descriptors of heterogeneity) features. Agnostic features are further classified in first, second and third order features[19]. The first order features are obtained from the analysis of the gray level histogram within a defined ROI, without considering spatial relations among pixels. Most common histogram-based features include mean (average of the pixels within the ROI), standard deviation (dispersion from the mean), skewness (asymmetric of the histogram), kurtosis (peakedness/flatness of the histogram), and entropy (image irregularity or complexity)[20]. The second order texture features consider the spatial relationship among pixels, and most commonly include grey level co-occurrence matrix (GLCM), that quantifies the arrangements of pairs of pixels with the same values in specific directions, and grey-level run length matrix (GLRLM), that quantifies consecutive pixels with the same intensity along specific directions. Third or higher order features evaluate spatial relationship among three or more pixels through statistical methods after applying filters or mathematical transforms. These features include fractal analysis, wavelet transform, and Laplacian transforms of Gaussian-filtered image. Due to the large number of extracted parameters, features reduction should be performed in order to excluded features that are not reproducible or with high similarity (*i.e.*, redundant features). This is a significant step to avoid overfitting problems, especially in small cohorts[18-20,24].

Only uncorrelated features with significant diagnostic performance are selected for final radiomics models. The choice of statistical methods and models may depend on multiple factors such as evaluation of primary outcome, number of features, and number of analyzed lesions[23]. These models can be also combined with other patient clinical characteristics in order to increase their predictive power[15]. Finally, radiomics models should be tested and validated using independent internal validation cohort or external population[18]. To assess the quality of radiomics studies, scores have been proposed, such as the Radiomics Quality Score developed by Lambin *et al*[28], which evaluates 16 key components of radiomics workflow[28,29].

Figure 1 Examples of lesion segmentation using a texture analysis software (LIFEx, www.lifexsoft.org) on axial (A), coronal (B) and sagittal (C) contrast-enhanced computed tomography images on venous phase in an 82-year-old man with 4.5 cm gastric gastrointestinal stromal tumor.

RADIOMICS METHODOLOGY IN GISTS

Existing articles of radiomics in GISTs (Table 1) have been performed with heterogeneous methodology regarding the imaging studies, type of radiomics features and analysis[30-44]. Up to May 2020, all the radiomics research studies on GISTs were performed in retrospective population, and only four studies were multicentric[31,32,35,44]. The number of included GISTs widely ranged from 15 to 440 lesions. All except one of radiomics GIST studies used CT imaging for features extraction, while only one study[36] evaluated the MRI. On CT studies, radiomics analysis was most commonly carried out on venous phase (48%), followed by arterial phase (38%), and pre-contrast images (14%) (Figure 2). No study included the delayed phase in radiomics evaluation. First, second, and third order features were extracted in 80%, 67%, and 20% of studies, respectively. Volumetric analysis (3D ROI) was performed in 60% of cases, while 2D ROIs were placed in 47% cases. Only one study[41] compared the accuracy of 2D *vs* 3D ROIs in GISTs, reporting an excellent agreement between the two segmentation methods.

Few studies have investigated the intra- and inter-reader variability of radiomics features in GISTs, with promising results for reproducibility of tumor segmentation and features extraction. A recent study[41] described an almost perfect intra- and inter-reader reproducibility of radiomics features (reported ICC > 0.98) using both single-ROI and whole lesions-ROI manual segmentations. Other studies assessed the inter-reader variability for manual segmentation, all reporting an excellent inter-observer agreement for whole tumor radiomics parameters extracted by two abdominal radiologists (ICC ranging from 0.85 to 0.99)[35,37-39].

Validation of radiomics models in independent cohorts was performed in 47% of studies. However only three of them[31,32,44] included external validation cohorts.

RADIOMICS APPLICATIONS IN GISTS

Differential diagnosis between GIST and other tumors

Stomach is the most common organ affected by GISTs. The differential diagnosis should be carried with other gastric benign mesenchymal neoplasms (*i.e.*, schwannomas and leiomyomas) or malignant tumors (*i.e.*, gastric adenocarcinomas and lymphomas), and it may be difficult due to the overlap in imaging appearance[45-47]. Using a texture analysis approach, Ba-Ssalamah *et al*[30] differentiated GISTs from gastric adenocarcinomas and lymphomas with a high successful rate on arterial and venous phase CT images.

Another challenging location for the differential diagnosis of GISTs from other gastrointestinal neoplasms is the duodenum[48]. GISTs occur rarely in the duodenum (less than 5% of cases) and the differentiation from more common duodenal adenocarcinomas (DACs), pancreatic ductal adenocarcinomas (PDACs), or pancreatic neuroendocrine tumors is significantly relevant for preoperative management and patient prognosis[48,49]. To improve the preoperative characterization of these lesions, a

Table 1 Summary of radiomics studies including gastrointestinal stromal tumors

Ref.	Number of lesions	Imaging	Radiomics analysis	Key radiomics results
Ba-Ssalamah *et al*[30]	15 GISTs, 27 gastric adenocarcinomas, 5 lymphomas	CT	Histogram-based, GLCM, GLRLM, absolute gradient, autoregressive model, Wavelet transform.	On AP texture features perfectly differentiated between GIST *vs* lymphoma. On PVP texture features differentiated GIST *vs* adenocarcinoma in 90% of cases and GIST *vs* lymphoma in 92% of cases.
Chen *et al*[31]	222 GISTs	CT	GLCM, GLRLM, GLSZM, NGTDM. Support Vector Machine for model building.	AUROC 0.84-0.86 of radiomics models for GIST risk stratification.
Chen *et al*[32]	147 GISTs	CT	Residual Neural Network for model building.	AUROC of 0.887-0.947 for ResNet nomogram and model for prediction of disease-free survival after surgical resection.
Choi *et al*[33]	145 GISTs	CT	Histogram-based.	AUROC of 0.782-0.779 of mpp and kurtosis for differentiation of high-risk GISTs.
Ekert *et al*[34]	25 GISTs	CT	Histogram-based, GLCM, GLDM, GLRLM, GLSZM, NGLDM.	Ten GLCM, GLRLM, NGLDM features significantly correlated with disease progression and progression free survival.
Feng *et al*[35]	90 GISTs	CT	Histogram-based.	AUROC of 0.823-0.830 of entropy for the differentiation of low from high-risk GISTs.
Fu *et al*[36]	51 GISTs	MRI	Fractal features, GLCM, GLRLM.	Texture features on DWI and ADC map correlated with overall survival in metastatic GISTs.
Liu *et al*[37]	78 GISTs	CT	Histogram-based.	AUROC of 0.637-0.811 for the identification of very low and low-risk GISTs.
Lu *et al*[38]	28 GISTs, 26 DACs, 20 PDACs	CT	Histogram-based.	AUROC of 0.809-0.936 of 90th percentile for differentiation of GISTs from DACs and PDACs.
Ren *et al*[39]	440 GISTs	CT	Histogram-based, GLCM.	AUROC of 0.933-0.935 for the differentiation of low from high-risk GISTs.
Wang *et al*[40]	333 GISTs	CT	Histogram-based, GLCM, GLRLM.	AUROC of 0.882-0.920 for the differentiation of low from high-risk GISTs. AUROC of 0.769-0.820 for the differentiation of low from high mitotic count.
Xu *et al*[41]	86 GISTs	CT	Histogram-based, GLCM, GLRLM.	AUROC of 0.904-0.962 of standard deviation for diagnosis of GIST without KIT exon 11 mutations.
Yan *et al*[42]	213 GISTs	CT	Histogram-based, GLCM, GLRLM, absolute gradient, autoregressive model, Wavelet transform.	AUROC of 0.933 of texture analysis model for preoperative risk stratification.
Zhang *et al*[43]	140 GISTs	CT	Histogram-based, shape-based, GLCM, GLRLM, GLSZM.	AUROC of 0.809-0.935 for discrimination of advanced GISTs and four risk categories of GISTs
Zhang *et al*[44]	339 GISTs	CT	GLCM, GLRLM, GLSZM, GLDM.	AUROC of 0.754-0.787 of radiomics features for prediction of high Ki67 expression.

AUROC: Area under the receiver operating characteristics curve; CT: Computed tomography; DACs: Duodenal adenocarcinomas; GIST: Gastrointestinal stromal tumors; GLCM: Grey level co-occurrence matrix; GLDM: Grey-level dependence matrix; GLRLM: Grey-level run length matrix; GLSZM, Gray-level size zone matrix; GLZLM: Grey-level zone length matrix; MRI: Magnetic resonance imaging; NGLDM: Neighborhood grey-level different matrix; NGTDM: Neighbourhood gray-tone difference matrix; PDACs: Pancreatic ductal adenocarcinomas.

study by Lu *et al*[38] investigated the whole lesion histogram analysis on contrast-enhanced CT, reporting an excellent discrimination of GISTs from DACs and PDACs in the periampullary region.

Risk stratification and prediction of prognosis of GISTs

Accurate evaluation of malignant risk and outcome in GISTs is mainly based on tumor size, location (gastric *vs* non-gastric tumors), and mitotic count obtained with resection specimens. These factors are combined in the National Institutes of Health 2008 criteria[50], which classified GISTs four risk classes: very low, low, intermediate and high-risk tumors. However, in clinical practice risk stratification may be limited by the evaluation of mitotic count in patients treated with neoadjuvant therapies, or by the assessment of biopsy specimens that could not be representative of the whole tumor. Therefore, several studies have tried to predict risk stratification based on preoperative CT imaging[51-53]. CT features like size, growth pattern, or enlarged feeding vessels have

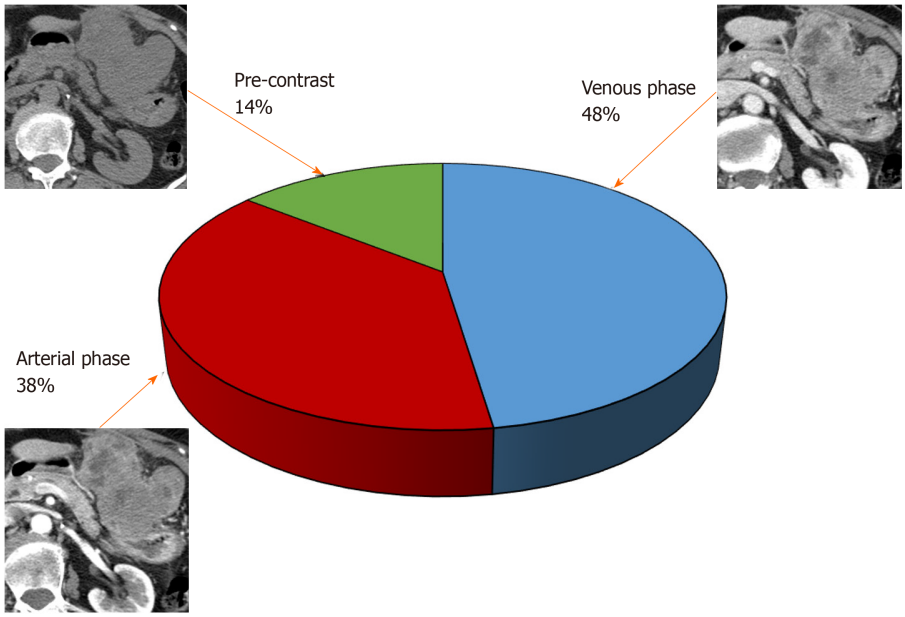

Figure 2 Chart shows the frequency of computed tomography imaging phases included in radiomics gastrointestinal stromal tumors studies. Corresponding computed tomography images shows an 8.6 cm gastric gastrointestinal stromal tumor in a 64-year-old woman.

been associated with high-risk tumors[51-53]. Nevertheless, risk stratification using qualitative imaging evaluation is affected by the readers' experience, heterogeneous definition of imaging features, and subjective assessment with suboptimal reproducibility of qualitative features[54].

Radiomics models have demonstrated to improve the preoperative prediction of high-risk GISTs compared to the conventional visual evaluation[33,42]. The added value of radiomics and texture analysis on contrast-enhanced CT was firstly investigated by Yan *et al*[42] in a retrospective cohort of 213 small bowel GISTs. In that study, texture analysis model achieved a similar diagnostic accuracy compared to that of clinical and subjective imaging features for preoperative risk prediction of GISTs[42]. When combining the clinical and texture analysis features, the diagnostic performance (AUROC of 0.943) significantly improved compared to the model incorporating clinical and imaging features only[42]. In a more recent study, Choi *et al*[33] investigated the diagnostic performance of histogram-based texture parameters and qualitative analysis of CT imaging features for the differentiation of low-risk from high-risk GISTs. Their results confirmed that the radiomics features showed a higher diagnostic performance (AUROC of 0.782-0.779) compared to conventional qualitative evaluation (AUROC of 0.59-0.70) by two radiologists in the differential diagnosis of low-risk from high-risk GISTs[33].

The potential of radiomics for the risk stratification in GISTs have been further evaluated by other evidences with promising results and excellent diagnostic performance[35,37,39,40,43]. Liu *et al*[37] applied CT-based texture analysis for the identification of very low and low risk GISTs in a cohort of 78 patients, reporting a fair diagnostic performance (AUROC of 0.637-0.811) for the most discriminant features obtained on pre-contrast, arterial and venous phases CT images. Feng *et al*[35] extracted histogram-based parameters from arterial and venous phase CT images of 90 small bowel GISTs. Among them, entropy showed the highest diagnostic accuracy on arterial and venous phases (AUROC of 0.823 and 0.830, respectively) for the identification of high-risk GISTs. Zhang *et al*[43] analyzed 140 GISTs using arterial phase CT images, reporting an excellent diagnostic performance for preoperative prediction of advanced (*i.e.*, high and intermediate risk) GISTs and four-class risk stratification (AUROC of 0.935 and 0.809, respectively).

In a large population of 440 pathologically proven GISTs, Ren *et al*[39] reported an excellent performance of radiomics models for the differentiation of low-risk from high-risk GISTs (AUROC of 0.935 and 0.933 in training and validation cohort, respectively). In that study, the prediction nomogram (incorporating lesion size, cystic degeneration, and texture-based mean) demonstrated a sensitivity of 90.6% and a specificity of 75.7% for the diagnosis of high-risk GISTs[39]. Similarly, Wang *et al*[40] analyzed the contrast-enhanced CT images of 333 GISTs and reported an excellent

discrimination capacity of radiomics models between low-risk and high-risk GISTs in both training and validation cohorts (AUROC of 0.882 and 0.920, respectively). In addition, radiomics models enable to discriminate GISTs with low and high mitotic count with a good-to-excellent performance (AUROC: 0.769-0.820)[40].

In two subsequent studies[31,32], Chen *et al*[31,32] built support vector machine and residual neural network based models to predict malignant potential or 3-year and 5-year recurrence-free survival after complete surgical resection of localized GISTs, respectively. In those researches, the Authors enrolled an internal patients' cohort for training the model, which was subsequently validated in internal and external cohorts, with a good-to almost perfect performance for GIST risk stratification and prediction of recurrence free survival at 3-year and 5-year, respectively[31,32].

Survival analysis for disease progression according to texture features was carried out also by Ekert *et al*[34] on contrast-enhanced CT, while only one study[36] has performed radiomics analysis on MRI. Fu *et al*[36] extracted texture features from T2-weighted, DWI and ADC map images to determine prognosis of metastatic GISTs, reporting that texture features on DWI and ADC map well-correlated with overall survival.

Finally, Ki67 index represents a marker of proliferation of tumor cells, which have also been associated with poor prognosis in GISTs[55]. In a study of 339 GISTs[44], radiomics signature from contrast-enhanced CT have demonstrated a significant correlation with Ki67 expression, providing an added value for prognosis assessment.

Assessment of mutational status

Genetic alterations and mutational status is crucial for GISTs optimal target therapy. About 80%-85% of GISTs have mutation in KIT genes, 10% of GISTs have mutations in PDGFRα, while the remaining 10%-15% GISTs are wild type due to the lack of mutations in either of these genes[6]. Particularly, PDGFRα and wild type GISTs have a lower response rate or resistance to the target therapies with tyrosine kinase inhibitors, depending on the specific mutational status[1,6].

Few data exist regarding the association between CT imaging features and mutations in GISTs[57,58]. The performance of radiomics features and radiologists visual analysis for the differentiation of GISTs with and without KIT exon 11 mutations have been explored by Xu *et al*[41] in a study cohort and validation group of 69 and 17 GISTs, respectively. In that investigation, the standard deviation was strongly correlated with absence of KIT exon 11 mutations, and achieved an AUROC of 0.904-0.962. Contrarily, there was no statistically significant differences in the visual ratings of lesions heterogeneity between GISTs with and without KIT exon 11 mutations. Further researches are needed to correlate the radiomics signature with the genomics patterns of mutational status (known as radiogenomics analysis[15]) in order to provide reliable information to guide the most appropriate treatment, especially in advanced GISTs that are not suitable for surgical resection.

LIMITATIONS AND FUTURE DIRECTIONS

Although radiomics has an enormous research potential for the improvement of quantitative tumors evaluation, there are some limitations that challenges its application in everyday clinical practice. Standardization of methodology is the primary problem for radiomics analysis. Differences in imaging acquisition, features extraction, and radiomics software challenge the comparisons between studies and the repeatability or application of radiomics models in different populations. All the current published studies on radiomics of GISTs are retrospective and mostly performed in single centers. The lack of standardization in CT and MRI acquisition is another major problem for radiomics assessment of GISTs. This latter is strictly related to the rarity of GISTs compared to other neoplasms, which require collection of imaging studies obtained during a long period of time. Moreover, the peculiar histopathological characteristics of GISTs, such as mitotic count and mutational status, require pathological diagnosis through resections specimens as reference standard for radiomics studies.

The evaluation of treatment response after tyrosine kinase inhibitors therapy needs also the be further investigated. Indeed, the response to target therapy may occur even without reduction of tumor size[58]. As consequence, Choi criteria[59], based on the measurements of CT attenuation values, have been adopted for the evaluation of treatment response in patients undergoing target therapies. The added values of radiomics in the imaging evaluation of treatment response is currently underexplored

and may be investigated in futures studies.

Further prospective multicentric studies will be needed to validate the optimal diagnostic performance of radiomics models provided by retrospective analysis. Future works are also warranted for optimization and standardization of radiomics software, imaging acquisition, features extraction and models analysis.

CONCLUSION

Radiomics is emerging as a promising tool for quantitative evaluation of GISTs, with excellent diagnostic performance for the differential diagnosis with other gastrointestinal neoplasms, prediction of risk stratification, and evaluation of mutational status. Future implementation of radiomics models in clinical practice may provide additional information from radiological images that will be helpful to guide patients management and more tailored treatments.

REFERENCES

1 **Parab TM**, DeRogatis MJ, Boaz AM, Grasso SA, Issack PS, Duarte DA, Urayeneza O, Vahdat S, Qiao JH, Hinika GS. Gastrointestinal stromal tumors: a comprehensive review. *J Gastrointest Oncol* 2019; **10**: 144-154 [PMID: 30788170 DOI: 10.21037/jgo.2018.08.20]

2 **Akahoshi K**, Oya M, Koga T, Shiratsuchi Y. Current clinical management of gastrointestinal stromal tumor. *World J Gastroenterol* 2018; **24**: 2806-2817 [PMID: 30018476 DOI: 10.3748/wjg.v24.i26.2806]

3 **Plumb AA**, Kochhar R, Leahy M, Taylor MB. Patterns of recurrence of gastrointestinal stromal tumour (GIST) following complete resection: implications for follow-up. *Clin Radiol* 2013; **68**: 770-775 [PMID: 23663875 DOI: 10.1016/j.crad.2013.03.002]

4 **D'Ambrosio L**, Palesandro E, Boccone P, Tolomeo F, Miano S, Galizia D, Manca A, Chiara G, Bertotto I, Russo F, Campanella D, Venesio T, Sangiolo D, Pignochino Y, Siatis D, De Simone M, Ferrero A, Pisacane A, Dei Tos AP, Aliberti S, Aglietta M, Grignani G. Impact of a risk-based follow-up in patients affected by gastrointestinal stromal tumour. *Eur J Cancer* 2017; **78**: 122-132 [PMID: 28448856 DOI: 10.1016/j.ejca.2017.03.025]

5 **Burkill GJ**, Badran M, Al-Muderis O, Meirion Thomas J, Judson IR, Fisher C, Moskovic EC. Malignant gastrointestinal stromal tumor: distribution, imaging features, and pattern of metastatic spread. *Radiology* 2003; **226**: 527-532 [PMID: 12563150 DOI: 10.1148/radiol.2262011880]

6 **Oppelt PJ**, Hirbe AC, Van Tine BA. Gastrointestinal stromal tumors (GISTs): point mutations matter in management, a review. *J Gastrointest Oncol* 2017; **8**: 466-473 [PMID: 28736634 DOI: 10.21037/jgo.2016.09.15]

7 **Vernuccio F**, Taibbi A, Picone D, LA Grutta L, Midiri M, Lagalla R, Lo Re G, Bartolotta TV. Imaging of Gastrointestinal Stromal Tumors: From Diagnosis to Evaluation of Therapeutic Response. *Anticancer Res* 2016; **36**: 2639-2648 [PMID: 27272772]

8 **Inoue A**, Ota S, Sato S, Nitta N, Shimizu T, Sonoda H, Tani M, Ban H, Inatomi O, Ando A, Kushima R, Murata K. Comparison of characteristic computed tomographic findings of gastrointestinal and non-gastrointestinal stromal tumors in the small intestine. *Abdom Radiol (NY)* 2019; **44**: 1237-1245 [PMID: 30600381 DOI: 10.1007/s00261-018-1865-9]

9 **Bartolotta TV**, Taibbi A, Galia M, Cannella I, Lo Re G, Sparacia G, Midiri M, Lagalla R. Gastrointestinal stromal tumour: 40-row multislice computed tomography findings. *Radiol Med* 2006; **111**: 651-660 [PMID: 16791466 DOI: 10.1007/s11547-006-0063-y]

10 **Xing GS**, Wang S, Sun YM, Yuan Z, Zhao XM, Zhou CW. Small Bowel Stromal Tumors: Different Clinicopathologic and Computed Tomography Features in Various Anatomic Sites. *PLoS One* 2015; **10**: e0144277 [PMID: 26646242 DOI: 10.1371/journal.pone.0144277]

11 **Baheti AD**, Shinagare AB, O'Neill AC, Krajewski KM, Hornick JL, George S, Ramaiya NH, Tirumani SH. MDCT and clinicopathological features of small bowel gastrointestinal stromal tumours in 102 patients: a single institute experience. *Br J Radiol* 2015; **88**: 20150085 [PMID: 26111069 DOI: 10.1259/bjr.20150085]

12 **Scola D**, Bahoura L, Copelan A, Shirkhoda A, Sokhandon F. Getting the GIST: a pictorial review of the various patterns of presentation of gastrointestinal stromal tumors on imaging. *Abdom Radiol (NY)* 2017; **42**: 1350-1364 [PMID: 28070658 DOI: 10.1007/s00261-016-1025-z]

13 **Yu MH**, Lee JM, Baek JH, Han JK, Choi BI. MRI features of gastrointestinal stromal tumors. *AJR Am J Roentgenol* 2014; **203**: 980-991 [PMID: 25341135 DOI: 10.2214/AJR.13.11667]

14 **Kang TW**, Kim SH, Jang KM, Choi D, Ha SY, Kim KM, Kang WK, Kim MJ. Gastrointestinal stromal tumours: correlation of modified NIH risk stratification with diffusion-weighted MR imaging as an imaging biomarker. *Eur J Radiol* 2015; **84**: 33-40 [PMID: 25466773 DOI: 10.1016/j.ejrad.2014.10.020]

15 **Gillies RJ**, Kinahan PE, Hricak H. Radiomics: Images Are More than Pictures, They Are Data. *Radiology* 2016; **278**: 563-577 [PMID: 26579733 DOI: 10.1148/radiol.2015151169]

16 **Vernuccio F**, Cannella R, Comelli A, Salvaggio G, Lagalla R, Midiri M. [Radiomics and artificial intelligence: new frontiers in medicine.]. *Recenti Prog Med* 2020; **111**: 130-135 [PMID: 32157259 DOI: 10.1701/3315.32853]

17 **Lubner MG**, Smith AD, Sandrasegaran K, Sahani DV, Pickhardt PJ. CT Texture Analysis: Definitions, Applications, Biologic Correlates, and Challenges. *Radiographics* 2017; **37**: 1483-1503 [PMID: 28898189 DOI: 10.1148/rg.2017170056]

18 **Wakabayashi T**, Ouhmich F, Gonzalez-Cabrera C, Felli E, Saviano A, Agnus V, Savadjiev P, Baumert TF,

Pessaux P, Marescaux J, Gallix B. Radiomics in hepatocellular carcinoma: a quantitative review. *Hepatol Int* 2019; **13**: 546-559 [PMID: 31473947 DOI: 10.1007/s12072-019-09973-0]
19 **Lewis S**, Hectors S, Taouli B. Radiomics of hepatocellular carcinoma. *Abdom Radiol (NY)* 2020 [PMID: 31925492 DOI: 10.1007/s00261-019-02378-5]
20 **Miranda Magalhaes Santos JM**, Clemente Oliveira B, Araujo-Filho JAB, Assuncao-Jr AN, de M Machado FA, Carlos Tavares Rocha C, Horvat JV, Menezes MR, Horvat N. State-of-the-art in radiomics of hepatocellular carcinoma: a review of basic principles, applications, and limitations. *Abdom Radiol (NY)* 2020; **45**: 342-353 [PMID: 31707435 DOI: 10.1007/s00261-019-02299-3]
21 **Kocak B**, Durmaz ES, Erdim C, Ates E, Kaya OK, Kilickesmez O. Radiomics of Renal Masses: Systematic Review of Reproducibility and Validation Strategies. *AJR Am J Roentgenol* 2020; **214**: 129-136 [PMID: 31613661 DOI: 10.2214/AJR.19.21709]
22 **Park HJ**, Park B, Lee SS. Radiomics and Deep Learning: Hepatic Applications. *Korean J Radiol* 2020; **21**: 387-401 [PMID: 32193887 DOI: 10.3348/kjr.2019.0752]
23 **Varghese BA**, Cen SY, Hwang DH, Duddalwar VA. Texture Analysis of Imaging: What Radiologists Need to Know. *AJR Am J Roentgenol* 2019; **212**: 520-528 [PMID: 30645163 DOI: 10.2214/AJR.18.20624]
24 **Berenguer R**, Pastor-Juan MDR, Canales-Vázquez J, Castro-García M, Villas MV, Mansilla Legorburo F, Sabater S. Radiomics of CT Features May Be Nonreproducible and Redundant: Influence of CT Acquisition Parameters. *Radiology* 2018; **288**: 407-415 [PMID: 29688159 DOI: 10.1148/radiol.2018172361]
25 **Ahn SJ**, Kim JH, Lee SM, Park SJ, Han JK. CT reconstruction algorithms affect histogram and texture analysis: evidence for liver parenchyma, focal solid liver lesions, and renal cysts. *Eur Radiol* 2019; **29**: 4008-4015 [PMID: 30456584 DOI: 10.1007/s00330-018-5829-9]
26 **Meyer M**, Ronald J, Vernuccio F, Nelson RC, Ramirez-Giraldo JC, Solomon J, Patel BN, Samei E, Marin D. Reproducibility of CT Radiomic Features within the Same Patient: Influence of Radiation Dose and CT Reconstruction Settings. *Radiology* 2019; **293**: 583-591 [PMID: 31573400 DOI: 10.1148/radiol.2019190928]
27 **Koçak B**, Durmaz EŞ, Ateş E, Kılıçkesmez Ö. Radiomics with artificial intelligence: a practical guide for beginners. *Diagn Interv Radiol* 2019; **25**: 485-495 [PMID: 31650960 DOI: 10.5152/dir.2019.19321]
28 **Lambin P**, Leijenaar RTH, Deist TM, Peerlings J, de Jong EEC, van Timmeren J, Sanduleanu S, Larue RTHM, Even AJG, Jochems A, van Wijk Y, Woodruff H, van Soest J, Lustberg T, Roelofs E, van Elmpt W, Dekker A, Mottaghy FM, Wildberger JE, Walsh S. Radiomics: the bridge between medical imaging and personalized medicine. *Nat Rev Clin Oncol* 2017; **14**: 749-762 [PMID: 28975929 DOI: 10.1038/nrclinonc.2017.141]
29 **Park JE**, Kim D, Kim HS, Park SY, Kim JY, Cho SJ, Shin JH, Kim JH. Quality of science and reporting of radiomics in oncologic studies: room for improvement according to radiomics quality score and TRIPOD statement. *Eur Radiol* 2020; **30**: 523-536 [PMID: 31350588 DOI: 10.1007/s00330-019-06360-z]
30 **Ba-Ssalamah A**, Muin D, Schernthaner R, Kulinna-Cosentini C, Bastati N, Stift J, Gore R, Mayerhoefer ME. Texture-based classification of different gastric tumors at contrast-enhanced CT. *Eur J Radiol* 2013; **82**: e537-e543 [PMID: 23910996 DOI: 10.1016/j.ejrad.2013.06.024]
31 **Chen T**, Ning Z, Xu L, Feng X, Han S, Roth HR, Xiong W, Zhao X, Hu Y, Liu H, Yu J, Zhang Y, Li Y, Xu Y, Mori K, Li G. Radiomics nomogram for predicting the malignant potential of gastrointestinal stromal tumours preoperatively. *Eur Radiol* 2019; **29**: 1074-1082 [PMID: 30116959 DOI: 10.1007/s00330-018-5629-2]
32 **Chen T**, Liu S, Li Y, Feng X, Xiong W, Zhao X, Yang Y, Zhang C, Hu Y, Chen H, Lin T, Zhao M, Liu H, Yu J, Xu Y, Zhang Y, Li G. Developed and validated a prognostic nomogram for recurrence-free survival after complete surgical resection of local primary gastrointestinal stromal tumors based on deep learning. *EBioMedicine* 2019; **39**: 272-279 [PMID: 30587460 DOI: 10.1016/j.ebiom.2018.12.028]
33 **Choi IY**, Yeom SK, Cha J, Cha SH, Lee SH, Chung HH, Lee CM, Choi J. Feasibility of using computed tomography texture analysis parameters as imaging biomarkers for predicting risk grade of gastrointestinal stromal tumors: comparison with visual inspection. *Abdom Radiol (NY)* 2019; **44**: 2346-2356 [PMID: 30923842 DOI: 10.1007/s00261-019-01995-4]
34 **Ekert K**, Hinterleitner C, Horger M. Prognosis assessment in metastatic gastrointestinal stromal tumors treated with tyrosine kinase inhibitors based on CT-texture analysis. *Eur J Radiol* 2019; **116**: 98-105 [PMID: 31153581 DOI: 10.1016/j.ejrad.2019.04.018]
35 **Feng C**, Lu F, Shen Y, Li A, Yu H, Tang H, Li Z, Hu D. Tumor heterogeneity in gastrointestinal stromal tumors of the small bowel: volumetric CT texture analysis as a potential biomarker for risk stratification. *Cancer Imaging* 2018; **18**: 46 [PMID: 30518436 DOI: 10.1186/s40644-018-0182-4]
36 **Fu J**, Fang MJ, Dong D, Li J, Sun YS, Tian J, Tang L. Heterogeneity of metastatic gastrointestinal stromal tumor on texture analysis: DWI texture as potential biomarker of overall survival. *Eur J Radiol* 2020; **125**: 108825 [PMID: 32035324 DOI: 10.1016/j.ejrad.2020.108825]
37 **Liu S**, Pan X, Liu R, Zheng H, Chen L, Guan W, Wang H, Sun Y, Tang L, Guan Y, Ge Y, He J, Zhou Z. Texture analysis of CT images in predicting malignancy risk of gastrointestinal stromal tumours. *Clin Radiol* 2018; **73**: 266-274 [PMID: 28969853 DOI: 10.1016/j.crad.2017.09.003]
38 **Lu J**, Hu D, Tang H, Hu X, Shen Y, Li Z, Peng Y, Kamel I. Assessment of tumor heterogeneity: Differentiation of periampullary neoplasms based on CT whole-lesion histogram analysis. *Eur J Radiol* 2019; **115**: 1-9 [PMID: 31084752 DOI: 10.1016/j.ejrad.2019.03.021]
39 **Ren C**, Wang S, Zhang S. Development and validation of a nomogram based on CT images and 3D texture analysis for preoperative prediction of the malignant potential in gastrointestinal stromal tumors. *Cancer Imaging* 2020; **20**: 5 [PMID: 31931874 DOI: 10.1186/s40644-019-0284-7]
40 **Wang C**, Li H, Jiaerken Y, Huang P, Sun L, Dong F, Huang Y, Dong D, Tian J, Zhang M. Building CT Radiomics-Based Models for Preoperatively Predicting Malignant Potential and Mitotic Count of Gastrointestinal Stromal Tumors. *Transl Oncol* 2019; **12**: 1229-1236 [PMID: 31280094 DOI: 10.1016/j.tranon.2019.06.005]
41 **Xu F**, Ma X, Wang Y, Tian Y, Tang W, Wang M, Wei R, Zhao X. CT texture analysis can be a potential tool to differentiate gastrointestinal stromal tumors without KIT exon 11 mutation. *Eur J Radiol* 2018; **107**: 90-97 [PMID: 30292279 DOI: 10.1016/j.ejrad.2018.07.025]

42 **Yan J**, Zhao X, Han S, Wang T, Miao F. Evaluation of Clinical Plus Imaging Features and Multidetector Computed Tomography Texture Analysis in Preoperative Risk Grade Prediction of Small Bowel Gastrointestinal Stromal Tumors. *J Comput Assist Tomogr* 2018; **42**: 714-720 [PMID: 30015796 DOI: 10.1097/RCT.0000000000000756]

43 **Zhang L**, Kang L, Li G, Zhang X, Ren J, Shi Z, Li J, Yu S. Computed tomography-based radiomics model for discriminating the risk stratification of gastrointestinal stromal tumors. *Radiol Med* 2020; **125**: 465-473 [PMID: 32048155 DOI: 10.1007/s11547-020-01138-6]

44 **Zhang QW**, Gao YJ, Zhang RY, Zhou XX, Chen SL, Zhang Y, Liu Q, Xu JR, Ge ZZ. Personalized CT-based radiomics nomogram preoperative predicting Ki-67 expression in gastrointestinal stromal tumors: a multicenter development and validation cohort. *Clin Transl Med* 2020; **9**: 12 [PMID: 32006200 DOI: 10.1186/s40169-020-0263-4]

45 **Choi JW**, Choi D, Kim KM, Sohn TS, Lee JH, Kim HJ, Lee SJ. Small submucosal tumors of the stomach: differentiation of gastric schwannoma from gastrointestinal stromal tumor with CT. *Korean J Radiol* 2012; **13**: 425-433 [PMID: 22778564 DOI: 10.3348/kjr.2012.13.4.425]

46 **Choi YR**, Kim SH, Kim SA, Shin CI, Kim HJ, Kim SH, Han JK, Choi BI. Differentiation of large (≥ 5 cm) gastrointestinal stromal tumors from benign subepithelial tumors in the stomach: radiologists' performance using CT. *Eur J Radiol* 2014; **83**: 250-260 [PMID: 24325848 DOI: 10.1016/j.ejrad.2013.10.028]

47 **Huh CW**, Jung DH, Kim JS, Shin YR, Choi SH, Kim BW. CT Versus Endoscopic Ultrasound for Differentiating Small (2-5 cm) Gastrointestinal Stromal Tumors From Leiomyomas. *AJR Am J Roentgenol* 2019; **213**: 586-591 [PMID: 31063418 DOI: 10.2214/AJR.18.20877]

48 **Cai PQ**, Lv XF, Tian L, Luo ZP, Mitteer RA Jr, Fan Y, Wu YP. CT Characterization of Duodenal Gastrointestinal Stromal Tumors. *AJR Am J Roentgenol* 2015; **204**: 988-993 [PMID: 25905932 DOI: 10.2214/AJR.14.12870]

49 **Ren S**, Chen X, Wang J, Zhao R, Song L, Li H, Wang Z. Differentiation of duodenal gastrointestinal stromal tumors from hypervascular pancreatic neuroendocrine tumors in the pancreatic head using contrast-enhanced computed tomography. *Abdom Radiol (NY)* 2019; **44**: 867-876 [PMID: 30293109 DOI: 10.1007/s00261-018-1803-x]

50 **Joensuu H**. Risk stratification of patients diagnosed with gastrointestinal stromal tumor. *Hum Pathol* 2008; **39**: 1411-1419 [PMID: 18774375 DOI: 10.1016/j.humpath.2008.06.025]

51 **Zhou C**, Duan X, Zhang X, Hu H, Wang D, Shen J. Predictive features of CT for risk stratifications in patients with primary gastrointestinal stromal tumour. *Eur Radiol* 2016; **26**: 3086-3093 [PMID: 26699371 DOI: 10.1007/s00330-015-4172-7]

52 **O'Neill AC**, Shinagare AB, Kurra V, Tirumani SH, Jagannathan JP, Baheti AD, Hornick JL, George S, Ramaiya NH. Assessment of metastatic risk of gastric GIST based on treatment-naïve CT features. *Eur J Surg Oncol* 2016; **42**: 1222-1228 [PMID: 27178777 DOI: 10.1016/j.ejso.2016.03.032]

53 **Li H**, Ren G, Cai R, Chen J, Wu X, Zhao J. A correlation research of Ki67 index, CT features, and risk stratification in gastrointestinal stromal tumor. *Cancer Med* 2018; **7**: 4467-4474 [PMID: 30123969 DOI: 10.1002/cam4.1737]

54 **Maldonado FJ**, Sheedy SP, Iyer VR, Hansel SL, Bruining DH, McCollough CH, Harmsen WS, Barlow JM, Fletcher JG. Reproducible imaging features of biologically aggressive gastrointestinal stromal tumors of the small bowel. *Abdom Radiol (NY)* 2018; **43**: 1567-1574 [PMID: 29110055 DOI: 10.1007/s00261-017-1370-6]

55 **Basilio-de-Oliveira RP**, Pannain VL. Prognostic angiogenic markers (endoglin, VEGF, CD31) and tumor cell proliferation (Ki67) for gastrointestinal stromal tumors. *World J Gastroenterol* 2015; **21**: 6924-6930 [PMID: 26078569 DOI: 10.3748/wjg.v21.i22.6924]

56 **Tateishi U**, Miyake M, Maeda T, Arai Y, Seki K, Hasegawa T. CT and MRI findings in KIT-weak or KIT-negative atypical gastrointestinal stromal tumors. *Eur Radiol* 2006; **16**: 1537-1543 [PMID: 16397744 DOI: 10.1007/s00330-005-0091-3]

57 **Yin YQ**, Liu CJ, Zhang B, Wen Y, Yin Y. Association between CT imaging features and KIT mutations in small intestinal gastrointestinal stromal tumors. *Sci Rep* 2019; **9**: 7257 [PMID: 31076599 DOI: 10.1038/s41598-019-43659-9]

58 **Apfaltrer P**, Meyer M, Meier C, Henzler T, Barraza JM Jr, Dinter DJ, Hohenberger P, Schoepf UJ, Schoenberg SO, Fink C. Contrast-enhanced dual-energy CT of gastrointestinal stromal tumors: is iodine-related attenuation a potential indicator of tumor response? *Invest Radiol* 2012; **47**: 65-70 [PMID: 21934517 DOI: 10.1097/RLI.0b013e31823003d2]

59 **Choi H**, Charnsangavej C, Faria SC, Macapinlac HA, Burgess MA, Patel SR, Chen LL, Podoloff DA, Benjamin RS. Correlation of computed tomography and positron emission tomography in patients with metastatic gastrointestinal stromal tumor treated at a single institution with imatinib mesylate: proposal of new computed tomography response criteria. *J Clin Oncol* 2007; **25**: 1753-1759 [PMID: 17470865 DOI: 10.1200/JCO.2006.07.3049]

World Journal of Gastroenterology

Submit a Manuscript: https://www.f6publishing.com

World J Gastroenterol 2020 August 28; 26(32): 4739-4752

DOI: 10.3748/wjg.v26.i32.4739

ISSN 1007-9327 (print) ISSN 2219-2840 (online)

MINIREVIEWS

Novel virulence factor *dupA* of *Helicobacter pylori* as an important risk determinant for disease manifestation: An overview

Jawed Alam, Avijit Sarkar, Bipul Chandra Karmakar, Mou Ganguly, Sangita Paul, Asish K Mukhopadhyay

ORCID number: Jawed Alam 0000-0003-1176-0876; Avijit Sarkar 0000-0002-3196-4959; Bipul Chandra Karmakar 0000-0003-0561-520X; Mou Ganguly 0000-0003-4330-5974; Sangita Paul 0000-0002-1547-9232; Asish K Mukhopadhyay 0000-0002-5638-4520.

Author contributions: Alam J and Mukhopadhyay AK was involved in the conceptualization; Alam J, Karmakar BC and Sarkar A were involved in the writing the original draft; Sarkar A and Paul S performed the methodology; Karmakar BC was involved in collecting research; Ganguly M took part in the visualization; Ganguly M and Paul S wrote and edited the review; Paul S performed the validation; Mukhopadhyay AK supervised, critically revised and edited the manuscript; All authors have read and approve the final manuscript.

Supported by Council of Scientific and Industrial Research, Government of India, No. 12458; Department of Science and Technology, India, No. IF140909; and the Council of Scientific and Industrial Research, India, No. 09/482(0065)/2017-EMR-1.

Conflict-of-interest statement: All authors declare no conflicts of interest.

Jawed Alam, Division of Infectious Diseases, Institute of Life Science, Bhubaneswar 751023, India

Avijit Sarkar, Bipul Chandra Karmakar, Mou Ganguly, Sangita Paul, Asish K Mukhopadhyay, Division of Bacteriology, ICMR-National Institute of Cholera and Enteric Diseases, Kolkata 700010, India

Corresponding author: Asish K Mukhopadhyay, PhD, Senior Scientist, Division of Bacteriology, ICMR-National Institute of Cholera and Enteric Diseases, P 33, CIT Road, Scheme XM, Beliaghata, Kolkata 700010, India. asish1967@gmail.com

Abstract

Helicobacter pylori (*H. pylori*) is a microaerophilic, Gram-negative, human gastric pathogen found usually in the mucous lining of stomach. It infects more than 50% of the world's population and leads to gastroduodenal diseases. The outcome of disease depends on mainly three factors: Host genetics, environment and bacterial factors. Among these, bacterial virulence factors such as *cagA*, *vacA* are well known for their role in disease outcomes. However, based on the global epidemiological results, none of the bacterial virulence (gene) factors was found to be associated with particular diseases like duodenal ulcer (DU) in all populations. Hence, substantial importance has been provided for research in strain-specific genes outside the *cag* pathogenicity island, especially genes located within the plasticity regions. *dupA* found within the plasticity regions was first demonstrated in 2005 and was proposed for duodenal ulcer development and reduced risk of gastric cancer in certain geographical regions. Due to the discrepancies in report from different parts of the world in DU development related to *H. pylori* virulence factor, *dupA* became an interesting area of research in elucidating the role of this gene in the disease progression. In this review, we shed light on the detailed information available on the polymorphisms in *dupA* and their clinical relevance. We have critically appraised several pertinent studies on *dupA* and discussed their merits and shortcomings. This review also highlights *dupA* gene as an important biomarker for DU in certain populations.

Key words: *Helicobacter pylori*; Plasticity region; Duodenal ulcer; Gastric cancer; *dupA* gene

Manuscript source: Invited manuscript

Received: February 20, 2020
Peer-review started: February 20, 2020
First decision: February 29, 2020
Revised: June 23, 2020
Accepted: August 3, 2020
Article in press: August 3, 2020
Published online: August 28, 2020

P-Reviewer: Fagoonee S, Huang YQ, Ulaşoğlu C
S-Editor: Yan JP
L-Editor: Filipodia
P-Editor: Zhang YL

Core tip: A novel virulence factor *dupA* located in the plasticity region of *Helicobacter pylori* genome was found to be associated with duodenal ulcer development in certain geographical regions. Well-known bacterial virulence factors in this pathogen like *cagA*, *vacA* are not found to be associated with duodenal ulcer in Asia. Studies focused on the epidemiology and clinical relevance of *dupA* around the world exhibit significant variations. Hence, we focused on the variations in *dupA* and the plausible role of such variation in disease etiology with the goal of bringing attention to this topic to the scientific community and eventually opening up avenues for further research.

Citation: Alam J, Sarkar A, Karmakar BC, Ganguly M, Paul S, Mukhopadhyay AK. Novel virulence factor *dupA* of *Helicobacter pylori* as an important risk determinant for disease manifestation: An overview. *World J Gastroenterol* 2020; 26(32): 4739-4752
URL: https://www.wjgnet.com/1007-9327/full/v26/i32/4739.htm
DOI: https://dx.doi.org/10.3748/wjg.v26.i32.4739

INTRODUCTION

Helicobacter pylori (*H. pylori*) is a curved rod-shaped, Gram-negative, microaerophilic bacterium found usually in the mucous lining of the stomach. *H. pylori* infects more than 50% of the world's population and 70%-80% of the Indian population[1,2]. *H. pylori* is acquired during childhood and remains in the stomach throughout the life if not treated effectively[3]. Infection with *H. pylori* causes duodenal ulcer (DU), gastric ulcer (GU), gastric cancer (GC) and gastric mucosa-associated lymphoid tissue lymphoma[4-7]. Considering its clinical importance, the World Health Organization has declared *H. pylori* as a class I carcinogen and enlisted GC as the fifth most common cancer and the third most common cause of cancer-related death[8,9]. Infection of *H. pylori* is comparatively more prevalent in developing countries than Western countries due to socioeconomic and sanitary conditions[10]. The mode of transmission of *H. pylori* is not clearly understood. However, most of the studies suggest that *H. pylori* is transmitted from person to person *via* oral-oral and fecal-oral route and also through contaminated food and water[11-14].

The enigma of *H. pylori* research is that the majority of infected patients remain asymptomatic, whereas around 15%-20% of infected individuals develop symptoms of peptic ulcer (duodenal or gastric) as a long-term consequence of infection. It is not clear what governs the manifestation of *H. pylori* infection in some people. This apparent puzzle prompted the proposal that the sheer presence of *H. pylori* in the stomach is inadequate to develop acute gastric disease and that other conditions are required. However, it is assumed that the responsible factors in *H. pylori*-associated diseases are due to its virulence factors, host genetics, immunity and environmental influences. Host factors like polymorphism in the genes (pro-inflammatory cytokine genes) increase the risk of the specific clinical outcome[15]. None of the *H. pylori* virulence factors such as *cagA*, *vacA*, the blood group antigen *babA* and *oipA* have been linked with specific diseases like DU or GC uniformly in all populations[16-20].

Analysis of the full genome sequences of different *H. pylori* strains reported specific genetic locus whose G+C content was lower than that of the rest of the *H. pylori* genome. This indicates the possibility of horizontal deoxyribonucleic acid (DNA) transfer from other species. *H. pylori* carry an open pan-genome, which maintain a discrete group of strain-specific genes. These strain-specific genes mostly reside in genomic regions that had earlier been coined as plasticity zones. This term was previously used to describe a specific genetic segment with high variation between the *H. pylori* genome sequences[21,22]. The complete genome sequence of *H. pylori* reveals that part of the plasticity zone is normally arranged as genomic islands that may be integrated in the genetic loci. About 50% of the strain-specific genes of *H. pylori* are located in the plasticity region. Here, our focus is on the gene *dupA*, which is located within the plasticity region. This gene was first reported in 2005 as an important biomarker for DU[23]. During subsequent years, several investigations were carried out on *dupA*, and this has become an interesting area of research, as shown in Table 1.

Table 1 Important finding on *dupA* of *Helicobacter pylori* in chronological order

Year	Observation and conclusion	Sample location	Sample size	Techniques used in the study	Proposed name	Ref.
2005	*dupA* was novel marker associated with increased risk for DU and reduced risk for gastric cancer in East Asia and South America	Japan, Korea, Colombia	500	PCR, southern blot	*dupA*	Lu *et al*[23]
2007	Significant association of *dupA* gene with DU	North India	166	PCR, Dot-blot hybridization, partial sequencing	*dupA*	Arachchi *et al*[24]
2007	Presence of *dupA* significantly associated with GC than DU	Belgium, South Africa, china, North America	258	PCR	*dupA*	Argent *et al*[25]
2008	*dupA* gene was not associated with any diseases outcome	Iran	157	PCR, partial sequencing	*dupA*	Douraghi *et al*[30]
2008	*dupA* was not associated with *H. pylori* associated diseases in children and adults	Brazil	482	PCR, partial sequencing	*dupA*	Gomes *et al*[26]
2008	*dupA* was associated with peptic ulcer in Iraqi population but not with Iranian population	Iraq and Iran	108	PCR	*dupA*	Hussein *et al*[29]
2008	There was no association between the occurrence of *dupA* and DU	Brazil (Sao Paulo)	79	PCR	*dupA*	Pacheco *et al*[27]
2008	The prevalence of *dupA* was significantly higher in DU patients than in gastric cancer	china	360	PCR	*dupA*	Zhang *et al*[38]
2009	There was no consistent association between *dupA* and DU or GC development	Sweden, Australia, Malaysia (ethnic groups Indian, Malaya)	243	PCR, partial sequencing	*dupA*	Schmidt *et al*[41]
2010	*dupA* was not associated with gastroduodenal diseases or IL-8 production	Japan	244	PCR, partial sequencing RT-PCR, IL-8 assay	*dupA*	Nguyen *et al*[45]
2010	*dupA* is not association with DU in patients from Turkey	Turkey	91	PCR	*dupA*	Tuncel *et al*[37]
2010	Meta-analysis of case control studies confirmed the presence of *dupA* gene for DU	Asian and western countries	2466	-	*dupA*	Shiota *et al*[44]
2010	Meta-analysis of previous report showed *dupA* gene promotes DU formation some population and GU and GC in others	Around the world	2358		*dupA*	Hussein *et al*[43]
2010	In Taiwanese female population, MMP-3 promoter polymorphism is correlated with DU rather than *dupA* gene	Taiwan female	181	PCR	*dupA*	Yeh *et al*[40]
2010	*dupA* and gastric cancer is negatively associated with GC in Japanese population	Japan	136	PCR	*dupA*	Imagawa *et al*[46]
2010	Proposed two alleles of *dupA* [*dupA*1 (intact), *dupA*2 (truncated)]. *dupA*1 (not *dupA*2) increased IL-12p40 and IL-12p70 production from $CD14^+$ mononuclear cell	United Kingdom, United States, Belgium, South Africa, China	34	PCR, full Sequencing, Cytokine ELISA, real tome PCR, flow cytometry	*dupA1*	Hussein *et al*[52]
2011	Presence of mutation on *dupA* at 1311 and 1426 leads to stop codon called truncated *dupA*	Brazil	252	PCR, full sequencing	*dupA*	Queiroz *et al*[50]
2011	Intact *dupA* (*dupA1*) without stop codon was associated with decreases rate of gastric carcinoma in Brazilian population	Brazil	6	Full sequencing	*dupA1*	Queiroz *et al*[57]
2012	Found a positive association between presence of *dupA* and DU [OR 24.2; 95%CI: 10.6-54.8] and inverse association	Iran	216	PCR	*dupA*	Abadi *et al*[31]

	between presence of *dupA* and GU [OR 0.34; 95%CI: 0.16-0.68] and GC [OR 0.16; 95%CI: 0.05-0.47]					
2012	Prevalence of *dupA* was higher in the eradication failure group than in the success group (36.3% *vs* 21.9%)	Japan	142	PCR, Drug sensitivity test	*dupA*	Shiota *et al*[60]
2012	The logistic analysis report in Brazilian population showed the presence of intact *dupA* independently associated with duodenal ulcer (OR = 5.06; 95%CI: 1.22-20.96, *P* = 0.02)	Brazil	75	Sequencing	Intact *dupA*	Moura *et al*[51]
2012	*dupA* gene was found to be significantly associated with DU than in NUD in south east Indian population	India	140	PCR, partial sequencing, real time PCR,	*dupA*	Alam *et al*[47]
2012	Found a significant association between *dupA*1 and DU (*P* < 0.01) along with a significant higher level of gastric mucosa IL-8 in *dupA1* than in *dupA2* or *dupA* negative Iraqi strain	Iran	68	PCR, full sequencing, IL-8 ELISA	*dupA1*	Hussein *et al*[54]
2012	classified *dupA* into two types (long types and short types) depend on the presence of 615 bp at the N-terminal of *dupA*. Found high prevalence of intact long type *dupA* (24.5%) than short type *dupA* (6.6%) and significantly associated with GU and GC than gastritis (*P* = 0.001 and *P* = 0.019) in Japanese population	Japan	319	PCR, full sequencing	Long type and short type	Takahashi *et al*[53]
2012	Complete *dupA* cluster (*dupA* with six *virB* homologues) was associated with DU rather than *dupA* gene only in United States population	United States	245	PCR and cytokine ELISA	*dupA* cluster	Jung *et al*[75]
2013	Prevalence of long type *dupA* (2499 bp) was significantly higher in GU, GC and DU (40.3%) than from gastritis (20.4%) (*P* = 0.02) in China	China	116	PCR, Full sequencing	*dupA* cluster	Wang *et al*[59]
2013	PUD was significantly associated with *cagA* (*P* ≤ 0.017; OR 0.4; 95%CI: 0.18-0.85) rather than *dupA*	Iraq	154	PCR	*dupA*	Salih *et al*[34]
2014	*dupA* was found to play an important role in the development of DU, BGU and dysplasia in South Korean population	South Korea	401	PCR	*dupA*	Kim *et al*[39]
2014	*dupA* was associated with *cagA* and *vacAs1m1* genotypes	Brazil	205	PCR	*dupA*	Pereira *et al*[28]
2014	The prevalence of *dupA* and *cagA* were more in MTZ, CLR and AML resistance strain as compared to other virulence factor in Pakistan	Pakistan	46	PCR	*dupA*	Rasheed *et al*[61]
2015	*cagA*, complete *dupA* cluster and smoking were significantly associated with increased level of IL-8 production from gastric mucosa of Iraqi population	Iraq	81	PCR, IL-8 ELISA	*dupA*	Hussein *et al*[55]
2015	Prevalence of *dupA*1 was significantly higher in DU than NUD (*P* = 0.02) in Indian strains and *dupA1* positive strains were similar to East Asian strains and distinct from western strains.	India	170	PCR, sequencing, IL-8 ELISA	*dupA1*	Alam *et al*[58]
2015	Significant association of complete *dupA* cluster with IL-8 production (*P* < 0.01) in north East of China	China	262	PCR, western blotting, IL-8 ELISA	*dupA* cluster	Wang *et al*[76]
2015	DupA protein have ATPase activity and play a role in apoptosis of gastric cancerous cells through mitochondrial pathway but neither adhere nor translocate to host cell	China	1 (WH21)	PCR, western blotting, ATPase, Adhesion, translocation and cytotoxic assay	Long type *dupA*	Wang *et al*[79]
2015	*dupA1* have a significant association with A2147G clarithromycin resistance strain but not with Il-8 production from gastric mucosa	Iraq	74	PCR, IL-8 ELISA, antibiotic susceptibility teat	*dupA1*	Hussein *et al*[56]
2015	Significant association between the presence of *dupA* and DU diseases (*P* = 0.03 OR 3.14, 95%CI: 1.47-7.8).	Iran	128	PCR	*dupA*	Haddadi *et al*[35]
2015	There was no significant relationship between *dupA* status and duodenal ulcer disease (*P* = 0.25) but, there was a converse relationship between *dupA* negative strains and gastric cancer disease (*P* = 0.02)	Iran	123	PCR	*dupA*	Souod *et al*[36]
2015	There was no association of *dupA* gene with the ethnic group (Indian, Chinese, Malaya) of Malaysia	Malaysia	105	PCR	*dupA*	Osman *et al*[42]

2017	Significant association of *dupA* gene with non-severe clinical outcome (P = 0.0032, OR 0.25, 95%CI: 0.09-0.65) and play a role in protecting against gastric cancer in Chile	Chile	132	PCR	*dupA*	Paredes *et al*[48]
2017	A complete *tfs* plasticity zone cluster including *dupA* is a virulence factor that may be important for the colonization of *H. pylori* and to the development of severe outcomes of the infection with *cagA*-positive strains	Portugal	18	PCR, whole genome sequencing, cytokine assay	*dupA*	Silva *et al*[78]
2019	*dupA* was significantly associated with decreased risk of duodenal ulcer (P = 0.024)	Costa Rica	151	PCR	*dupA*	Molina Castro *et al*[49]
2019	Significant relationship was observed between the occurrence of DU and the presence of the 112 bp segment (P = 0.002; OR 6.98; 95%CI: 1.94-25.00)	Iran	143	PCR	*dupA*	Fatahi *et al*[32]
2019	The prevalence of *dupA* was 53.4% in South African population, but it was not associated with duodenal ulcer	South Africa	234	PCR	*dupA*	Idowu *et al*[64]
2019	The prevalence of *dupA* was higher (30.4%) in peptic ulcer (mild diseases) than gastric cancer (severe diseases) 18.2%	Northern Spain	102	PCR	*dupA*	Fernandez-Reyes *et al*[72]
2019	*dupA* was present in 10/41 (24.4%) of population, and it was not associated with severe gastritis	Switzerland	41	Whole genome sequence	*dupA*	Imkamp *et al*[63]
2019	Significant association was found between metronidazole resistance and *dupA* genotypes (P = 0.0001)	Iran	68	PCR	*dupA*	Farzi *et al*[33]

CI: Confidence interval; DU: Duodenal ulcer; GC: Gastric cancer; GU: Gastric ulcer; IL-8: Interleukin-8; MMP-3: Matrix metalloproteinase -3; NUD: Non-ulcer dyspepsia; OR: Odds ratio; PCR: Polymerase chain reaction.

METHODOLOGY

To review the importance of *dupA*, we have searched the "NCBI-PubMed" using the keywords: "*dupA*", "*H. pylori*" and a total of 80 articles were found, of which 76 were published in English till January 2020. Out of 76, 13 are published as review articles and two as meta-analysis of previous data. The remaining 61 documented as research articles. The research on *dupA* has spanned 15 years with contradictory findings. In this review, we summarize the result of relevant studies and discuss the pathogenesis of *dupA* since its early stage to recent advancements. Finally, this review highlights the significance of *dupA* gene of *H. pylori* as a virulence factor (virulence marker) and its role in pathogenesis including the progression of DU.

DISCREPANCIES OF *DUPA* WITH CLINICAL OUTCOMES

Studies conducted with *H. pylori* strains from East Asia and South America identified a novel *H. pylori* virulence factor encoded in the *dupA* that was associated with increased risk of DU and decreased risk of GC. However, this perception seems to be region specific. This *dupA* was homologous to *virB*4 gene, located in the plasticity zone of *H. pylori*. *dupA* contained two open reading frames (ORFs), *jhp0917* and *jhp0918*, with an overlap of twelve bases and an insertion of either base thymine (T) or cytosine (C) after the position 1385 of the *jhp0917* that leads to continuous gene of 1839 bp. Since 2005, several studies have been conducted from different geographical areas to check the

association of *dupA* with disease outcome considering the *dupA* has two ORFs (*jhp0917/jhp0918*) with the insertion of one base (T/C) at position 1385 of *jhp0917*. Studies performed in North India during 2007 support the finding of Lu *et al*[24]. However, studies conducted in different countries (Belgium, South Africa, China, North America and Brazil) found that *dupA* is not associated with DU in the respective population[25-27].

Investigations made in Sao Paulo, Brazil showed that *dupA* was detected in *H. pylori* strains of 41.5% patients, which was less from a previous study made by Gomes *et al*[26] (2008), in which *dupA* was present in 89.5% patients[28]. This study showed an association of *dupA* with *cagA* and *vacA s1m1* genotypes but without any link to disease outcome. The difference in the results of these two studies from Brazil could be explained by variation in geographic regions, a re-arrangement in the plasticity zone distribution in *H. pylori* and various methods used for the analysis.

The distribution of *dupA* in *H. pylori* was similar in Iraqi and Iranian population, but there was an association between peptic ulcer and *dupA* only in the Iraqi population[29]. An independent study by Douraghi *et al*[30] (2008) reported a non-significant higher distribution of *dupA* in DU than non-cardia GC patients in the Iranian population[30]. Another study by Talebi Bezmin Abadi *et al*[31] (2012) found a positive association between the presence of *dupA* and DU along with an inverse association between *dupA* and GU in Iranian population[31]. The discrepancy in the finding of Douraghi *et al*[30] (2008) and Talebi Bezmin Abadi *et al*[31] (2012) may be due to differences in the study populations. Douraghi *et al*[30] (2008) focused mainly in Tehran (the densely populated capital of Iran), whereas Talebi Bezmin Abadi *et al*[31] (2012) collected samples from the extremely rural northern areas of Iran. Recently, Fatahi *et al*[32] (2019) tested a highly conserved region of *dupA* and showed a significant relationship between the occurrence of DU and the presence of an 112 bp segment of *dupA* in the Iranian population[32]. Another group from Iran studied the relationship between antibiotic resistance pattern and virulence genotype among 68 *H. pylori* strains and found that metronidazole resistance was significantly associated with the strains harboring *cagA, sabA* and *dupA*[33]. One study from Kurdistan region of Northern Iraq reported that *cagA* gene was significantly associated with peptic ulcer disease rather than *dupA*, which contradict the result of Hussein *et al*[29] (2008). This might be due to the differences in sample size and also in the geographical location of Iraq[34]. In the Shiraz area of Iran, a significant relationship was found between strains with *dupA*, CagA motif (ABC types) and DU disease, which supports the previous finding in this region[35]. Another study from Western Iran indicated that presence of *dupA* gene could be considered as a marker for the onset of severe gastroduodenal diseases[36]. However, there was no association of *dupA* with DU in the results obtained from the Turkish population[37].

In China and South Korea, presence of *dupA* in clinical *H. pylori* isolates is significantly associated with DU and peptic ulcer (DU, benign GU, dysplasia), respectively[38,39]. In the Taiwanese female population, the host factor matrix metalloproteinase-3/tissue inhibitor matrix metalloproteinase-1 genotypes rather than *dupA* was found to increase the risk of DU in *H. pylori* infected cases[40]. A case control study conducted in Sweden, Australia, Malaysia and Singapore showed that there was significant variation in the prevalence of *dupA* in different locations and among different ethnic groups (Chinese, Indian and Malaya) within a country[41]. Another study in ethnic groups (Indian, Chinese and Malaya) of Malaysia reported that the prevalence of *dupA* was 22.9% in patients, which was in line with previous data (21.3%) conducted in Malaysia by Schmidt *et al*[41] (2009). In the later study, there was no association between *dupA* and clinical outcome[42].

Two independent systematic review and meta-analyses showed that *dupA* is more associated with DU in some Asian populations than in Western populations[43,44]. Between 2005 and 2009, almost all the studies used polymerase chain reaction (PCR) of two ORFs *jhp0917, jhp0918* and sequencing to identify the *dupA*. Functional analysis of *dupA* in the Japanese population showed no association with DU but another study from different parts of Japan showed that *dupA* is inversely related to GC[45,46].

Results from a study using different molecular methods [PCR, dot-blot hybridization, sequencing and reverse transcription PCR (RT-PCR)] indicated that *dupA* gene was prevalent more than six times in DU than in non-ulcer dyspepsia patients, indicating its significant association in India[47]. This result also corroborated the finding of Arachchi *et al*[24] (2007) from North India. The RT-PCR analysis of South and East Indian population revealed that all PCR positive strains were not able to produce *dupA* transcripts, which was inconsistent with the finding of Nguyen *et al*[45] (2009) where all the *dupA* positive strains showed the expression of the gene[47]. Further, the real-time PCR analysis revealed that the expression level of the *dupA*

transcripts varied from strain to strain in this study.

Studies conducted in Chile supported a significant association of *dupA* gene with non-severe clinical outcome like DU and also played a role in protecting severe diseases like GC[48]. The Costa Rica study with 151 dyspeptic patients showed that presence of *dupA* was significantly associated with decreased risk of DU[49].

Some of the above-mentioned studies verified the finding of Lu *et al*[23] (2005), but others could not find an association between *dupA* and disease outcome in their study populations. The differences in the results could be explained due to variation in the distribution of plasticity region genes and differences in the study population and techniques chosen for detection of *dupA* gene. Several studies on *dupA* were restricted to PCR of *jhp0917* and *jhp0918* along with sequencing of only the 3' region of *jhp0917* to find the insertion of T/C at 1385 position of *jhp0917*. Numerous studies have shown the presence of frame shift mutation within *dupA* gene leading to the formation of truncated non-functional DupA. These findings provide evidence that only PCR based analysis of *dupA* may yield erroneous interpretation. Studies conducted by Queiroz *et al*[50] (2011) and Moura *et al*[51] (2012) from Brazil showed the presence of a mutation in *dupA* that results in a stop codon, making the gene truncated or non-functional. In addition, these studies revealed the importance of sequence analysis of *dupA* amplicons[50,51]. Truncated *dupA* might not be involved in the pathogenesis of *H. pylori*.

Hussein *et al*[52] (2010) coined the term "*dupA*1". The *dupA* positive *H. pylori* strains were categorized into two alleles based on the sequence; *dupA1* (intact 1884 bp) and *dupA2* (truncated). It was shown that the intact *dupA1* positive strains induced the production of interleukin (IL)-12 subunit p40 (IL-12p40) and IL-12p70 from CD14 (+) mononuclear cells and IL-8 expression in the human stomach, respectively[52]. Takahashi *et al*[53] (2012) first reported the presence of an additional 615 bp in the 5' region of ORF *jhp0917* (absent in strain J99) and 45 bp in the 3' of *jhp0918* (consist of 37 bp of intergenic region of *jhp0918-jhp0919* and 8 bp of 5' region of *jhp0919* in J99) to make 2499 bp of *dupA* in the Japanese population (Figure 1). This variation formed the basis for classification of *dupA* into two types; "long and short types". The long type of intact 2499 bp (with an additional 615 bp at 5' region of *jhp0917*) has been considered as an actual virulence factor, and the absence of the additional segment should be interpreted with caution[53].

None of the *H. pylori* strains from Iraq carried the complete *dupA* cluster containing *virB8*, *virB9*, *virB10*, *virB11*, *virD4* and *virD2*, but there was a significant association between *dupA*1 and DU. Moreover, higher levels of gastric mucosa IL-8 production were documented in *dupA1* than in *dupA2* or *dupA* negative strains[54]. Further studies with *H. pylori* infected patients showed that *cagA*, complete *dupA* cluster and smoking habit were associated with increased levels of IL-8 production from gastric mucosa[55]. It was also shown in another study that the high IL-8 level in gastric mucosa was neither significantly associated with *dupA1* positive strains nor with *dupA* negative strains[56]. A significant association has also been found between *dupA1* and A2147G clarithromycin resistance mutation. However, the result of *dupA1* and IL-8 association in the Iraqi population was not well elucidated. In Brazilian *H. pylori* strains, it was found that *H. pylori* strains had the 45 base at the 3' end of *dupA*, similar to that of *dupA1*[57].

dupA gene of Indian *H. pylori* strains has been classified into two forms based on the presence of additional 615 bp at the 5' region of *dupA* followed *by* a stop codon. This includes *dupA*1 without any frameshift mutation (either long type or short type) and *dupA*2 with the truncated version having frameshift mutation[58]. Among these, *dupA*1 (intact *dupA*) was significantly associated with DU. Phylogenetic analysis of complete *dupA* gene sequencing revealed that Indian *H. pylori* strains intermingled with the East Asian strains, but differed from European strains[58]. *dupA* is the first known genetic element of Indian *H. pylori* strains, which phylogenetically formed the same cluster with the East Asian strains. *In vitro* study showed that IL-8 production was significantly associated with DU in intact *dupA*1 rather than truncated *dupA*2 or *dupA* negative strains[58]. In Chinese strains, the prevalence of long type *dupA* (2499 bp) was significantly higher in patients with GU, GC and DU than in those with gastritis[59].

In the Japanese population, prevalence of *dupA* was higher in the group where *H. pylori* cannot be eradicated, indicating that *dupA* may be an associated risk factor in the eradication failure[60]. A study from Pakistan on the influence of *dupA* in the eradication failure showed that *H. pylori* strains harboring *dupA* and *cagA* were multidrug (metronidazole, clarithromycin and amoxicillin) resistant as compared to strains having other virulence factors. This finding was similar to the observation made in the Japanese population[61]. In the northern part of Spain, *dupA* was more prevalent in mild diseases (peptic ulcer) than severe diseases (GC)[62]. In Switzerland and South Africa, *dupA* of *H. pylori* was not associated with severe gastritis or DU[63,64].

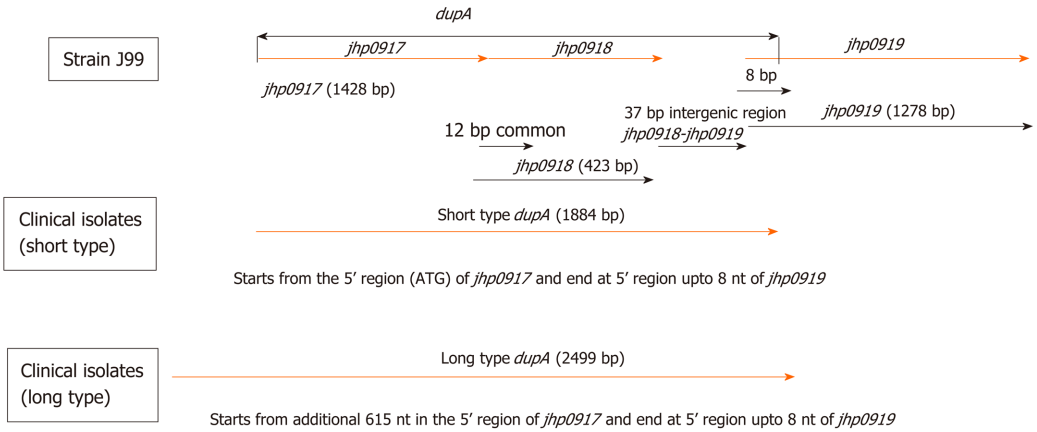

Figure 1 Schematic representation of the *jhp0917*, *jhp0918* and *jhp0919* gene in strain J99 and that of the *dupA* alleles in the clinical isolates. The long type *dupA* (2499 nt) in some clinical isolates contained an additional 615 nt in 5' region before *jhp0917* gene and ended 5 bp after the start codon of *jph0919* gene. The short type *dupA* (1884 nt) in some clinical isolates starts from the 5' region of *jhp0917* gene and ended 5 bp after the start codon of *jph0919* gene.

DUPA CLUSTER: THIRD TYPE IV SECRETION SYSTEM (T4SS) OF *H. PYLORI*

The T4SS is an important bacterial transport system, and it is involved in the transport of large molecules (*e.g.*, DNA, protein, *etc*). across the bacterial cell envelope[65,66]. Till now, three types of T4SS have been identified in *H. pylori*, of which much work has been done for the first two categories (*cag*PAI and ComB) and little is known about the third T4SS termed *dupA* cluster or *tfs*3 (Figure 2)[67,68]. The third putative type IV secretion system (*tfs3)* is a 16 kb gene fragment present in the plasticity zone of *H. pylori*, whose seven ORFs (*viB4*, *virB8, virB9, virB10, virB11, virD4* and *virD2*) were homologous to virB4/D of *Agrobacterium tumefecians* (*A. tumefecians*). The function of the *tfs3* elements is not yet clear as there is no direct evidence to show its role in transformation, conjugation or mouse colonization[69,70]. Some researchers divided the *tfs3* into *tfs3a* (all six *virB* homologues with *dupA*) and *tfs3b* (all six *virB* homologues with *virB4*), whereas others named all six *virB* homologues with virB4 as *tfs3* and all six *vir*B homologues with *dupA* as *tfs4*[71-73]. In order to avoid confusion, we will use the term *tfs3a* or *dupA* cluster (all six *virB* homologues with *dupA*). VirB8, VirB9 and VirB10 are expected to form the core complex that bridges cytoplasm and the outer membrane. The VirB4, VirB11, VirD4 may be localized to the inner bacterial membrane and recognize the substrate and energize translocation and assembly of T4SS[74]. Further, the novel putative T4SS (*tfs3a*) or *dupA* cluster has been divided into three groups: Viz, a complete *dupA* cluster (*dupA*-positive and all six *virB* genes-positive), an incomplete *dupA* cluster (*dupA*-positive but one/more than one *virB* genes negative) and *dupA*-negative group (*dupA* negative and *virB* gene positive/negative).

The study of *dupA* cluster from the United States population showed that the complete *dupA* cluster (*dupA* with six *virB* homologues) was associated with DU rather than *dupA* gene only[75]. Another report from the northeast part of China showed a significant association of complete *dupA* cluster with IL-8 production ($P < 0.01$), but it did not show any correlation between *dupA* cluster and disease outcome[76]. The studies from United States and China were conducted to check the prevalence of *tfs3a* or *dupA* cluster in their population by PCR only. However, the mere presence of the gene does not express functional protein and there is no direct evidence that shows *tfs3a* or *dupA* cluster forming a functional T4SS. The earlier studies on *tfs3a*did not find a direct pathogenic role of *tfs3a* in *H. pylori*, but found increased colonization fitness and up-regulation of pro-inflammatory signaling from cultured cells. A novel pathogenicity island (PAI) called *tfs3*-PAI was identified in China that had 17 ORFs, of which six are functionally homologues of T4SS and coordinate with the well-studied *cag*-PAI[77]. The complete *tfs* plasticity cluster was associated with IL-8 induction. The expression of some of the genes of *tfs3a/tfs*4 (*virB2*, *virB4*, *virB6*, *virB8*, *virB10*) in *H. pylori* is up-regulated in low pH and enhances bacterial adhesion that support the role of *tfs3a/tfs4* in the colonization and virulence[78]. It is not known whether the *virB* genes of *dupA* cluster work independently or in a coordinated manner by interacting among themselves or complementing each other's function. We checked the interaction of

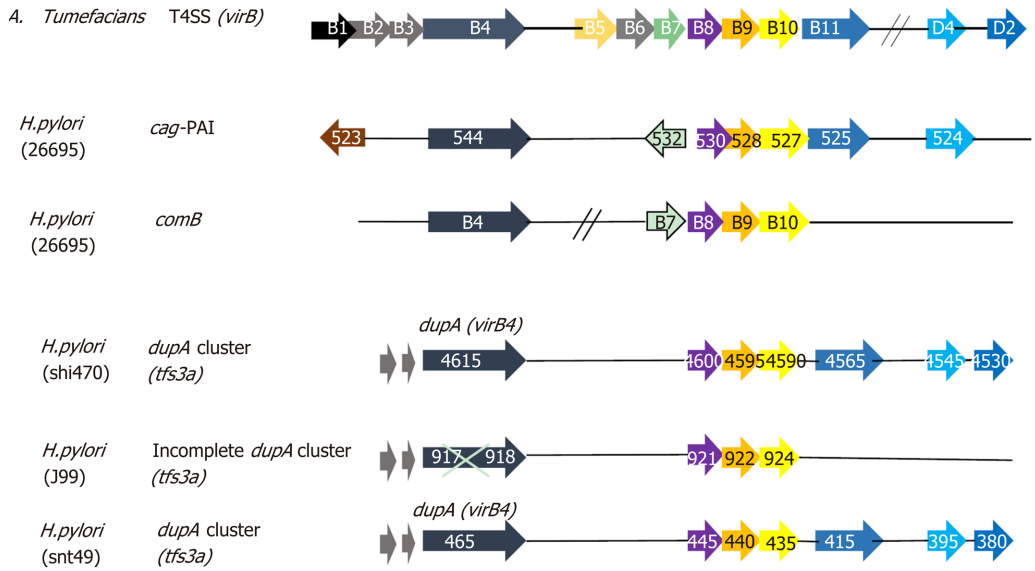

Figure 2 Organization of three types of type IV secretion system in the *Helicobacter pylori* compared to *Agrobacterium tumefaciens* prototype type IV secretion system. Genes are not drawn to scale. *H. pylori*: *Helicobacter pylori*; *A. tumefaciens*: *Agrobacterium tumefaciens*; T4SS: Type IV secretion system.

dupA with six *virB* genes of *tfs3a* to identify the assembly and function of complete *tfs3* using *in vivo* studies (yeast two-hybrid system) and found that *dupA* gene did not interact directly with any *virB* gene. It seems that *dupA* may interact with some intermediates or work independently (unpublished data). This interpretation supports our earlier finding that *tfs3* is not significantly associated with DU in Indian population. More studies are required to know the structure, assembly and functions of the VirB proteins in *H. pylori*.

THE PROSPECTIVE FUNCTIONS OF DUPA

The bioinformatics analysis (PDB search tool, UniProt database) showed that the *dupA* gene is homologous to VirB4 adenosine triphosphate (ATP)ase of virB/virD of *A. tumefecians* and is predicted to be involved in DNA/protein transfer. The N-terminal of long type DupA has no homologous motif. Only the middle portion (*jhp0917*) and C-terminal (part of *jhp0918*) showed homologous motifs suggesting that the N-terminal region might act as signal sequence. The amino acid sequence (210-406 AA) of *jhp0917* gene protein was homologous to CagE_TrbE_VirB family, a component of type IV transporter secretion system. The first middle region of the DupA protein (430-500 AA) is homologous to FtsK/SpoIIIE family, which contains ATP binding P-loop motif. This was found in the Ftsk protein of *Escherichia coli* involved in peptidoglycan synthesis and spoIIIE of *Bacillus subtilis*, facilitating in the intercellular chromosomal DNA transfer.

The second middle region (464-503aa) is homologous to TrwB, which has an ATP binding domain, and a part of T4SS may be responsible for the DNA binding and horizontal DNA transfer. The C-terminal region (668-738aa) is homologous to TraG_C_D, which is involved in the interaction of DNA-processing (Dtr) and mating pair formation (Mpf) system, leading to DNA transfer in bacterial conjugation. Many reports have shown that the growth rate of *dupA* positive strains is higher in low pH as compared to *dupA* deleted/negative strains. This phenomenon indicates that DupA protein acts as an interactive protein and hence regulates urease secretion in *H. pylori* [79].

The *in vitro* and *in vivo* studies showed the role of *dupA* gene in the activation of transcription factors nuclear factor kappa light chain enhancer of activated B cells and activator protein-1, which leads to IL-8 production. DupA protein act as an ATPase associated efflux pump, which probably confers its virulence. Evidence suggests that *DupA* is involved in the pathogenesis of *H. pylori* by activating the mitochondria dependent apoptotic pathway of the host's cell, which ultimately inhibits gastric cell growth.

Studies to understand the apoptotic effect of *dupA* on human gastric adenocarcinoma epithelial cell line (commonly known as AGS) by propidium iodide staining and fragmentation assay determined that *dupA* gene can induce apoptosis in AGS cells during an early stage of infection (unpublished data). This finding supports the results of Wang *et al*[79] (2015) and finds that *dupA* may act as a pathogenic factor of *H. pylori* to cause gastroduodenal diseases. Further studies are required to confirm the pathogenic effect of *dupA* in an *in vivo* model.

The growth kinetics between wild type *dupA* positive strains and its isogenic mutant strain showed that exponential phase was retarded in *dupA* mutant cells as compared to the wild type strain. Our growth curve results, supported by the microarray data, showed that cell division gene in the mutant *H. pylori* was downregulated (unpublished data). It has also been suggested that motility is an essential feature in the colonization and therefore the pathogenicity of *H. pylori*. The decrease in motility in *dupA* mutant strain as compared to wild type inferred the role of *dupA* gene in the motility. This motility result was further confirmed by the gene expression profile of *dupA* mutant strain whose flagella proteins (FlgE, FliD and FliG) were found to be down-regulated (unpublished data). It might be possible that *dupA* gene is directly or indirectly involved in negatively affecting the expression of cell division and flagellar genes of *H. pylori*.

As predicted from the bioinformatics analysis, our experimental data (unpublished data) have shown that natural transformation ability in *dupA* mutant strains has been totally inhibited in comparison to their wild type counterparts. There is a need for more studies on the heat-shock transformation efficiency, which will confirm the natural transformation assay, if any. Resistance to antimicrobials is of serious concern in *H. pylori* infection, as this may be the basis for eradication failure. It is important to use therapeutic regimens based on the results of antibiotic susceptibility testing. Metronidazole is considered a key drug in several therapies against *H. pylori* infection. The results of the metronidazole susceptibility test showed that inactivation of *dupA* gene transforms the *H. pylori* strains to resistance phenotype. This phenomenon has not been explained very well. It is possible that the *dupA* gene might help in the DNA/protein/drug import (unpublished data).

The *dupA* or *dupA* cluster may have an intermediate function to link *cag*PAI and *comB* system, as *dupA* gene shows homology with *cagE* of *cag*PAI and *comB4* of *comB* system. So, there is a need of an *in vivo* study to establish the precise function of *dupA*. It is assumed that the *dupA* in combination with other six *vir* genes form a novel third T4SS called *tfs3a* or *dupA* cluster that might play a pathogenic role in gastroduodenal diseases.

CONCLUSION

H. pylori is one of the most diverse bacterial species. *H. pylori* demonstrate panmictic population structure. DNA-fingerprint of two strains isolated from two different persons generally displays a non-identical pattern, which suggests genetic exchange along with co-evolution of this gastric pathogen with its host. One study from the Indian population demonstrated that all the tested patients carried multiple *H. pylori* strains in their gastric mucosa[80]. Analyses of certain genetic loci showed the micro diversity among the colonies from a single patient, which may be due to the recombination events during long-term carriage of the pathogen. From the results of this study, researchers predicted that many patients from the developing world acquired infections of *H. pylori* due to repeated exposure to this pathogen with different genetic make-up[80]. This may enhance the probability of super infections, which favor genetic exchanges among these unrelated *H. pylori* strains. As a result, this led to the genesis of certain *H. pylori* variants with different genetic makeup than the parental strain, which in turn increases the chance of the severe infection. Therefore, the exploration of appropriate biomarker(s) that envisage the clinical condition in *H. pylori*-infected patient is a challenging area of research.

There is a lack of relevant biomarker(s) capable of predicting important digestive diseases in clinical settings. Even though there is ample information regarding the *dupA* of *H. pylori*, many unanswered questions still exist, especially regarding the specificity of the *dupA* proposed for clinical manifestation. *dupA* was categorized as long and short types in one study, but in another study, this gene was typed as *dupA*1 (intact *dupA1* may be long type or short type) and *dupA*2 (truncated version). This gene classification should be resolved for international use to avoid any misperception. We propose the long *dupA* as *dupA*1 and short type *dupA* as *dupA*2, and the truncated

version of *dupA* has to be disregarded, as it has no role in pathogenesis. *dupA* should be screened by PCR, sequencing of the full-length gene (1884 and 2499 nt) and western blotting. Nevertheless, the discrepancy prevails between the association of *dupA* (short type or long type) or *dupA* cluster and the disease outcome. Currently, the prevalence of intact *dupA* in East Asian countries is lower than Western countries. DupA with another six Vir proteins (VirB8, VirB9, VirB10, VirB11, VirD4 and VirD2) predicted to form novel third type-IV secretion system (*tfs3a*), which may be involved in transformation/conjugation or injection of DNA/new effector molecules in gastric epithelial cells. However, the function of specific Vir protein of complete *dupA* cluster (*tfs3a*) is not well characterized. Recent reports and other unpublished data showed that DupA has multifunctional biological activities, and it can be considered as an important biomarker for DU. It is also not clear whether the DupA works alone or in combination with other VirB proteins. There is an urgent need for reliable *in vitro* and animal models from diverse geographical areas of the world to elucidate further the pathogenic role of *dupA* and *dupA* cluster in gastroduodenal diseases, particularly the DU and GC.

REFERENCES

1 **Buzás GM**. Benign and malignant gastroduodenal diseases associated with Helicobacter pylori: a narrative review and personal remarks in 2018. *Minerva Gastroenterol Dietol* 2018; **64**: 280-296 [PMID: 29458240 DOI: 10.23736/S1121-421X.18.02481-9]

2 **Misra V**, Pandey R, Misra SP, Dwivedi M. Helicobacter pylori and gastric cancer: Indian enigma. *World J Gastroenterol* 2014; **20**: 1503-1509 [PMID: 24587625 DOI: 10.3748/wjg.v20.i6.1503]

3 **Abadi AT**, Kusters JG. Management of Helicobacter pylori infections. *BMC Gastroenterol* 2016; **16**: 94 [PMID: 27520775 DOI: 10.1186/s12876-016-0496-2]

4 **Wotherspoon AC**, Ortiz-Hidalgo C, Falzon MR, Isaacson PG. Helicobacter pylori-associated gastritis and primary B-cell gastric lymphoma. *Lancet* 1991; **338**: 1175-1176 [PMID: 1682595 DOI: 10.1016/0140-6736(91)92035-z]

5 **Parsonnet J**, Friedman GD, Vandersteen DP, Chang Y, Vogelman JH, Orentreich N, Sibley RK. Helicobacter pylori infection and the risk of gastric carcinoma. *N Engl J Med* 1991; **325**: 1127-1131 [PMID: 1891020 DOI: 10.1056/NEJM199110173251603]

6 **Suerbaum S**, Michetti P. Helicobacter pylori infection. *N Engl J Med* 2002; **347**: 1175-1186 [PMID: 12374879 DOI: 10.1056/NEJMra020542]

7 **Pellicano R**, Ribaldone DG, Fagoonee S, Astegiano M, Saracco GM, Mégraud F. A 2016 panorama of Helicobacter pylori infection: key messages for clinicians. *Panminerva Med* 2016; **58**: 304-317 [PMID: 27716738]

8 Schistosomes, liver flukes and Helicobacter pylori. IARC Working Group on the Evaluation of Carcinogenic Risks to Humans. *IARC Monogr Eval Carcinog Risks Hum* 1994; **61**: 1-241 [PMID: 7715068]

9 **McGuire S**. World Cancer Report 2014. Geneva, Switzerland: World Health Organization, International Agency for Research on Cancer, WHO Press, 2015. *Adv Nutr* 2016; **7**: 418-419 [PMID: 26980827 DOI: 10.3945/an.116.012211]

10 **Smith S**, Fowora M, Pellicano R. Infections with *Helicobacter pylori* and challenges encountered in Africa. *World J Gastroenterol* 2019; **25**: 3183-3195 [PMID: 31333310 DOI: 10.3748/wjg.v25.i25.3183]

11 **Mamishi S**, Eshaghi H, Mahmoudi S, Bahador A, Hosseinpour Sadeghi R, Najafi M, Farahmand F, Khodadad A, Pourakbari B. Intrafamilial transmission of Helicobacter pylori: genotyping of faecal samples. *Br J Biomed Sci* 2016; **73**: 38-43 [PMID: 27182676 DOI: 10.1080/09674845.2016.1150666]

12 **Bui D**, Brown HE, Harris RB, Oren E. Serologic Evidence for Fecal-Oral Transmission of Helicobacter pylori. *Am J Trop Med Hyg* 2016; **94**: 82-88 [PMID: 26598563 DOI: 10.4269/ajtmh.15-0297]

13 **Ranjbar R**, Khamesipour F, Jonaidi-Jafari N, Rahimi E. Helicobacter pylori isolated from Iranian drinking water: vacA, cagA, iceA, oipA and babA2 genotype status and antimicrobial resistance properties. *FEBS Open Bio* 2016; **6**: 433-441 [PMID: 27419049 DOI: 10.1002/2211-5463.12054]

14 **Talaei R**, Souod N, Momtaz H, Dabiri H. Milk of livestock as a possible transmission route of Helicobacter pylori infection. *Gastroenterol Hepatol Bed Bench* 2015; **8**: S30-S36 [PMID: 26171135]

15 **Amieva MR**, El-Omar EM. Host-bacterial interactions in Helicobacter pylori infection. *Gastroenterology* 2008; **134**: 306-323 [PMID: 18166359 DOI: 10.1053/j.gastro.2007.11.009]

16 **Yamaoka Y**, Kwon DH, Graham DY. A M(r) 34,000 proinflammatory outer membrane protein (oipA) of Helicobacter pylori. *Proc Natl Acad Sci USA* 2000; **97**: 7533-7538 [PMID: 10852959 DOI: 10.1073/pnas.130079797]

17 **Covacci A**, Censini S, Bugnoli M, Petracca R, Burroni D, Macchia G, Massone A, Papini E, Xiang Z, Figura N. Molecular characterization of the 128-kDa immunodominant antigen of Helicobacter pylori associated with cytotoxicity and duodenal ulcer. *Proc Natl Acad Sci USA* 1993; **90**: 5791-5795 [PMID: 8516329 DOI: 10.1073/pnas.90.12.5791]

18 **Censini S**, Lange C, Xiang Z, Crabtree JE, Ghiara P, Borodovsky M, Rappuoli R, Covacci A. cag, a pathogenicity island of Helicobacter pylori, encodes type I-specific and disease-associated virulence factors. *Proc Natl Acad Sci USA* 1996; **93**: 14648-14653 [PMID: 8962108 DOI: 10.1073/pnas.93.25.14648]

19 **Atherton JC**, Cao P, Peek RM Jr, Tummuru MK, Blaser MJ, Cover TL. Mosaicism in vacuolating cytotoxin alleles of Helicobacter pylori. Association of specific vacA types with cytotoxin production and peptic ulceration. *J Biol Chem* 1995; **270**: 17771-17777 [PMID: 7629077 DOI: 10.1074/jbc.270.30.17771]

20 **Ghosh P**, Sarkar A, Ganguly M, Raghwan, Alam J, De R, Mukhopadhyay AK. Helicobacter pylori strains

harboring babA2 from Indian sub population are associated with increased virulence in ex vivo study. *Gut Pathog* 2016; **8**: 1 [PMID: 26759607 DOI: 10.1186/s13099-015-0083-z]

21 **Fischer W**, Breithaupt U, Kern B, Smith SI, Spicher C, Haas R. A comprehensive analysis of Helicobacter pylori plasticity zones reveals that they are integrating conjugative elements with intermediate integration specificity. *BMC Genomics* 2014; **15**: 310 [PMID: 24767410 DOI: 10.1186/1471-2164-15-310]

22 **Ganguly M**, Sarkar S, Ghosh P, Sarkar A, Alam J, Karmakar BC, De R, Saha DR, Mukhopadhyay AK. Helicobacter pylori plasticity region genes are associated with the gastroduodenal diseases manifestation in India. *Gut Pathog* 2016; **8**: 10 [PMID: 27006705 DOI: 10.1186/s13099-016-0093-5]

23 **Lu H**, Hsu PI, Graham DY, Yamaoka Y. Duodenal ulcer promoting gene of Helicobacter pylori. *Gastroenterology* 2005; **128**: 833-848 [PMID: 15825067 DOI: 10.1053/j.gastro.2005.01.009]

24 **Arachchi HS**, Kalra V, Lal B, Bhatia V, Baba CS, Chakravarthy S, Rohatgi S, Sarma PM, Mishra V, Das B, Ahuja V. Prevalence of duodenal ulcer-promoting gene (dupA) of Helicobacter pylori in patients with duodenal ulcer in North Indian population. *Helicobacter* 2007; **12**: 591-597 [PMID: 18001398 DOI: 10.1111/j.1523-5378.2007.00557.x]

25 **Argent RH**, Burette A, Miendje Deyi VY, Atherton JC. The presence of dupA in Helicobacter pylori is not significantly associated with duodenal ulceration in Belgium, South Africa, China, or North America. *Clin Infect Dis* 2007; **45**: 1204-1206 [PMID: 17918084 DOI: 10.1086/522177]

26 **Gomes LI**, Rocha GA, Rocha AM, Soares TF, Oliveira CA, Bittencourt PF, Queiroz DM. Lack of association between Helicobacter pylori infection with dupA-positive strains and gastroduodenal diseases in Brazilian patients. *Int J Med Microbiol* 2008; **298**: 223-230 [PMID: 17897881 DOI: 10.1016/j.ijmm.2007.05.006]

27 **Pacheco AR**, Proença-Módena JL, Sales AI, Fukuhara Y, da Silveira WD, Pimenta-Módena JL, de Oliveira RB, Brocchi M. Involvement of the Helicobacter pylori plasticity region and cag pathogenicity island genes in the development of gastroduodenal diseases. *Eur J Clin Microbiol Infect Dis* 2008; **27**: 1053-1059 [PMID: 18560912 DOI: 10.1007/s10096-008-0549-8]

28 **Pereira WN**, Ferraz MA, Zabaglia LM, de Labio RW, Orcini WA, Bianchi Ximenez JP, Neto AC, Payão SL, Rasmussen LT. Association among H. pylori virulence markers dupA, cagA and vacA in Brazilian patients. *J Venom Anim Toxins Incl Trop Dis* 2014; **20**: 1 [PMID: 24456629 DOI: 10.1186/1678-9199-20-1]

29 **Hussein NR**, Mohammadi M, Talebkhan Y, Doraghi M, Letley DP, Muhammad MK, Argent RH, Atherton JC. Differences in virulence markers between Helicobacter pylori strains from Iraq and those from Iran: potential importance of regional differences in H. pylori-associated disease. *J Clin Microbiol* 2008; **46**: 1774-1779 [PMID: 18353934 DOI: 10.1128/JCM.01737-07]

30 **Douraghi M**, Mohammadi M, Oghalaie A, Abdirad A, Mohagheghi MA, Hosseini ME, Zeraati H, Ghasemi A, Esmaieli M, Mohajerani N. dupA as a risk determinant in Helicobacter pylori infection. *J Med Microbiol* 2008; **57**: 554-562 [PMID: 18436587 DOI: 10.1099/jmm.0.47776-0]

31 **Talebi Bezmin Abadi A**, Taghvaei T, Wolfram L, Kusters JG. Infection with Helicobacter pylori strains lacking dupA is associated with an increased risk of gastric ulcer and gastric cancer development. *J Med Microbiol* 2012; **61**: 23-30 [PMID: 21903829 DOI: 10.1099/jmm.0.027052-0]

32 **Fatahi G**, Talebi Bezmin Abadi A, Peerayeh SN, Forootan M. Carrying a 112 bp-segment in Helicobacter pylori dupA may associate with increased risk of duodenal ulcer. *Infect Genet Evol* 2019; **73**: 21-25 [PMID: 30981881 DOI: 10.1016/j.meegid.2019.04.009]

33 **Farzi N**, Yadegar A, Sadeghi A, Asadzadeh Aghdaei H, Marian Smith S, Raymond J, Suzuki H, Zali MR. High Prevalence of Antibiotic Resistance in Iranian *Helicobacter pylori* Isolates: Importance of Functional and Mutational Analysis of Resistance Genes and Virulence Genotyping. *J Clin Med* 2019; **8**: 2004 [PMID: 31744181 DOI: 10.3390/jcm8112004]

34 **Salih AM**, Goreal A, Hussein NR, Abdullah SM, Hawrami K, Assafi M. The distribution of cagA and dupA genes in Helicobacter pylori strains in Kurdistan region, northern Iraq. *Ann Saudi Med* 2013; **33**: 290-293 [PMID: 23793434 DOI: 10.5144/0256-4947.2013.290]

35 **Haddadi MH**, Bazargani A, Khashei R, Fattahi MR, Bagheri Lankarani K, Moini M, Rokni Hosseini SM. Different distribution of Helicobacter pylori EPIYA- cagA motifs and dupA genes in the upper gastrointestinal diseases and correlation with clinical outcomes in iranian patients. *Gastroenterol Hepatol Bed Bench* 2015; **8**: S37-S46 [PMID: 26171136 DOI: 10.1016/j.ccep.2012.02.001]

36 **Souod N**, Sarshar M, Dabiri H, Momtaz H, Kargar M, Mohammadzadeh A, Abdi S. The study of the oipA and dupA genes in Helicobacter pylori strains and their relationship with different gastroduodenal diseases. *Gastroenterol Hepatol Bed Bench* 2015; **8**: S47-S53 [PMID: 26171137]

37 **Tuncel IE**, Hussein NR, Bolek BK, Arikan S, Salih BA. Helicobacter pylori virulence factors and their role in peptic ulcer diseases in Turkey. *Acta Gastroenterol Belg* 2010; **73**: 235-238 [PMID: 20690562 DOI: 10.1007/s00261-009-9502-2]

38 **Zhang Z**, Zheng Q, Chen X, Xiao S, Liu W, Lu H. The Helicobacter pylori duodenal ulcer promoting gene, dupA in China. *BMC Gastroenterol* 2008; **8**: 49 [PMID: 18950522 DOI: 10.1186/1471-230X-8-49]

39 **Kim JY**, Kim N, Nam RH, Suh JH, Chang H, Lee JW, Kim YS, Kim JM, Choi JW, Park JG, Lee YS, Lee DH, Jung HC. Association of polymorphisms in virulence factor of Helicobacter pylori and gastroduodenal diseases in South Korea. *J Gastroenterol Hepatol* 2014; **29**: 984-991 [PMID: 24372834 DOI: 10.1111/jgh.12509]

40 **Yeh YC**, Cheng HC, Chang WL, Yang HB, Sheu BS. Matrix metalloproteinase-3 promoter polymorphisms but not dupA-H. pylori correlate to duodenal ulcers in H. pylori-infected females. *BMC Microbiol* 2010; **10**: 218 [PMID: 20707923 DOI: 10.1186/1471-2180-10-218]

41 **Schmidt HM**, Andres S, Kaakoush NO, Engstrand L, Eriksson L, Goh KL, Fock KM, Hilmi I, Dhamodaran S, Forman D, Mitchell H. The prevalence of the duodenal ulcer promoting gene (dupA) in Helicobacter pylori isolates varies by ethnic group and is not universally associated with disease development: a case-control study. *Gut Pathog* 2009; **1**: 5 [PMID: 19338650 DOI: 10.1186/1757-4749-1-5]

42 **Osman HA**, Hasan H, Suppian R, Hassan S, Andee DZ, Abdul Majid N, Zilfalil BA. Prevalence of Helicobacter pylori cagA, babA2, and dupA genotypes and correlation with clinical outcome in Malaysian patients with dyspepsia. *Turk J Med Sci* 2015; **45**: 940-946 [PMID: 26422871 DOI: 10.3906/sag-1409-77]

43 **Hussein NR**. The association of dupA and Helicobacter pylori-related gastroduodenal diseases. *Eur J Clin Microbiol Infect Dis* 2010; **29**: 817-821 [PMID: 20419465 DOI: 10.1007/s10096-010-0933-z]

44 **Shiota S**, Matsunari O, Watada M, Hanada K, Yamaoka Y. Systematic review and meta-analysis: the relationship between the Helicobacter pylori dupA gene and clinical outcomes. *Gut Pathog* 2010; **2**: 13 [PMID: 21040520 DOI: 10.1186/1757-4749-2-13]

45 **Nguyen LT**, Uchida T, Tsukamoto Y, Kuroda A, Okimoto T, Kodama M, Murakami K, Fujioka T, Moriyama M. Helicobacter pylori dupA gene is not associated with clinical outcomes in the Japanese population. *Clin Microbiol Infect* 2010; **16**: 1264-1269 [PMID: 19832706 DOI: 10.1111/j.1469-0691.2009.03081.x]

46 **Imagawa S**, Ito M, Yoshihara M, Eguchi H, Tanaka S, Chayama K. Helicobacter pylori dupA and gastric acid secretion are negatively associated with gastric cancer development. *J Med Microbiol* 2010; **59**: 1484-1489 [PMID: 20829397 DOI: 10.1099/jmm.0.021816-0]

47 **Alam J**, Maiti S, Ghosh P, De R, Chowdhury A, Das S, Macaden R, Devarbhavi H, Ramamurthy T, Mukhopadhyay AK. Significant association of the dupA gene of Helicobacter pylori with duodenal ulcer development in a South-east Indian population. *J Med Microbiol* 2012; **61**: 1295-1302 [PMID: 22653921 DOI: 10.1099/jmm.0.038398-0]

48 **Paredes-Osses E**, Sáez K, Sanhueza E, Hebel S, González C, Briceño C, García Cancino A. Association between cagA, vacAi, and dupA genes of Helicobacter pylori and gastroduodenal pathologies in Chilean patients. *Folia Microbiol (Praha)* 2017; **62**: 437-444 [PMID: 28283946 DOI: 10.1007/s12223-017-0514-y]

49 **Molina-Castro S**, Garita-Cambronero J, Malespín-Bendaña W, Une C, Ramírez V. Virulence factor genotyping of Helicobacter pylori isolated from Costa Rican dyspeptic patients. *Microb Pathog* 2019; **128**: 276-280 [PMID: 30654009 DOI: 10.1016/j.micpath.2019.01.018]

50 **Queiroz DM**, Rocha GA, Rocha AM, Moura SB, Saraiva IE, Gomes LI, Soares TF, Melo FF, Cabral MM, Oliveira CA. dupA polymorphisms and risk of Helicobacter pylori-associated diseases. *Int J Med Microbiol* 2011; **301**: 225-228 [PMID: 21050811 DOI: 10.1016/j.ijmm.2010.08.019]

51 **Moura SB**, Costa RF, Anacleto C, Rocha GA, Rocha AM, Queiroz DM. Single nucleotide polymorphisms of Helicobacter pylori dupA that lead to premature stop codons. *Helicobacter* 2012; **17**: 176-180 [PMID: 22515354 DOI: 10.1111/j.1523-5378.2011.00933.x]

52 **Hussein NR**, Argent RH, Marx CK, Patel SR, Robinson K, Atherton JC. Helicobacter pylori dupA is polymorphic, and its active form induces proinflammatory cytokine secretion by mononuclear cells. *J Infect Dis* 2010; **202**: 261-269 [PMID: 20533870 DOI: 10.1086/653587]

53 **Takahashi A**, Shiota S, Matsunari O, Watada M, Suzuki R, Nakachi S, Kinjo N, Kinjo F, Yamaoka Y. Intact long-type dupA as a marker for gastroduodenal diseases in Okinawan subpopulation, Japan. *Helicobacter* 2013; **18**: 66-72 [PMID: 23067336 DOI: 10.1111/j.1523-5378.2012.00994.x]

54 **Hussein NR**, Abdullah SM, Salih AM, Assafi MA. dupA1 is associated with duodenal ulcer and high interleukin-8 secretion from the gastric mucosa. *Infect Immun* 2012; **80**: 2971-2; author reply 2973 [PMID: 22811495 DOI: 10.1128/IAI.00076-12]

55 **Hussein NR**, Tuncel IE. Helicobacter pylori dupA and smoking are associated with increased levels of interleukin-8 in gastric mucosa in Iraq. *Hum Pathol* 2015; **46**: 929-930 [PMID: 25791584 DOI: 10.1016/j.humpath.2015.01.021]

56 **Hussein NR**, Tunjel I, Majed HS, Yousif ST, Aswad SI, Assafi MS. Duodenal ulcer promoting gene 1 (dupA1) is associated with A2147G clarithromycin-resistance mutation but not interleukin-8 secretion from gastric mucosa in Iraqi patients. *New Microbes New Infect* 2015; **6**: 5-10 [PMID: 26042186 DOI: 10.1016/j.nmni.2015.02.005]

57 **Queiroz DM**, Moura SB, Rocha AM, Costa RF, Anacleto C, Rocha GA. The genotype of the Brazilian dupA-positive Helicobacter pylori strains is dupA1. *J Infect Dis* 2011; **203**: 1033-1034 [PMID: 21402555 DOI: 10.1093/infdis/jiq147]

58 **Alam J**, Ghosh P, Ganguly M, Sarkar A, De R, Mukhopadhyay AK. Association of Intact dupA (dupA1) rather than dupA1 cluster with duodenal ulcer in Indian population. *Gut Pathog* 2015; **7**: 9 [PMID: 25829953 DOI: 10.1186/s13099-015-0056-2]

59 **Wang MY**, Chen C, Gao XZ, Li J, Yue J, Ling F, Wang XC, Shao SH. Distribution of Helicobacter pylori virulence markers in patients with gastroduodenal diseases in a region at high risk of gastric cancer. *Microb Pathog* 2013; **59-60**: 13-18 [PMID: 23583809 DOI: 10.1016/j.micpath.2013.04.001]

60 **Shiota S**, Nguyen LT, Murakami K, Kuroda A, Mizukami K, Okimoto T, Kodama M, Fujioka T, Yamaoka Y. Association of helicobacter pylori dupA with the failure of primary eradication. *J Clin Gastroenterol* 2012; **46**: 297-301 [PMID: 22298090 DOI: 10.1097/MCG.0b013e318243201c]

61 **Rasheed F**, Campbell BJ, Alfizah H, Varro A, Zahra R, Yamaoka Y, Pritchard DM. Analysis of clinical isolates of Helicobacter pylori in Pakistan reveals high degrees of pathogenicity and high frequencies of antibiotic resistance. *Helicobacter* 2014; **19**: 387-399 [PMID: 24827414 DOI: 10.1111/hel.12142]

62 **Fernández-Reyes M**, Tamayo E, Rojas-Rengifo D, Fischer W, Carrasco-García E, Alonso M, Lizasoain J, Bujanda L, Cosme Á, Montes M. Helicobacter pylori pathogenicity and primary antimicrobial resistance in Northern Spain. *Eur J Clin Invest* 2019; **49**: e13150 [PMID: 31192451 DOI: 10.1111/eci.13150]

63 **Imkamp F**, Lauener FN, Pohl D, Lehours P, Vale FF, Jehanne Q, Zbinden R, Keller PM, Wagner K. Rapid Characterization of Virulence Determinants in *Helicobacter pylori* Isolated from Non-Atrophic Gastritis Patients by Next-Generation Sequencing. *J Clin Med* 2019; **8**: 1030 [PMID: 31336977 DOI: 10.3390/jcm8071030]

64 **Idowu A**, Mzukwa A, Harrison U, Palamides P, Haas R, Mbao M, Mamdoo R, Bolon J, Jolaiya T, Smith S, Ally R, Clarke A, Njom H. Detection of Helicobacter pylori and its virulence genes (cagA, dupA, and vacA) among patients with gastroduodenal diseases in Chris Hani Baragwanath Academic Hospital, South Africa. *BMC Gastroenterol* 2019; **19**: 73 [PMID: 31088381 DOI: 10.1186/s12876-019-0986-0]

65 **Christie PJ**. Type IV secretion: intercellular transfer of macromolecules by systems ancestrally related to conjugation machines. *Mol Microbiol* 2001; **40**: 294-305 [PMID: 11309113 DOI: 10.1046/j.1365-2958.2001.02302.x]

66 **Fischer W**, Püls J, Buhrdorf R, Gebert B, Odenbreit S, Haas R. Systematic mutagenesis of the Helicobacter pylori cag pathogenicity island: essential genes for CagA translocation in host cells and induction of

interleukin-8. *Mol Microbiol* 2001; **42**: 1337-1348 [PMID: 11886563 DOI: 10.1046/j.1365-2958.2003.03406.x]

67 **Backert S**, Ziska E, Brinkmann V, Zimny-Arndt U, Fauconnier A, Jungblut PR, Naumann M, Meyer TF. Translocation of the Helicobacter pylori CagA protein in gastric epithelial cells by a type IV secretion apparatus. *Cell Microbiol* 2000; **2**: 155-164 [PMID: 11207572 DOI: 10.1046/j.1462-5822.2000.00043.x]

68 **Karnholz A**, Hoefler C, Odenbreit S, Fischer W, Hofreuter D, Haas R. Functional and topological characterization of novel components of the comB DNA transformation competence system in Helicobacter pylori. *J Bacteriol* 2006; **188**: 882-893 [PMID: 16428391 DOI: 10.1128/JB.188.3.882-893.2006]

69 **Kersulyte D**, Velapatiño B, Mukhopadhyay AK, Cahuayme L, Bussalleu A, Combe J, Gilman RH, Berg DE. Cluster of type IV secretion genes in Helicobacter pylori's plasticity zone. *J Bacteriol* 2003; **185**: 3764-3772 [PMID: 12813069 DOI: 10.1128/jb.185.13.3764-3772.2003]

70 **Kersulyte D**, Lee W, Subramaniam D, Anant S, Herrera P, Cabrera L, Balqui J, Barabas O, Kalia A, Gilman RH, Berg DE. Helicobacter Pylori's plasticity zones are novel transposable elements. *PLoS One* 2009; **4**: e6859 [PMID: 19727398 DOI: 10.1371/journal.pone.0006859]

71 **Delahay RM**, Croxall NJ, Stephens AD. Phylogeographic diversity and mosaicism of the *Helicobacter pylori tfs* integrative and conjugative elements. *Mob DNA* 2018; **9**: 5 [PMID: 29416569 DOI: 10.1186/s13100-018-0109-4]

72 **Fernandez-Gonzalez E**, Backert S. DNA transfer in the gastric pathogen Helicobacter pylori. *J Gastroenterol* 2014; **49**: 594-604 [PMID: 24515309 DOI: 10.1007/s00535-014-0938-y]

73 **Grove JI**, Alandiyjany MN, Delahay RM. Site-specific relaxase activity of a VirD2-like protein encoded within the tfs4 genomic island of Helicobacter pylori. *J Biol Chem* 2013; **288**: 26385-26396 [PMID: 23900838 DOI: 10.1074/jbc.M113.496430]

74 **Vergunst AC**, Schrammeijer B, den Dulk-Ras A, de Vlaam CM, Regensburg-Tuïnk TJ, Hooykaas PJ. VirB/D4-dependent protein translocation from Agrobacterium into plant cells. *Science* 2000; **290**: 979-982 [PMID: 11062129 DOI: 10.1126/science.290.5493.979]

75 **Jung SW**, Sugimoto M, Shiota S, Graham DY, Yamaoka Y. The intact dupA cluster is a more reliable Helicobacter pylori virulence marker than dupA alone. *Infect Immun* 2012; **80**: 381-387 [PMID: 22038914 DOI: 10.1128/IAI.05472-11]

76 **Wang MY**, Shao C, Li J, Yang YC, Wang SB, Hao JL, Wu CM, Gao XZ, Shao SH. Helicobacter pylori with the Intact dupA Cluster is more Virulent than the Strains with the Incomplete dupA Cluster. *Curr Microbiol* 2015; **71**: 16-23 [PMID: 25847580 DOI: 10.1007/s00284-015-0812-z]

77 **Wang GQ**, Xu JT, Xu GY, Zhang Y, Li F, Suo J. Predicting a novel pathogenicity island in Helicobacter pylori by genomic barcoding. *World J Gastroenterol* 2013; **19**: 5006-5010 [PMID: 23946608 DOI: 10.3748/wjg.v19.i30.5006]

78 **Silva B**, Nunes A, Vale FF, Rocha R, Gomes JP, Dias R, Oleastro M. The expression of Helicobacter pylori tfs plasticity zone cluster is regulated by pH and adherence, and its composition is associated with differential gastric IL-8 secretion. *Helicobacter* 2017; 22 [PMID: 28436598 DOI: 10.1111/hel.12390]

79 **Wang MY**, Chen C, Shao C, Wang SB, Wang AC, Yang YC, Yuan XY, Shao SH. Intact long-type DupA protein in Helicobacter pylori is an ATPase involved in multifunctional biological activities. *Microb Pathog* 2015; **81**: 53-59 [PMID: 25745877 DOI: 10.1016/j.micpath.2015.03.002]

80 **Patra R**, Chattopadhyay S, De R, Ghosh P, Ganguly M, Chowdhury A, Ramamurthy T, Nair GB, Mukhopadhyay AK. Multiple infection and microdiversity among Helicobacter pylori isolates in a single host in India. *PLoS One* 2012; **7**: e43370 [PMID: 22952670 DOI: 10.1371/journal.pone.0043370]

World Journal of Gastroenterology

Submit a Manuscript: https://www.f6publishing.com

World J Gastroenterol 2020 August 28; 26(32): 4753-4762

DOI: 10.3748/wjg.v26.i32.4753

ISSN 1007-9327 (print) ISSN 2219-2840 (online)

MINIREVIEWS

Etiology and management of liver injury in patients with COVID-19

Rui-Xu Yang, Rui-Dan Zheng, Jian-Gao Fan

ORCID number: Rui-Xu Yang 0000-0001-9384-6408; Rui-Dan Zheng 0000-0003-3556-8563; Jian-Gao Fan 0000-0001-7443-5056.

Author contributions: Yang RX wrote the paper; Zheng RD contributed to the preparation of the tables and figure; and Fan JG critically revised the manuscript.

Supported by the National Key Research and Development Program, No. 2017YFC0908903; National Natural Science Foundation of China, No. 81873565 and No. 81900507; and Hospital Funded Clinical Research, Xinhua Hospital Affiliated to Shanghai Jiao Tong University School of Medicine, No. 17CSK04.

Conflict-of-interest statement: The authors declare no conflicts of interest for this article.

Rui-Xu Yang, Center for Fatty Liver, Department of Gastroenterology, Xinhua Hospital Affiliated to Shanghai Jiao Tong University School of Medicine, Shanghai 200092, China

Rui-Dan Zheng, Diagnosis and Treatment Center for Liver Diseases, Zhengxing Hospital, Zhangzhou 363000, Fujian Province, China

Jian-Gao Fan, Center for Fatty Liver, Department of Gastroenterology, Xinhua Hospital Affiliated to Shanghai Jiao Tong University School of Medicine, Shanghai Key Lab of Pediatric Gastroenterology and Nutrition, Shanghai 200092, China

Corresponding author: Jian-Gao Fan, MD, PhD, Chief Doctor, Professor, Center for Fatty Liver, Department of Gastroenterology, Xinhua Hospital Affiliated to Shanghai Jiao Tong University School of Medicine, Shanghai Key Lab of Pediatric Gastroenterology and Nutrition, No. 1665 Kongjiang Road, Shanghai 200092, China. fanjiangao@xinhuamed.com.cn

Abstract

The outbreak of novel coronavirus disease 2019 (COVID-19) has resulted in global emergence. With the expansion of related research, in addition to respiratory symptoms, digestive system involvement such as nausea, vomiting, and diarrhea have also been reported with COVID-19. Besides, abnormal liver function is also frequent in biochemical tests of COVID-19 patients, which is correlated with the severity and mortality of the disease course. The etiology of liver injury in patients with COVID-19 might include viral immunologic injury, drug-induced liver injury, the systemic inflammatory response, hypoxic hepatitis, and the exacerbation of preexisting liver disease. Although liver injuries in COVID-19 are often transient and reversible, health workers need to pay attention to preexisting liver disease, monitor liver function, strengthen supportive treatment, and reduce the chance of drug-induced liver injury. This article reviews the epidemiological characteristics, etiology, management, and preventive strategies for liver injury in patients with COVID-19.

Key words: COVID-19; SARS-CoV-2; Coronavirus; Liver injury; Function test, Liver; Etiology

Core tip: The pandemic of coronavirus disease 2019 (COVID-19) has aroused a global threat to human health. With the deepening of related research, it was found that in

Manuscript source: Invited manuscript

Received: May 8, 2020
Peer-review started: May 8, 2020
First decision: May 15, 2020
Revised: May 23, 2020
Accepted: August 12, 2020
Article in press: August 12, 2020
Published online: August 28, 2020

P-Reviewer: Gencdal G, Khayyat YM, Marcos R, Sargsyants N
S-Editor: Zhang L
L-Editor: Wang TQ
P-Editor: Zhang YL

addition to respiratory symptoms, digestive involvements and liver injury were reported in COVID-19. Viral immunologic injury, drug-induced liver injury, secondary liver injury induced by systemic inflammatory response or hypoxia, and the exacerbation of pre-existing liver disease might be the etiologic factors for liver injury in COVID-19. Health workers need to pay attention to the management of pre-existing liver disease, monitor the liver function and strengthen supportive treatment, and reduce the chance of drug-induced liver injury with COVID-19.

Citation: Yang RX, Zheng RD, Fan JG. Etiology and management of liver injury in patients with COVID-19. *World J Gastroenterol* 2020; 26(32): 4753-4762
URL: https://www.wjgnet.com/1007-9327/full/v26/i32/4753.htm
DOI: https://dx.doi.org/10.3748/wjg.v26.i32.4753

INTRODUCTION

In December 2019, an outbreak of novel coronavirus disease 2019 (COVID-19, previously known as 2019-nCoV) was reported in Wuhan, Hubei Province, China, and rapidly spread to other areas and countries. As of May 23, 2020, there were 5.2 million confirmed cases, causing 336 thousand fatalities globally. The COVID-19 pandemic has become a global threat to human health, which has constituted a public health emergency of international concern. The pandemic is caused by severe acute respiratory syndrome coronavirus 2 (SARS-CoV-2), which was identified as a type of beta coronavirus cluster and shares 79.6% sequence identity with SARS-CoV[1]. COVID-19 is generally a self-limiting disease but can also be deadly, with a fatality rate of approximately 2.3% in China[2], ranging from 5.8% in Wuhan to 0.7% in the rest of China[3]. The proportion of severe or fatal infections may vary by country and area, which may be related to distinct demographics of infection. Most of the fatal cases have occurred in patients with advanced age or underlying medical comorbidities (obesity, hypertension, diabetes, cardiovascular disease, chronic lung disease, and cancer)[2,4,5].

The onset of COVID-19 presents mainly with fever, cough, and dyspnea, and some patients can progress to acute respiratory distress syndrome and septic shock. With the increase in cases and the expansion of related research, it was found that in addition to respiratory symptoms, digestive system involvement such as nausea, vomiting, and diarrhea have also been reported[6,7]. In addition, some patients with COVID-19 also have shown different degrees of liver injury, presenting mainly with elevated serum transaminase and lactate dehydrogenase (LDH) levels and hypoalbuminemia[4,5,8-24]. It has been suggested that there might be a certain relationship between coronavirus infection and liver injury. The issue of liver injury in patients with COVID-19 has aroused extensive discussion and attention. This article reviews the epidemiological characteristics, etiologies, and management and prevention strategies for liver injury in patients with COVID-19.

CLINICAL CHARACTERISTICS OF LIVER INJURY IN COVID-19

Based on recent studies, COVID-19 onset clusters with the common symptoms of fever and cough. However, other clinical features, such as diarrhea (1.25%-10.1%), nausea and vomiting (1%-10.1%), and loss of appetite (43%), were also reported in several studies (Table 1), and 11.4% of patients presented with at least one digestive system symptom[4,5,7]. Fecal specimen nucleic detection also showed positive results in COVID-19 patients[16,25,27], suggesting the possible enteric involvement of SARS-CoV-2[28]. However, fecal-oral transmission has not been clinically described in the spread of COVID-19. Liver injury in patients with coronavirus infection has been reported in patients with SARS and Middle East respiratory syndrome[29,30]. Abnormal liver function was also observed in cases of COVID-19, manifesting mainly as isolated elevated serum transaminase and LDH levels[4,5,9-23] (Table 2). The first case of COVID-19 in the United States was reported to have progressive elevation of alanine aminotransferase (ALT), aspartate aminotransferase (AST), alkaline phosphatase (ALP), and LDH levels during hospitalization, while the bilirubin level and prothrombin time remained normal[16]. In a study from Jin Yin-tan Hospital, among the

Table 1 Digestive system involvement in coronavirus disease 2019

Ref.	City	Sample size (*n*)	Disease severity	Preexisting digestive system diseases (%)	Digestive system symptoms
Guan *et al*[4]	Multicenter, China	1099	Nonsevere (84.3%); severe (15.7%)	Hepatitis B infection (2.1%)	Diarrhea (3.8%); nausea and vomiting (5.0%)
Zhou *et al*[5]	Wuhan, China	191	General (38%); severe (35%); critical (28%)	NA	Diarrhea (5%); nausea or vomiting (4%)
Chen *et al*[9]	Wuhan, China	99	NA	Digestive system disease (11%)	Diarrhea (2%); nausea and vomiting (1%)
Shi *et al*[10]	Wuhan, China	81	NA	Chronic liver disease (9%)	Diarrhea (4%); vomiting (5%)
Huang *et al*[11]	Wuhan, China	41	Nonsevere (68.3%); severe (31.7%)	Chronic liver disease (2%)	Diarrhea (3%)
Wu *et al*[12]	Jiangsu, China	80	Mild (35.0%); moderate (61.25%); severe (3.75%); critical (0%)	Digestive system disease (3.75%); chronic liver disease (1.25%);	Diarrhea (1.25%); nausea and vomiting (1.25%)
Xu *et al*[13]	Zhejiang, China	62	NA	Chronic liver disease (11%)	Diarrhea (8%)
Yang *et al*[14]	Wuhan, China	52	Critical (100%)	NA	Vomiting (4%)
Wang *et al*[15]	Wuhan, China	138	Nonsevere (73.9%); severe (26.1%)	Chronic liver disease (2.9%)	Diarrhea (10.1%); nausea (10.1%); vomiting (3.6%); abdominal pain (2.2%)
Pan *et al*[18]	Wuhan, China	21	Nonsevere (100%)	NA	Loss of appetite (43%)
Jin *et al*[7]	Zhejiang, China	651	Nonsevere (90.2%); severe/critical (9.8%)	Chronic liver disease (3.8%)	Nausea, vomiting, or diarrhea (11.4%)
Xie *et al*[20]	Wuhan, China	79	Moderate (64.6%); severe (35.4%)	NA	Diarrhea (8.9%)
Chen *et al*[22]	Hubei, China	274	Recovered (58.8%); died (41.2%)	Gastrointestinal diseases (1%); hepatitis B virus positivity (4%)	Diarrhea (28%); nausea (9%); vomiting (6%); abdominal pain (7%)

COVID-19: Coronavirus disease 2019.

99 patients confirmed to have COVID-19, 43 had ALT or AST levels above the normal range, 75 were reported to have elevated LDH levels, and one had severely impaired liver function (ALT, 7590 U/L; AST, 1445 U/L), while basic liver disease was not reported in these cases[9]. Imported cases outside of Wuhan were reported to have a lower proportion of liver injury, accounting for 3.75% of the total cases in Jiangsu Province[12]. Xie *et al*[20] analyzed liver function among non-intensive care unit patients and demonstrated that liver dysfunction is more likely to occur in males than in females[20]. In pediatric cases, liver injury was found in 22% of children and occurred mostly between 2 and 18 d of hospitalization[31].

Among the hospitalized confirmed patients in Wuhan, liver injury rates were increased in intensive care unit patients and nonsurvivors, indicating that liver injury is most likely to occur in critically ill cases[5,11,15]. In a study of critical patients, 52 patients who required mechanical ventilation or with a at least 60% fraction of inspired oxygen were included. Twenty-nine percent of the critical patients presented with liver injury, 15% with acute kidney injury, and 15% with cardiac injury[14]. In a multicenter study including 1099 patients and 552 hospitals, liver function abnormalities were more common in critically ill subjects, and jaundice was less common in patients with COVID-19. Elevation of total bilirubin was observed in 10% of patients, whereas the percentage was higher in severe cases than in controls (20.5% *vs* 9.8%)[4]. A multicenter retrospective cohort study including 5771 patients in Hubei Province suggested that liver injury indicators, particularly AST, are strongly associated with mortality risk in COVID-19[23].

In current reports, liver injury was not the first occurrence in COVID-19, while secondary liver injury is more common, and liver failure directly caused by COVID-19 has not been reported. Based on published data, secondary liver injury is most common in critically ill patients who have diabetes and hypertension[9,11,15]. Patients with mild conditions rarely have secondary liver injury, even if basic liver diseases

Table 2 Characteristics of liver injury in coronavirus disease 2019

Ref.	City	Sample size (*n*)	Disease severity	Preexisting liver diseases (%)	AST (U/L)	ALT (U/L)	LDH (U/L)	Percentage with abnormal liver function
Guan *et al*[4]	Multicenter, China	1099	Nonsevere (84.3%); severe (15.7%)	2.1	NA	NA	NA	AST (22.2%); ALT (21.3%); total bilirubin (10.5%); LDH (41.0%)
Zhou *et al*[5]	Wuhan, China	191	General (38%); severe (35%); critical (28%)	NA	NA	30 (17-46)	300 (234-407)	ALT (31%); LDH (67%); ALT and LDH significantly increased in nonsurvivors
Chen *et al*[9]	Wuhan, China	99	NA	NA	34 (26-48)	39 (22-53)	336 (260-447)	AST (28%); ALT (35%); total bilirubin (18%); LDH (76%)
Shi *et al*[10]	Wuhan, China	81	NA	9	40.8 ± 17.9	46.2 ± 29.5	NA	AST (53%)
Huang *et al*[11]	Wuhan, China	41	Nonsevere (68.3%); severe (31.7%)	2	34 (26-48)	32 (21-50)	286 (242-408)	AST (37%); LDH (73%); ALT, AST, and LDH levels in ICU patients significantly higher than those in non-ICU patients
Wu *et al*[12]	Jiangsu, China	80	Mild (35.0%); moderate (61.25%); severe (3.75%); critical (0%)	1.25	30 (19-39)	24 (12-38)	226 (182-308)	ALT or AST (3.75%); LDH (21.25%)
Xu *et al*[13]	Zhejiang, China	62	NA	11	26 (20-32)	22 (14-34)	205 (184-260.5)	AST (16.1%); LDH (27%)
Yang *et al*[14]	Wuhan, China	52	Critical (100%)	NA	NA	NA	NA	Liver dysfunction (29%)
Wang *et al*[15]	Wuhan, China	138	Nonsevere (73.9%); severe (26.1%)	2.9	31 (24-51)	24 (16-40)	261 (182-403)	ALT, AST, total bilirubin, LDH levels in ICU patients significantly higher than those in non-ICU patients
Liu *et al*[17]	Multicenter, China	32	Nonsevere (87.5%); severe (12.5%)	3.13	25 (19-32)	27 (17-46)	NA	AST (6.2%); ALT (28.1%)
Pan *et al*[18]	Wuhan, China	21	Nonsevere (100%)	NA	32 (15-95)	42 (12-107)	242 (156-377)	NA
Zhang *et al*[19]	Wuhan, China	115	Nonsevere (73.0%); severe (27.0%)	NA	28.30 ± 15.66	25.71 ± 21.08	222.77 ± 159.07	ALT (9.6%); AST (14.8%); ALP (5.2%); GGT (13.0%); TB (6.1%); LDH (22.6%)
Xie *et al*[20]	Wuhan, China	79	Moderate (64.6%); severe (35.4%)	NA	34.5 (25.3-55.3)	36.5 (17.5-71.5)	NA	ALT (31.6%); AST (35.4%); TB (5.1%)
Wu *etal* [21]	Wuhan, China	201	NA	3.5	33 (26-45)	31 (19.75-47.00)	307.5 (232.25-389.25)	NA
Chen *et al*[22]	Wuhan, China	274	Recovered (58.8%); died (41.2%)	4	23 (15-38)	30 (22-46)	321.5 (249.8-510.5)	ALT (22%); AST (31%); LDH (42%)
Lei *et al*[23]	Wuhan, China	5771	Nonsevere (79.4%); severe (20.6%)	1.4	24 (17-35)	24 (15.1-39)	NA	NA

COVID-19: Coronavirus disease 2019; AST: Aspartate aminotransferase; ALT: Alanine aminotransferase; LDH: Lactate dehydrogenase; ICU: Intensive care unit.

coexist. The liver injury in COVID-19 is hepatocellular rather than cholestatic, manifesting mainly as elevations of ALT, AST, and LDH levels. And the hepatocellar injury marker such as AST was associated with mortality risk in COVID-19[23]. The laboratory markers of bile duct injury, such as ALP and GGT levels, did not increase significantly, and jaundice is uncommon in patients with COVID-19. The markers of bile duct injury seems not to be related to the severity of the disease[20]. Notably, COVID-19 may cause damage to multiple organs, including the myocardium, skeletal muscles, and kidney. Skeletal muscle and myocardial injury could also result in the elevation of serum transaminase and LDH levels, as shown in Table 2. Compared to ALT, LDH is more likely to be increased.

ETIOLOGY OF LIVER INJURY IN COVID-19

Viral immunologic injury

Liver impairment in patients with COVID-19 might be directly caused by viral infection (Figure 1). A previous study demonstrated the liver pathology of patients with SARS and showed SARS-associated coronavirus in liver tissues, suggesting that hepatic impairment might be due to viral infection of the liver[29]. Based on recent studies, clinical features such as nausea, vomiting, and diarrhea can be present in COVID-19[4,32], and fecal specimen and blood nucleic acid detection also have shown positive results in COVID-19 patients, suggesting that there might be enteric involvement of the virus[16,25,28].

Angiotensin-converting enzyme 2 (ACE2) is the host cell receptor for SARS-CoV and has recently been demonstrated to mediate SARS-CoV-2 infection[33-35]. Zhou *et al*[1] used HeLa cells that expressed ACE2 and confirmed that ACE2 is the cell receptor through which SARS-CoV-2 enters cells[1]. Liang *et al*[32] examined the expression profiles of ACE2 in various human tissues and found that ACE2 was highly expressed in the small intestine, indicating that the virus may infect through fecal-oral transmission and cause gastrointestinal symptoms[32]. Recently, it was found that cholangiocytes could specifically express ACE2, while ACE2 expression is low in hepatocytes, at 20-fold less than the expression level in cholangiocytes. The expression pattern of ACE2 reveals that SARS-CoV-2 may directly infect cholangiocytes and cause bile duct dysfunction. Cholangiocytes are multifunctional and play critical roles in liver regeneration and immune responses, indicating that viral immunologic injury might play a role in liver injury in COVID-19. However, clinical data have shown that there are increased AST, ALT, and LDH levels in COVID-19, while ALP and GGT levels, which represent bile duct injury, did not increase significantly in patients with COVID-19. Furthermore, autopsy of a patient with COVID-19 showed that viral inclusions were not observed in the liver tissue[36]. Given the multiorgan complications such as cardiopulmonary insufficiency, renal impairment, systemic inflammation status and the use of multiple drugs, direct liver damage from the virus is not considered to be the key factor.

Drug-induced liver injury

The clinical picture of drug-induced liver injury ranges from pure hepatocellular to cholestatic variants. The liver function abnormalities in COVID-19 are characterized mainly as hepatocellular injury. The initial presentation of COVID-19 is manifested mainly by fever, cough, fatigue, and dyspnea. Thus, some patients have a history of using antipyretic drugs, and most of these drugs contain acetaminophen. These agents are recognized as common drugs that cause direct hepatocyte toxicity. In addition, some citizens may use multiple patent Chinese medicines to prevent infection, which may also induce liver injury. Recent liver pathological findings from COVID-19 cases showed moderate microvascular steatosis and mild lobular inflammation, suggesting that there might be drug-induced liver injury[36]. Although there are currently no recognized effective antiviral drugs for COVID-19, antiviral therapies such as oseltamivir, arbidol, lopinavir, and ritonavir are prescribed in nearly half of critical patients[14]. These antiviral drugs might lead to abnormal liver function. In addition, hemolysis caused by ribavirin could induce or exacerbate tissue hypoxia, which may also induce increased serum liver enzyme levels. Patients with chronic liver disease, such as those with hepatitis B or hepatitis C, which may have preexisting elevated transaminase levels before treatment, could pose an increased risk of drug-induced liver injury. Thus, for patients comorbid with basic liver disease, when antipyretic drugs, traditional herbal medicine, or antiviral medicine is clinically used, physicians must take into account the risk of liver damage, and such patients should be closely monitored to take timely measures to prevent drug-induced liver damage.

Systemic inflammatory response

It has been reported that some of the patients with COVID-19 had mild early onset, but they might progress rapidly into later stages with multiple organ failure. This progression is considered to be related to the sudden initiation of an inflammatory storm, *i.e.*, systemic inflammatory response syndrome, driven by viral infection. Cytokine storm syndromes can induce the exuberant release of multiple pro-inflammatory cytokines and inflammatory markers, such as tumor necrosis factor, interleukin-2 (IL-2), IL-6, IL-7, IL-18, granulocyte-colony stimulating factor, interferon-γ, and ferritin[11]. Fulminant and fatal hypercytokinemia could initiate a chain of events that lead to tissue injury and multiorgan injuries or failure, including in the liver[37].

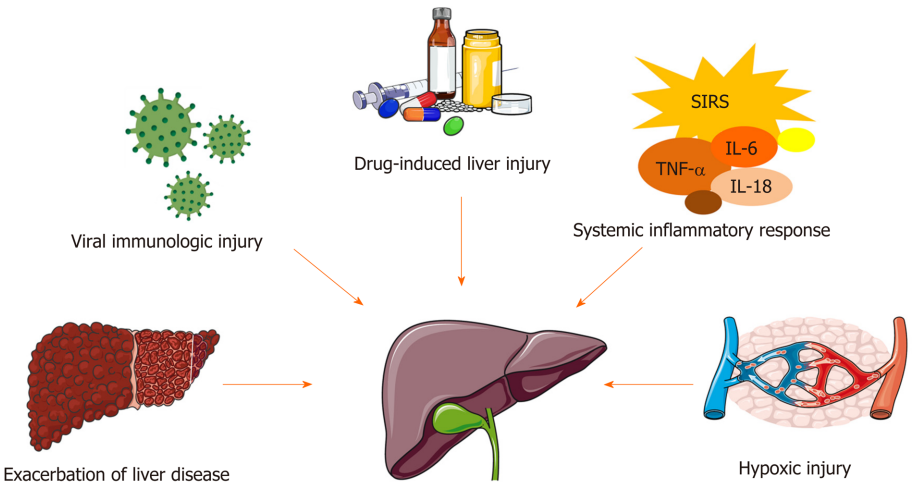

Figure 1 Etiology of liver injury in coronavirus disease 2019 patients. SIRS: Systemic inflammatory response syndrome; TNF-α: Tumor necrosis factor-alpha; IL-6: Interleukin-6; IL-18: Interleukin-18.

The inflammatory response could cause hepatomegaly and elevated serum transaminase levels, as well as jaundice and hepatic encephalopathy.

Hypoxic injury

The complex vascular supply and high metabolic activity of the liver make it particularly vulnerable to circulatory disturbances. Hypoxic hepatitis, also called ischemic hepatitis, is frequently encountered in critically ill patients and represents a complication of underlying cardiac, circulatory, or respiratory failure, causing passive congestion or diminished perfusion of the liver[38,39]. Under situations of systemic stress, there is a compensatory decrease in peripheral and splanchnic blood flow, resulting in a decrease in hepatic blood flow and thereby leading to hepatocellular hypoxia, especially in zone 3[40]. Reperfusion injury is mediated by the generation of reactive oxygen species when ischemic hepatocytes are reexposed to oxygen, leading to cell injury *via* lipid peroxidation[41]. In addition, Kupffer cells could produce cytokines in response to ischemia and trigger the recruitment and activation of polymorphonuclear leukocytes[41]. This phenomenon usually rapidly progresses with severe elevation of transaminase levels (20 Upper Limit Of Normal), accompanied by LDH level elevation, which can recover as hypoxia is corrected[38]. Hospitalized patients present with different degrees of hypoxemia, and these patients need oxygenation support, which is administered to patients according to the severity of hypoxemia, such as nasal cannula (66%), noninvasive ventilation (24%), invasive mechanical ventilation (5%) and extracorporeal membrane oxygenation (5%)[11]. Approximately 1.1%-20% of patients are comorbid with septic shock, and 23% of patients have heart failure in COVID-19[5,9,15]. Therefore, hypoxemia and reperfusion or passive congestion followed by heart failure may be causes of liver damage in patients with COVID-19.

Exacerbation of preexisting liver disease

According to the current reports, 1.25%-11% of patients with COVID-19 had preexisting liver diseases (Table 2). In a large cohort of 1099 patients from 552 hospitals, 261 (23.7%) were reported to have at least one comorbidity, and 23 (2.1%) were comorbid with hepatitis B, which is more common in severe cases, indicating that the comorbidity of hepatitis B is associated with poorer clinical outcome in patients[4]. Lymphocytopenia is common and has been associated with increased disease severity in COVID-19[14,42], which might affect the immunotolerant status of hepatitis B virus and might cause reactivation of hepatitis B. For patients under antiviral therapy, discontinuation of drugs during the course of COVID-19 or the administration of glucocorticoids may also induce the activation of hepatitis B and induce hepatic injuries. For patients with cirrhosis, the systemic inflammation, hypoxia, and circulatory disturbances driven by COVID-19 could induce secondary infection or hepatic decompensation, leading to the exacerbation of preexisting liver disease. Qiu *et al*[43] had reported acute-on-chronic liver failure secondary to the SARS-CoV-2 infection in a patient with alcoholic cirrhosis[43]. Nonalcoholic fatty liver disease

(NAFLD) is the common cause of liver function abnormalities in the general population; thus, it could also be the cause of liver injuries in COVID-19. Metabolic factors such as obesity and diabetes are highly prevalent in critical cases and associated with mortality in COVID-19[5,9]. Ji *et al*[44] reported that 37.6% of patients with COVID-19 were comorbid with NAFLD, and patients with NAFLD had an increased risk of severe COVID-19 and prolonged viral shedding time[44]. However, the combination of other liver diseases, such as autoimmune liver diseases, in COVID-19 requires further exploration.

PREVENTION AND MANAGEMENT

Prevention of liver injury in COVID-19

For all patients with COVID-19, liver biochemical indicators, such as ALT/AST, bilirubin, albumin, and prothrombin time, should be monitored to detect liver damage. If serum AST and LDH levels were elevated while the ALT level was normal, skeletal muscle or myocardial damage rather than liver injury should be considered. Given that chronic liver disease is also a major burden among elderly patients with COVID-19, clinicians need to pay attention to the management of preexisting liver disease. In the management of chronic hepatitis B, discontinuation of antiviral medicine should be avoided to prevent reactivation of hepatitis B, and anti-HBV agents should be considered when patients are under glucocorticoid treatment. For patients with autoimmune liver disease who are treated with glucocorticoids or immunosuppressants, infection should be closely monitored during the treatment of COVID-19. For patients with cirrhosis, their immunocompromised status requires intensive monitoring for the incidence of complications and secondary infections. In COVID-19, the novel coronavirus induces a cytokine storm and produces a series of immune responses. Some patients can quickly progress to acute respiratory distress syndrome and septic shock and eventually multiorgan failure or death. Therefore, timely treatment of critical cases is of great importance in the prevention of secondary liver injuries. In addition, antiviral drugs, glucocorticoids, nonsteroidal anti-inflammatory drugs (NSAIDs), and traditional Chinese herbs might be administered in the clinical management of COVID-19. It is suggested that the treatment should be streamlined and the use of redundant types, doses, and durations of medicine should be avoided to reduce the chance of drug-induced liver injury.

Management of liver injury in COVID-19

In COVID-19, current therapy is mainly supportive treatment, such as intensive care, correcting hypoxemia through oxygenation support or mechanical ventilation, continuous renal replacement therapy for cytokine storm syndrome, and maintaining effective blood volume, which are essential for the prevention and treatment of multiple organ failure, including liver damage[45]. Intravenous glucocorticoids were commonly used in patients with SARS and Middle East respiratory syndrome, but their efficacy remains controversial. Clinical evidence does not support glucocorticoids in the treatment for COVID-19 unless there are other indications (*e.g.*, exacerbation of chronic obstructive pulmonary disease)[46]. Although some clinicians have suggested that the use of NSAIDs in the early course may have a negative impact on the outcome of COVID-19[47,48], the World Health Organization does not recommend that NSAIDs be avoided when clinically indicated. Although a number of investigation agents are being explored for antiviral treatment, such as remdesivir, chloroquine/hydroxychloroquine, tocilizumab, and lopinavir-ritonavir[49-51], their use for COVID-19 remains investigational. Therefore, etiological treatment of SARS-CoV-2 infection is difficult to achieve at this time.

Liver injuries in COVID-19 cases are often transient and reversible without special treatment, and liver failure is rarely reported. However, on occasion of severe or acute liver damage, careful evaluation to identify any underlying diseases is needed, and the degree of liver damage should be evaluated to predict the onset of liver failure. Initial screening includes a careful history of preexisting liver disease, exposure to hepatotoxins (alcohol, drugs, herbs, and chemicals), hypoxia, and circulation status. Circulation and respiratory support should be strengthened for those with hypoxic hepatitis. Continuous renal replacement therapy could be considered for cytokine storm syndrome. For those suspected of drug-induced liver injury, prompt discontinuation or reduction of doses of suspected drugs should be considered. Antiinflammatory liver-protecting drugs can be used in hepatocellular injury, and administration of L-ornithine-L-aspartate could be used in the management of

hyperammonemia with hepatic encephalopathy. However, these medications are only an adjuvant treatment and should not be overemphasized. In addition, prebiotics and probiotics could be considered to ensure intestinal microecological balance and prevent bacterial infections.

CONCLUSION

In summary, digestive system symptoms and liver function abnormities are common in patients with COVID-19, especially in critical cases. Liver injuries are often transient and mild and present mostly with hepatocellular injury rather than cholestatic injury. Although there might be a link with virus-directed liver injuries, the mechanism of SARS-CoV-2-related liver injury requires further investigation. Drug-induced liver injury and secondary liver injury induced by systemic inflammatory response syndrome or hypoxia might be major etiologic factors for liver injury in COVID-19. Health workers need to pay attention to the management of preexisting liver disease and monitor the liver function of patients with COVID-19. Timely treatment of critical cases is of great importance in the prevention of secondary liver injuries. Attempts should be made to streamline treatment and prevent the use of redundant types, doses, and durations of medicines to reduce the chance of drug-induced liver injury. When treating the underlying disease, control of inflammatory storms, correction of tissue hypoxia, and maintenance of effective blood volume are important in the prevention and treatment of liver injury. The utilization of antiinflammatory liver-protecting drugs could be considered in the management of liver injury in COVID-19.

REFERENCES

1 **Zhou P**, Yang XL, Wang XG, Hu B, Zhang L, Zhang W, Si HR, Zhu Y, Li B, Huang CL, Chen HD, Chen J, Luo Y, Guo H, Jiang RD, Liu MQ, Chen Y, Shen XR, Wang X, Zheng XS, Zhao K, Chen QJ, Deng F, Liu LL, Yan B, Zhan FX, Wang YY, Xiao GF, Shi ZL. A pneumonia outbreak associated with a new coronavirus of probable bat origin. *Nature* 2020; **579**: 270-273 [PMID: 32015507 DOI: 10.1038/s41586-020-2012-7]

2 **Wu Z**, McGoogan JM. Characteristics of and Important Lessons from the Coronavirus Disease 2019 (COVID-19) Outbreak in China: Summary of a Report of 72â€¯314 Cases from the Chinese Center for Disease Control and Prevention. *JAMA* 2020; **323**: 1239-1242 [PMID: 32091533 DOI: 10.1001/jama.2020.2648]

3 **WHO**. Report of the WHO-China Joint Mission on Coronavirus Disease 2019 (COVID-2019). February 16-24, 2020

4 **Guan WJ**, Ni ZY, Hu Y, Liang WH, Ou CQ, He JX, Liu L, Shan H, Lei CL, Hui DSC, Du B, Li LJ, Zeng G, Yuen KY, Chen RC, Tang CL, Wang T, Chen PY, Xiang J, Li SY, Wang JL, Liang ZJ, Peng YX, Wei L, Liu Y, Hu YH, Peng P, Wang JM, Liu JY, Chen Z, Li G, Zheng ZJ, Qiu SQ, Luo J, Ye CJ, Zhu SY, Zhong NS; China Medical Treatment Expert Group for Covid-19. Clinical Characteristics of Coronavirus Disease 2019 in China. *N Engl J Med* 2020; **382**: 1708-1720 [PMID: 32109013 DOI: 10.1056/NEJMoa2002032]

5 **Zhou F**, Yu T, Du R, Fan G, Liu Y, Liu Z, Xiang J, Wang Y, Song B, Gu X, Guan L, Wei Y, Li H, Wu X, Xu J, Tu S, Zhang Y, Chen H, Cao B. Clinical course and risk factors for mortality of adult inpatients with COVID-19 in Wuhan, China: a retrospective cohort study. *Lancet* 2020; **395**: 1054-1062 [PMID: 32171076 DOI: 10.1016/s0140-6736(20)30566-3]

6 **Mao R**, Liang J, Shen J, Ghosh S, Zhu LR, Yang H, Wu KC, Chen MH; Chinese Society of IBD, Chinese Elite IBD Union; Chinese IBD Quality Care Evaluation Center Committee. Implications of COVID-19 for patients with pre-existing digestive diseases. *Lancet Gastroenterol Hepatol* 2020; **5**: 425-427 [PMID: 32171057 DOI: 10.1016/S2468-1253(20)30076-5]

7 **Jin X**, Lian JS, Hu JH, Gao J, Zheng L, Zhang YM, Hao SR, Jia HY, Cai H, Zhang XL, Yu GD, Xu KJ, Wang XY, Gu JQ, Zhang SY, Ye CY, Jin CL, Lu YF, Yu X, Yu XP, Huang JR, Xu KL, Ni Q, Yu CB, Zhu B, Li YT, Liu J, Zhao H, Zhang X, Yu L, Guo YZ, Su JW, Tao JJ, Lang GJ, Wu XX, Wu WR, Qv TT, Xiang DR, Yi P, Shi D, Chen Y, Ren Y, Qiu YQ, Li LJ, Sheng J, Yang Y. Epidemiological, clinical and virological characteristics of 74 cases of coronavirus-infected disease 2019 (COVID-19) with gastrointestinal symptoms. *Gut* 2020; **69**: 1002-1009 [PMID: 32213556 DOI: 10.1136/gutjnl-2020-320926]

8 **Hu LL**, Wang WJ, Zhu QJ, Yang L. [Novel coronavirus pneumonia-related liver injury: etiological analysis and treatment strategy]. *Zhonghua Gan Zang Bing Za Zhi* 2020; **28**: 97-99 [PMID: 32075364 DOI: 10.3760/cma.j.issn.1007-3418.2020.02.001]

9 **Chen N**, Zhou M, Dong X, Qu J, Gong F, Han Y, Qiu Y, Wang J, Liu Y, Wei Y, Xia J, Yu T, Zhang X, Zhang L. Epidemiological and clinical characteristics of 99 cases of 2019 novel coronavirus pneumonia in Wuhan, China: a descriptive study. *Lancet* 2020; **395**: 507-513 [PMID: 32007143 DOI: 10.1016/S0140-6736(20)30211-7]

10 **Shi H**, Han X, Jiang N, Cao Y, Alwalid O, Gu J, Fan Y, Zheng C. Radiological findings from 81 patients with COVID-19 pneumonia in Wuhan, China: a descriptive study. *Lancet Infect Dis* 2020; **20**: 425-434 [PMID: 32105637 DOI: 10.1016/s1473-3099(20)30086-4]

11 **Huang C**, Wang Y, Li X, Ren L, Zhao J, Hu Y, Zhang L, Fan G, Xu J, Gu X, Cheng Z, Yu T, Xia J, Wei Y, Wu W, Xie X, Yin W, Li H, Liu M, Xiao Y, Gao H, Guo L, Xie J, Wang G, Jiang R, Gao Z, Jin Q, Wang J, Cao B. Clinical features of patients infected with 2019 novel coronavirus in Wuhan, China. *Lancet* 2020;

395: 497-506 [PMID: 31986264 DOI: 10.1016/S0140-6736(20)30183-5]
12 **Wu J**, Liu J, Zhao X, Liu C, Wang W, Wang D, Xu W, Zhang C, Yu J, Jiang B, Cao H, Li L. Clinical Characteristics of Imported Cases of Coronavirus Disease 2019 (COVID-19) in Jiangsu Province: A Multicenter Descriptive Study. *Clin Infect Dis* 2020; **71**: 706-712 [PMID: 32109279 DOI: 10.1093/cid/ciaa199]
13 **Xu XW**, Wu XX, Jiang XG, Xu KJ, Ying LJ, Ma CL, Li SB, Wang HY, Zhang S, Gao HN, Sheng JF, Cai HL, Qiu YQ, Li LJ. Clinical findings in a group of patients infected with the 2019 novel coronavirus (SARS-Cov-2) outside of Wuhan, China: retrospective case series. *BMJ* 2020; **368**: m606 [PMID: 32075786 DOI: 10.1136/bmj.m606]
14 **Yang X**, Yu Y, Xu J, Shu H, Xia J, Liu H, Wu Y, Zhang L, Yu Z, Fang M, Yu T, Wang Y, Pan S, Zou X, Yuan S, Shang Y. Clinical course and outcomes of critically ill patients with SARS-CoV-2 pneumonia in Wuhan, China: a single-centered, retrospective, observational study. *Lancet Respir Med* 2020; **8**: 475-481 [PMID: 32105632 DOI: 10.1016/s2213-2600(20)30079-5]
15 **Wang D**, Hu B, Hu C, Zhu F, Liu X, Zhang J, Wang B, Xiang H, Cheng Z, Xiong Y, Zhao Y, Li Y, Wang X, Peng Z. Clinical Characteristics of 138 Hospitalized Patients With 2019 Novel Coronavirus-Infected Pneumonia in Wuhan, China. *JAMA* 2020 [PMID: 32031570 DOI: 10.1001/jama.2020.1585]
16 **Holshue ML**, DeBolt C, Lindquist S, Lofy KH, Wiesman J, Bruce H, Spitters C, Ericson K, Wilkerson S, Tural A, Diaz G, Cohn A, Fox L, Patel A, Gerber SI, Kim L, Tong S, Lu X, Lindstrom S, Pallansch MA, Weldon WC, Biggs HM, Uyeki TM, Pillai SK; Washington State 2019-nCoV Case Investigation Team. First Case of 2019 Novel Coronavirus in the United States. *N Engl J Med* 2020; **382**: 929-936 [PMID: 32004427 DOI: 10.1056/NEJMoa2001191]
17 **Liu C**, Jiang ZC, Shao CX, Zhang HG, Yue HM, Chen ZH, Ma BY, Liu WY, Huang HH, Yang J, Wang Y, Liu HY, Xu D, Wang JT, Yang JY, Pan HQ, Zou SQ, Li FJ, Lei JQ, Li X, He Q, Gu Y, Qi XL. [Preliminary study of the relationship between novel coronavirus pneumonia and liver function damage: a multicenter study]. *Zhonghua Gan Zang Bing Za Zhi* 2020; **28**: 107-111 [PMID: 32077660 DOI: 10.3760/cma.j.issn.1007-3418.2020.02.003]
18 **Pan F**, Ye T, Sun P, Gui S, Liang B, Li L, Zheng D, Wang J, Hesketh RL, Yang L, Zheng C. Time Course of Lung Changes at Chest CT during Recovery from Coronavirus Disease 2019 (COVID-19). *Radiology* 2020; **295**: 715-721 [PMID: 32053470 DOI: 10.1148/radiol.2020200370]
19 **Zhang Y**, Zheng L, Liu L, Zhao M, Xiao J, Zhao Q. Liver impairment in COVID-19 patients: A retrospective analysis of 115 cases from a single centre in Wuhan city, China. *Liver Int* 2020 [PMID: 32239796 DOI: 10.1111/liv.14455]
20 **Xie H**, Zhao J, Lian N, Lin S, Xie Q, Zhuo H. Clinical characteristics of non-ICU hospitalized patients with coronavirus disease 2019 and liver injury: A retrospective study. *Liver Int* 2020; **40**: 1321-1326 [PMID: 32239591 DOI: 10.1111/liv.14449]
21 **Wu C**, Chen X, Cai Y, Xia J, Zhou X, Xu S, Huang H, Zhang L, Zhou X, Du C, Zhang Y, Song J, Wang S, Chao Y, Yang Z, Xu J, Zhou X, Chen D, Xiong W, Xu L, Zhou F, Jiang J, Bai C, Zheng J, Song Y. Risk Factors Associated With Acute Respiratory Distress Syndrome and Death in Patients With Coronavirus Disease 2019 Pneumonia in Wuhan, China. *JAMA Intern Med* 2020 [PMID: 32167524 DOI: 10.1001/jamainternmed.2020.0994]
22 **Chen T**, Wu D, Chen H, Yan W, Yang D, Chen G, Ma K, Xu D, Yu H, Wang H, Wang T, Guo W, Chen J, Ding C, Zhang X, Huang J, Han M, Li S, Luo X, Zhao J, Ning Q. Clinical characteristics of 113 deceased patients with coronavirus disease 2019: retrospective study. *BMJ* 2020; **368**: m1091 [PMID: 32217556 DOI: 10.1136/bmj.m1091]
23 **Lei F**, Liu YM, Zhou F, Qin JJ, Zhang P, Zhu L, Zhang XJ, Cai J, Lin L, Ouyang S, Wang X, Yang C, Cheng X, Liu W, Li H, Xie J, Wu B, Luo H, Xiao F, Chen J, Tao L, Cheng G, She ZG, Zhou J, Wang H, Lin J, Luo P, Fu S, Zhou J, Ye P, Xiao B, Mao W, Liu L, Yan Y, Liu L, Chen G, Li H, Huang X, Zhang BH, Yuan Y. Longitudinal association between markers of liver injury and mortality in COVID-19 in China. *Hepatology* 2020 [PMID: 32359177 DOI: 10.1002/hep.31301]
24 **Li J**, Fan JG. Characteristics and Mechanism of Liver Injury in 2019 Coronavirus Disease. *J Clin Transl Hepatol* 2020; **8**: 13-17 [PMID: 32274341 DOI: 10.14218/JCTH.2020.00019]
25 **Zhang J**, Wang S, Xue Y. Fecal specimen diagnosis 2019 novel coronavirus-infected pneumonia. *J Med Virol* 2020; **92**: 680-682 [PMID: 32124995 DOI: 10.1002/jmv.25742]
26 **Zheng S**, Fan J, Yu F, Feng B, Lou B, Zou Q, Xie G, Lin S, Wang R, Yang X, Chen W, Wang Q, Zhang D, Liu Y, Gong R, Ma Z, Lu S, Xiao Y, Gu Y, Zhang J, Yao H, Xu K, Lu X, Wei G, Zhou J, Fang Q, Cai H, Qiu Y, Sheng J, Chen Y, Liang T. Viral load dynamics and disease severity in patients infected with SARS-CoV-2 in Zhejiang province, China, January-March 2020: retrospective cohort study. *BMJ* 2020; **369**: m1443 [PMID: 32317267 DOI: 10.1136/bmj.m1443]
27 **Cheung KS**, Hung IFN, Chan PPY, Lung KC, Tso E, Liu R, Ng YY, Chu MY, Chung TWH, Tam AR, Yip CCY, Leung KH, Fung AY, Zhang RR, Lin Y, Cheng HM, Zhang AJX, To KKW, Chan KH, Yuen KY, Leung WK. Gastrointestinal Manifestations of SARS-CoV-2 Infection and Virus Load in Fecal Samples From a Hong Kong Cohort: Systematic Review and Meta-analysis. *Gastroenterology* 2020; **159**: 81-95 [PMID: 32251668 DOI: 10.1053/j.gastro.2020.03.065]
28 **Yeo C**, Kaushal S, Yeo D. Enteric involvement of coronaviruses: is faecal-oral transmission of SARS-CoV-2 possible? *Lancet Gastroenterol Hepatol* 2020; **5**: 335-337 [PMID: 32087098 DOI: 10.1016/S2468-1253(20)30048-0]
29 **Chau TN**, Lee KC, Yao H, Tsang TY, Chow TC, Yeung YC, Choi KW, Tso YK, Lau T, Lai ST, Lai CL. SARS-associated viral hepatitis caused by a novel coronavirus: report of three cases. *Hepatology* 2004; **39**: 302-310 [PMID: 14767982 DOI: 10.1002/hep.20111]
30 **Lee JY**, Kim YJ, Chung EH, Kim DW, Jeong I, Kim Y, Yun MR, Kim SS, Kim G, Joh JS. The clinical and virological features of the first imported case causing MERS-CoV outbreak in South Korea, 2015. *BMC Infect Dis* 2017; **17**: 498 [PMID: 28709419 DOI: 10.1186/s12879-017-2576-5]
31 **Wang D**, Ju XL, Xie F, Lu Y, Li FY, Huang HH, Fang XL, Li YJ, Wang JY, Yi B, Yue JX, Wang J, Wang LX, Li B, Wang Y, Qiu BP, Zhou ZY, Li KL, Sun JH, Liu XG, Li GD, Wang YJ, Cao AH, Chen YN. [Clinical analysis of 31 cases of 2019 novel coronavirus infection in children from six provinces

(autonomous region) of northern China]. *Zhonghua Er Ke Za Zhi* 2020; **58**: 269-274 [PMID: 32118389 DOI: 10.3760/cma.j.cn112140-20200225-00138]
32 **Liang W**, Feng Z, Rao S, Xiao C, Xue X, Lin Z, Zhang Q, Qi W. Diarrhoea may be underestimated: a missing link in 2019 novel coronavirus. *Gut* 2020; **69**: 1141-1143 [PMID: 32102928 DOI: 10.1136/gutjnl-2020-320832]
33 **Kuhn JH**, Li W, Choe H, Farzan M. Angiotensin-converting enzyme 2: a functional receptor for SARS coronavirus. *Cell Mol Life Sci* 2004; **61**: 2738-2743 [PMID: 15549175 DOI: 10.1007/s00018-004-4242-5]
34 **Hamming I**, Timens W, Bulthuis ML, Lely AT, Navis G, van Goor H. Tissue distribution of ACE2 protein, the functional receptor for SARS coronavirus. A first step in understanding SARS pathogenesis. *J Pathol* 2004; **203**: 631-637 [PMID: 15141377 DOI: 10.1002/path.1570]
35 **Walls AC**, Park YJ, Tortorici MA, Wall A, McGuire AT, Veesler D. Structure, Function, and Antigenicity of the SARS-CoV-2 Spike Glycoprotein. *Cell* 2020; **181**: 281-292.e6 [PMID: 32155444 DOI: 10.1016/j.cell.2020.02.058]
36 **Xu Z**, Shi L, Wang Y, Zhang J, Huang L, Zhang C, Liu S, Zhao P, Liu H, Zhu L, Tai Y, Bai C, Gao T, Song J, Xia P, Dong J, Zhao J, Wang FS. Pathological findings of COVID-19 associated with acute respiratory distress syndrome. *Lancet Respir Med* 2020; **8**: 420-422 [PMID: 32085846 DOI: 10.1016/s2213-2600(20)30076-x]
37 **Mehta P**, McAuley DF, Brown M, Sanchez E, Tattersall RS, Manson JJ; HLH Across Speciality Collaboration, UK. COVID-19: consider cytokine storm syndromes and immunosuppression. *Lancet* 2020; **395**: 1033-1034 [PMID: 32192578 DOI: 10.1016/s0140-6736(20)30628-0]
38 **Waseem N**, Chen PH. Hypoxic Hepatitis: A Review and Clinical Update. *J Clin Transl Hepatol* 2016; **4**: 263-268 [PMID: 27777895 DOI: 10.14218/jcth.2016.00022]
39 **Lightsey JM**, Rockey DC. Current concepts in ischemic hepatitis. *Curr Opin Gastroenterol* 2017; **33**: 158-163 [PMID: 28346236 DOI: 10.1097/mog.0000000000000355]
40 **Dunn GD**, Hayes P, Breen KJ, Schenker S. The liver in congestive heart failure: a review. *Am J Med Sci* 1973; **265**: 174-189 [PMID: 4573728 DOI: 10.1097/00000441-197303000-00001]
41 **Rosser BG**, Gores GJ. Liver cell necrosis: cellular mechanisms and clinical implications. *Gastroenterology* 1995; **108**: 252-275 [PMID: 7806049 DOI: 10.1016/0016-5085(95)90032-2]
42 **Henry BM**. COVID-19, ECMO, and lymphopenia: a word of caution. *Lancet Respir Med* 2020; **8**: e24 [PMID: 32178774 DOI: 10.1016/s2213-2600(20)30119-3]
43 **Qiu H**, Wander P, Bernstein D, Satapathy SK. Acute on chronic liver failure from novel severe acute respiratory syndrome coronavirus 2 (SARS-CoV-2). *Liver Int* 2020; **40**: 1590-1593 [PMID: 32369658 DOI: 10.1111/liv.14506]
44 **Ji D**, Qin E, Xu J, Zhang D, Cheng G, Wang Y, Lau G. Non-alcoholic fatty liver diseases in patients with COVID-19: A retrospective study. *J Hepatol* 2020; **73**: 451-453 [PMID: 32278005 DOI: 10.1016/j.jhep.2020.03.044]
45 **Ronco C**, Navalesi P, Vincent JL. Coronavirus epidemic: preparing for extracorporeal organ support in intensive care. *Lancet Respir Med* 2020; **8**: 240-241 [PMID: 32035509 DOI: 10.1016/S2213-2600(20)30060-6]
46 **Russell CD**, Millar JE, Baillie JK. Clinical evidence does not support corticosteroid treatment for 2019-nCoV lung injury. *Lancet* 2020; **395**: 473-475 [PMID: 32043983 DOI: 10.1016/s0140-6736(20)30317-2]
47 **Day M**. Covid-19: European drugs agency to review safety of ibuprofen. *BMJ* 2020; **368**: m1168 [PMID: 32205306 DOI: 10.1136/bmj.m1168]
48 **Day M**. Covid-19: ibuprofen should not be used for managing symptoms, say doctors and scientists. *BMJ* 2020; **368**: m1086 [PMID: 32184201 DOI: 10.1136/bmj.m1086]
49 **Wang M**, Cao R, Zhang L, Yang X, Liu J, Xu M, Shi Z, Hu Z, Zhong W, Xiao G. Remdesivir and chloroquine effectively inhibit the recently emerged novel coronavirus (2019-nCoV) in vitro. *Cell Res* 2020; **30**: 269-271 [PMID: 32020029 DOI: 10.1038/s41422-020-0282-0]
50 **Yao X**, Ye F, Zhang M, Cui C, Huang B, Niu P, Liu X, Zhao L, Dong E, Song C, Zhan S, Lu R, Li H, Tan W, Liu D. In Vitro Antiviral Activity and Projection of Optimized Dosing Design of Hydroxychloroquine for the Treatment of Severe Acute Respiratory Syndrome Coronavirus 2 (SARS-CoV-2). *Clin Infect Dis* 2020; **71**: 732-739 [PMID: 32150618 DOI: 10.1093/cid/ciaa237]
51 **Cao B**, Wang Y, Wen D, Liu W, Wang J, Fan G, Ruan L, Song B, Cai Y, Wei M, Li X, Xia J, Chen N, Xiang J, Yu T, Bai T, Xie X, Zhang L, Li C, Yuan Y, Chen H, Li H, Huang H, Tu S, Gong F, Liu Y, Wei Y, Dong C, Zhou F, Gu X, Xu J, Liu Z, Zhang Y, Li H, Shang L, Wang K, Li K, Zhou X, Dong X, Qu Z, Lu S, Hu X, Ruan S, Luo S, Wu J, Peng L, Cheng F, Pan L, Zou J, Jia C, Wang J, Liu X, Wang S, Wu X, Ge Q, He J, Zhan H, Qiu F, Guo L, Huang C, Jaki T, Hayden FG, Horby PW, Zhang D, Wang C. A Trial of Lopinavir-Ritonavir in Adults Hospitalized with Severe Covid-19. *N Engl J Med* 2020; **382**: 1787-1799 [PMID: 32187464 DOI: 10.1056/NEJMoa2001282]

World Journal of Gastroenterology

Submit a Manuscript: https://www.f6publishing.com

World J Gastroenterol 2020 August 28; 26(32): 4763-4785

DOI: 10.3748/wjg.v26.i32.4763

ISSN 1007-9327 (print) ISSN 2219-2840 (online)

ORIGINAL ARTICLE

Basic Study

Immune and microRNA responses to *Helicobacter muridarum* infection and indole-3-carbinol during colitis

Rasha Raheem Alkarkoushi, Yvonne Hui, Abbas S Tavakoli, Udai Singh, Prakash Nagarkatti, Mitzi Nagarkatti, Ioulia Chatzistamou, Marpe Bam, Traci L Testerman

ORCID number: Rasha Raheem Alkarkoushi 0000-0003-2816-7550; Yvonne Hui 0000-0001-8012-1838; Abbas S Tavakoli 0000-0003-2527-7017; Udai Singh 0000-0002-7048-4325; Prakash Nagarkatti 0000-0003-2663-0759; Mitzi Nagarkatti 0000-0002-5977-5615; Ioulia Chatzistamou 0000-0002-6632-8469; Marpe Bam 0000-0002-8321-8958; Traci L Testerman 0000-0002-3883-6407.

Author contributions: Alkarkoushi RR, Hui Y, Tavakoli AS, Testerman TL and Singh U assisted with conceptualization, performed experiments, analyzed data, and drafted the manuscript; Nagarkatti P and Nagarkatti M assisted with conceptualization and funding acquisition; Chatzistamou I performed histopathological analysis; Bam M analyzed microRNA data; Testerman TL conceptualized assisted with funding acquisition, and wrote and edited the manuscript.

Supported by the National Institutes of Health, No. P20GM103641.

Institutional review board statement: This study did not involve human subjects.

Institutional animal care and use committee statement: All

Rasha Raheem Alkarkoushi, Yvonne Hui, Prakash Nagarkatti, Mitzi Nagarkatti, Ioulia Chatzistamou, Marpe Bam, Traci L Testerman, Department of Pathology, Microbiology and Immunology, University of South Carolina School of Medicine, Columbia, SC 29209, United States

Abbas S Tavakoli, College of Nursing, University of South Carolina, University of South Carolina, Columbia, SC 29208, United States

Udai Singh, Department of Medicine, Hematology and Oncology, University of Virginia School of Medicine, Charlottesville, VA 22908, United States

Corresponding author: Traci L Testerman, PhD, Assistant Professor, Department of Pathology, Microbiology and Immunology, University of South Carolina School of Medicine, 6439 Garners Ferry Road, Columbia, SC 29209, United States. traci.testerman@uscmed.sc.edu

Abstract

BACKGROUND

Indole-3-carbinol (I3C) and other aryl hydrocarbon receptor agonists are known to modulate the immune system and ameliorate various inflammatory and autoimmune diseases in animal models, including colitis induced by dextran sulfate sodium (DSS). MicroRNAs (miRNAs) are also gaining traction as potential therapeutic agents or diagnostic elements. Enterohepatic *Helicobacter* (EHH) species are associated with an increased risk of inflammatory bowel disease, but little is known about how these species affect the immune system or response to treatment.

AIM

To determine whether infection with an EHH species alters the response to I3C and how the immune and miRNA responses of an EHH species compare with responses to DSS and inflammatory bowel disease.

METHODS

We infected C57BL/6 mice with *Helicobacter muridarum* (*H. muridarum*), with and without DSS and I3C treatment. Pathological responses were evaluated by histological examination, symptom scores, and cytokine responses. MiRNAs analysis was performed on mesenteric lymph nodes to further evaluate the regional immune response.

RESULTS

H. muridarum infection alone caused colonic inflammation and upregulated proinflammatory, macrophage-associated cytokines in the colon similar to changes seen in DSS-treated mice. Further upregulation occurred upon treatment with DSS. *H. muridarum* infection caused broad changes in mesenteric lymph node miRNA expression, but colitis-associated miRNAs were regulated similarly in *H. muridarum*-infected and uninfected, DSS-treated mice. In spite of causing colitis exacerbation, *H. muridarum* infection did not prevent disease amelioration by I3C. I3C normalized both macrophage- and T cell-associated cytokines.

CONCLUSION

Thus, I3C may be useful for inflammatory bowel disease patients regardless of EHH infection. The miRNA changes associated with I3C treatment are likely the result of, rather than the cause of immune response changes.

Key words: *Helicobacter muridarum*; MicroRNA; Immune; T regulatory cell; T helper 17 cell; Colitis; Cytokine

Core tip: The immune response to *Helicobacter muridarum* (*H. muridarum*), an enterohepatic *Helicobacter* species, mimics responses seen during chemically induced colitis and human inflammatory bowel disease (IBD) in terms of local and systemic cytokine responses and microRNA changes. Most microRNAs that are altered in IBD are also altered by *H. muridarum* infection with or without dextran sodium sulfate treatment. Furthermore, *H. muridarum* does not alter activity of an aryl hydrocarbon receptor agonist, indole-3-carbinol, a natural compound being explored as a treatment for IBD. Therefore, *H. muridarum* infection provides a viable model for predicting the effects of enterohepatic *Helicobacter* species on IBD.

Citation: Alkarkoushi RR, Hui Y, Tavakoli AS, Singh U, Nagarkatti P, Nagarkatti M, Chatzistamou I, Bam M, Testerman TL. Immune and microRNA responses to *Helicobacter muridarum* infection and indole-3-carbinol during colitis. *World J Gastroenterol* 2020; 26(32): 4763-4785

URL: https://www.wjgnet.com/1007-9327/full/v26/i32/4763.htm

DOI: https://dx.doi.org/10.3748/wjg.v26.i32.4763

INTRODUCTION

Ulcerative colitis (UC) is a chronic, idiopathic inflammatory bowel disease (IBD) characterized by inflammation of the colon. In the past decade, inflammatory bowel disease has emerged as a public health challenge and a global disease with increasing incidence in newly industrialized and industrialized countries worldwide, especially in North America, and Europe[1]. In 2015, 3.1 million adults in the United States were living with IBD[2], with direct and indirect costs estimated to be between $14.6 and $31.6 billion in 2014 alone[3]. The pathogenesis of IBD is complex and influenced by genetic susceptibility, dysregulation of the innate and adaptive immune systems, environmental factors, and intestinal dysbiosis; however, a crucial feature of UC is the imbalance between T regulatory (Treg) cells and T helper 17 (Th17) cells[4].

The best-known member of the *Helicobacter* genus is *Helicobacter pylori* (*H. pylori*), which colonizes the stomach, causing gastritis, gastric cancer, and a range of extragastric diseases[5]. Enterohepatic *Helicobacter* (EHH) species colonize the colon and sometimes the biliary tree. Some of these poorly studied organisms commonly cause persistent, asymptomatic infections, but occasionally cause intestinal diseases or even cancer in species ranging from rodents to primates[6-8]. Several studies suggest that EHH species are associated with IBD in humans[9-11]. The prevalence of EHH species in human populations is not clearly known, but one study found 9% infection in healthy control patients[11]. *Helicobacter muridarum* (*H. muridarum*) is an enterohepatic *Helicobacter* (EHH) species that was initially described as a member of the normal flora of conventional rodents[12]. Subsequent studies, however, showed that *H. muridarum*

experimental procedures were conducted in accordance with the guidelines for the use of experimental animals and were approved by the Institutional Review Committee on Animal Care and Use at the University of South Carolina.

Conflict-of-interest statement: The authors have nothing to disclose.

Data sharing statement: Raw data have been provided as supplemental material.

ARRIVE guidelines statement: The authors have read the ARRIVE guidelines, and the manuscript was prepared and revised according to the ARRIVE guidelines.

Manuscript source: Unsolicited manuscript

Received: March 19, 2020
Peer-review started: March 20, 2020
First decision: April 8, 2020
Revised: July 16, 2020
Accepted: August 12, 2020
Article in press: August 12, 2020
Published online: August 28, 2020

P-Reviewer: Cheng H, Huang YQ
S-Editor: Zhang L
L-Editor: A
P-Editor: Zhang YL

could induce colitis and gastritis in mice, suggesting a potential pathogenic role for the bacterium[13-15].

Dextran sodium sulfate (DSS)-induced colitis is the most widely used mouse colitis model for studying acute colitis and inflammation-associated colon cancer. DSS is a water-soluble, negatively charged, sulfated polysaccharide with a highly variable molecular weight. DSS-induced murine colitis, which most closely resembles human UC, employs DSS at a molecular weight of 40000 Da[16,17]. The mechanism by which DSS induces intestinal inflammation is disruption of tight junctions, allowing dissemination of proinflammatory intestinal contents[18]. In conjunction with colonic damage, DSS induces a range of proinflammatory cytokines and a Th1/Th17 response[17,19].

The aryl hydrocarbon receptor (AhR) regulates several signaling pathways relevant to intestinal health, including the balance between Tregs and Th17 cells[20,21]. AhR is needed for the survival of intraepithelial lymphocytes and also the organogenesis of lymphoid structures in the gastrointestinal tract[22]. Indole-3-carbinol (I3C), a dietary compound from cruciferous vegetables such as broccoli, activates AhR, as does its acidic condensation product, 3,3′-diindolylmethane (DIM)[23]. Both I3C and DIM have been investigated as treatments for a range of inflammatory diseases and cancers, including colitis[24-26], but the effects of *Helicobacter* infection on the response to I3C has not been studied. I3C and DIM are available for purchase as dietary supplements.

MicroRNAs (miRNAs) are being investigated as potential diagnostic and treatment tools. MiRNAs are highly conserved, noncoding, single-stranded, small ribonucleic acid molecules (17–27 nucleotides) that control gene expression post-transcriptionally. They typically bind at the 3′ untranslated region of the target gene messenger RNA (mRNA) leading to the degradation of the target RNA or inhibition of the translation of the RNA[27,28]. MiRNAs regulate genes involved in a wide range of cellular signaling pathways, including the Immune response. During the past ten years, much research has been done to uncover their roles in cellular proliferation, differentiation, maturation, and apoptosis[27]. Moreover, substantial scientific evidence underlines the functional roles and potential value of these tiny ribonucleic acid molecules for regulating autoimmunity and inflammation by affecting the differentiation, maturation, and functions of various immune cells in diseases including colitis[28,29]. Furthermore, many pieces of evidence show the participation of miRNAs in the regulation of T-cell development, differentiation, maturation, and activation[30]. Since the Treg/Th17 balance is crucial to intestinal health[31], understanding how miRNA expression is controlled by inflammatory and anti-inflammatory signals, such as I3C, could lead to identification of miRNAs capable of rebalancing the immune response in the inflamed colon.

The aims of this study were to examine the relative effects of *H. muridarum* and I3C on mouse colon pathology, immune response, and miRNA expression. We used the standard mouse model of DSS-induced colitis in C57BL/6 mice. Some groups were infected with *H. muridarum* and treated with I3C. Treatment responses were monitored in the colon and mesenteric lymph nodes.

MATERIALS AND METHODS

Animals

The research described in this manuscript (including the acquisition of animals and all protocols for their use) was approved by the University of South Carolina Institutional Animal Care and Use Committee prior to commencement of studies. University of South Carolina is an AALAC accredited institution and all animal care procedures followed the NIH Guide for the Care and Use of Laboratory Animals. Female C57BL/6J mice (aged 8-10 wk) were purchased from The Jackson Laboratory, Bar Harbor, Maine, United States. Animals were housed in a controlled environment (12 h light/dark cycle) with food and water ad libitum. After one week of acclimation on a normal chow diet, the mice were randomly divided into groups. Groups of 5-7 animals were used in each experiment. The experimental groups included control (Ctrl), *H. muridarum*, *H. muridarum* plus DSS, *H. muridarum* plus DSS plus I3C, DSS, and DSS plus I3C (DSS/I3C). Each experiment included either all male or all female mice, as indicated in the text.

Bacterial strains, cultivation, and infection

H. muridarum strain ATCC4982 was purchased from the American Type Culture Collection and was cultured in a humidified environment at 37 °C with 10% CO_2, 5%

O_2 in Ham's F-12 medium containing 20 mL/L fetal calf serum in tissue culture flasks. *H. muridarum* bacteria were passaged every 2 to 3 d. After microscopically verifying appropriate morphology and motility, the culture was centrifuged at 25°C at 4500 rpm for 20 min, then the pellet was suspended in 9 g/L sodium chloride to produce a suspension containing approximately 28465 to 142072 adenosine triphosphate (ATP) relative luminescence units per 200 μL, as determined using the luminescent BacTiter-Glo ATP viability assay (Promega Corp.,Madison, Wisconsin, United States). Mice were inoculated by orogastric gavage (200 μL) every other day for a total of four inoculations. Viability of the remaining bacterial suspension was reconfirmed using the luminescent BacTiter-Glo ATP assay.

Infection was confirmed by polymerase chain reaction (PCR) of stool DNA using *H. muridarum*-specific primers as follows. Fecal samples were collected and stored at -80°C until analysis. Fecal DNA was isolated using the EZNA stool DNA kit (Omega Bio-Tek, Inc., Norcross Georgia, United States) according to the manufacturer's recommendations. Fecal PCR was performed using *H. muridarum* 16S rRNA gene-specific primers (H. m. p30f, 5'-ATGGGTAAGAAAAAAAAAGATTGCAA-3', and H. m. p30r, 5'-CTATTTCATATCCGCTCTTGAGAATC-3'), which amplify an 800 bp conserved region of the 16S rRNA, as previously described[32].

Induction of colitis with DSS

DSS (MW 40 000, Chem-Impex International, Inc, Wood Dale, Illinois, United States) at a concentration of 1-30 g/L was provided in drinking water for 10-13 d. The volume of DSS consumed, animal weight, diarrhea score, and stool blood score were recorded daily. The disease activity index was calculated from weight, diarrhea, and stool blood scores as previously described[33,34]. Stool blood was detected using a colorimetric fecal occult blood test (Helena Laboratories, ColoScreen catalog No. 5083). Briefly, we determined the disease activity index using the following variables: Stool blood (0, negative; 1, weakly positive; 2, strongly positive; 3, rusty-colored stool and 4, gross bleeding), changes in weight (0, < 1%; 1, 1%-5%; 2, 6%-10%; 3, 11%-15%; and 4, > 15%), and stool consistency (0-1, normal; 2-3, loose stools; and 4, diarrhea).

I3C preparation and dosage

For treatment groups, I3C purchased from Chem-Impex International, Inc. was suspended in DMSO prior to dilution in corn oil. I3C was administered orogastrically at a dose of 40 mg/kg in a total volume of 100 μL, as described previously[24]. Animals were treated with either I3C or vehicle (20 mL/L DMSO in corn oil) daily, beginning on the first day of the DSS cycle.

Histopathological colitis score

Formalin-fixed colon tissue was embedded in paraffin and cut into 5 μm thick sections. Next, the colon sections were stained using hematoxylin and eosin (H and E). Four randomly chosen, non-overlapping fields of each stained section were analyzed and assigned a colitis severity score by a pathologist using methods described previously[34,35]. In short, the degree of colitis was scored on the basis of the following parameters: Extent of the injury (0, none; 1, mucosa; 2, mucosa and submucosa; and 3, transmural), inflammation severity (0, none; 1, mild; 2, moderate; and 3, severe), and crypt damage (0, none; 1, basal one-third damaged; 2, basal two-thirds damaged; 3, crypt loss and the presence of surface epithelium; and 4, loss of the entire crypt and epithelium). Then the degrees for each of these aforementioned parameters were multiplied by an extent score that represented the percentage of each parameter that had a given feature as follows: 1, 0-25%; 2, 26%-50%; 3, 51%-75%; and 4, 76%-100%. We defined the total score as the sum of the three parameters. The bottom limit total colitis score was 0; the upper limit total

Characterization of CD4+ T cells in the mesenteric lymph node and spleen

For flow cytometry, the mesenteric lymph nodes (MLN) and spleens were pooled from each group of mice and placed in ice-cold medium. These tissues were mechanically disrupted, teased into single-cell suspensions, filtered through a cell strainer (70 μm), and placed in complete medium (RPMI-1640 containing 100 mL/L of heat-inactivated fetal bovine serum). The isolated cell suspension was stimulated with a cell stimulation cocktail (eBioscience™) plus protein transport inhibitors (Invitrogen, catalog 00-4975), for 4-6 h. Stimulated cells were incubated with anti-CD4 mAb and anti-CD25 mAb for 15 min on ice (Biolegend, United States). For intracellular cytokine staining, the cell suspension was incubated with anti-IFNγ, Interleukin-17 after treating the cells with Fixation/permeabilization kit (BD Biosciences catalog 554714).

For Treg identification, we used FOXP3/Transcription Factor Staining Buffer set (eBioscience Invitrogen) before adding anti-FOXP3. Staining and washing were carried out in complete medium on ice. The stained cells were analyzed with a Beckman Coulter FC500 flow cytometer.

Enzyme linked immunosorbent assays

Interleukin-17 (IL-17), IL-6, IL-10, IL-4, IL-6, IL-21, IL-22, IL-23, IL-1β, transforming growth factor beta 1 (TGF-β1) , tumor necrosis factor-alpha (TNF-α) and interferon gamma (INF-γ), in the plasma and/or in colonic tissue lysates were quantified by ELISA kits (R and D Systems, Minneapolis, MN, United States) following the manufacturer's recommendations. Colon tissues were prepared for ELISA as described previously[33]. Briefly, the mouse colons where washed immediately with cold phosphate buffered saline and frozen at -70°C until use. The samples were homogenized in 200 μL protein analysis buffer [10 mL of 1 mol/L Tris-hydrochloric acid (pH 8.0), 6 mL of 5 mol/L sodium chloride and 2 mL of Triton X-100 to 182 mL of sterilized distilled water][33] in 2 mL microcentrifuge tubes with a 0.9-2.0 mm stainless steel bead blend and homogenized with a tissue homogenizer (MP FastPrep-24) at a speed of 0.4 m/s for 20 s. Samples were frozen and thawed, and homogenized three times, then centrifuged at 30000 *g* for 30 min at 4°C. The supernatant was collected, and the pellet was re-suspended in phosphate buffer. Protein concentrations were determined using a bicinchoninic acid assay (Bio-Rad). Samples were frozen until the ELISA assays were performed and 0.5-1.0 mg/mL of protein was used for each run, depending on the interleukin type.

Sample collection and RNA isolation

Mesenteric lymph nodes were collected from the groups on the day of the sacrifice and immediately frozen at -70°C prior to use. Mesenteric lymph nodes were ground with mortar and pestle in liquid nitrogen. QIAzol Lysis Reagent (Qiagen, catalog 217004) was added to the samples and they were then homogenized by MP FastPrep-24 with 0.9-2.0 mm stainless steel beads (0.4 m/s for 10 s). Total RNA, including mRNA, miRNA and other small RNA molecules, were isolated from all the mesenteric lymph node with the miRNeasy Kit (Qiagen, Germany), following the manufacturer's procedure. The concentration and purity of the isolated RNA was determined using a Beckman Coulter DU800 UV/visible spectrophotometer. RNA quality was assessed by measuring the absorbance (A260/A280, A260/A230) of isolated samples and by agarose gel electrophoresis.

MicroRNA array analysis

The microarray was performed at the University of South Carolina School of Medicine following the protocol described by Bam *et al*[36,37]. Briefly, total RNA isolated as described above was hybridized to an Affymetrix miRNA-v3 gene chip (Affymetrix, Sunnyvale, CA, United States) as directed by the manufacturer. Raw data was processed in the Transcriptome Analysis Console (Affymetrix). The heat map was generated in Genesis[38]. The data from Transcriptome Analysis Console were used to calculate the linear fold-change of the expression of miRNAs to compare the miRNA expression differences among treatment groups. A linear fold-change of at least ± 1.5 was used as a cutoff value for the inclusion of a miRNA for further analysis. Moreover, only the miRNAs which were significant on the basis of P value (< 0.05) calculated using student's t-test, were included in the analysis.

MiRNA-target gene prediction

Ingenuity Pathway Analysis (IPA, Qiagen, Redwood City, CA, United States) was used to predict the targets of the differentially expressed miRNAs. Networks relevant to regulatory T cells were generated to identify relevant miRNA species for testing. Other databases [TargetScan (http://www.targetscan.org/vert_72/), miRWalk (http://mirwalk.umm.uni-heidelberg.de/)] were also used to identify genes targeted by specific miRNAs.

Quantitative real-time PCR analysis of miRNA and gene expression

Total RNA from MLN was isolated and purified with the miRNeasy Kit (Qiagen, Valencia, CA, United States), following the manufacturer's procedure. The miScript II RT complementary DNA (cDNA) synthesis kit (Qiagen, Germany) was used according to the manufacturer's specifications to reverse-transcribe cDNA by taking 1 μg each of total RNA in a 20 μL total volume. The quantitative real-time (qRT-PCR) reactions were carried out using miScript Primer Assays or miScript Precursors (Qiagen,

Germany) according to manufacturer instructions. U6, SnorD96, Snor68, Snor234, and Snor202 were evaluated for stability among groups and SnorD96 was chosen for normalization. SnorD96 has also been used by others[39,40]. Primers were purchased from Qiagen, Maryland.

For mRNA expression analysis, cDNA was made from total RNA as described. A two-step amplification qRT-PCR was carried out using SsoAdvanced™ SYBR® green supermix from Bio-Rad (Hercules, CA, United States) with the mouse primers shown in Table 1. The real-time PCR conditions were as follows: Initial step at 95°C for 10 s followed by cycles (n = 40) consisting of 30 s at 95°C, followed by 30 s annealing/extension at 60°C and a final extension step for 30 s at 72°C. Data are normalized to expression of the reference gene encoding β-actin. Primers were purchased from Integrated Technologies and from Invitrogen. Melting temperatures ranged from 56.0°C to 64.5°C. Primer efficiency was measured for each primer set. All reactions were performed in triplicate. The qPCR experiments were carried out on a CFX96 Touch Real-Time PCR Detection System (Bio-Rad, Hercules, CA, United States). Fold changes were calculated using the $2^{-\Delta\Delta CT}$ (Livak) method.

Statistical analysis

Significance of differences between groups at single time points were determined using the Mann-Whitney U-test using GraphPad Prism software (Version 8.2). P values less than 0.05 were considered significant. Colitis symptom time course data were analyzed using a repeated measure analysis with 13 measures taken per animal (day one to day thirteen) randomly assigned to six groups (Ctrl, *H. muridarum*, *H. muridarum*/DSS, *H. muridarum*/DSS/I3C, DSS/I3C) and three experiments. Descriptive statistics were computed on the variables. For categorical variables, the univariate constructions will be included frequency distributions. For continuous variable statistics included measure of central tendency (mean and median) and measure of spread (standard deviation and range). Descriptive statistics for main variables were carried out for each group. In the analysis, expected mean squares were calculated and the appropriate combination used for hypothesis tests with specific functions of the repeated measures. General linear model analyses in SAS (MIXED procedure) were used to examine the effects of day, group, and day by group interaction. Post-hoc comparisons for the appropriate effects were examined. In addition, parameter estimates of the effects of covariate (experiment) and of the appropriate structure for the repeated observations was estimated. Adjusted Tukey-Kramer multiple comparison was used for significant effects. Significance levels are indicated as $^{a}P \leq 0.05$; $^{b}P \leq 0.01$; $^{c}P \leq 0.001$; $^{d}P \leq 0.0001$.

RESULTS

Exacerbation of colitis by H. muridarum is counteracted by I3C treatment

In three independent experiments, female wild-type C57BL/6 mice were infected with live *H. muridarum* bacteria seven, five, three, and one days prior to commencement of DSS treatment (day zero). Pathology in mice treated with 30 g/L DSS was so severe that one *H. muridarum*/DSS treated mouse required euthanasia. For this reason, 10 g/L DSS was used in subsequent experiments. Figure 1 shows average values from three independent experiments. Statistical analysis results are shown in Table 2 and Table S1. Overall disease activity was increased by each treatment except *H. muridarum* when compared to the control group. *H. muridarum* alone occasionally induced stool softening and a small amount of fecal occult blood, yet *H. muridarum* decreased diarrhea scores in DSS-treated mice (Figure 1A and Table 2). On the other hand, *H. muridarum* increased fecal occult blood and weight loss in DSS-treated mice. I3C was as effective in ameliorating colitis symptoms in *H. muridarum* mice as it was in uninfected mice. Significant shortening of the colon, an indicator of inflammation, occurred in *H. muridarum*-infected mice compared with control mice (Figure 1B). DSS treatment of *H. muridarum* mice caused additional shortening and colon length was similar to DSS mice. I3C significantly increased colon length in both infected and uninfected mice. It is evident from the pathology scores that the infection with *H. muridarum* alone can induce pathology such as dilatation of glandular crypts, edema, and destruction of epithelium and glands (Figure 1B). In some cases, pathology caused by *H. muridarum* alone is comparable to that caused by DSS treatment, yet damage to the mucosa was not reflected in symptom scores in these mice. Treatment of *H. muridarum*-infected mice with DSS further worsened pathology.

Table 1 Primers used for transcription analysis

Gene	Forward primer (5'-3')	Reverse primer (5'-3')
Actb (β-actin)	TCACCCACACTGTGCCCATCTACG	CAGCGGAACCGCTCATTGCCAATGG
Il17a	TCAGCGTGTCCAAACACTGAG	CGCCAAGGGAGTAAAGACTT
Foxp3	AGCAGTCCACTTCACCAAGG	GGATAACGCCAGAGGAGCTG
Rorc	CCGCTGAGAGGGCTTCAC	TGCAGGAGTAGGCCACATTACA
Il10	TGAATTCCCTGGGTGAGAAGC	ATCACTCTTCACCTCCAC
Il6	AGCCAGAGTCCTTCAGAGAGAT	AAAAAGTGCCGCTACCCTGA

Table 2 Colitis symptom score *P* values

Treatment groups[2]		% Weight	Stool blood	Diarrhea	DAI
Ctrl *vs*	Hm	0.2495	0.6142[1]	0.0248[1]	0.0659[1]
	Hm/DSS	< 0.0001[1]	< 0.0001[1]	< 0.0001[1]	< 0.0001[1]
	Hm/DSS/I3C	0.9574	< 0.0001[1]	< 0.0001[1]	< 0.0001[1]
	DSS	0.0552	< 0.0001[1]	< 0.0001[1]	< 0.0001[1]
	DSS/I3C	0.1381	< 0.0001[1]	< 0.0001[1]	< 0.0001[1]
Hm *vs*	DSS	0.9823	< 0.0001[1]	< 0.0001[1]	< 0.0001[1]
	Hm/DSS	< 0.0001[1]	< 0.0001[1]	< 0.0001[1]	< 0.0001[1]
Hm/DSS *vs*	DSS	< 0.0001[1]	0.0007[1]	0.0041[1]	< 0.0001[1]
	Hm/DSS/I3C	< 0.0001[1]	< 0.0001[1]	< 0.0001[1]	< 0.0001[1]
DSS *vs*	DSS/I3C	0.9977	0.0026[1]	< 0.0001[1]	< 0.0001[1]

[1]Significant *P* values.
[2]Ctrl: Control; Hm: *Helicobacter muridarum;* Hm/DSS: *Helicobacter muridarum* plus DSS; Hm/DSS/I3C: *Helicobacter muridarum* plus DSS plus I3C; DSS/I3C: DSS plus I3C.

Effects of H. muridarum, DSS, and I3C on miRNA expression

Since miRNAs contribute to immune cell differentiation, we sought to determine which miRNAs were regulated by I3C, which were regulated by *H. muridarum*, and whether *H. muridarum* affected the I3C response. To accomplish this, we performed miRNA analysis on total RNA isolated from the mesenteric lymph nodes of all groups from one of the experiments. A heat map was constructed highlighting the differences in miRNA abundance among the groups (Figure 2A). We found that each group had a pattern that was distinct from all others. For example, *H. muridarum* infection alone altered miRNA expression and miRNA expression in DSS, I3C treated mice was different depending on whether they were infected or uninfected.

We sought to determine whether I3C-regulated miRNAs are associated with regulation of the major Treg and Th17 transcriptional regulators, FOXP3 and RORC. To this end, we used *in silico* analysis of predicted miRNA targets and pathways as well as online databases to search for miRNAs induced by I3C in *H. muridarum* /DSS mice that could target *Foxp3* and *Rorc* genes. Among these potential miRNAs, we identified 3 candidates that had acceptable alignment scores and were highly predicted to target *Foxp3* or *Rorc*. These miRNAs included miR-let7a-5p and miR-29a-3p, which target RORC, and miR-874-5p and miR-6906-5p, which target *FoxP3*. It should be noted that other members of the let-7 family also target *Rorc* and some were similarly regulated by I3C in *H. muridarum*-infected mice. We performed qRT-PCR on cDNA samples reverse transcribed from total MLN RNA. As predicted, we found increased expression of miR-23a-3p and let-7a-2, which target *Rorc* (Figure 2B). Differences between untreated and I3C-treated groups were only significant for *H. muridarum*-infected mice, but the *Rorc*-targeted miRNAs miR-29a-3p and let-7a trended higher in uninfected mice. We also found that I3C decreased expression of *Foxp3*-targeting miR-874-5p and miR-6906-5p in *H. muridarum*-infected mice, but only

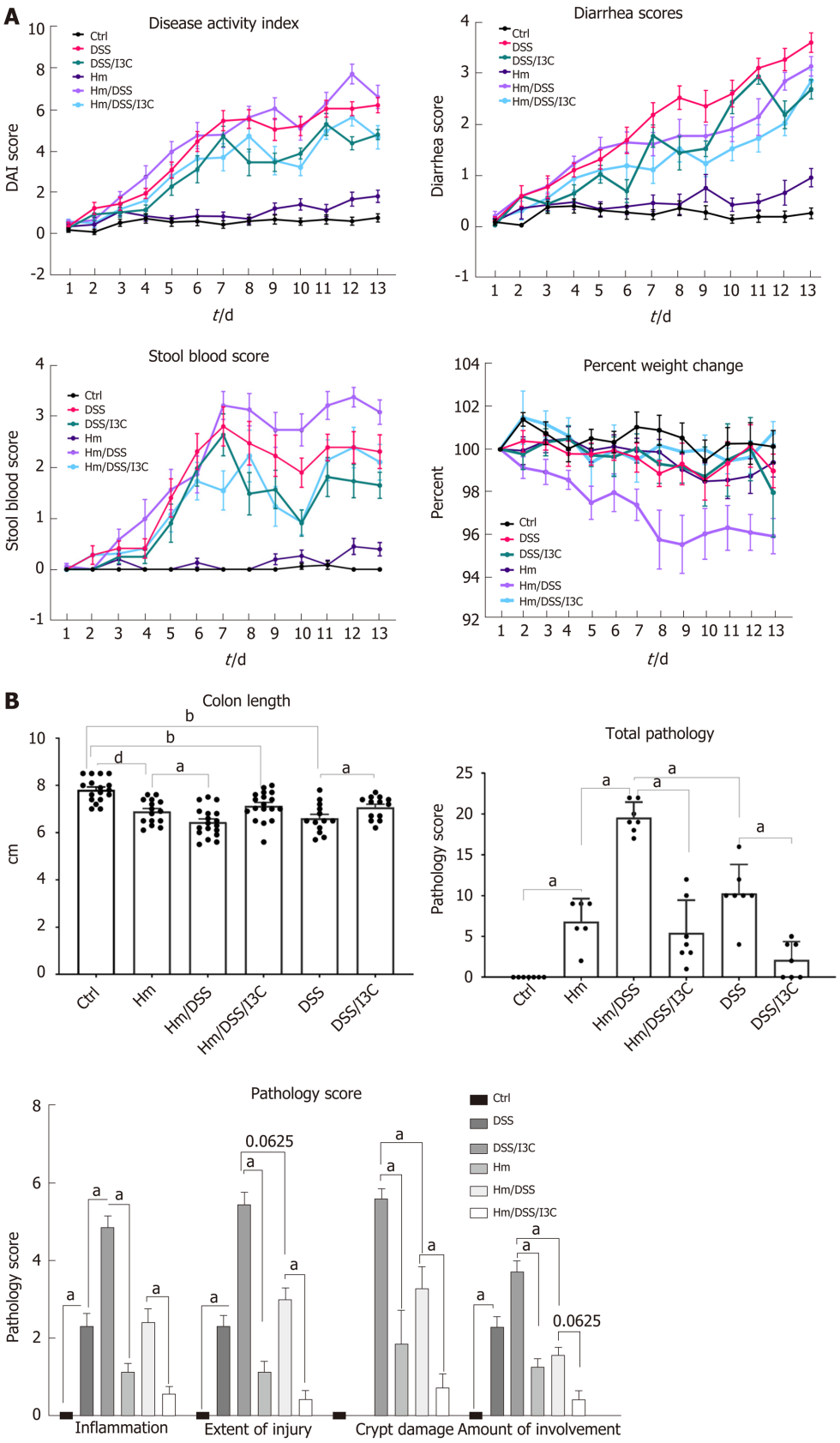

Figure 1 Symptom scores and histopathology. A: Colitis symptom scores (n = 17-21 per group); B: Colon length (n = 17-21 per group) and histopathology scores (n = 7 per group). $^{a}P \leq 0.05$; $^{b}P \leq 0.01$; $^{c}P \leq 0.001$; $^{d}P \leq 0.0001$. Ctrl: Control; Hm: *Helicobacter muridarum;* Hm/DSS: *Helicobacter muridarum* plus DSS; Hm/DSS/I3C: *Helicobacter muridarum* plus DSS plus I3C; DSS/I3C: DSS plus I3C.

miR-6906-5p was reduced in uninfected mice. This is not surprising since miR-874-5p was not predicted to be elevated by DSS in uninfected mice, but it highlights the different miRNA responses seen among groups. The miRNAs miR-15b and miR-16

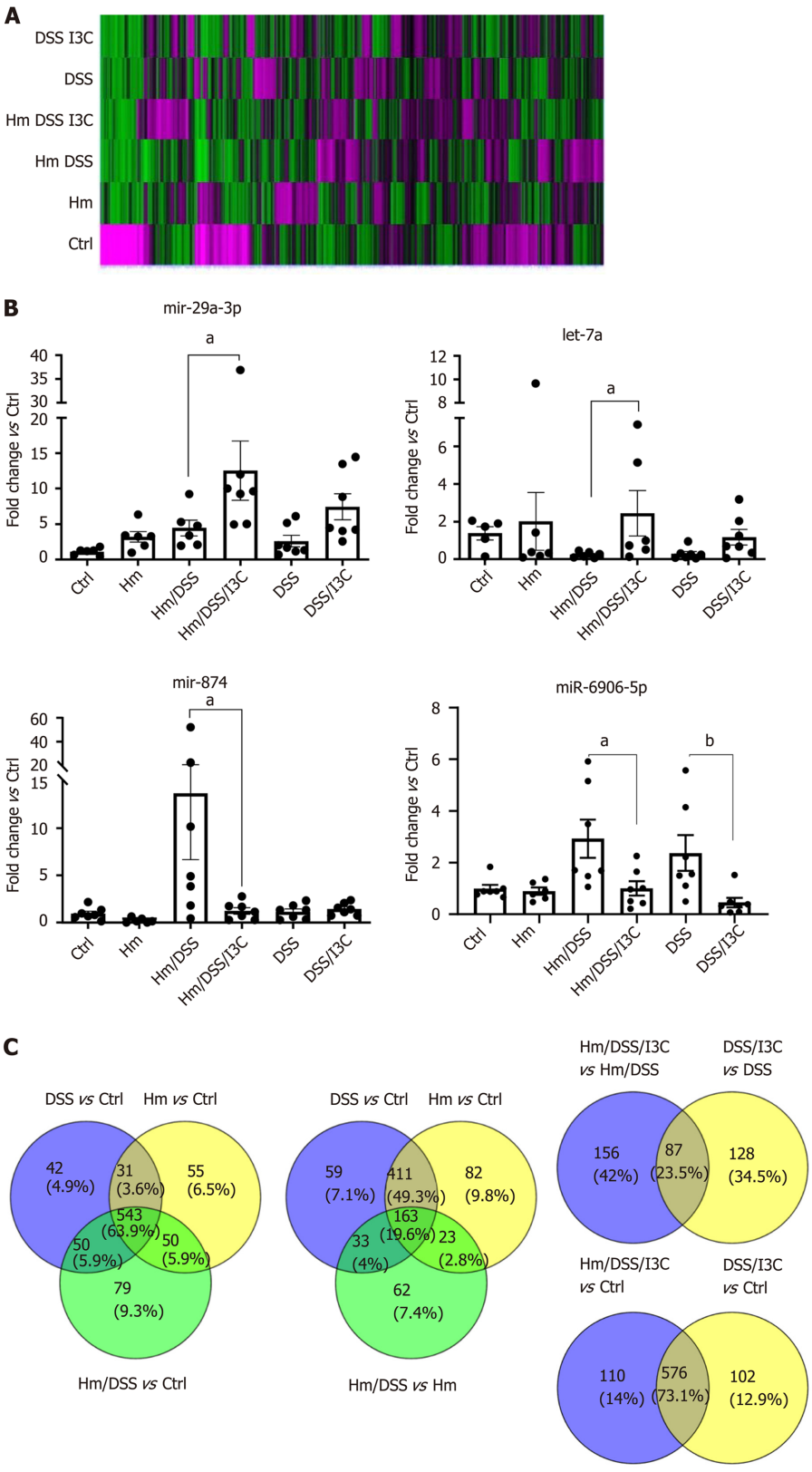

Figure 2 MicroRNA expression analysis. A: A heat map of expression intensities for each group was generated using Genesis software with red representing high expression and green representing low expression; B: Expression of microRNA as determined by quantitative real time PCR. All values are normalized to expression in the control group (n = 7); and C: Venn diagrams generated using Venny 2.1 demonstrate microRNA expression changes common to different treatment conditions. [a]$P \leq 0.05$; [b]$P \leq 0.01$. Ctrl: Control; Hm: *Helicobacter muridarum;* Hm/DSS: *Helicobacter muridarum* plus DSS; Hm/DSS/I3C: *Helicobacter muridarum* plus DSS plus I3C; DSS/I3C: DSS plus I3C.

support Treg development by targeting a suppressor of Treg development and miR-15b/16 previously have been shown to be induced by DIM[41,42]. We also found these miRNAs to be increased by I3C in *H. muridarum*-infected, DSS-treated mice (Figure S1

), but their expressions were predicted to be oppositely regulated in uninfected mice.

A closer look at miRNA microarray data was illuminating. The first Venn diagram shown in Figure 2C highlights miRNAs that displayed a greater than 2-fold change in the colitis groups compared with the control group. The *H. muridarum* group has 679 miRNAs up or down-regulated compared with the control, *vs* 666 miRNAs in the DSS group, and 722 miRNAs in the *H. muridarum* /DSS group. Interestingly, the majority (n = 574) of the miRNA changes are shared between the *H. muridarum* group and the DSS group and most of these (n = 543) are also shared with the *H. muridarum* /DSS group as well. This demonstrates that the miRNA response to *H. muridarum* infection is very similar to the response induced by DSS treatment. More importantly, miRNAs common between the *H. muridarum* group and the DSS group were almost all regulated in the same direction. All miRNA data are found in Table S2.

A second Venn diagram further highlights the effect of DSS treatment by substituting the *H. muridarum* /DSS *vs* *H. muridarum* comparison for the *H. muridarum* *vs* control comparison. Not surprisingly, the number of miRNAs changed between *H. muridarum* /DSS and *H. muridarum* (n = 281) is much smaller than the effect of *H. muridarum* /DSS compared to Ctrl (n = 722), but the majority of those miRNAs (69.8%) are also altered by DSS. It should be noted that 80.1% of the miRNAs altered by DSS treatment of *H. muridarum* mice are found within the *H. muridarum* /DSS *vs* Ctrl comparison. 85.7% if miRNAs common between DSS *vs* Ctrl and *H. muridarum*/DSS *vs* *H. muridarum* were concordant in the direction of change. This recapitulates the findings shown in the first Venn diagram, indicating that *H. muridarum* infection and DSS treatment have similar effects.

A third Venn diagram was constructed to study the effects of I3C treatment. In I3C-treated animals (Figure 2C), there was less overlap between *H. muridarum*-infected and –uninfected animals (87 miRNAs, or 23.5%). Oddly, most of the 87 common miRNAs (71.2%) were oppositely regulated in *H. muridarum*-infected and uninfected mice. In most cases, miRNAs were upregulated by I3C in *H. muridarum*-infected mice, but downregulated by I3C in uninfected mice. The predicted fold changes were also larger in *H. muridarum*-infected mice. The reason for this odd regulation pattern is discussed in the next paragraph. An alternative method for Identifying I3C effects is to compare *H. muridarum* /DSS/I3C *vs* control with DSS/I3C *vs* Ctrl (Figure 2C). These miRNA populations overlap heavily (73.1%). Most of the 87 previously identified miRNAs (56/87) are found in the overlap group. Since there is also heavy overlap between the putative I3C-regulated miRNAs and DSS-regulated miRNAs (529/666), it is not clear whether any of the miRNAs are strictly responsive to I3C; however, the overlap is consistent with the hypothesis that I3C normalizes miRNAs involved in colitis.

Examination of specific miRNAs provides a clearer demonstration of the effects of *H. muridarum*, DSS, and I3C and an explanation for the differential regulation of miRNAs by I3C in infected *vs* uninfected mice. We examined a list of 45 miRNAs that are altered in human IBD[43-45]. Almost all of the human IBD-associated miRNAs were altered by *H. muridarum* and/or DSS. Table 3 shows raw expression data and fold changes for the selected miRNAs. When compared with control values, these miRNAs were all downregulated, whereas many were upregulated compared to healthy controls in humans[43]. Possible reasons for this are discussed later. Expression decreases are mostly modest in *H. muridarum* *vs* Ctrl, but extreme in *H. muridarum* /DSS *vs* Ctrl- up to 3,646-fold decreased. The expression reductions were less extreme in the *H. muridarum* /DSS/I3C group compared to Ctrl. Expression of the selected miRNAs was lower in DSS/I3C group than the DSS group, but in many cases, the reductions were less than two-fold, which is why those miRNAs did not show up as common between infected and uninfected mice treated with I3C. It should be noted that there was not a global decrease in miRNA expression in any treated groups *vs* Ctrls; the decreases are specific to certain miRNAs. All 45 human IBD-associated miRNAs were among the 576 miRNAs in the putative I3C regulated group (Figure 2C) and all but two of the 45 were regulated by *H. muridarum* and/or DSS. Bian *et al*[46] also reported that many of these miRNAs are differentially regulated in DSS-treated mice, suggesting that a core set of miRNAs are relevant to colitis in both humans and mice[46].

H. muridarum infection alters T helper cell profiles.

Since miRNAs are pleotropic in their effects, we sought to confirm predicted effects on Treg and Th17 populations. MLN transcript analysis by qRT-PCR demonstrated that I3C decreased RORC and increased FOXP3 expression, consistent with a switch from Th17 to Treg (Figure 3). These results were mirrored by the decrease in IL17 and increase in IL10 expression. Expression of *Il6*, which is involved in Th17 induction, is also shown. RORC and IL17 were more strongly induced by DSS in *H. muridarum*-

Table 3 MicroRNA expression

	Raw expression data						Fold changes						
miRNA	Ctrl	Hm	Hm/DSS	DSS/Hm/ I3C	DSS	DSS/ I3C	Hm *vs* Ctrl	Hm/DSS *vs* Ctrl	DSS/Hm/I3C *vs* Ctrl	DSS *vs* Ctrl	DI *vs* Ctrl	DMI *vs*DHM	DI *vs* DSS
mmu-let-7a-5p	12.93	11.14	5.72	9.11	10.71	10.59	-3.45	-147.58	-14.06	-4.65	-5.07	10.5	-1.09
mmu-let-7b-5p	14.14	11.84	7.97	10.45	11.21	10.89	-4.92	-72.01	-12.96	-7.62	-9.56	5.56	-1.25
mmu-let-7d-5p	13.76	11.52	8.09	10.44	11.1	10.86	-4.71	-50.67	-9.97	-6.29	-7.42	5.08	-1.18
mmu-let-7e-5p	11.06	10.06	1.7	8.39	9.6	9.23	-2	-654.64	-6.34	-2.74	-3.54	103.31	-1.29
mmu-let-7g-5p	10.31	6.71	1.37	2.01	7.52	6.16	-12.19	-491.93	-317.1	-6.92	-17.81	1.55	-2.58
mmu-miR-103-3p	11.85	10.44	6.42	10.09	10.88	10.02	-2.66	-43.07	-3.39	-1.96	-3.57	12.7	-1.82
mmu-miR-106a-5p	9.29	5.45	1.15	2.03	5.51	2.78	-14.34	-282.96	-153.91	-13.78	-91.54	1.84	-6.64
mmu-miR-127-3p	7.9	4.55	0.95	2.8	2.43	1.91	-10.18	-123.98	-34.2	-44.34	-63.55	3.63	-1.43
mmu-miR-128-3p	5.81	0.79	0.94	1.04	0.77	1.3	-32.4	-29.23	-27.31	-33.04	-22.87	1.07	1.44
mmu-miR-135a-1-3p	3.64	1.3	1.8	1.26	1.43	2.12	-5.04	-3.57	-5.19	-4.62	-2.86	-1.45	1.62
mmu-miR-140-3p	10.2	9.92	1.83	7.91	9.62	8.3	-1.21	-329.16	-4.87	-1.49	-3.73	67.62	-2.51
mmu-miR-140-5p	6.33	1.38	0.79	1.02	1.38	0.87	-30.86	-46.56	-39.48	-30.86	-43.84	1.18	-1.42
mmu-miR-142-5p	2.9	0.99	1.35	0.99	1.16	1.01	-3.78	-2.93	-3.78	-3.34	-3.72	-1.29	-1.11
mmu-miR-145a-5p	12.99	11.51	6.79	10.2	11.15	10.28	-2.78	-73.5	-6.89	-3.57	-6.55	10.66	-1.83
mmu-miR-146a-5p	10.34	7.84	1.24	3.54	7.72	7.84	-5.65	-550.48	-111.6	-6.13	-22.7	4.93	-3.7
mmu-miR-150-5p	13.4	11.1	4.14	8.96	10.4	9.76	-4.92	-614.48	-21.78	-8.01	-12.51	28.22	-1.56
mmu-miR-155-5p	9.86	8.15	1.54	3.58	7.65	5.31	-3.27	-320.03	-77.72	-4.61	-23.48	4.12	-5.09
mmu-miR-15b-5p	11.17	10.17	1.48	8	9.92	8.84	-1.99	-824.5	-9.01	-2.37	-5.02	91.56	-2.12
mmu-miR-16-5p	13.18	10.38	1.35	9.1	10.8	9.11	-7	-3646.25	-16.92	-5.22	-16.9	215.51	-3.23
mmu-miR-17-5p	10.71	9.01	1.33	7.8	9.29	7.82	-3.25	-666.3	-7.53	-2.67	-7.43	88.54	-2.78
mmu-miR-185-5p	9.27	6.58	0.99	5.64	5.86	5.07	-6.45	-310.71	-12.33	-10.58	-18.36	25.19	-1.74
mmu-miR-18a-5p	7.32	1.37	0.84	1.37	1.41	1.74	-61.84	-89.41	-61.84	-60.29	-47.91	1.45	1.26
mmu-miR-195a-5p	10.59	8.03	1.91	5.03	8.22	7.39	-5.89	-409.38	-47.19	-5.17	-9.14	8.68	-1.77
mmu-miR-196b-5p	3.11	0.94	0.94	1.08	1.05	0.83	-4.49	-4.49	-4.09	-4.19	-4.86	1.1	-1.16
mmu-miR-199a-5p	9.5	4.56	1.77	2.01	7.72	1.77	-2.03	-101.88	-21.49	-3.71	-78.21	4.74	-21.08

mmu-miR-19a-3p	4.08	1.56	1.39	0.91	1.24	1.25	-5.73	-6.45	-9.02	-7.15	-7.13	-1.4	1
mmu-miR-19b-3p	9.43	6.13	1.18	5.87	7.97	5.61	-9.84	-303.99	-11.79	-2.74	-14.07	25.78	-5.14
mmu-miR-20b-5p	9.03	4.87	1.76	2.29	5.85	1.96	-17.77	-154.33	-106.75	-9.05	-133.96	1.45	-14.8
mmu-miR-221-3p	9.19	6.07	1.24	1.42	7.45	5.25	-8.65	-246.56	-218.06	-3.34	-15.34	1.13	-4.59
mmu-miR-222-3p	8.89	7.65	1.12	4.11	6.24	4.58	-2.36	-219.12	-27.5	-6.29	-19.86	7.97	-3.16
mmu-miR-223-3p	5.45	1.57	1.01	0.99	1.84	0.87	-14.69	-21.58	-21.99	-12.14	-23.85	-1.02	-1.96
mmu-miR-24-2-5p	12.74	10.84	1.78	9.51	10.8	10.12	-56.17	-101.73	-64.83	-72.38	-48.35	1.57	1.5
mmu-miR-27a-3p	9.96	5.94	1.35	1.57	8.22	5.2	-16.28	-390.62	-337.26	-3.34	-27.11	1.16	-8.12
mmu-miR-28a-3p	7.53	4.75	0.83	1.4	1.49	1.12	-6.86	-103.85	-69.7	-65.83	-84.8	1.49	-1.29
mmu-miR-29a-3p	10.97	8.84	2.38	7.73	9.45	7.38	-4.37	-386.19	-9.45	-2.86	-12.06	40.85	-4.21
mmu-miR-29c-3p	5.38	0.87	1.23	1.28	2.05	1.8	-22.8	-17.81	-17.22	-10.08	-12.01	1.03	-1.19
mmu-miR-30e-5p	7.8	1.13	1.64	1.64	3.46	1.32	-101.76	-71.46	-71.46	-14.68	-89.04	1	-4.42
mmu-miR-345-5p	5.41	2.46	2.85	3.65	2.81	1.18	-7.76	-5.93	-3.41	-6.1	-18.84	1.74	-3.09
mmu-miR-374b-5p	4.34	0.92	1.19	0.89	1.58	1.13	-10.7	-8.87	-10.91	-6.78	-9.23	-1.23	-1.36
mmu-miR-423-5p	7.07	3.13	1.29	4.25	2.56	1.26	-15.33	-54.69	-7.03	-22.66	-55.78	7.78	-2.46
mmu-miR-491-5p	2.95	1.39	1.15	1.01	1.34	1.07	-2.96	-3.49	-3.84	-3.06	-3.7	-1.1	-1.21
mmu-miR-532-5p	8.4	5.55	0.89	3.43	3.45	1.75	-7.22	-183.34	-31.45	-30.94	-101.04	5.83	-3.27
mmu-miR-760-3p	2.44	0.99	0.74	1.1	1.15	1.17	-2.73	-3.25	-2.54	-2.46	-2.42	1.28	1.02
mmu-miR-877-5p	4.05	3.56	1.93	2.14	3.28	1.8	-1.4	-4.35	-3.75	-1.7	-4.76	1.16	-2.79
mmu-miR-93-5p	10.41	8.67	1.86	7.64	8.66	6.85	-3.34	-373.43	-6.79	-3.35	-11.77	54.98	-3.52

Ctrl: Control; Hm: *Helicobacter muridarum;* Hm/DSS: *Helicobacter muridarum* plus DSS; Hm/DSS/I3C: *Helicobacter muridarum* plus DSS plus I3C; DSS/I3C: DSS plus I3C.

infected mice than in uninfected mice, consistent with the increased pathology. Although FOXP3 was less strongly induced by I3C in *H. muridarum*-infected mice, IL10 expression was similar to that of uninfected mice treated with I3C. These results were corroborated by flow cytometry (Figure S2). The Th17 cell population increased sharply following DSS treatment of *H. muridarum*-infected animals and decreased following I3C treatment while the Treg population increased.

Production of cytokines in colon tissue and plasma

Our gene expression and flow cytometry data from the mesenteric lymph nodes

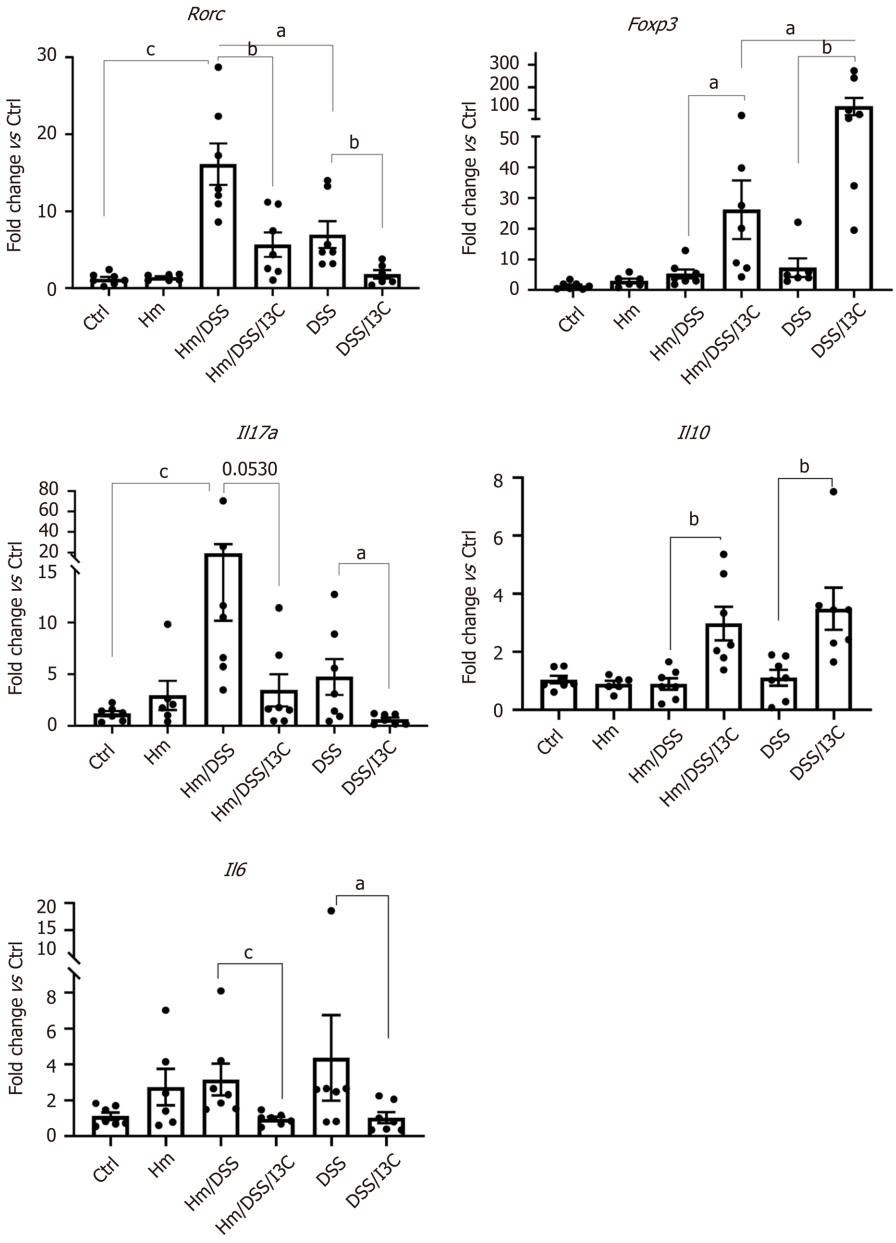

Figure 3 Expression of T helper 17 and Treg-associated genes in mesenteric lymph nodes. Gene expression was determined from total complementary DNA using qRT-PCR and values were normalized to the control group (n = 7). [a]$P \leq 0.05$; [b]$P \leq 0.01$; [c]$P \leq 0.001$. Ctrl: Control; Hm: *Helicobacter muridarum;* Hm/DSS: *Helicobacter muridarum* plus DSS; Hm/DSS/I3C: *Helicobacter muridarum* plus DSS plus I3C; DSS/I3C: DSS plus I3C.

clearly show that DSS and *H. muridarum* shift the T helper cell profile towards a Th17-dominated response, whereas I3C increases the Treg population. We next measured cytokine concentrations in colon homogenates to assess local immune cell and epithelial responses. These measurements encompass both epithelial cells and inflammatory cells. In most cases, production of pro-inflammatory cytokines was altered by multiple variables. Infection with *H. muridarum* alone increased all pro-inflammatory cytokines tested except IL-17 and IL-23 compared with control mice (Figure 4). In fact, cytokine levels in *H. muridarum*-infected mice were similar to those in uninfected, DSS-treated mice. Treatment of *H. muridarum*-infected mice with DSS caused trends towards further increases in most cytokines, but this was only significant in the case of IL-17. I3C treatment reduced secretion of all pro-inflammatory cytokines in DSS-treated, *H. muridarum*-infected and/or uninfected mice.

Levels of the anti-inflammatory cytokines IL-10 and TGFβ were only significantly altered by I3C, though TGFβ levels trended lower in DSS-treated mice (Figure 4). There were trends towards decreased IL-4 levels in uninfected mice treated with I3C, but not in *H. muridarum* infected mice treated with I3C. To summarize, I3C both decreases secretion of pro-inflammatory cytokines an increases secretion of anti-

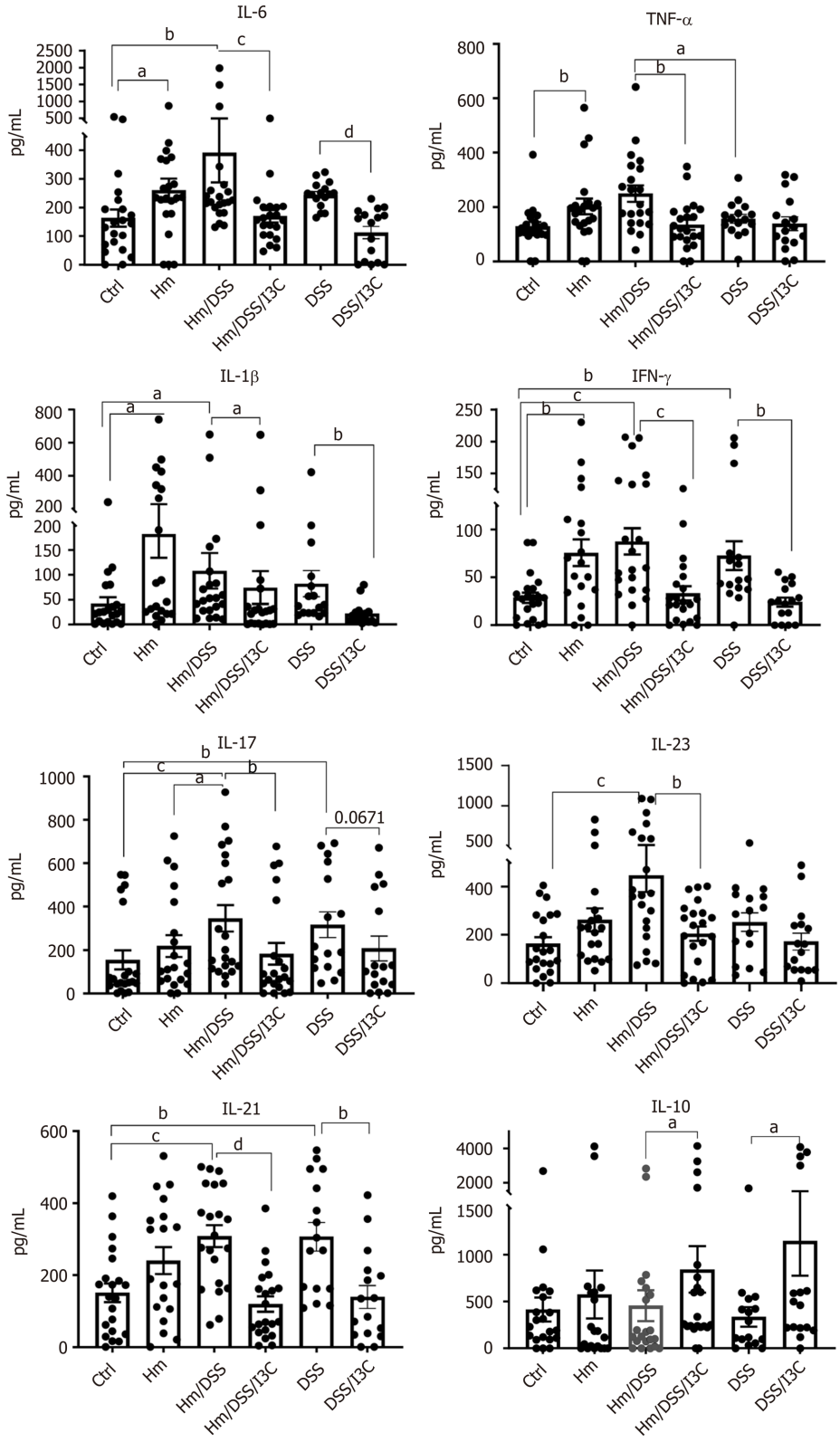
IL-6
TNF-α
IL-1β
IFN-γ
IL-17
IL-23
IL-21
IL-10
pg/mL
Ctrl
Hm
Hm/DSS
Hm/DSS/I3C
DSS
DSS/I3C
0.0671

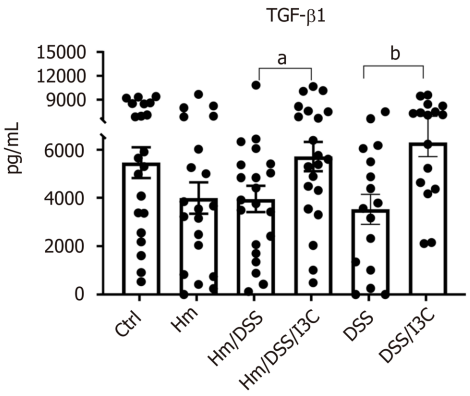

Figure 4 Colon cytokine production. Protein levels were determined by ELISA using colon homogenates (n = 17-21). [a]$P \leq 0.05$; [b]$P \leq 0.01$; [c]$P \leq 0.001$; [d]$P \leq 0.0001$. Ctrl: Control; Hm: *Helicobacter muridarum;* Hm/DSS: *Helicobacter muridarum* plus DSS; Hm/DSS/I3C: *Helicobacter muridarum* plus DSS plus I3C; DSS/I3C: DSS plus I3C.

inflammatory cytokines.

Plasma cytokines showed less dramatic changes than colon cytokines, the proinflammatory IL-17 and IL-6 cytokine concentrations were elevated in the *H. muridarum* /DSS group and to a lesser extent in the DSS group. I3C treatment reduced both to control levels. IL-10 was elevated by I3C in *H. muridarum*-infected mice and trended higher in the DSS/I3C group (Figure 5). TGFβ was reduced only in *H. muridarum*-infected mice and did not respond to I3C treatment. IL-4 and IL-22 were not significantly altered under any condition (Figure S3). Serum amyloid a levels were significantly increased only in *H. muridarum* /DSS mice, consistent with more severe pathology in that group. The neutrophil marker myeloperoxidase was strongly increased by *H. muridarum* infection, even in the absence of DSS treatment (Figure 5).

DISCUSSION

Effects of H. muridarum on susceptibility to DSS-induced colitis and treatment with I3C

Several models of inflammation and inflammatory bowel disease suggest that bacteria are necessary, but insufficient triggers of IBD[47] and several studies have reported that EHH species modulate IBD. As an example, *H. macacae* has been connected with chronic idiopathic colitis in young rhesus macaques and a study of children with CD reported PCR evidence for *Helicobacter* infection in 59% of patients *vs* 9% of healthy controls[11,48]. Similarly, Laharie *et al*[10] found that *H. pullorum* or *H. canadensis* infection was considerably related to CD in adults[10]. Finally, *H. canis*, another EHH species, has been detected in duodenal ulcerations associated with CD[49]. Therefore, certain *Helicobacter* species are almost certainly involved in IBD pathogenesis; however, the exact mechanism of EHH involvement remains undiscovered.

Th17 cells have a crucial role in colitis development in both humans and mouse models[50,51]. *H. pylori* is known to induce a Th17 response in the gastric mucosa[52-54], yet *H. pylori* infection is associated with a decreased risk of IBD[55]. *H. pylori* only colonizes the gastric mucosa, meaning that any effects of *H. pylori* on the colon are likely due to systemic effects of infection. Furthermore, EHH species lack the major *H. pylori* virulence factors *cagA* and *vacA*. Thus, one cannot assume that mucosal or immune effects of *H. pylori* infection will match those caused by EHH species. It is therefore necessary to use infection with EHH species to investigate potential mechanisms of EHH-mediated contributions to IBD.

The present study extends existing knowledge on *H. muridarum* pathogenesis. *H. muridarum* infection has been previously shown to induce colitis in C57BL/6 mice treated with DSS and in monoassociated severe combined immunodeficiency mice following the transfer of certain T cell populations[13,35,56]. We found increased weight loss and stool blood in *H. muridarum*-infected mice treated with DSS compared with DSS treatment alone, but diarrhea was actually lessened. Increased stool blood suggests damage to the mucosal barrier, potentially increasing exposure to other members of the gut microbiota. Though *H. muridarum* alone did not cause appreciable colitis symptoms, it caused modest colon shortening and inflammatory infiltrates.

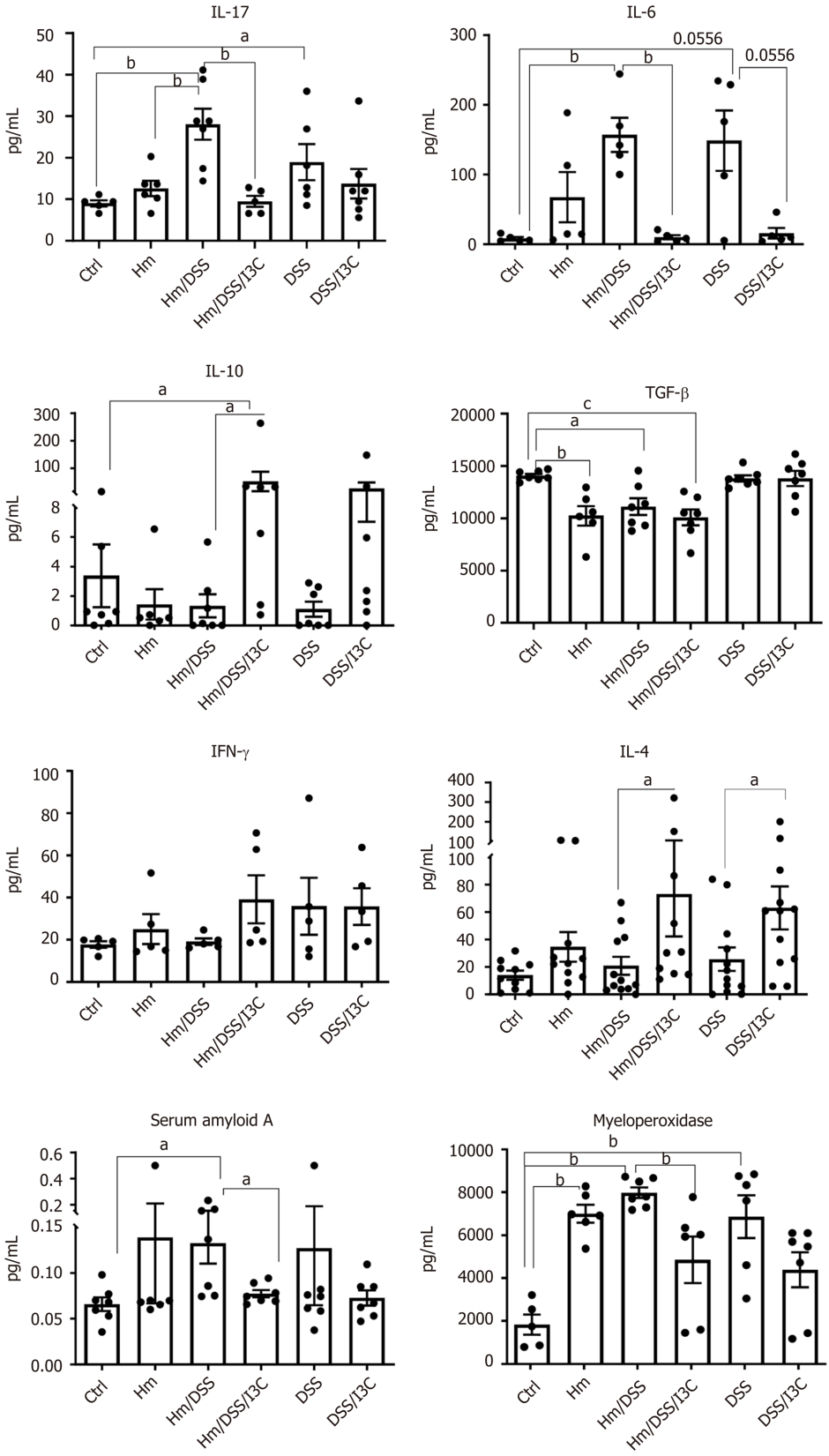

Figure 5 Plasma cytokine and inflammatory protein markers. Protein levels were determined by ELISA using plasma collected at the time of euthanasia (n = 5-7). $^{a}P \leq 0.05$; $^{b}P \leq 0.01$; $^{c}P \leq 0.001$. Ctrl: Control; Hm: *Helicobacter muridarum;* Hm/DSS: *Helicobacter muridarum* plus DSS; Hm/DSS/I3C: *Helicobacter muridarum* plus DSS plus I3C; DSS/I3C: DSS plus I3C.

Effects of H. muridarum, DSS, and I3C on microRNA expression

There is increasing interest in the use of miRNAs to diagnose and treat a wide variety of diseases and cancers. We examined mesenteric lymph node miRNA expression to

determine whether miRNA signatures explained the effects of *H. muridarum* and I3C. Many studies show that miRNAs participate in the regulation of crucial lymphocyte functions such as lymphocyte development, maturation, activation, and differentiation[19,28,57,58]. When considering the roles of miRNAs in Treg and Th17 function, it is necessary to distinguish between miRNAs involved in T cell differentiation and miRNAs involved in function. For example, miRNAs binding to the Treg transcriptional regulator gene FOXP3 prevent differentiation of Tregs and must be downregulated to allow Treg differentiation. Some miRNAs promote FoxP3 expression by downregulating expression of other genes, while others are induced by FoxP3 and influence Treg function. Still other miRNAs act in an autocrine manner, being both induced by FoxP3 and inducing FOXP3 expression[59]. Therefore, miRNA expression patterns can differ between naïve and mature T cells and between highly active and anergic T cells. A further complication of miRNA interpretation is that the same miRNA can have different effects depending on the cell type in which it is expressed. For example, miR-155 reportedly induces both Treg and Th17 cell differentiation[60] making it impossible to predict whether increased miR-155 in the lymph node, or even within the T cell population, favors a Treg or Th17 phenotype. Relative concentrations of miRNAs within each cell most likely dictate the cell phenotype.

These nuances explain the often disparate and contradictory results published in the literature. For example, Iborra *et al*[43] sought to compare serum and mucosal miRNAs profiles in human ulcerative colitis and Crohn's disease[43]. They found little overlap between serum and tissue miRNAs and many differences between their results and those published by others. Each miRNA has hundreds or thousands of targets[61] and each gene is likely controlled by dozens of miRNAs. In the context of IBD and colon cancer, miR-15b/16 is reported to regulate Tregs, macrophages, TP53, aquaporin 8, and the adenosine A2a receptor[41,62-65]. Surprisingly, miR-16 has even been suggested as a stable reference miRNA[66]. The multiple targets of miR-15b/16 may then explain why treatment of mice with miR-16 precursors ameliorates colitis, yet elevated miR-16 in human blood samples is associated with more severe IBD[62,67,68].

Interpretation of miRNA data in our study proved similarly challenging; however, there was remarkable overlap between the responses to *H. muridarum*, DSS, and I3C. Nonetheless, the direction of regulation was not always as expected. For example, when looking at a set of colitis-associated miRNAs, expression dropped following treatment with either *H. muridarum* or DSS, whereas human studies found increases in these miRNAs in IBD patients *vs* controls[43-45]. The human studies used either peripheral blood or colon biopsies as a source of miRNAs, whereas we used mesenteric lymph nodes. Lymph nodes differ in cellular composition compared to peripheral blood[69] and since the cell subsets change following *H. muridarum* infection or DSS treatment, the ratios of T cells to dendritic or other cell populations may change as well. Because colitis-associated miRNAs are likely expressed in multiple cell types, the meaning of a miRNA increase or decrease cannot be deciphered without knowing whether they rise or fall in each cell subtype. Presorting cells by flow cytometry would provide better data for understanding the effects of miRNA expression changes, but would not be feasible for most clinical samples due to the limited amounts of tissue available.

One would think that if DSS or *H. muridarum* decreases miRNA expression, then I3C treatment should increase it back to the control value. This was not necessarily the case for the same reasons mentioned above. I3C increased the number of cells found in MLN, and likely the ratios of cell types. The fact that I3C altered roughly the same subset of miRNAs as DSS or *H. muridarum* is consistent with its known anti-inflammatory effects, but does not shed light on the mechanism of I3C activity. Rather, the results are consistent with the hypothesis that miRNA changes due to I3C result from, rather than cause, immune response normalization.

We did not find measurable effects of *H. muridarum* infection alone on cytokine expression in the lymph nodes or on plasma cytokine levels; however, there were clear pro-inflammatory changes in the colon, which were further exacerbated by DSS administration. The cytokines induced by *H. muridarum* (TNFα, IL-1β, IL-6, and IFNγ) are typical of those induced by DSS treatment[17]. It is therefore not surprising that *H. muridarum* further increased production of inflammatory cytokines and worsened pathology following DSS treatment. In humans with IBD, increases in mucosal TNFα, IL-1β, IL-6, IL-23 and IFNγ are due to lamina propria monocytes or macrophages[70-72]. IFNγ is also produced by Th1 cells or potentially a new intraepithelial lymphocyte subtype, IL-17$^+$ IFNγ$^+$ T cells[73]. Regardless of cell source, IFNγ plays an important role in IBD pathology in humans and mice[74,75]. Thus, the effects of *H. muridarum* in our mouse model will likely be relevant to humans infected with enterohepatic species. In

general, *H. muridarum* infection more strongly influenced production of monocyte/dendritic cell-associated cytokines (TNFα, IL-1β, IL-6 , IL-23) compared to T cell-associated cytokines (IFNγ, IL-4, IL-10, IL-17, IL-21, IL-22), although IFNγ was increased by *H. muridarum* alone.

Cytokines secreted by monocytes or dendritic cells can drive T cell differentiation. TGFβ and IL-6 can drive several differentiation pathways depending upon which other cytokines are present[76]. The combination TGFβ, IL-6, and IL-23 efficiently induce Th17 differentiation[77]. In spite of local cytokine responses suggestive of a Th17-promoting milieu, we did not find evidence of a substantial T cell shift in mice infected with *H. muridarum* alone. DSS treatment was required for enhanced expression of RORC and IL17 in lymph nodes or increased plasma IL-17. In contrast, there was no apparent difference in Treg markers in lymph nodes or plasma between infected and uninfected mice. These data suggest that local effects of *H. muridarum* are conducive to, but not sufficient for Th17 polarization. This is consistent with a "two hit" hypothesis, although in this case, the two hits are *H. muridarum* and an irritant rather than host genetics and the microbiome.

I3C shifts the immune balance

The use of alternative medicine to treat inflammatory disorders is appealing to many patients. Numerous studies demonstrate that dietary indoles possess anti-cancer properties such as anti-oxidant activity, regulation of cell cycle and apoptosis, and control of endocrine metabolism[78-83]. DIM is sold over the counter as BioResponse DIM® with claims that it promotes breast health, prostate health, and weight management. Before such products can be confidently recommended, their mechanisms of action must be uncovered. In the case of IBD, it is prudent to investigate the effect of gut microbiota on response to treatment.

Several natural compounds, including I3C, are AhR ligands[84]. AhR is now known to govern differentiation and function of both T cells and macrophages[85-87]. Several studies have shown that AhR plays a vital role in regulation of immune responses specifically promoting the generation of Tregs while suppressing Th17 cells[88,89]. Previous studies have provided convincing proof that Foxp3-positive Treg cells are essential for gastrointestinal immune homeostasis[90] and that increased Th17 differentiation promotes colitis[50,51]. Consistent with other reports from various disease models, we found that I3C increases the Treg population and decreases the Th17 population[91-93]. The shift from Th17 to Treg was not inhibited by *H. muridarum* infection. Additionally, we found that I3C reduced production of every other pro-inflammatory cytokine tested, except for IL-22, which was not affected in any treatment group. Though we did not specifically analyze macrophages, others have shown that I3C or DIM suppresses IL-6, TNFα, IL-1β, IL-23 and IFNγ[94-96]. Therefore, I3C most likely inhibits colitis development via effects on both T cells and macrophages.

In summary, our studies suggest that *H. muridarum* increases susceptibility to DSS-induced colitis by inducing macrophage-associated cytokines and creating a mucosal milieu conducive to Th17 polarization. I3C ameliorates colitis via induction of Tregs, suppression of Th17 cells, and suppression of macrophage-associated pro-inflammatory cytokines. While no mouse model perfectly replicates human IBD, the identities of miRNAs altered by *H. muridarum* and DSS were similar to colitis studies in both mice and humans, although the direction of change was not always consistent. I3C is equally effective in the presence and absence of *H. muridarum*. Further research is warranted on the roles of EHH species in human IBD and the use of I3C or similar AhR agonists for the treatment of inflammatory bowel disease.

ARTICLE HIGHLIGHTS

Research background

Enterohepatic *Helicobacter* (EHH) species can infect humans and many animal species. Some of these species are known to cause disease in animals, while others have been described as commensal. In humans, epidemiological evidence suggests that EHH species are associated with inflammatory bowel disease (IBD), but the specific species involved and mechanisms of action are unknown. New treatments being tested for IBD include natural compounds and microRNA (miRNA)-based therapies. MiRNA is also being investigated as a diagnostic tool.

Research motivation

Given the limitations of performing IBD research in humans, an animal model of EHH-mediated pathology is needed. Such a model should reflect the biological changes seen during human IBD. *Helicobacter muridarum* (*H. muridarum*) has been referred to as a commensal in mice, yet we previously determined that *H. muridarum* worsens colitis resulting from dextran sodium sulfate (DSS). This suggested that EHH species could represent environmental factors that cause or worsen IBD in genetically susceptible individuals. It is also important to determine whether phytochemicals being investigated as IBD treatments are influenced by infection with EHH species because there are no commercially available tests for EHH infection in humans.

Research objectives

We sought to determine how the immune and miRNA profiles of *H. muridarum*-infected wild-type mice compared with DSS-treated mice and with published immune and miRNA profiles of IBD patients. We also determined whether efficacy of a broccoli-derived anti-inflammatory compound, indole-3-carbinol (I3C), was reduced by *H. muridarum* infection.

Research methods

We measured changes in body weight, stool consistency, and stool blood following *H. muridarum* infection, DSS treatment, and/or I3C treatment. We then measured cytokine responses in the colon and plasma and histopathological changes in the colon. MiRNA changes and T cell population changes were measured in mesenteric lymph nodes.

Research results

While *H. muridarum* infection alone did not cause clinical symptoms, it did cause colonic inflammation and induced proinflammatory cytokines. As expected, *H. muridarum* worsened colitis caused by DSS treatment, but it did not prevent amelioration of colitis by I3C treatment. Both the miRNA changes and cytokine responses to *H. muridarum* infection were similar to those seen in human IBD and due to DSS treatment. Changes in cytokines and miRNA were consistent with a Th17 response.

Research conclusions

H. muridarum causes subclinical colitis that increases vulnerability to DSS treatment. Since I3C is an aryl hydrocarbon receptor agonist, the efficacy of I3C in the presence of *H. muridarum* suggests that *H. muridarum* does not influence the aryl hydrocarbon receptor agonist pathway. The strong similarities between cytokine and miRNA profiles induced by DSS and those induced by *H. muridarum* suggest that similar mechanisms could be at play and that the mouse model is suitable for studying host interactions with EHH species.

Research perspectives

This research supports the hypothesis that EHH species could contribute to human IBD by exacerbating the response to other inflammatory stimuli. More research is needed on the prevalence of EHH species in humans and the mechanisms underlying EHH-mediated colonic damage.

REFERENCES

1 **Ng SC**, Shi HY, Hamidi N, Underwood FE, Tang W, Benchimol EI, Panaccione R, Ghosh S, Wu JCY, Chan FKL, Sung JJY, Kaplan GG. Worldwide incidence and prevalence of inflammatory bowel disease in the 21st century: a systematic review of population-based studies. *Lancet* 2018; **390**: 2769-2778 [PMID: 29050646 DOI: 10.1016/S0140-6736(17)32448-0]

2 **Dahlhamer JM**, Zammitti EP, Ward BW, Wheaton AG, Croft JB. Prevalence of Inflammatory Bowel Disease Among Adults Aged ≥18 Years - United States, 2015. *MMWR Morb Mortal Wkly Rep* 2016; **65**: 1166-1169 [PMID: 27787492 DOI: 10.15585/mmwr.mm6542a3]

3 **Mehta F**. Report: economic implications of inflammatory bowel disease and its management. *Am J Manag Care* 2016; **22**: s51-s60 [PMID: 27269903]

4 **Geremia A**, Biancheri P, Allan P, Corazza GR, Di Sabatino A. Innate and adaptive immunity in inflammatory bowel disease. *Autoimmun Rev* 2014; **13**: 3-10 [PMID: 23774107 DOI: 10.1016/j.autrev.2013.06.004]

5 **Testerman TL**, Morris J. Beyond the stomach: an updated view of Helicobacter pylori pathogenesis, diagnosis, and treatment. *World J Gastroenterol* 2014; **20**: 12781-12808 [PMID: 25278678 DOI:

10.3748/wjg.v20.i36.12781]
6 **Fox JG**. The non-H pylori helicobacters: their expanding role in gastrointestinal and systemic diseases. *Gut* 2002; **50**: 273-283 [PMID: 11788573 DOI: 10.1136/gut.50.2.273]
7 **Fox JG**, Ge Z, Whary MT, Erdman SE, Horwitz BH. Helicobacter hepaticus infection in mice: models for understanding lower bowel inflammation and cancer. *Mucosal Immunol* 2011; **4**: 22-30 [PMID: 20944559 DOI: 10.1038/mi.2010.61]
8 **Saunders KE**, Shen Z, Dewhirst FE, Paster BJ, Dangler CA, Fox JG. Novel intestinal Helicobacter species isolated from cotton-top tamarins (Saguinus oedipus) with chronic colitis. *J Clin Microbiol* 1999; **37**: 146-151 [PMID: 9854080 DOI: 10.1128/JCM.37.1.146-151.1999]
9 **Yu Q**, Zhang S, Li L, Xiong L, Chao K, Zhong B, Li Y, Wang H, Chen M. Enterohepatic Helicobacter Species as a Potential Causative Factor in Inflammatory Bowel Disease: A Meta-Analysis. *Medicine (Baltimore)* 2015; **94**: e1773 [PMID: 26559250 DOI: 10.1097/MD.0000000000001773]
10 **Laharie D**, Asencio C, Asselineau J, Bulois P, Bourreille A, Moreau J, Bonjean P, Lamarque D, Pariente A, Soulé JC, Charachon A, Coffin B, Perez P, Mégraud F, Zerbib F. Association between entero-hepatic Helicobacter species and Crohn's disease: a prospective cross-sectional study. *Aliment Pharmacol Ther* 2009; **30**: 283-293 [PMID: 19438427 DOI: 10.1111/j.1365-2036.2009.04034.x]
11 **Man SM**, Zhang L, Day AS, Leach S, Mitchell H. Detection of enterohepatic and gastric helicobacter species in fecal specimens of children with Crohn's disease. *Helicobacter* 2008; **13**: 234-238 [PMID: 18665930 DOI: 10.1111/j.1523-5378.2008.00607.x]
12 **Phillips MW**, Lee A. Isolation and characterization of a spiral bacterium from the crypts of rodent gastrointestinal tracts. *Appl Environ Microbiol* 1983; **45**: 675-683 [PMID: 6402981 DOI: 10.1128/AEM.45.2.675-683.1983]
13 **Jiang HQ**, Kushnir N, Thurnheer MC, Bos NA, Cebra JJ. Monoassociation of SCID mice with Helicobacter muridarum, but not four other enterics, provokes IBD upon receipt of T cells. *Gastroenterology* 2002; **122**: 1346-1354 [PMID: 11984521 DOI: 10.1053/gast.2002.32959]
14 **Lee A**, Chen M, Coltro N, O'Rourke J, Hazell S, Hu P, Li Y. Long term infection of the gastric mucosa with Helicobacter species does induce atrophic gastritis in an animal model of Helicobacter pylori infection. *Zentralbl Bakteriol* 1993; **280**: 38-50 [PMID: 8280955 DOI: 10.1016/s0934-8840(11)80939-4]
15 **Queiroz DM**, Contigli C, Coimbra RS, Nogueira AM, Mendes EN, Rocha GA, Moura SB. Spiral bacterium associated with gastric, ileal and caecal mucosa of mice. *Lab Anim* 1992; **26**: 288-294 [PMID: 1447907 DOI: 10.1258/002367792780745760]
16 **Okayasu I**, Hatakeyama S, Yamada M, Ohkusa T, Inagaki Y, Nakaya R. A novel method in the induction of reliable experimental acute and chronic ulcerative colitis in mice. *Gastroenterology* 1990; **98**: 694-702 [PMID: 1688816 DOI: 10.1016/0016-5085(90)90290-h]
17 **Perše M**, Cerar A. Dextran sodium sulphate colitis mouse model: traps and tricks. *J Biomed Biotechnol* 2012; **2012**: 718617 [PMID: 22665990 DOI: 10.1155/2012/718617]
18 **Laroui H**, Ingersoll SA, Liu HC, Baker MT, Ayyadurai S, Charania MA, Laroui F, Yan Y, Sitaraman SV, Merlin D. Dextran sodium sulfate (DSS) induces colitis in mice by forming nano-lipocomplexes with medium-chain-length fatty acids in the colon. *PLoS One* 2012; **7**: e32084 [PMID: 22427817 DOI: 10.1371/journal.pone.0032084]
19 **Singh UP**, Murphy AE, Enos RT, Shamran HA, Singh NP, Guan H, Hegde VL, Fan D, Price RL, Taub DD, Mishra MK, Nagarkatti M, Nagarkatti PS. miR-155 deficiency protects mice from experimental colitis by reducing T helper type 1/type 17 responses. *Immunology* 2014; **143**: 478-489 [PMID: 24891206 DOI: 10.1111/imm.12328]
20 **Kimura A**, Naka T, Nohara K, Fujii-Kuriyama Y, Kishimoto T. Aryl hydrocarbon receptor regulates Stat1 activation and participates in the development of Th17 cells. *Proc Natl Acad Sci USA* 2008; **105**: 9721-9726 [PMID: 18607004 DOI: 10.1073/pnas.0804231105]
21 **Quintana FJ**, Basso AS, Iglesias AH, Korn T, Farez MF, Bettelli E, Caccamo M, Oukka M, Weiner HL. Control of T(reg) and T(H)17 cell differentiation by the aryl hydrocarbon receptor. *Nature* 2008; **453**: 65-71 [PMID: 18362915 DOI: 10.1038/nature06880]
22 **Veldhoen M**. Direct interactions between intestinal immune cells and the diet. *Cell Cycle* 2012; **11**: 426-427 [PMID: 22262170 DOI: 10.4161/cc.11.3.19163]
23 **Hanieh H**. Toward understanding the role of aryl hydrocarbon receptor in the immune system: current progress and future trends. *Biomed Res Int* 2014; **2014**: 520763 [PMID: 24527450 DOI: 10.1155/2014/520763]
24 **Busbee PB**, Nagarkatti M, Nagarkatti PS. Natural indoles, indole-3-carbinol (I3C) and 3,3'-diindolylmethane (DIM), attenuate staphylococcal enterotoxin B-mediated liver injury by downregulating miR-31 expression and promoting caspase-2-mediated apoptosis. *PLoS One* 2015; **10**: e0118506 [PMID: 25706292 DOI: 10.1371/journal.pone.0118506]
25 **Wang X**, He H, Lu Y, Ren W, Teng KY, Chiang CL, Yang Z, Yu B, Hsu S, Jacob ST, Ghoshal K, Lee LJ. Indole-3-carbinol inhibits tumorigenicity of hepatocellular carcinoma cells via suppression of microRNA-21 and upregulation of phosphatase and tensin homolog. *Biochim Biophys Acta* 2015; **1853**: 244-253 [PMID: 25447674 DOI: 10.1016/j.bbamcr.2014.10.017]
26 **Licznerska B**, Baer-Dubowska W. Indole-3-Carbinol and Its Role in Chronic Diseases. *Adv Exp Med Biol* 2016; **928**: 131-154 [PMID: 27671815 DOI: 10.1007/978-3-319-41334-1_6]
27 **Miska EA**. How microRNAs control cell division, differentiation and death. *Curr Opin Genet Dev* 2005; **15**: 563-568 [PMID: 16099643 DOI: 10.1016/j.gde.2005.08.005]
28 **Xu XM**, Zhang HJ. miRNAs as new molecular insights into inflammatory bowel disease: Crucial regulators in autoimmunity and inflammation. *World J Gastroenterol* 2016; **22**: 2206-2218 [PMID: 26900285 DOI: 10.3748/wjg.v22.i7.2206]
29 **McKenna LB**, Schug J, Vourekas A, McKenna JB, Bramswig NC, Friedman JR, Kaestner KH. MicroRNAs control intestinal epithelial differentiation, architecture, and barrier function. *Gastroenterology* 2010; **139**: 1654-1664, 1664.e1 [PMID: 20659473 DOI: 10.1053/j.gastro.2010.07.040]
30 **Geginat J**, Paroni M, Maglie S, Alfen JS, Kastirr I, Gruarin P, De Simone M, Pagani M, Abrignani S. Plasticity of human CD4 T cell subsets. *Front Immunol* 2014; **5**: 630 [PMID: 25566245 DOI:

10.3389/fimmu.2014.00630]
31 **Maloy KJ**, Powrie F. Intestinal homeostasis and its breakdown in inflammatory bowel disease. *Nature* 2011; **474**: 298-306 [PMID: 21677746 DOI: 10.1038/nature10208]
32 **Feng S**, Ku K, Hodzic E, Lorenzana E, Freet K, Barthold SW. Differential detection of five mouse-infecting helicobacter species by multiplex PCR. *Clin Diagn Lab Immunol* 2005; **12**: 531-536 [PMID: 15817762 DOI: 10.1128/CDLI.12.4.531-536.2005]
33 **Kim JJ**, Shajib MS, Manocha MM, Khan WI. Investigating intestinal inflammation in DSS-induced model of IBD. *J Vis Exp* 2012 [PMID: 22331082 DOI: 10.3791/3678]
34 **Cooper HS**, Murthy SN, Shah RS, Sedergran DJ. Clinicopathologic study of dextran sulfate sodium experimental murine colitis. *Lab Invest* 1993; **69**: 238-249 [PMID: 8350599]
35 **Monceaux CP**, Testerman TL, Boktor M, Jordan P, Adegboyega P, McGee DJ, Jennings MH, Parker CP, Gupta S, Yi P, Ganta VC, Galous H, Manas K, Alexander JS. Helicobacter infection decreases basal colon inflammation, but increases disease activity in experimental IBD. *Open Journal of Gastroenterology* 2013; **3**: 177-189 [DOI: 10.4236/ojgas.2013.33029]
36 **Bam M**, Yang X, Zumbrun EE, Zhong Y, Zhou J, Ginsberg JP, Leyden Q, Zhang J, Nagarkatti PS, Nagarkatti M. Dysregulated immune system networks in war veterans with PTSD is an outcome of altered miRNA expression and DNA methylation. *Sci Rep* 2016; **6**: 31209 [PMID: 27510991 DOI: 10.1038/srep31209]
37 **Bam M**, Yang X, Zumbrun EE, Ginsberg JP, Leyden Q, Zhang J, Nagarkatti PS, Nagarkatti M. Decreased AGO2 and DCR1 in PBMCs from War Veterans with PTSD leads to diminished miRNA resulting in elevated inflammation. *Transl Psychiatry* 2017; **7**: e1222 [PMID: 28850112 DOI: 10.1038/tp.2017.185]
38 **Sturn A**, Quackenbush J, Trajanoski Z. Genesis: cluster analysis of microarray data. *Bioinformatics* 2002; **18**: 207-208 [PMID: 11836235 DOI: 10.1093/bioinformatics/18.1.207]
39 **Laferriere NR**, Kurata WE, Grayson CT 3rd, Stecklow KM, Pierce LM. Inhibition of microRNA-124-3p as a novel therapeutic strategy for the treatment of Gulf War Illness: Evaluation in a rat model. *Neurotoxicology* 2019; **71**: 16-30 [PMID: 30503814 DOI: 10.1016/j.neuro.2018.11.008]
40 **Becker W**, Nagarkatti M, Nagarkatti PS. miR-466a Targeting of TGF-β2 Contributes to FoxP3$^+$ Regulatory T Cell Differentiation in a Murine Model of Allogeneic Transplantation. *Front Immunol* 2018; **9**: 688 [PMID: 29686677 DOI: 10.3389/fimmu.2018.00688]
41 **Singh Y**, Garden OA, Lang F, Cobb BS. MicroRNA-15b/16 Enhances the Induction of Regulatory T Cells by Regulating the Expression of Rictor and mTOR. *J Immunol* 2015; **195**: 5667-5677 [PMID: 26538392 DOI: 10.4049/jimmunol.1401875]
42 **Rouse M**, Rao R, Nagarkatti M, Nagarkatti PS. 3,3'-diindolylmethane ameliorates experimental autoimmune encephalomyelitis by promoting cell cycle arrest and apoptosis in activated T cells through microRNA signaling pathways. *J Pharmacol Exp Ther* 2014; **350**: 341-352 [PMID: 24898268 DOI: 10.1124/jpet.114.214742]
43 **Iborra M**, Bernuzzi F, Correale C, Vetrano S, Fiorino G, Beltrán B, Marabita F, Locati M, Spinelli A, Nos P, Invernizzi P, Danese S. Identification of serum and tissue micro-RNA expression profiles in different stages of inflammatory bowel disease. *Clin Exp Immunol* 2013; **173**: 250-258 [PMID: 23607522 DOI: 10.1111/cei.12104]
44 **Coskun M**, Bjerrum JT, Seidelin JB, Troelsen JT, Olsen J, Nielsen OH. miR-20b, miR-98, miR-125b-1*, and let-7e* as new potential diagnostic biomarkers in ulcerative colitis. *World J Gastroenterol* 2013; **19**: 4289-4299 [PMID: 23885139 DOI: 10.3748/wjg.v19.i27.4289]
45 **Takagi T**, Naito Y, Mizushima K, Hirata I, Yagi N, Tomatsuri N, Ando T, Oyamada Y, Isozaki Y, Hongo H, Uchiyama K, Handa O, Kokura S, Ichikawa H, Yoshikawa T. Increased expression of microRNA in the inflamed colonic mucosa of patients with active ulcerative colitis. *J Gastroenterol Hepatol* 2010; **25** Suppl 1: S129-S133 [PMID: 20586854 DOI: 10.1111/j.1440-1746.2009.06216.x]
46 **Bian Z**, Li L, Cui J, Zhang H, Liu Y, Zhang CY, Zen K. Role of miR-150-targeting c-Myb in colonic epithelial disruption during dextran sulphate sodium-induced murine experimental colitis and human ulcerative colitis. *J Pathol* 2011; **225**: 544-553 [PMID: 21590770 DOI: 10.1002/path.2907]
47 **Jantchou P**, Monnet E, Carbonnel F. [Environmental risk factors in Crohn's disease and ulcerative colitis (excluding tobacco and appendicectomy)]. *Gastroenterol Clin Biol* 2006; **30**: 859-867 [PMID: 16885870 DOI: 10.1016/s0399-8320(06)73333-4]
48 **Fox JG**, Boutin SR, Handt LK, Taylor NS, Xu S, Rickman B, Marini RP, Dewhirst FE, Paster BJ, Motzel S, Klein HJ. Isolation and characterization of a novel helicobacter species, "Helicobacter macacae," from rhesus monkeys with and without chronic idiopathic colitis. *J Clin Microbiol* 2007; **45**: 4061-4063 [PMID: 17928421 DOI: 10.1128/JCM.01100-07]
49 **Tankovic J**, Smati M, Lamarque D, Delchier JC. First detection of Helicobacter canis in chronic duodenal ulcerations from a patient with Crohn's disease. *Inflamm Bowel Dis* 2011; **17**: 1830-1831 [PMID: 21744440 DOI: 10.1002/ibd.21610]
50 **Hyun YS**, Han DS, Lee AR, Eun CS, Youn J, Kim HY. Role of IL-17A in the development of colitis-associated cancer. *Carcinogenesis* 2012; **33**: 931-936 [PMID: 22354874 DOI: 10.1093/carcin/bgs106]
51 **Martin M**, Kesselring RK, Saidou B, Brunner SM, Schiechl G, Mouris VF, Wege AK, Rümmele P, Schlitt HJ, Geissler EK, Fichtner-Feigl S. RORγt(+) hematopoietic cells are necessary for tumor cell proliferation during colitis-associated tumorigenesis in mice. *Eur J Immunol* 2015; **45**: 1667-1679 [PMID: 25820779 DOI: 10.1002/eji.201444915]
52 **Caruso R**, Fina D, Paoluzi OA, Del Vecchio Blanco G, Stolfi C, Rizzo A, Caprioli F, Sarra M, Andrei F, Fantini MC, MacDonald TT, Pallone F, Monteleone G. IL-23-mediated regulation of IL-17 production in Helicobacter pylori-infected gastric mucosa. *Eur J Immunol* 2008; **38**: 470-478 [PMID: 18200634 DOI: 10.1002/eji.200737635]
53 **Chang LL**, Hsu WH, Kao MC, Chou CC, Lin CC, Liu CJ, Weng BC, Kuo FC, Kuo CH, Lin MH, Wang CJ, Lin CH, Wu DC, Huang SK. Stromal C-type lectin receptor COLEC12 integrates H. pylori, PGE2-EP2/4 axis and innate immunity in gastric diseases. *Sci Rep* 2018; **8**: 3821 [PMID: 29491476 DOI: 10.1038/s41598-018-20957-2]
54 **Bagheri N**, Razavi A, Pourgheysari B, Azadegan-Dehkordi F, Rahimian G, Pirayesh A, Shafigh M,

Rafieian-Kopaei M, Fereidani R, Tahmasbi K, Shirzad H. Up-regulated Th17 cell function is associated with increased peptic ulcer disease in Helicobacter pylori-infection. *Infect Genet Evol* 2018; **60**: 117-125 [PMID: 29481961 DOI: 10.1016/j.meegid.2018.02.020]

55 **Luther J**, Dave M, Higgins PD, Kao JY. Association between Helicobacter pylori infection and inflammatory bowel disease: a meta-analysis and systematic review of the literature. *Inflamm Bowel Dis* 2010; **16**: 1077-1084 [PMID: 19760778 DOI: 10.1002/ibd.21116]

56 **Dijkstra G**, Yuvaraj S, Jiang HQ, Bun JC, Moshage H, Kushnir N, Peppelenbosch MP, Cebra JJ, Bos NA. Early bacterial dependent induction of inducible nitric oxide synthase (iNOS) in epithelial cells upon transfer of CD45RB(high) CD4(+) T cells in a model for experimental colitis. *Inflamm Bowel Dis* 2007; **13**: 1467-1474 [PMID: 17879278 DOI: 10.1002/ibd.20262]

57 **Ma X**, Zhou J, Zhong Y, Jiang L, Mu P, Li Y, Singh N, Nagarkatti M, Nagarkatti P. Expression, regulation and function of microRNAs in multiple sclerosis. *Int J Med Sci* 2014; **11**: 810-818 [PMID: 24936144 DOI: 10.7150/ijms.8647]

58 **Zhou J**, Nagarkatti P, Zhong Y, Ginsberg JP, Singh NP, Zhang J, Nagarkatti M. Dysregulation in microRNA expression is associated with alterations in immune functions in combat veterans with post-traumatic stress disorder. *PLoS One* 2014; **9**: e94075 [PMID: 24759737 DOI: 10.1371/journal.pone.0094075]

59 **Hippen KL**, Loschi M, Nicholls J, MacDonald KPA, Blazar BR. Effects of MicroRNA on Regulatory T Cells and Implications for Adoptive Cellular Therapy to Ameliorate Graft-versus-Host Disease. *Front Immunol* 2018; **9**: 57 [PMID: 29445371 DOI: 10.3389/fimmu.2018.00057]

60 **Yao R**, Ma YL, Liang W, Li HH, Ma ZJ, Yu X, Liao YH. MicroRNA-155 modulates Treg and Th17 cells differentiation and Th17 cell function by targeting SOCS1. *PLoS One* 2012; **7**: e46082 [PMID: 23091595 DOI: 10.1371/journal.pone.0046082]

61 **Giza DE**, Vasilescu C, Calin GA. Key principles of miRNA involvement in human diseases. *Discoveries (Craiova)* 2014; **2**: e34 [PMID: 26317116 DOI: 10.15190/d.2014.26]

62 **Huang Z**, Ma J, Chen M, Jiang H, Fu Y, Gan J, Dong L, Zhang J, Chen J. Dual TNF-α/IL-12p40 Interference as a Strategy to Protect Against Colitis Based on miR-16 Precursors With Macrophage Targeting Vectors. *Mol Ther* 2015; **23**: 1611-1621 [PMID: 26073885 DOI: 10.1038/mt.2015.111]

63 **Kanaan Z**, Rai SN, Eichenberger MR, Barnes C, Dworkin AM, Weller C, Cohen E, Roberts H, Keskey B, Petras RE, Crawford NP, Galandiuk S. Differential microRNA expression tracks neoplastic progression in inflammatory bowel disease-associated colorectal cancer. *Hum Mutat* 2012; **33**: 551-560 [PMID: 22241525 DOI: 10.1002/humu.22021]

64 **Min M**, Peng LH, Sun G, Guo MZ, Qiu ZW, Yang YS. Aquaporin 8 expression is reduced and regulated by microRNAs in patients with ulcerative colitis. *Chin Med J (Engl)* 2013; **126**: 1532-1537 [PMID: 23595390]

65 **Tian T**, Zhou Y, Feng X, Ye S, Wang H, Wu W, Tan W, Yu C, Hu J, Zheng R, Chen Z, Pei X, Luo H. MicroRNA-16 is putatively involved in the NF-κB pathway regulation in ulcerative colitis through adenosine A2a receptor (A2aAR) mRNA targeting. *Sci Rep* 2016; **6**: 30824 [PMID: 27476546 DOI: 10.1038/srep30824]

66 **Buonpane C**, Ares G, Benyamen B, Yuan C, Hunter CJ. Identification of suitable reference microRNA for qPCR analysis in pediatric inflammatory bowel disease. *Physiol Genomics* 2019; **51**: 169-175 [PMID: 30978148 DOI: 10.1152/physiolgenomics.00126.2018]

67 **Paraskevi A**, Theodoropoulos G, Papaconstantinou I, Mantzaris G, Nikiteas N, Gazouli M. Circulating MicroRNA in inflammatory bowel disease. *J Crohns Colitis* 2012; **6**: 900-904 [PMID: 22386737 DOI: 10.1016/j.crohns.2012.02.006]

68 **Schönauen K**, Le N, von Arnim U, Schulz C, Malfertheiner P, Link A. Circulating and Fecal microRNAs as Biomarkers for Inflammatory Bowel Diseases. *Inflamm Bowel Dis* 2018; **24**: 1547-1557 [PMID: 29668922 DOI: 10.1093/ibd/izy046]

69 **Backteman K**, Andersson C, Dahlin LG, Ernerudh J, Jonasson L. Lymphocyte subpopulations in lymph nodes and peripheral blood: a comparison between patients with stable angina and acute coronary syndrome. *PLoS One* 2012; **7**: e32691 [PMID: 22396788 DOI: 10.1371/journal.pone.0032691]

70 **Reimund JM**, Wittersheim C, Dumont S, Muller CD, Baumann R, Poindron P, Duclos B. Mucosal inflammatory cytokine production by intestinal biopsies in patients with ulcerative colitis and Crohn's disease. *J Clin Immunol* 1996; **16**: 144-150 [PMID: 8734357 DOI: 10.1007/bf01540912]

71 **Reinecker HC**, Steffen M, Witthoeft T, Pflueger I, Schreiber S, MacDermott RP, Raedler A. Enhanced secretion of tumour necrosis factor-alpha, IL-6, and IL-1 beta by isolated lamina propria mononuclear cells from patients with ulcerative colitis and Crohn's disease. *Clin Exp Immunol* 1993; **94**: 174-181 [PMID: 8403503 DOI: 10.1111/j.1365-2249.1993.tb05997.x]

72 **Kamada N**, Hisamatsu T, Okamoto S, Chinen H, Kobayashi T, Sato T, Sakuraba A, Kitazume MT, Sugita A, Koganei K, Akagawa KS, Hibi T. Unique CD14 intestinal macrophages contribute to the pathogenesis of Crohn disease via IL-23/IFN-gamma axis. *J Clin Invest* 2008; **118**: 2269-2280 [PMID: 18497880 DOI: 10.1172/JCI34610]

73 **Globig AM**, Hennecke N, Martin B, Seidl M, Ruf G, Hasselblatt P, Thimme R, Bengsch B. Comprehensive intestinal T helper cell profiling reveals specific accumulation of IFN-γ+IL-17+coproducing CD4+ T cells in active inflammatory bowel disease. *Inflamm Bowel Dis* 2014; **20**: 2321-2329 [PMID: 25248005 DOI: 10.1097/MIB.0000000000000210]

74 **Neurath MF**. Cytokines in inflammatory bowel disease. *Nat Rev Immunol* 2014; **14**: 329-342 [PMID: 24751956 DOI: 10.1038/nri3661]

75 **Ito R**, Shin-Ya M, Kishida T, Urano A, Takada R, Sakagami J, Imanishi J, Kita M, Ueda Y, Iwakura Y, Kataoka K, Okanoue T, Mazda O. Interferon-gamma is causatively involved in experimental inflammatory bowel disease in mice. *Clin Exp Immunol* 2006; **146**: 330-338 [PMID: 17034586 DOI: 10.1111/j.1365-2249.2006.03214.x]

76 **Tripathi SK**, Lahesmaa R. Transcriptional and epigenetic regulation of T-helper lineage specification. *Immunol Rev* 2014; **261**: 62-83 [PMID: 25123277 DOI: 10.1111/imr.12204]

77 **Ganjalikhani Hakemi M**, Ghaedi K, Andalib A, Hosseini M, Rezaei A. Optimization of human Th17 cell differentiation in vitro: evaluating different polarizing factors. *In Vitro Cell Dev Biol Anim* 2011; **47**: 581-592 [PMID: 21853398 DOI: 10.1007/s11626-011-9444-1]

78 **Aggarwal BB**, Ichikawa H. Molecular targets and anticancer potential of indole-3-carbinol and its derivatives. *Cell Cycle* 2005; **4**: 1201-1215 [PMID: 16082211 DOI: 10.4161/cc.4.9.1993]

79 **Weng JR**, Bai LY, Chiu CF, Wang YC, Tsai MH. The dietary phytochemical 3,3'-diindolylmethane induces G2/M arrest and apoptosis in oral squamous cell carcinoma by modulating Akt-NF-κB, MAPK, and p53 signaling. *Chem Biol Interact* 2012; **195**: 224-230 [PMID: 22290291 DOI: 10.1016/j.cbi.2012.01.003]

80 **Zhong MC**, Kerlero de Rosbo N, Ben-Nun A. Multiantigen/multiepitope-directed immune-specific suppression of "complex autoimmune encephalomyelitis" by a novel protein product of a synthetic gene. *J Clin Invest* 2002; **110**: 81-90 [PMID: 12093891 DOI: 10.1172/JCI15692]

81 **Coombes JL**, Robinson NJ, Maloy KJ, Uhlig HH, Powrie F. Regulatory T cells and intestinal homeostasis. *Immunol Rev* 2005; **204**: 184-194 [PMID: 15790359 DOI: 10.1111/j.0105-2896.2005.00250.x]

82 **Sarkar FH**, Li Y. Indole-3-carbinol and prostate cancer. *J Nutr* 2004; **134**: 3493S-3498S [PMID: 15570059 DOI: 10.1093/jn/134.12.3493S]

83 **Adachi J**, Mori Y, Matsui S, Takigami H, Fujino J, Kitagawa H, Miller CA 3rd, Kato T, Saeki K, Matsuda T. Indirubin and indigo are potent aryl hydrocarbon receptor ligands present in human urine. *J Biol Chem* 2001; **276**: 31475-31478 [PMID: 11425848 DOI: 10.1074/jbc.C100238200]

84 **Busbee PB**, Rouse M, Nagarkatti M, Nagarkatti PS. Use of natural AhR ligands as potential therapeutic modalities against inflammatory disorders. *Nutr Rev* 2013; **71**: 353-369 [PMID: 23731446 DOI: 10.1111/nure.12024]

85 **Nguyen NT**, Hanieh H, Nakahama T, Kishimoto T. The roles of aryl hydrocarbon receptor in immune responses. *Int Immunol* 2013; **25**: 335-343 [PMID: 23580432 DOI: 10.1093/intimm/dxt011]

86 **Veldhoen M**, Hirota K, Westendorf AM, Buer J, Dumoutier L, Renauld JC, Stockinger B. The aryl hydrocarbon receptor links TH17-cell-mediated autoimmunity to environmental toxins. *Nature* 2008; **453**: 106-109 [PMID: 18362914 DOI: 10.1038/nature06881]

87 **Veldhoen M**, Hirota K, Christensen J, O'Garra A, Stockinger B. Natural agonists for aryl hydrocarbon receptor in culture medium are essential for optimal differentiation of Th17 T cells. *J Exp Med* 2009; **206**: 43-49 [PMID: 19114668 DOI: 10.1084/jem.20081438]

88 **Singh NP**, Singh UP, Singh B, Price RL, Nagarkatti M, Nagarkatti PS. Activation of aryl hydrocarbon receptor (AhR) leads to reciprocal epigenetic regulation of FoxP3 and IL-17 expression and amelioration of experimental colitis. *PLoS One* 2011; **6**: e23522 [PMID: 21858153 DOI: 10.1371/journal.pone.0023522]

89 **Nakahama T**, Hanieh H, Nguyen NT, Chinen I, Ripley B, Millrine D, Lee S, Nyati KK, Dubey PK, Chowdhury K, Kawahara Y, Kishimoto T. Aryl hydrocarbon receptor-mediated induction of the microRNA-132/212 cluster promotes interleukin-17-producing T-helper cell differentiation. *Proc Natl Acad Sci U S A* 2013; **110**: 11964-11969 [PMID: 23818645 DOI: 10.1073/pnas.1311087110]

90 **Akimova T**, Xiao H, Liu Y, Bhatti TR, Jiao J, Eruslanov E, Singhal S, Wang L, Han R, Zacharia K, Hancock WW, Beier UH. Targeting sirtuin-1 alleviates experimental autoimmune colitis by induction of Foxp3+ T-regulatory cells. *Mucosal Immunol* 2014; **7**: 1209-1220 [PMID: 24549276 DOI: 10.1038/mi.2014.10]

91 **Rouse M**, Singh NP, Nagarkatti PS, Nagarkatti M. Indoles mitigate the development of experimental autoimmune encephalomyelitis by induction of reciprocal differentiation of regulatory T cells and Th17 cells. *Br J Pharmacol* 2013; **169**: 1305-1321 [PMID: 23586923 DOI: 10.1111/bph.12205]

92 **Huang Z**, Jiang Y, Yang Y, Shao J, Sun X, Chen J, Dong L, Zhang J. 3,3'-Diindolylmethane alleviates oxazolone-induced colitis through Th2/Th17 suppression and Treg induction. *Mol Immunol* 2013; **53**: 335-344 [PMID: 23085552 DOI: 10.1016/j.molimm.2012.09.007]

93 **Liu Y**, She W, Wang F, Li J, Wang J, Jiang W. 3, 3'-Diindolylmethane alleviates steatosis and the progression of NASH partly through shifting the imbalance of Treg/Th17 cells to Treg dominance. *Int Immunopharmacol* 2014; **23**: 489-498 [PMID: 25281898 DOI: 10.1016/j.intimp.2014.09.024]

94 **Jiang J**, Kang TB, Shim do W, Oh NH, Kim TJ, Lee KH. Indole-3-carbinol inhibits LPS-induced inflammatory response by blocking TRIF-dependent signaling pathway in macrophages. *Food Chem Toxicol* 2013; **57**: 256-261 [PMID: 23597448 DOI: 10.1016/j.fct.2013.03.040]

95 **Cho HJ**, Seon MR, Lee YM, Kim J, Kim JK, Kim SG, Park JH. 3,3'-Diindolylmethane suppresses the inflammatory response to lipopolysaccharide in murine macrophages. *J Nutr* 2008; **138**: 17-23 [PMID: 18156398 DOI: 10.1093/jn/138.1.17]

96 **Mohammadi S**, Memarian A, Sedighi S, Behnampour N, Yazdani Y. Immunoregulatory effects of indole-3-carbinol on monocyte-derived macrophages in systemic lupus erythematosus: A crucial role for aryl hydrocarbon receptor. *Autoimmunity* 2018; **51**: 199-209 [PMID: 30289282 DOI: 10.1080/08916934.2018.1494161]

World Journal of Gastroenterology

Submit a Manuscript: https://www.f6publishing.com

World J Gastroenterol 2020 August 28; 26(32): 4786-4801

DOI: 10.3748/wjg.v26.i32.4786

ISSN 1007-9327 (print) ISSN 2219-2840 (online)

ORIGINAL ARTICLE

Basic Study

Dual targeting of Polo-like kinase 1 and baculoviral inhibitor of apoptosis repeat-containing 5 in TP53-mutated hepatocellular carcinoma

Yan Li, Zhen-Gang Zhao, Yin Luo, Hao Cui, Hao-Yu Wang, Yan-Fang Jia, Ying-Tang Gao

ORCID number: Yan Li 0000-0003-2602-7423; Zhen-Gang Zhao 0000-0001-7249-4474; Yin Luo 0000-0003-0252-0053; Hao Cui 0000-0002-5629-7814; Hao-Yu Wang 0000-0001-6672-2733; Yan-Fang Jia 0000-0002-0974-1337; Ying-Tang Gao 0000-0002-5564-1986.

Author contributions: Li Y, Zhao ZG, Luo Y, and Jia YF performed the majority of experiments and analyzed the data; Cui H and Wang HY were responsible for animal experiments; Li Y and Gao YT designed and coordinated the research; Li Y, Luo Y, and Gao YT wrote the paper; all authors approved the final version of the article.

Supported by National Science and Technology Major Project, No. 2018ZX10732-202-004; Tianjin Science and Technology Plan Project, No. 17JCYBJC26100 and No. 19ZXDBSY00030.

Institutional review board statement: This study/paper was reviewed and approved by the Ethics Committee of Tianjin Third Central Hospital.

Institutional animal care and use committee statement: All animal experiments and procedures were

Yan Li, Zhen-Gang Zhao, Hao Cui, Hao-Yu Wang, Department of Hepatology, Nankai University Affiliated Third Center Hospital, Tianjin 300170, China

Yin Luo, Ying-Tang Gao, Tianjin Key Laboratory of Extracorporeal Life Support for Critical Diseases, Institute of Hepatobiliary Disease, Nankai University Affiliated Third Center Hospital, Tianjin 300170, China

Yan-Fang Jia, Tianjin Key Laboratory of Extracorporeal Life Support for Critical Diseases, Tianjin Medical University Third Center Clinical College, Tianjin 300170, China

Corresponding author: Ying-Tang Gao, PhD, Professor, Tianjin Key Laboratory of Extracorporeal Life Support for Critical Diseases, Institute of Hepatobiliary Disease, Nankai University Affiliated Third Center Hospital, No. 83, Jintang Road, Hedong District, Tianjin 300170, China. gaoyt816@163.com

Abstract

BACKGROUND

Hepatocellular carcinoma (HCC), often diagnosed at advanced stages without curative therapies, is the fifth most common malignant cancer and the second leading cause of cancer-related mortality. Polo-like kinase 1 (PLK1) is activated in the late G2 phase of the cell cycle and is required for entry to mitosis. Interestingly, PLK1 is overexpressed in many HCC patients and is highly associated with poor clinical outcome. Baculoviral inhibitor of apoptosis repeat-containing 5 (BIRC5) is also highly overexpressed in HCC and plays key roles in this malignancy.

AIM

To determine the expression patterns of PLK1 and BIRC5, as well as their correlation with p53 mutation status and patient clinical outcome.

METHODS

The expression patterns of PLK1 and BIRC5, and their correlation with p53 mutation status or patient clinical outcome were analyzed using a TCGA HCC dataset. Cell viability, cell apoptosis, and cell cycle arrest assays were conducted to investigate the efficacy of the PLK1 inhibitors volasertib and GSK461364 and the BIRC5 inhibitor YM155, alone or in combination. The *in vivo* efficacy of

volasertib and YM155, alone or in combination, was assessed in p53-mutated Huh7-derived xenograft models in immune-deficient NSIG mice.

RESULTS

Our bioinformatics analysis using a TCGA HCC dataset revealed that PLK1 and BIRC5 were overexpressed in the same patient subset and their expression was highly correlated. The overexpression of both PLK1 and BIRC5 was more frequently detected in HCC with p53 mutations. High PLK1 or BIRC5 expression significantly correlated with poor clinical outcome. PLK1 inhibitors (volasertib and GSK461364) or a BIRC5 inhibitor (YM155) selectively targeted Huh7 cells with mutated p53, but not HepG2 cells with wild-type p53. The combination treatment of volasertib and YM155 synergistically inhibited the viability of Huh7 cells *via* apoptotic pathway. The efficacy of volasertib and YM155, alone or in combination, was validated *in vivo* in a Huh7-derived xenograft model.

CONCLUSION

PLK1 and BIRC5 are highly co-expressed in p53-mutated HCC and inhibition of both PLK1 and BIRC5 synergistically compromises the viability of p53-mutated HCC cells *in vitro* and *in vivo*.

Key words: Polo-like kinase 1; Baculoviral inhibitor of apoptosis repeat-containing 5; p53; Co-expression; Hepatocellular carcinoma; Bioinformatics analysis

Core tip: A bioinformatics analysis using a TCGA hepatocellular carcinoma (HCC) dataset revealed that Polo-like kinase 1 (PLK1) and baculoviral inhibitor of apoptosis repeat-containing 5 (BIRC5) were overexpressed in the same patient subset and their expression was highly correlated. Overexpression of both PLK1 and BIRC5 was more frequently detected in HCC with p53 mutations. High PLK1 or BIRC5 expression significantly correlated with poor clinical outcome. The PLK1 inhibitors volasertib and GSK461364 or BIRC5 inhibitor YM155 selectively targeted Huh7 cells with mutated p53, but not HepG2 cells with wild-type p53. Combination treatment with volasertib and YM155 synergistically inhibited the viability of Huh7 cells by inducing apoptosis. The efficacy of volasertib and YM155, alone or in combination, was validated *in vivo* in a Huh7-derived xenograft model in immuno-deficient NSIG mice.

Citation: Li Y, Zhao ZG, Luo Y, Cui H, Wang HY, Jia YF, Gao YT. Dual targeting of Polo-like kinase 1 and baculoviral inhibitor of apoptosis repeat-containing 5 in TP53-mutated hepatocellular carcinoma. *World J Gastroenterol* 2020; 26(32): 4786-4801
URL: https://www.wjgnet.com/1007-9327/full/v26/i32/4786.htm
DOI: https://dx.doi.org/10.3748/wjg.v26.i32.4786

INTRODUCTION

According to the World Health Organization: GLOBOCAN, hepatocellular carcinoma (HCC) is the fifth most common cancer worldwide. More than 800000 new cases are diagnosed each year, and China alone accounts for more than half (55%) of all cases[1]. Most HCC patients (80%) are diagnosed at advanced stages, with a median survival of only 6-8 mo due to the lack of effective therapies. Overall, HCC has an extremely high mortality rate (95%) and is the second leading cause of cancer mortality. The most common risk factors for HCC are chronic infection with two liver tropic viruses [hepatitis B virus (HBV) and hepatitis C virus (HCV)], exposure to dietary aflatoxin B1, or alcohol consumption, all of which can lead to liver cirrhosis[2].

In recent years, extensive efforts have focused on the molecular carcinogenesis of HCC. The tumor suppressor p53 is one of the most frequently mutated genes in all cancers, including HCC[3-7]. Mutations in p53 resulting in p53 inactivation or gain of function significantly contribute to disease malignancies; chemo-resistance to cisplatin (CDDP), doxorubicin, and 5-fluorouracil (5-FU); and drug resistance to targeted therapies including histone deacetylase inhibitors[8,9].

conducted under the protocol approved by the Animal Care and Use Committee of Nankai University.

Conflict-of-interest statement: All authors have nothing to disclose.

Data sharing statement: No additional data are available.

ARRIVE guidelines statement: The authors have read the ARRIVE guidelines, and the manuscript was prepared and revised according to the ARRIVE guidelines.

Manuscript source: Unsolicited manuscript

Received: May 7, 2020
Peer-review started: May 7, 2020
First decision: May 21, 2020
Revised: June 4, 2020
Accepted: August 4, 2020
Article in press: August 4, 2020
Published online: August 28, 2020

P-Reviewer: Pandey V
S-Editor: Gong ZM
L-Editor: Wang TQ
P-Editor: Ma YJ

Cell cycle dysregulation and apoptosis are essential cellular processes required for cancer cells to survive, proliferate, and evade immune elimination and therapeutic treatments. Polo-like kinase 1 (PLK1) is a master cell cycle regulator in mitosis that mediates centrosome disjunction and movement, CDK1/cyclin B activation, spindle assembly, and cytokinesis[10,11]. PLK1 has been shown to be an oncogene in many cancer types including HCC[12]. PLK1 expression is tightly regulated in a cell cycle-dependent manner in normal cells and is upregulated in various cancers[13-15], suggesting that it is a promising therapeutic target. Indeed, it has been shown that PLK1 inhibitors have potent activity in targeting various cancer types, including HCC.

Baculoviral inhibitor of apoptosis repeat-containing 5 (BIRC5), also known as Survivin, is the smallest family member of the inhibitor of apoptosis (IAP) proteins. BIRC5 expression is tightly regulated and only expressed during G2-M phase in normal cells[16]. Transcriptomic analysis identified BIRC5 as the fourth most highly transcribed gene in cancer cells compared to normal cells[17]. BIRC5 is a multifunctional protein that regulates chromosome segregation and cytokinesis during the cell cycle and promotes cell survival by inhibiting both intrinsic and extrinsic apoptosis pathways[16]. Furthermore, suppression of BIRC5 expression in cancer cells induces cell apoptosis and growth inhibition[16-18].

However, how p53, PLK1, and BIRC5 interact in HCC has not been well defined. In this study, we revealed that PLK1 and BIRC5 are significantly co-expressed in HCC together with a number of other important cell cycle factors. More interestingly, PLK1 and BIRC5 expression were observed to be highly upregulated in HCC cells with mutated p53 compared to those wild-type p53. Both PLK1 inhibitors and a BIRC5 inhibitor selectively targeted p53-mutated HCC cells. Furthermore, dual targeting of PLK1 and BIRC5 showed synergistic effects both *in vitro* and *in vivo* in p53-mutated cells and their derived xenografts.

MATERIALS AND METHODS

Cells and reagents

HepG2 and Huh7 cell lines were obtained from our laboratory for long-term storage. The cells were cultured in DMEM (high glucose) containing 10% fetal bovine serum and 1% penicillin/streptomycin. GSK461364 (S2193), volasertib (S2235), and YM155 (S1130) were purchased from Selleck. A CellTiter-Glo 2.0 cell viability assay kit (G9241) was purchased from Promega. Annexin V-FITC (Cat#: 1001) and propidium iodide (Cat#: 1056) were purchased from BioVision.

Bioinformatic analysis

The Liver Hepatocellular Carcinoma (TCGA, PanCancer Atlas) dataset was downloaded from the Cancer Genome Atlas website. The data were normalized using the RNA-Seq with the Expectation Maximization (RSEM) algorithm[19]. Co-expression data were downloaded using cBioPortal and the co-expression heatmap was generated using GraphPad Prism. Individual pairs of co-expressed gene plots, differential expression of PLK1 and BIRC5 in p53/RB1-wild-type and -mutated HCC patients, and the PLK1 and BIRC5 associated pathway networks were generated using cBioPortal. The Wilcoxon rank-sum test was used to assess the differences in PLK1 and BIRC5 expression between groups. For both overall clinical survival and disease/progression-free survival analysis, we generated Kaplan-Meier survival plots using the cBioPortal to compare patients with high PLK1 or BIRC5 expression levels and those with low PLK1 or BIRC5 levels. The log-rank test was used to compare the survival distribution between patients with differential expression of PLK1 or BIRC5.

Cell viability assay

The cell viability assay was performed following the manufacturer's instructions. Briefly, 2000 HepG2 or Huh7 cells were seeded into each well of white 96-well plates overnight. The cells were then treated with a 2-fold serial dilution of GSK461364 (0-50 nM), volasertib (0-50 nmol/L), or YM155 (0-20 M). At 72 h post treatment, the cells were lysed using CellTiter-Glo 2.0 Reagent, and cell viability was then measured using a VICTOR Nivo Multimode Microplate Reader from PerkinElmer.

Cell apoptosis assay

The cell apoptosis assay was performed following the manufacturer's instructions. Briefly, 100000 HepG2 or Huh7 cells were seeded into each well of 6-well plates

overnight. The cells were then treated with GSK461364, volasertib, or YM155. At 24 h post treatment, all the cells, including attached and detached cells, were harvested by trypsin treatment. Subsequently, the cells were stained with annexin V and propidium iodide, and analyzed by flow cytometry. Then, the percentage of annexin V-positive cells for each sample was calculated and plotted.

Cell cycle arrest assay

To assess cell cycle arrest, 100000 HepG2 or Huh7 cells were seeded into each well of 6-well plates overnight. The cells were then treated with GSK461364, volasertib, or YM155. At 24 h post treatment, all the cells, including attached and detached cells, were harvested by trypsin treatment. Subsequently, the cells were fixed with chilled 100% ethanol, stained with propidium iodide, and analyzed by flow cytometry. Then, the percentage of each cell cycle phase for each sample was calculated and plotted.

Mouse xenograft tumor model

All animal experiments and procedures were conducted under the protocol approved by the Animal Care and Use Committee at Nankai University. Eight-week-old male NOD-PrkdcscidIL2rgtm1-HFK (NSIG) mice were purchased from Beijing HFK Bioscience Co. Ltd. The mice were fed in a controlled environment (22 ± 2 °C, 50% ± 10% humidity, 12-h light/dark cycle, free access to water and standard diet). After 1 week of adaptive feeding, the mice were subcutaneously injected with 2×10^6 of Huh7 cells that had been harvested from cell culture and suspended in a 2:1 mixture of appropriate medium and Matrigel. Following cell inoculation, the mice were monitored daily for tumor engraftment and health conditions. When the tumor size became palpable, the mice were treated with vehicle or volasertib (10 mg/kg) weekly for 4 wk *via* the intraperitoneal route or received a continuous infusion of YM155 (3 mg/kg) for 7 d and off for the last 3 wk using a Alzet Osmotic pumps (Model 1007D), alone or in combination. The tumor growth and mouse health conditions were monitored daily and body weight was measured every week. At the end of the 4-wk treatment, the mice were euthanized using CO_2, and the tumor mass was dissected, weighed, and imaged.

Statistical analysis

Statistical analyses were performed with SPSS 22.0. The results are presented as the means ± SD from at least three independent experiments. Differences among multiple groups were analyzed using one-way ANOVA, while comparisons between two groups were conducted using Student's *t*-test. A P value of < 0.05 was considered statistically significant.

RESULTS

PLK1 and BIRC5 co-expressed in HCC cells

Both PLK1 and BIRC5 are expressed at the G2/M phase and play key roles in regulating the cell cycle in normal cells[10,11,16]. The expression of PLK1 and BIRC5 is frequently upregulated in cancer cells[12,17,18]. To assess the expression of PLK1 and BIRC5 in HCC tumor cells, we analyzed a transcriptome dataset (n = 374) available at TCGA and observed that PLK1 and BIRC5 were highly expressed in a subset of HCC patients. More interestingly, the expression of PLK1 and BIRC5 was significantly correlated in the same subset together with a number of other important cell cycle factors, including CCNB1, CCNB2, CDK1, FOXM1, AURKA, AURKB, and CDC25C (Figure 1A and B). Notably, PLK1 and PLK4, but not other family members PLK2 or PLK3, showed higher co-expression in the same subset (Figure 1A). Similarly, BIRC5 was not co-expressed with other family members BIRC2 or BIRC3, or other apoptotic genes, such as BCL-2 and MCL-1 (Figure 1A). In addition, we did not detect any significant correlation between FUBP1 expression and that of either PLK1 or BIRC5, although FuBP1 is overexpressed in 80% of HCC tumors with chronic hepatitis C (CHC)[20]. Altogether, these results indicated that PLK1 and BIRC5 may coordinate to mediate HCC malignancy.

In addition, poor overall clinical survival and disease/progression-free survival after initial treatment were observed to be significantly correlated with high PLK1 expression in patients with HCC (n = 134 and 109, respectively) compared to HCC patients with low PLK1 expression (n = 231 and 204, respectively) (Figure 2A and B). Similarly, poor overall clinical survival and disease/progression-free survival after

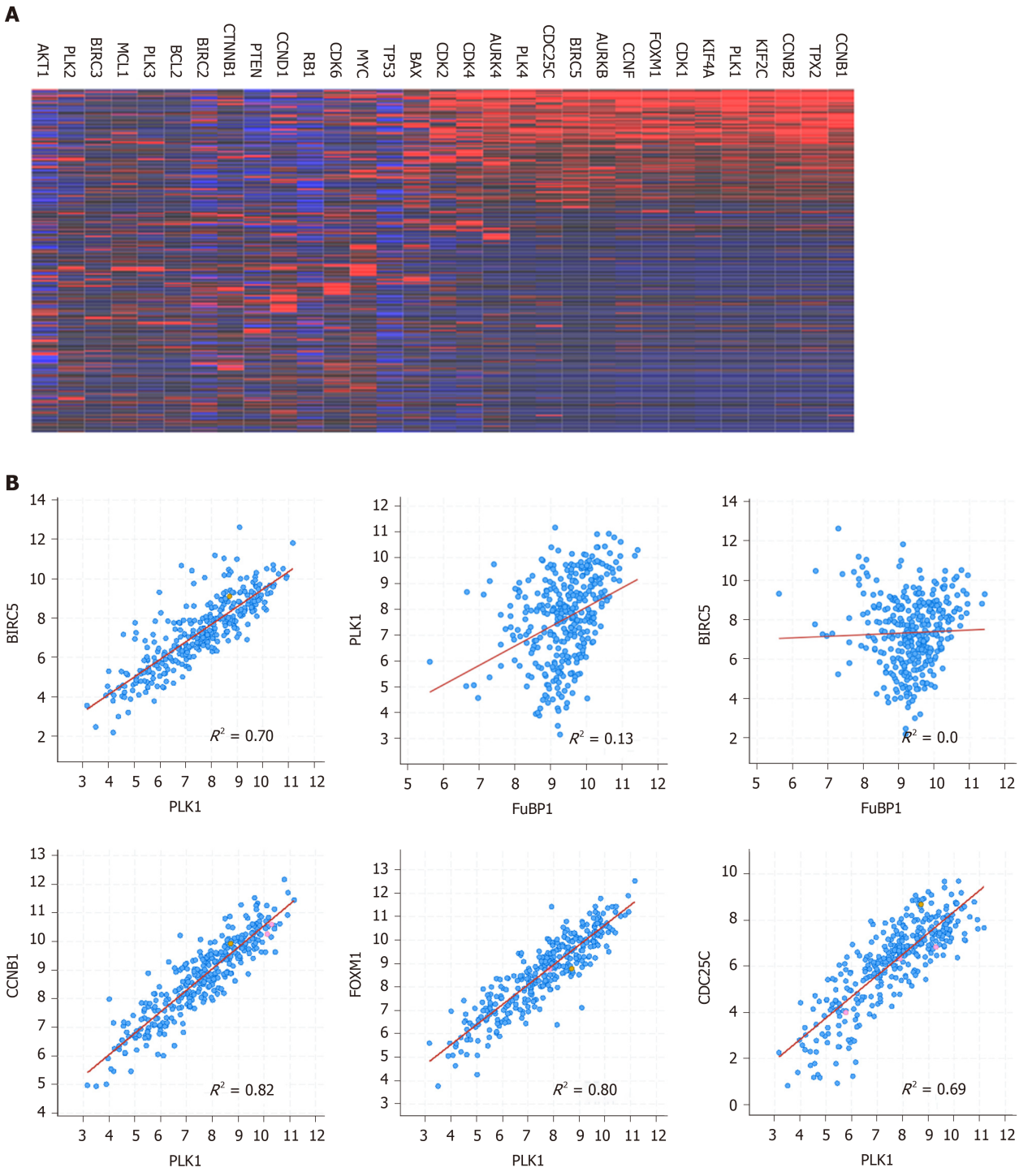
A
AKT1
PLK2
BIRC3
MCL1
PLK3
BCL2
BIRC2
CTNNB1
PTEN
CCND1
RB1
CDK6
MYC
TP53
BAX
CDK2
CDK4
AURK4
PLK4
CDC25C
BIRC5
AURKB
CCNF
FOXM1
CDK1
KIF4A
PLK1
KIF2C
CCNB2
TPX2
CCNB1
B
BIRC5
PLK1
R^2 = 0.70
PLK1
FuBP1
R^2 = 0.13
BIRC5
FuBP1
R^2 = 0.0
CCNB1
PLK1
R^2 = 0.82
FOXM1
PLK1
R^2 = 0.80
CDC25C
PLK1
R^2 = 0.69

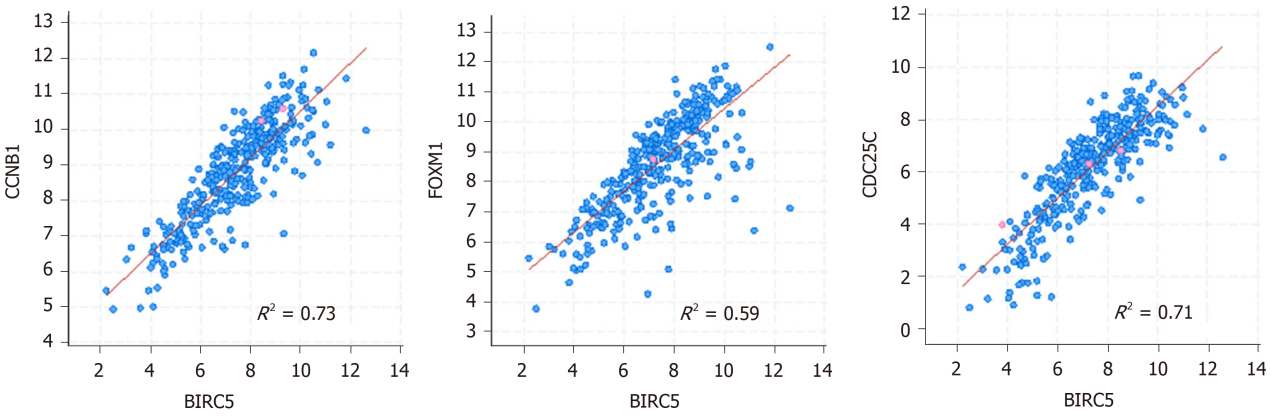

Figure 1 Co-expression of Polo-like kinase 1 and baculoviral inhibitor of apoptosis repeat-containing 5 in hepatocellular carcinoma. A: Heatmap of genes co-expressed with Polo-like kinase 1 in hepatocellular carcinoma; B: Correlations of representative genes that are co-expressed in hepatocellular carcinoma. The dataset used in these analysis was Liver Hepatocellular Carcinoma (TCGA, PanCancer Atlas). PLK1: Polo-like kinase 1; BIRC5: Baculoviral inhibitor of apoptosis repeat-containing 5.

initial treatment were observed to be significantly correlated high BIRC5 expression in patients with HCC (n = 126 and 104, respectively) compared to HCC patients with low BIRC5 expression (n = 239 and 209, respectively) (Figure 3A and B). These data suggested that dual targeting of PLK1 and BIRC5 in HCC patients with high expression of both PLK1 and BIRC5 may be a promising therapeutic strategy for anti-tumor treatments.

PLK1 and BIRC5 expression in HCC patients with wild-type and mutant p53

Previous studies have shown that p53 regulates the expression of PLK1 and BIRC5[21,22] and that PLK1, in turn, regulates p53 turnover (Figure 4A)[23]. In this study, we observed that both PLK1 and BIRC5 were upregulated in patients with p53-mutated HCC compared to those with wild-type p53 HCC (Figure 4B and C). These results suggest that mutations in or the functional loss of p53 in HCC may contribute to upregulation of PLK1 and BIRC5 expression, resulting in poor clinical outcome (Figures 2 and 3). In contrast, only high expression of PLK1, but not BIRC5, was observed in patients with RB1-mutated HCC compared to those with wild-type RB1 HCC (Figure 4D and E). These results suggest that the mutation status of the tumor suppressor p53 is more relevant than that of the tumor suppressor RB1 in mediating PLK1 and BIRC5 co-expression in HCC patients.

PLK1 inhibitors GSK461364 and volasertib selectively target Huh7 cells with mutant p53 over HepG2 cells with wild-type p53

In this study, we investigated the *in vitro* efficacy of two potent and selective PLK1 inhibitors, GSK462364 and volasertib, against the p53-mutated HCC cell line Huh7 and the p53-wild-type HCC cell line HepG2. These two independently developed PLK1 inhibitors showed potent anti-tumor activity against both cell lines 72 h post treatment, but significantly lower IC50 values were observed in p53-mutated Huh7 cells (IC_{50} = 3.2 and 4.9 nmol/L, respectively) compared to those measured for p53-wild-type HepG2 cells (IC_{50} = 15.7 and 19.2 nmol/L, respectively) (Figure 5A and B). Treatment with both inhibitors induced robust apoptosis in both cell lines in a dose-dependent manner. In line with the cell viability assay results (Figure 5A and B), these PLK1 inhibitors more potently induced cell apoptosis in Huh7 cells than in HepG2 cells in a dose-dependent manner (12.5 and 25 nmol/L for GSK361464; 50 and 100 nmol/L for volasertib, respectively) 24 h post treatment (Figure 5C and D). Treatment with both PLK1 inhibitors for 24 h induced greater cellular morphological changes in Huh7 cells than in HepG2 cells (Figure 5E). Moreover, both inhibitors induced substantial cell cycle arrest at G2/M phase in Huh7 and HepG2 cells in a dose-dependent manner 24 h post treatment (Figure 5F-I).

BIRC5 inhibitor YM155 selectively target Huh7 cells with mutant p53 over HepG2 cells with wild-type p53

YM155 is a selective BIRC5 suppressor that inhibits BIRC5 expression at the transcriptional level. In this study, treatment with YM155 (dose range of 0-20 μmol/L)

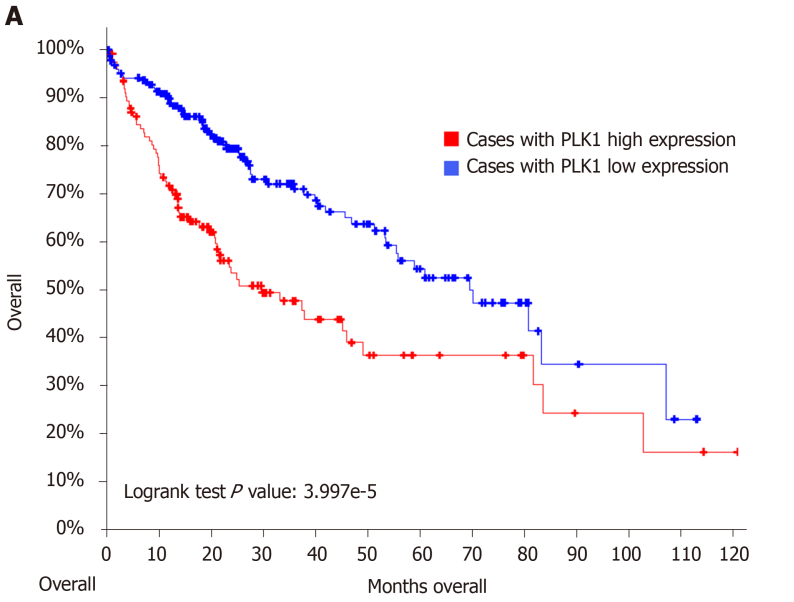

	Number of cases, total	Number of cases, deceased	Median months survival
Cases with PLK1 high expression	134	63	29.56
Cases with PLK1 low expression	231	66	69.57

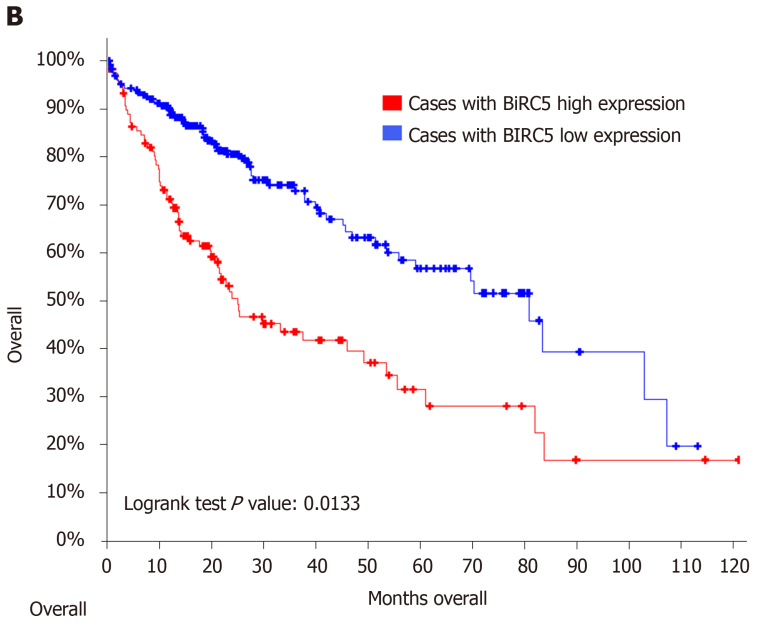

	Number of cases, total	Number of cases, deceased	Median months survival
Cases with BIRC5 high expression	109	54	13.15
Cases with BIRC5 low expression	204	87	33.93

Figure 2 High Polo-like kinase 1 expression correlates with a poor overall survival in patients with hepatocellular carcinoma. A: Kaplan-Meier estimate of overall clinical survival in patients with high Polo-like kinase 1 (PLK1) expression (PLK1: Exp > 0.1) and in patients with low PLK1 expression (PLK1: Exp ≤ 0.1). Total cases, deceased cased, and survival months for either group are also indicated in the bottom of the figure; B: Kaplan-Meier estimate of disease/progression-free survival after the initial treatment in patients with high PLK1 expression (PLK1: Exp > 0.1) and in patients with low PLK1 expression (PLK1: Exp ≤ 0.1). The *P* values generated by log-rank test are also shown. The dataset used in these analyses was Liver Hepatocellular Carcinoma (TCGA, PanCancer Atlas). PLK1: Polo-like kinase 1.

induced growth inhibition in p53-mutated Huh7 cells but not in p53-wild-type HepG2 cells 72 h post treatment (Figure 6A). These data suggest that the BIRC5 inhibitor YM155 is highly selective in targeting p53-mutated Huh7 cells over p53-wild-type

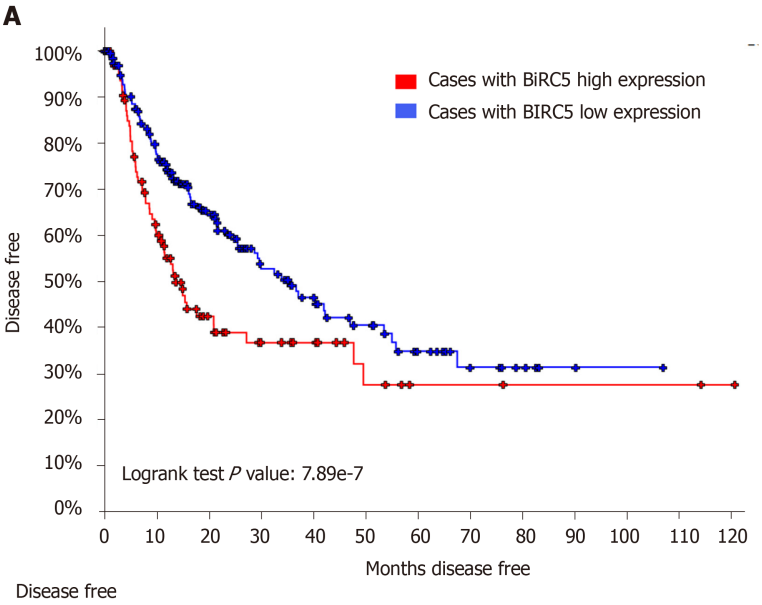

	Number of cases, total	Number of cases, deceased	Median months survival
Cases with BIRC5 high expression	126	65	24.89
Cases with BIRC5 low expression	239	64	80.74

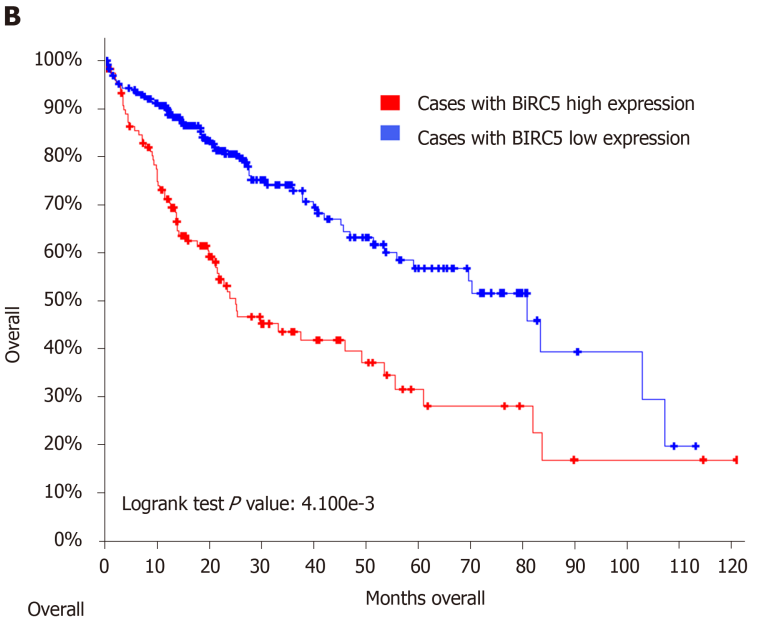

	Number of cases, total	Number of cases, deceased	Median months survival
Cases with BIRC5 high expression	104	54	13.64
Cases with BIRC5 low expression	209	87	35.61

Figure 3 High baculoviral inhibitor of apoptosis repeat-containing 5 expression correlates with a poor overall survival in patients with hepatocellular carcinoma. A: Kaplan-Meier estimate of overall clinical survival in patients with high baculoviral inhibitor of apoptosis repeat-containing 5 (BIRC5) expression (BIRC5: Exp > 0.1) and in patients with low BIRC5 expression (BIRC5: Exp ≤ 0.1). Total cases, deceased cased, and survival months for either group are also indicated in the bottom of the figure; B: Kaplan-Meier estimate of disease/progression-free survival after the initial treatment in patients with high BIRC5 expression (BIRC5: Exp > 0.1) and in patients with low BIRC5 expression (BIRC5: Exp ≤ 0.1). The *P* values generated by log-rank test are also shown. The dataset used in this analysis was Liver Hepatocellular Carcinoma (TCGA, PanCancer Atlas). BIRC5: Baculoviral inhibitor of apoptosis repeat-containing 5.

HepG2 cells. YM155 treatment for 24 h induced robust cell apoptosis in a dose-dependent manner in Huh7 cells (Figure 6B). Similar to the assayed PLK1 inhibitors,

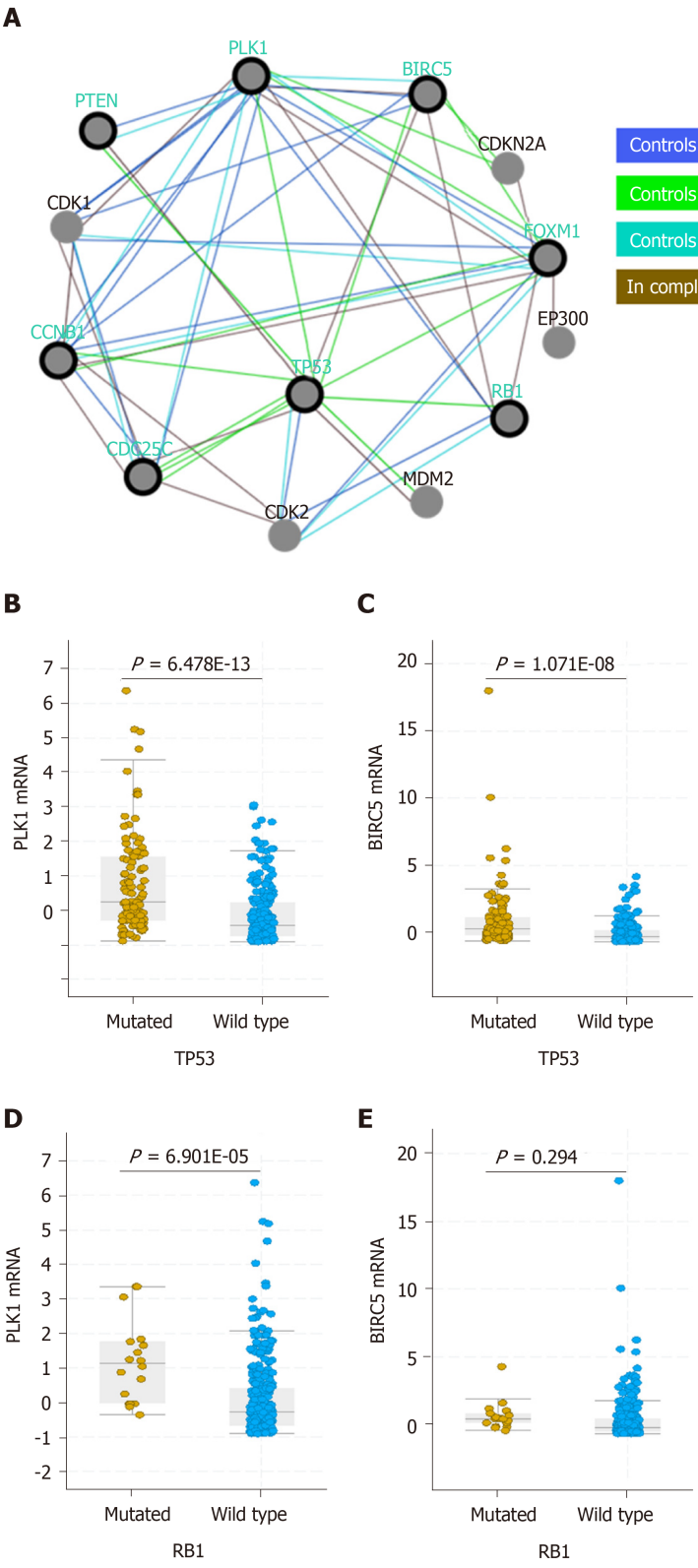

Figure 4 High expression of Polo-like kinase 1 and baculoviral inhibitor of apoptosis repeat-containing 5 in TP53-mutated hepatocellular carcinoma patients. A: PLK1- and BIRC5-associated pathway networks; B and C: Polo-like kinase 1 (PLK1) (B) or baculoviral inhibitor of apoptosis repeat-containing 5 (BIRC5) (C) expression in hepatocellular carcinoma (HCC) patients with wild-type and mutated TP53; D and E: PLK1 (D) or BIRC5 (E) expression in HCC patients with wild-type and mutated RB1. The dataset used in these analysis was Liver Hepatocellular Carcinoma (TCGA, PanCancer Atlas). PLK1: Polo-like kinase 1; BIRC5: Baculoviral inhibitor of apoptosis repeat-containing 5.

YM155 treatment for 24 h in Huh7 cells induced cell cycle arrest at G2/M phase in a dose-dependent manner (Figure 6C), but to a much less extent than that observed for the PLK1 inhibitors.

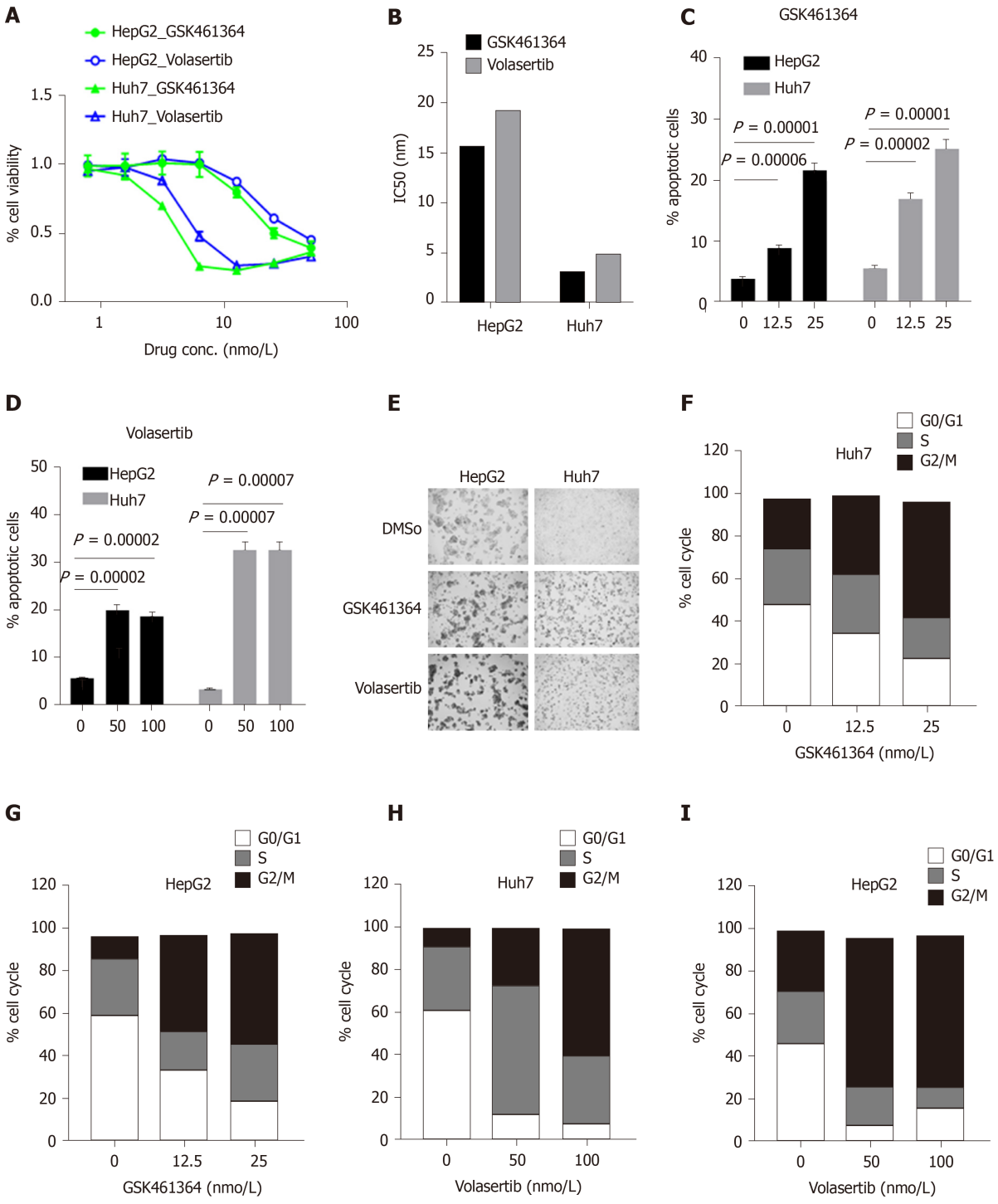

Figure 5 Polo-like kinase 1 inhibitors GSK461364 and volasertib selectively target Huh7 cells with mutated p53 over HepG2 cells with wild-type p53. A and B: *In vitro* efficacy of the Polo-like kinase 1 inhibitors GSK461364 and volasertib in HepG2 and Huh7 cells after 72 h of treatment as assessed through cell viability assays (A) and IC_{50} values for the inhibitors were also calculated and plotted (B); C and D: Percentage of apoptotic HepG2 and Huh7 cells treated with GSK461364 (C) or volasertib (D) for 24 h at the indicated dosage; E: Representative bright-field images of HepG2 and Huh7 cells treated with GSK461364 or volasertib for 24 h; F-I: Cell cycle status of Huh7 (F and H) and HepG2 (G and I) cells treated with GSK461364 (F and G) or volasertib (H and I) for 24 h at the indicated dosage.

Dual targeting of PLK1 and BIRC5 shows synergistic anti-tumor effects toward Huh7 cells

Co-expression of PLK1 and BIRC5 in the same subset of HCC patients suggested that dual targeting of PLK1 and BIRC5 may be a promising therapeutic strategy for these patients. Therefore, we investigated the *in vitro* efficacy of combining the PLK1 inhibitor volasertib, which reached a phase III clinical trial, and the BIRC5 inhibitor YM155, which reached a phase II clinical trial, in p53-mutated Huh7 cells. The

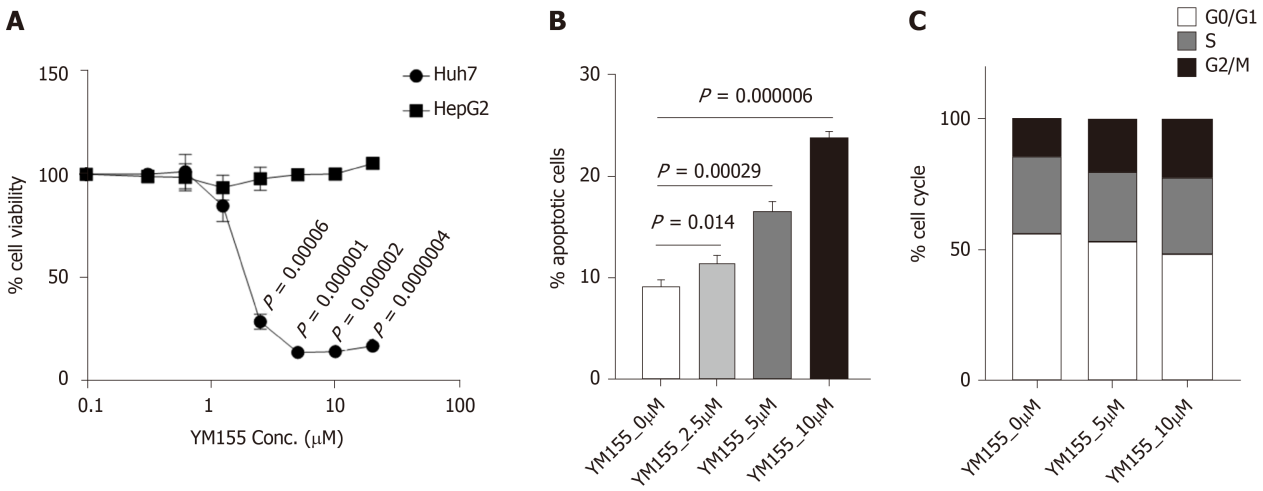

Figure 6 Baculoviral inhibitor of apoptosis repeat-containing 5 inhibitor YM155 selectively target Huh7 cells with mutated p53 over HepG2 cells with wild-type p53. A: *In vitro* efficacy of the baculoviral inhibitor of apoptosis repeat-containing 5 inhibitor YM155 in HepG2 and Huh7 cells after 72 h of treatment as assessed through cell viability assays; B: Percentage of apoptotic Huh7 cells treated with YM155 for 24 h at the indicated dosage; C: Cell cycle status of Huh7 cells treated with YM155 for 24 h at the indicated dosage.

combination treatment of volasertib (dose range: 0-50 nmol/L) and YM155 (dose range: 0-20 μmol/L) exhibited synergistic anti-tumor activity in the *in vitro* cell viability assay 72 h post treatment (Figure 7A). Consistent with these results, this combination treatment also showed synergistic induction of cell apoptosis 24 h post treatment (Figure 7B). In line with the data presented in Figures 5H and 6C, treatment with volasertib or YM155 alone markedly induced cell cycle arrest at G2/M phase, while the combination treatment of volasertib and YM155 showed less G2/M arrest than volasertib alone but more than that using YM155 alone (Figure 7C).

To validate the synergistic effect of the volasertib and YM155 combination treatment, we subcutaneously injected p53-mutated Huh7 cells into immunodeficient NSIG mice to establish mouse xenograft models. When the tumor became palpable, the mice were treated with volasertib (10 mg/kg, IP, weekly) for 4 wk and YM155 (3 mg/kg, continuous infusion for the first week and off for the following 3 wk), alone or in combination (Figure 8A). Single-agent treatment with volasertib or YM155 significantly inhibited tumor growth *in vivo*, and their combined use resulted in even smaller tumor masses in 3 out of 5 mice and no tumor masses in the last two mice in the group (Figure 8B and C). Furthermore, no toxicity was observed under the combination treatment schedule (Figure 8D).

DISCUSSION

In this study, we performed bioinformatic analysis for a TCGA RNA sequencing dataset from a large cohort of HCC patients (n = 374). Our analysis showed that two potential therapeutic targets, PLK1 and BIRC5, were highly expressed in a subset of HCC patients and that their expression correlated well in all patients. More interestingly, upregulation of PLK1/BIRC5 expression was frequently observed in HCC patients with mutations in p53. This observation led use to hypothesize that dual targeting PLK1 and BIRC5 in these patients would have superior therapeutic efficacy and could allow for the development of precision medicine to treat HCC patients with high PLK1 and BIRC5 expression, especially when p53 is also mutated.

In HCC cells with high co-expression of PLK1 and BIRC5, other cell cycle factors, including CCNB1, CCNB2, CDK1, FOXM1, AURKA, AURKB, and CDC25C were also observed to be highly expressed. In contrast, other PLK family members (PLK2 and PLK3), IAP family members (BIRC2 and BIRC3), and BCL-2 family members (BCL-2 and MCL-1) were not co-expressed with PLK1 and BIRC5. These results may provide a gene signature panel to identify HCC patients who will likely respond to PLK1 inhibition and BIRC5 treatment, although this possibility requires further validation.

For the first time, we provide a link between PLK1/BIRC5 co-expression and upregulation to the mutation status of p53, but not the p53 expression status, in HCC patients. The tumor suppressor p53 plays key roles in cell cycle arrest, DNA repair,

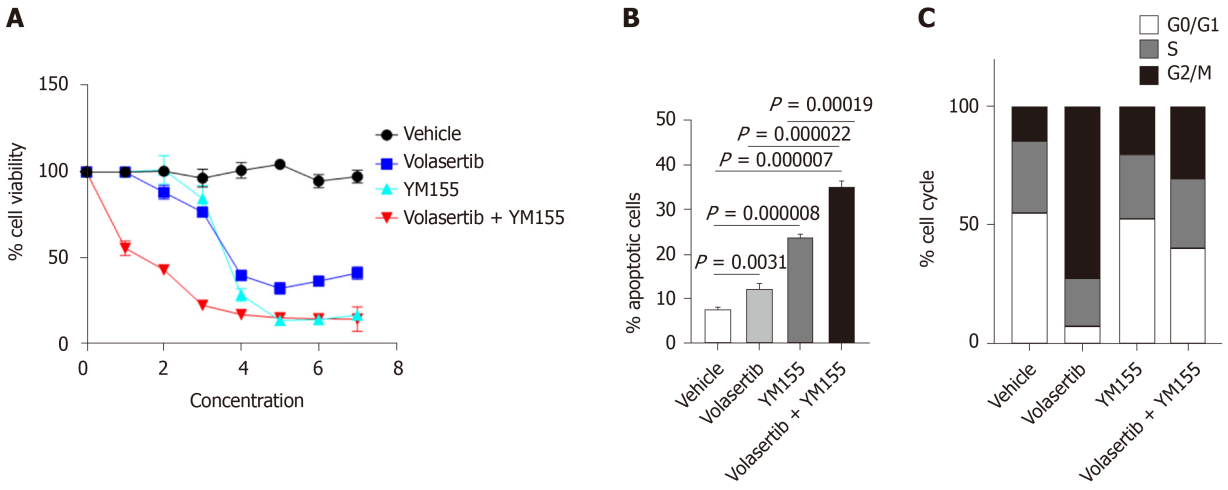

Figure 7 Dual targeting of Polo-like kinase 1 and baculoviral inhibitor of apoptosis repeat-containing 5 shows synergistic anti-tumor effects in p53 mutated Huh7 cells. A: *In vitro* efficacy of the combination treatment of the baculoviral inhibitor of apoptosis repeat-containing 5 inhibitor YM155 (0-20 μmol/L) and the Polo-like kinase 1 inhibitor volasertib (0-50 nmol/L) against Huh7 cells after 72 h of treatment as assessed through cell viability assays; B: Percentage of apoptotic Huh7 cells treated with YM155 and volasertib for 24 h; C: Cell cycle status of Huh7 cells treated with YM155 and volasertib for 24 h.

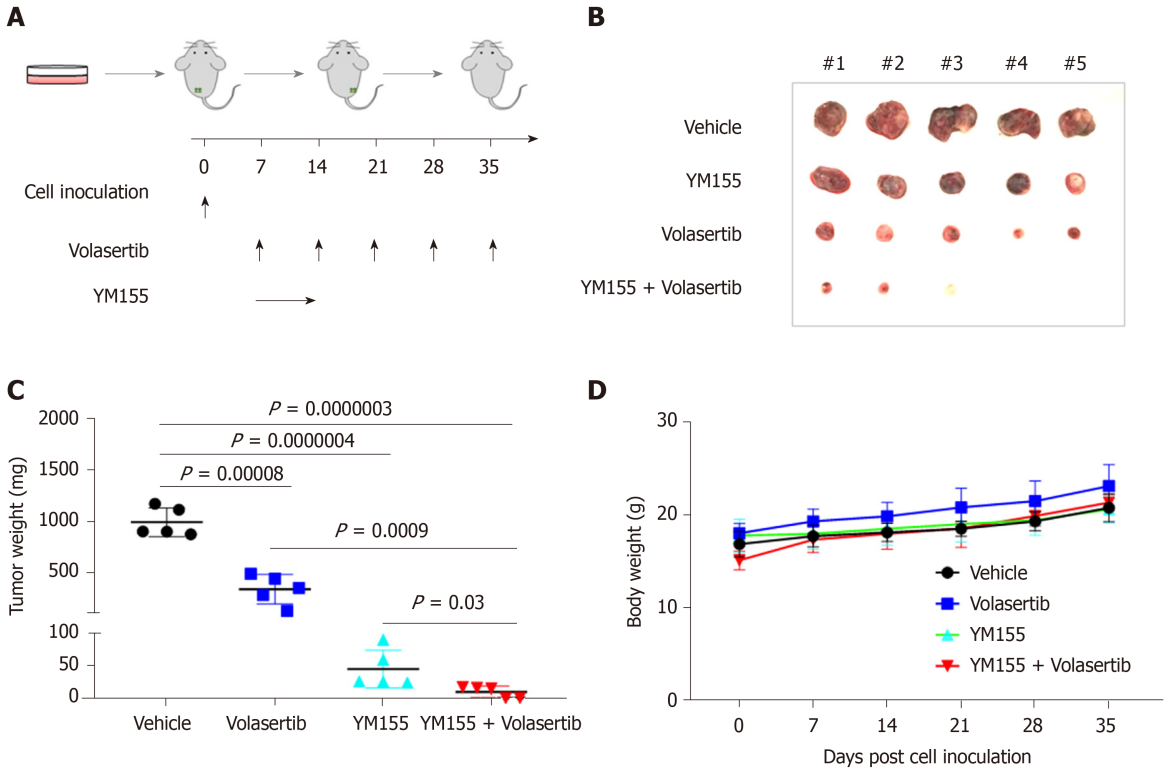

Figure 8 Dual targeting of Polo-like kinase 1 and baculoviral inhibitor of apoptosis repeat-containing 5 potently inhibits p53-mutated Huh7 cell-derived xenografts. A: Schematic of the experimental set up for the *in vivo* xenograft model. Huh7 cells were injected into NSG mice (n = 5 per group). The mice were treated with vehicle or volasertib (10 mg/kg, ip, weekly) for 4 wk, or continuously infused with YM155 (3 mg/kg) for 7 d and off for the next 3 wk; B and C: The mice were euthanized and dissected at the end of experiments. The xenografts were imaged (B) and weighed (C); D: The body weight of mice were measured once a week.

and apoptosis. PLK1 is a direct target for the p53 transcription factor, which binds to the PLK1 promoter to suppress its expression[21]. In response to DNA damage, wild-type p53 but not mutant p53 suppresses PLK1 expression in an E2F1-dependent manner[24]. Therefore, PLK1 expression is suppressed in cells with wild-type p53, and PLK1 is upregulated in cells with mutated p53 that lead to the loss or inactivation of p53. Functioning within a negative regulatory feedback loop, PLK1 negatively regulates p53 transcriptional activation *via* physical interaction and through the

phosphorylation of PLK1[25]. A similar scenario may also apply to the p53-BIRC5 axis, since wild-type but not mutant p53 also transcriptionally represses BIRC5 expression to promote p53-dependent cell apoptosis[22,26,27]. BIRC5 overexpression negatively regulates the expression of wild-type p53[28]. BIRC5 and PLK1 interact during mitosis, and PLK1 phosphorylates BIRC5 at serine 20[29]. In turn, BIRC5 regulates PLK1 localization to the kinetochore for the recruitment and dynamic localization of the BIRC5-containing chromosomal passenger complex (CPC) during cell division throughout mitosis[30,31]. However, no direct interaction between BIRC5 and p53 has been reported yet. Altogether, these results may explain why HCC cells with mutated p53 express higher levels of PLK1 and BIRC5 and suggest that PLK1 and BIRC5 work coordinately in contributing to cancer malignancies in cancer cells with p53 mutations. Based on this, one would expect that HCC cells with mutated p53 would be more sensitive to PLK1 and BIRC5 inhibition. Inhibition of PLK1 using small molecules such as GSK461364A and volasertib was previously shown to have differential anti-tumor activity and cell apoptosis based on p53 mutation status[32-35]. Inhibition of BIRC5 by YM155 leads to decreased BIRC5 expression and increased expression of PUMA, a direct target of p53, which results in cell apoptosis[36]. Indeed, this phenomenon is observed in Huh7 cells with mutated p53 and in HepG2 cells with wild-type p53. It has been shown that HuH7 cells harbor a homozygous p53 mutation (Y220C), which is a destabilizing mutation that results in partial DNA-binding activity compared to wild-type p53[37]. This type of mutant p53 can be pharmaceutically reactivated and functionally rescued by p53 activators such as ARP-246[38,39]. FuBP1 is overexpressed in 80% of HCC tumors with chronic hepatitis C[20] and has been shown to inhibit p53 function[37]. However, we did not detect any significant correlation between FUBP1 expression and that of either PLK1 or BIRC5, indicating that FUBP1 is not functionally correlated with PLK1 and BIRC5 in contributing to HCC malignancy.

Our data also showed that expression of PLK1 was upregulated in HCC patients with mutations in the tumor suppressor RB1 compared to those with wild-type RB1. It has also been shown that RB1 loss is associated with a higher sensitivity to PLK1 inhibitors in triple-negative breast cancer[40]. In contrast to PLK1, BIRC5 did not show differential expression in HCC patients with/without RB1 mutations. This result indicated that high co-expression of PLK1/BIRC5 is selective for HCC patients with p53 mutations and therefore provides strong evidence for the potential value of single or dual targeting of PLK1 and BIRC5 in p53-mutated HCC cells.

Moreover, the results of our study showed that dual targeting of PLK1 and BIRC5 showed synergistic antitumor activity *in vitro* and *in vivo* in p53-mutated Huh7 cells. Therefore, our study provides valuable insights for therapeutic development targeting PLK1 and BIRC5 for the subset of HCC patient population with the PLK1/BIRC5 co-expression signature in p53-mutated HCC patients as well as other cancer models.

ARTICLE HIGHLIGHTS

Research background

Hepatocellular carcinoma (HCC) is the fifth most common malignant cancer and the second leading cause of cancer-related mortality. HCC is often diagnosed at advanced stages without curative therapies. Therefore, there is an unmet need of preclinical studies to develop novel therapeutic strategies to treat HCC, especially at advanced stages. Polo-like kinase 1 (PLK1) is activated at the late G2 phase of the cell cycle and is required for entry to mitosis. Interestingly, PLK1 is overexpressed in many HCC patients and is highly associated with poor clinical outcome. Baculoviral inhibitor of apoptosis repeat-containing 5 (BIRC5) is also highly overexpressed in HCC and plays key roles in HCC cell survival, cell proliferation, and disease progression of HCC.

Research motivation

More biomarkers are required for the diagnosis and treatment of HCC. However, how p53, PLK1, and BIRC5 interact in HCC has not been well defined.

Research objectives

To determine the expression pattern of PLK1 and BIRC5, as well as their correlation with mutation status of p53 and patient clinical outcome.

Research methods

The expression of PLK1 and BIRC5 and their correlation with the mutation status p53

were analyzed using a TCGA HCC dataset. Cell-based studies were conducted to investigate the efficacy of PLK1 and BIRC5 inhibitors, alone or in combination, the results of which were further validated in p53-mutated Huh7-derived xenografts in immune-deficient NSIG mice.

Research results

Our bioinformatic analysis using an HCC dataset from TCGA revealed that PLK1 and BIRC5 were overexpressed in the same subset of HCC patients and that their expression was highly correlated in all HCC patients. Both PLK1 and BIRC5 overexpression was more frequently detected in HCC with p53 mutations, compared to that observed in HCC with wild-type p53. High PLK1 or BIRC5 expression was significantly correlated with poor clinical outcome. Both PLK1 inhibitors volasertib and GSK461364 or the BIRC5 inhibitor YM155 selectively targeted Huh7 cells, which express Y220C-mutated p53 that is aberrantly stable and transcriptionally inactive, but not HepG2 cells, which express wild-type p53. Combination treatment with volasertib and YM155 synergistically inhibited the cell viability of Huh7 cells by promoting cell apoptosis. The efficacy of volasertib and YM155, alone or in combination, was further validated *in vivo* in a Huh7-derived xenograft model in immuno-deficient NSIG mice.

Research conclusions

PLK1 and BIRC5 are highly co-expressed in p53-mutated HCC and dual targeting of PLK1 and BIRC5 synergistically inhibits the cell viability of p53-mutated HCC cells *in vitro* through the induction of cell apoptosis as well as the tumor growth of p53-mutated HCC cells *in vivo*.

Research perspectives

The results of this study provides valuable insights for therapeutic development for the subset of the HCC patient population with the PLK1/BIRC5 co-expression signature in p53-mutated HCC patients as well as for other cancer models in the future.

ACKNOWLEDGEMENTS

The authors would like to thank Li C from the Animal Laboratory of Tianjin Third Central Hospital for her help in animal preparation and Professor Li SJ from Nankai University for aid in biostatistics during the preparation of this manuscript.

REFERENCES

1 **Ferlay J**, Soerjomataram I, Dikshit R, Eser S, Mathers C, Rebelo M, Parkin DM, Forman D, Bray F. Cancer incidence and mortality worldwide: sources, methods and major patterns in GLOBOCAN 2012. *Int J Cancer* 2015; **136**: E359-E386 [PMID: 25220842 DOI: 10.1002/ijc.29210]
2 **Janevska D**, Chaloska-Ivanova V, Janevski V. Hepatocellular Carcinoma: Risk Factors, Diagnosis and Treatment. *Open Access Maced J Med Sci* 2015; **3**: 732-736 [PMID: 27275318 DOI: 10.3889/oamjms.2015.111]
3 **Zhou X**, Hao Q, Lu H. Mutant p53 in cancer therapy-the barrier or the path. *J Mol Cell Biol* 2019; **11**: 293-305 [PMID: 30508182 DOI: 10.1093/jmcb/mjy072]
4 **Hussain SP**, Schwank J, Staib F, Wang XW, Harris CC. TP53 mutations and hepatocellular carcinoma: insights into the etiology and pathogenesis of liver cancer. *Oncogene* 2007; **26**: 2166-2176 [PMID: 17401425 DOI: 10.1038/sj.onc.1210279]
5 **Tornesello ML**, Buonaguro L, Tatangelo F, Botti G, Izzo F, Buonaguro FM. Mutations in TP53, CTNNB1 and PIK3CA genes in hepatocellular carcinoma associated with hepatitis B and hepatitis C virus infections. *Genomics* 2013; **102**: 74-83 [PMID: 23583669 DOI: 10.1016/j.ygeno.2013.04.001]
6 **Shirabe K**, Toshima T, Taketomi A, Taguchi K, Yoshizumi T, Uchiyama H, Harimoto N, Kajiyama K, Egashira A, Maehara Y. Hepatic aflatoxin B1-DNA adducts and TP53 mutations in patients with hepatocellular carcinoma despite low exposure to aflatoxin B1 in southern Japan. *Liver Int* 2011; **31**: 1366-1372 [PMID: 21745313 DOI: 10.1111/j.1478-3231.2011.02572.x]
7 **Parrales A**, Iwakuma T. Targeting Oncogenic Mutant p53 for Cancer Therapy. *Front Oncol* 2015; **5**: 288 [PMID: 26732534 DOI: 10.3389/fonc.2015.00288]
8 **Li S**, Gao M, Li Z, Song L, Gao X, Han J, Wang F, Chen Y, Li W, Yang J. p53 and P-glycoprotein influence chemoresistance in hepatocellular carcinoma. *Front Biosci (Elite Ed)* 2018; **10**: 461-468 [PMID: 29772519 DOI: 10.2741/e833]
9 **Hientz K**, Mohr A, Bhakta-Guha D, Efferth T. The role of p53 in cancer drug resistance and targeted chemotherapy. *Oncotarget* 2017; **8**: 8921-8946 [PMID: 27888811 DOI: 10.18632/oncotarget.13475]
10 **Combes G**, Alharbi I, Braga LG, Elowe S. Playing polo during mitosis: PLK1 takes the lead. *Oncogene*

2017; **36**: 4819-4827 [PMID: 28436952 DOI: 10.1038/onc.2017.113]
11 **Colicino EG**, Hehnly H. Regulating a key mitotic regulator, polo-like kinase 1 (PLK1). *Cytoskeleton (Hoboken)* 2018; **75**: 481-494 [PMID: 30414309 DOI: 10.1002/cm.21504]
12 **Jeong SB**, Im JH, Yoon JH, Bui QT, Lim SC, Song JM, Shim Y, Yun J, Hong J, Kang KW. Essential Role of Polo-like Kinase 1 (Plk1) Oncogene in Tumor Growth and Metastasis of Tamoxifen-Resistant Breast Cancer. *Mol Cancer Ther* 2018; **17**: 825-837 [PMID: 29437878 DOI: 10.1158/1535-7163.MCT-17-0545]
13 **Ramani P**, Nash R, Sowa-Avugrah E, Rogers C. High levels of polo-like kinase 1 and phosphorylated translationally controlled tumor protein indicate poor prognosis in neuroblastomas. *J Neurooncol* 2015; **125**: 103-111 [PMID: 26318737 DOI: 10.1007/s11060-015-1900-4]
14 **Tut TG**, Lim SH, Dissanayake IU, Descallar J, Chua W, Ng W, de Souza P, Shin JS, Lee CS. Upregulated Polo-Like Kinase 1 Expression Correlates with Inferior Survival Outcomes in Rectal Cancer. *PLoS One* 2015; **10**: e0129313 [PMID: 26047016 DOI: 10.1371/journal.pone.0129313]
15 **Zhang R**, Shi H, Ren F, Liu H, Zhang M, Deng Y, Li X. Misregulation of polo-like protein kinase 1, P53 and P21WAF1 in epithelial ovarian cancer suggests poor prognosis. *Oncol Rep* 2015; **33**: 1235-1242 [PMID: 25592872 DOI: 10.3892/or.2015.3723]
16 **Mita AC**, Mita MM, Nawrocki ST, Giles FJ. Survivin: key regulator of mitosis and apoptosis and novel target for cancer therapeutics. *Clin Cancer Res* 2008; **14**: 5000-5005 [PMID: 18698017 DOI: 10.1158/1078-0432.CCR-08-0746]
17 **Velculescu VE**, Madden SL, Zhang L, Lash AE, Yu J, Rago C, Lal A, Wang CJ, Beaudry GA, Ciriello KM, Cook BP, Dufault MR, Ferguson AT, Gao Y, He TC, Hermeking H, Hiraldo SK, Hwang PM, Lopez MA, Luderer HF, Mathews B, Petroziello JM, Polyak K, Zawel L, Kinzler KW. Analysis of human transcriptomes. *Nat Genet* 1999; **23**: 387-388 [PMID: 10581018 DOI: 10.1038/70487]
18 **Garg H**, Suri P, Gupta JC, Talwar GP, Dubey S. Survivin: a unique target for tumor therapy. *Cancer Cell Int* 2016; **16**: 49 [PMID: 27340370 DOI: 10.1186/s12935-016-0326-1]
19 **Li B**, Dewey CN. RSEM: accurate transcript quantification from RNA-Seq data with or without a reference genome. *BMC Bioinformatics* 2011; **12**: 323 [PMID: 21816040 DOI: 10.1186/1471-2105-12-323]
20 **Rabenhorst U**, Beinoraviciute-Kellner R, Brezniceanu ML, Joos S, Devens F, Lichter P, Rieker RJ, Trojan J, Chung HJ, Levens DL, Zörnig M. Overexpression of the far upstream element binding protein 1 in hepatocellular carcinoma is required for tumor growth. *Hepatology* 2009; **50**: 1121-1129 [PMID: 19637194 DOI: 10.1002/hep.23098]
21 **McKenzie L**, King S, Marcar L, Nicol S, Dias SS, Schumm K, Robertson P, Bourdon JC, Perkins N, Fuller-Pace F, Meek DW. p53-dependent repression of polo-like kinase-1 (PLK1). *Cell Cycle* 2010; **9**: 4200-4212 [PMID: 20962589 DOI: 10.4161/cc.9.20.13532]
22 **Mirza A**, McGuirk M, Hockenberry TN, Wu Q, Ashar H, Black S, Wen SF, Wang L, Kirschmeier P, Bishop WR, Nielsen LL, Pickett CB, Liu S. Human survivin is negatively regulated by wild-type p53 and participates in p53-dependent apoptotic pathway. *Oncogene* 2002; **21**: 2613-2622 [PMID: 11965534 DOI: 10.1038/sj.onc.1205353]
23 **Dias SS**, Hogan C, Ochocka AM, Meek DW. Polo-like kinase-1 phosphorylates MDM2 at Ser260 and stimulates MDM2-mediated p53 turnover. *FEBS Lett* 2009; **583**: 3543-3548 [PMID: 19833129 DOI: 10.1016/j.febslet.2009.09.057]
24 **Zhou Z**, Cao JX, Li SY, An GS, Ni JH, Jia HT. p53 Suppresses E2F1-dependent PLK1 expression upon DNA damage by forming p53-E2F1-DNA complex. *Exp Cell Res* 2013; **319**: 3104-3115 [PMID: 24076372 DOI: 10.1016/j.yexcr.2013.09.012]
25 **Ando K**, Ozaki T, Yamamoto H, Furuya K, Hosoda M, Hayashi S, Fukuzawa M, Nakagawara A. Polo-like kinase 1 (Plk1) inhibits p53 function by physical interaction and phosphorylation. *J Biol Chem* 2004; **279**: 25549-25561 [PMID: 15024021 DOI: 10.1074/jbc.M314182200]
26 **Zhou M**, Gu L, Li F, Zhu Y, Woods WG, Findley HW. DNA damage induces a novel p53-survivin signaling pathway regulating cell cycle and apoptosis in acute lymphoblastic leukemia cells. *J Pharmacol Exp Ther* 2002; **303**: 124-131 [PMID: 12235242 DOI: 10.1124/jpet.102.037192]
27 **Hoffman WH**, Biade S, Zilfou JT, Chen J, Murphy M. Transcriptional repression of the anti-apoptotic survivin gene by wild type p53. *J Biol Chem* 2002; **277**: 3247-3257 [PMID: 11714700 DOI: 10.1074/jbc.M106643200]
28 **Wang Z**, Fukuda S, Pelus LM. Survivin regulates the p53 tumor suppressor gene family. *Oncogene* 2004; **23**: 8146-8153 [PMID: 15361831 DOI: 10.1038/sj.onc.1207992]
29 **Colnaghi R**, Wheatley SP. Liaisons between survivin and Plk1 during cell division and cell death. *J Biol Chem* 2010; **285**: 22592-22604 [PMID: 20427271 DOI: 10.1074/jbc.M109.065003]
30 **Sun SC**, Liu HL, Sun QY. Survivin regulates Plk1 localization to kinetochore in mouse oocyte meiosis. *Biochem Biophys Res Commun* 2012; **421**: 797-800 [PMID: 22554510 DOI: 10.1016/j.bbrc.2012.04.089]
31 **Chu Y**, Yao PY, Wang W, Wang D, Wang Z, Zhang L, Huang Y, Ke Y, Ding X, Yao X. Aurora B kinase activation requires survivin priming phosphorylation by PLK1. *J Mol Cell Biol* 2011; **3**: 260-267 [PMID: 21148584 DOI: 10.1093/jmcb/mjq037]
32 **Tyagi S**, Bhui K, Singh R, Singh M, Raisuddin S, Shukla Y. Polo-like kinase1 (Plk1) knockdown enhances cisplatin chemosensitivity via up-regulation of p73α in p53 mutant human epidermoid squamous carcinoma cells. *Biochem Pharmacol* 2010; **80**: 1326-1334 [PMID: 20655883 DOI: 10.1016/j.bcp.2010.07.025]
33 **Degenhardt Y**, Greshock J, Laquerre S, Gilmartin AG, Jing J, Richter M, Zhang X, Bleam M, Halsey W, Hughes A, Moy C, Liu-Sullivan N, Powers S, Bachman K, Jackson J, Weber B, Wooster R. Sensitivity of cancer cells to Plk1 inhibitor GSK461364A is associated with loss of p53 function and chromosome instability. *Mol Cancer Ther* 2010; **9**: 2079-2089 [PMID: 20571075 DOI: 10.1158/1535-7163.MCT-10-0095]
34 **Van den Bossche J**, Domen A, Peeters M, Deben C, De Pauw I, Jacobs J, De Bruycker S, Specenier P, Pauwels P, Vermorken JB, Lardon F, Wouters A. Radiosensitization of Non-Small Cell Lung Cancer Cells by the Plk1 Inhibitor Volasertib Is Dependent on the p53 Status. *Cancers (Basel)* 2019; **11** [PMID: 31795121 DOI: 10.3390/cancers11121893]
35 **Van den Bossche J**, Deben C, De Pauw I, Lambrechts H, Hermans C, Deschoolmeester V, Jacobs J, Specenier P, Pauwels P, Vermorken JB, Peeters M, Lardon F, Wouters A. In vitro study of the Polo-like

kinase 1 inhibitor volasertib in non-small-cell lung cancer reveals a role for the tumor suppressor p53. *Mol Oncol* 2019; **13**: 1196-1213 [PMID: 30859681 DOI: 10.1002/1878-0261.12477]

36 **Yan X**, Su H. YM155 Down-Regulates Survivin and Induces P53 Up-Regulated Modulator of Apoptosis (PUMA)-Dependent in Oral Squamous Cell Carcinoma Cells. *Med Sci Monit* 2017; **23**: 1963-1972 [PMID: 28435150 DOI: 10.12659/msm.901643]

37 **Dixit U**, Pandey AK, Liu Z, Kumar S, Neiditch MB, Klein KM, Pandey VN. FUSE Binding Protein 1 Facilitates Persistent Hepatitis C Virus Replication in Hepatoma Cells by Regulating Tumor Suppressor p53. *J Virol* 2015; **89**: 7905-7921 [PMID: 25995247 DOI: 10.1128/JVI.00729-15]

38 **Zhang Q**, Bykov VJN, Wiman KG, Zawacka-Pankau J. APR-246 reactivates mutant p53 by targeting cysteines 124 and 277. *Cell Death Dis* 2018; **9**: 439 [PMID: 29670092 DOI: 10.1038/s41419-018-0463-7]

39 **Lehmann S**, Bykov VJ, Ali D, Andrén O, Cherif H, Tidefelt U, Uggla B, Yachnin J, Juliusson G, Moshfegh A, Paul C, Wiman KG, Andersson PO. Targeting p53 in vivo: a first-in-human study with p53-targeting compound APR-246 in refractory hematologic malignancies and prostate cancer. *J Clin Oncol* 2012; **30**: 3633-3639 [PMID: 22965953 DOI: 10.1200/JCO.2011.40.7783]

40 **Witkiewicz AK**, Chung S, Brough R, Vail P, Franco J, Lord CJ, Knudsen ES. Targeting the Vulnerability of RB Tumor Suppressor Loss in Triple-Negative Breast Cancer. *Cell Rep* 2018; **22**: 1185-1199 [PMID: 29386107 DOI: 10.1016/j.celrep.2018.01.022]

World Journal of Gastroenterology

Submit a Manuscript: https://www.f6publishing.com

World J Gastroenterol 2020 August 28; 26(32): 4802-4816

DOI: 10.3748/wjg.v26.i32.4802

ISSN 1007-9327 (print) ISSN 2219-2840 (online)

ORIGINAL ARTICLE

Basic Study

Promising xenograft animal model recapitulating the features of human pancreatic cancer

Jin-Xin Miao, Jian-Yao Wang, Hao-Ze Li, Hao-Ran Guo, Louisa S Chard Dunmall, Zhong-Xian Zhang, Zhen-Guo Cheng, Dong-Ling Gao, Jian-Zeng Dong, Zhong-De Wang, Yao-He Wang

ORCID number: Jin-Xin Miao 0000-0003-1688-3066; Jian-Yao Wang 0000-0001-6685-5253; Hao-Ze Li 0000-0002-3899-7120; Hao-Ran Guo 0000-0001-8924-202X; Louisa S Chard Dunmall 0000-0003-2380-0900; Zhong-Xian Zhang 0000-0001-6411-4814; Zhen-Guo Cheng 0000-0001-6375-3438; Dong-Ling Gao 0000-0002-1012-9751; Jian-Zeng Dong 0000-0001-7299-7805; Zhong-De Wang 0000-0003-2441-4729; Yao-He Wang 0000-0003-2367-6313.

Author contributions: Wang YH and Wang ZD conceived and supervised the study; Miao JX and Wang YH designed all experiments; Miao JX performed most experiments with Wang JY, Li HZ, Guo HR, and Zhang ZX; Gao DL did the histopathology staining and Cheng ZG reviewed histopathology; Dong JZ and Chard Dunmall LS revised the manuscript; Miao JX, Wang YH, and Wang ZD interpreted all results and wrote the manuscript.

Supported by the National Key R and D Program of China, No. 2016YFE0200800; Nature Sciences Foundation of China, No. 81771776; Nature Sciences Foundation of China, No. U1704282; and Medical Research of Council, No. MR/M015696/1.

Jin-Xin Miao, Jian-Yao Wang, Hao-Ze Li, Hao-Ran Guo, Zhong-Xian Zhang, Zhen-Guo Cheng, Dong-Ling Gao, Yao-He Wang, Sino-British Research Centre for Molecular Oncology, National Centre for International Research in Cell and Gene Therapy, Academy of Medical Sciences, Zhengzhou University, Zhengzhou 450000, Henan Province, China

Jin-Xin Miao, Academy of Chinese Medical Sciences, Henan University of Chinese Medicine, Zhengzhou 450000, Henan Province, China

Louisa S Chard Dunmall, Yao-He Wang, Centre for Biomarkers and Biotherapeutics, Barts Cancer Institute, Queen Mary University of London, London EC1M6BQ, United Kingdom

Jian-Zeng Dong, Department of Cardiology, Beijing Anzhen Hospital, Capital Medical University, Beijing 100029, China

Zhong-De Wang, Department of Animal Dairy, and Veterinary Sciences, Utah State University, Logan UT 84341, United States

Corresponding author: Yao-He Wang, MD, PhD, Professor, Sino-British Research Centre for Molecular Oncology, National Centre for International Research in Cell and Gene Therapy, Academy of Medical Sciences, Zhengzhou University, No. 100 Kexue Road, Zhengzhou 450000, Henan Province, China. yaohe.wang@qmul.ac.uk

Abstract

BACKGROUND

Multiple sites of metastasis and desmoplastic reactions in the stroma are key features of human pancreatic cancer (PC). There are currently no simple and reliable animal models that can mimic these features for accurate disease modeling.

AIM

To create a new xenograft animal model that can faithfully recapitulate the features of human PC.

METHODS

Interleukin 2 receptor subunit gamma (*IL2RG*) gene knockout Syrian hamster was created and characterized. A panel of human PC cell lines were transplanted into *IL2RG* knockout Syrian hamsters and severe immune-deficient mice

Institutional review board statement: The study was reviewed and approved by the Academy of Medical Sciences, Zhengzhou University Institutional Review Board.

Institutional animal care and use committee statement: All animal experiments conformed to the Provision and General Recommendation of Chinese Experimental Animals Administration Legislation accepted principles for the care and use of laboratory animals (IACUC-ZZU-2016/Wang, The Ethics Committee on Animal Experiment of Zhengzhou University, Zhengzhou, Henan, China).

Conflict-of-interest statement: The authors disclose that they have no competing interests.

Data sharing statement: No additional data are available.

ARRIVE guidelines statement: The authors have read the ARRIVE guidelines, and the manuscript was prepared and revised according to the ARRIVE guidelines.

Manuscript source: Unsolicited manuscript

Received: April 14, 2020
Peer-review started: April 14, 2020
First decision: June 18, 2020
Revised: July 1, 2020
Accepted: August 4, 2020
Article in press: August 4, 2020

subcutaneously or orthotopically. Tumor growth, local invasion, remote organ metastasis, histopathology, and molecular alterations of tumor cells and stroma were compared over time.

RESULTS

The Syrian hamster with *IL2RG* gene knockout (named ZZU001) demonstrated an immune-deficient phenotype and function. ZZU001 hamsters faithfully recapitulated most features of human PC, in particular, they developed metastasis at multiple sites. PC tissues derived from ZZU001 hamsters displayed desmoplastic reactions in the stroma and epithelial to mesenchymal transition phenotypes, whereas PC tissues derived from immune-deficient mice did not present such features.

CONCLUSION

ZZU001 hamsters engrafted with human PC cells are a superior animal model compared to immune-deficient mice. ZZU001 hamsters can be a valuable animal model for better understanding the molecular mechanism of tumorigenesis and metastasis and the evaluation of new drugs targeting human PC.

Key words: Pancreatic cancer; Xenotrans plantation; Syrian hamster; IL-2 receptor gamma chain gene; Metastasis; Animal model

Core tip: Xenograft cell transplantation into immune-deficient mice has become the gold standard for assessing tumor progression and efficacy of cancer drugs. However, xenografting human pancreatic cancer (PC) models in nude mice rarely results in development of metastasis and thus does not accurately reflect tumor progression as seen in the human disease. Here, we created a new immune-deficient Syrian hamster with interleukin 2 receptor subunit gamma (*IL2RG*) gene knockout and demonstrated that the *IL2RG*-/- Syrian hamster is a promising animal model that can faithfully recapitulate most features of human PC, notably multiple sites of metastasis. Furthermore, this model can present other key features of human PC, such as stromal reaction and the communication between stromal cells and PC cells.

Citation: Miao JX, Wang JY, Li HZ, Guo HR, Dunmall LSC, Zhang ZX, Cheng ZG, Gao DL, Dong JZ, Wang ZD, Wang YH. Promising xenograft animal model recapitulating the features of human pancreatic cancer. *World J Gastroenterol* 2020; 26(32): 4802-4816
URL: https://www.wjgnet.com/1007-9327/full/v26/i32/4802.htm
DOI: https://dx.doi.org/10.3748/wjg.v26.i32.4802

INTRODUCTION

Pancreatic cancer (PC) is one of the most deadly human diseases, with a 5-year survival rate of less than 7%. It is predicted to be the second leading cause of cancer-associated mortality within the next decade in developed countries[1]. Even when primary cancer can be removed by radical surgery, the recurrence rate of PC is as high as 85%[2,3]. Multiple-sites of metastasis from PC remains a significant hurdle in treating this disease. Thus, reliable animal models that can mimic the clinical features of PC are needed for better understanding the molecular mechanisms of tumorigenesis, development of practical approaches for early diagnosis, and evaluation of novel therapeutic agents.

In preclinical studies, there have been several models developed for human PC research, such as human PC cell lines, cell line-based xenografts, patient-derived tumor xenografts, transgenic mice models, as well as recently developed pancreatic ductal organoids, three-dimensional culture systems, and organoid-based xenografts[4]. Among these models, xenografting of human tumor cells into immune-deficient mice has become the gold standard for assessing tumor progression and the preclinical efficacy of cancer drugs. However, subcutaneous xenograft PC tumor models in nude mice rarely develop metastasis[5]. The orthotopic model of human PC

Published online: August 28, 2020

P-Reviewer: Sun XT, Wang XB, Zhang XB
S-Editor: Zhang L
L-Editor: Filipodia
P-Editor: Zhang YL

in nude mice provides a better way to evaluate tumor growth, but metastasis to the lung or/and other organs occurs rarely from most human PC cell lines tested[6,7]. Furthermore, it has been shown that cell-line based xenografts in immune-deficient mice could not consistently predict therapeutic response of human PC[8-11]. The lack of predictive drug responsiveness using xenograft models is likely due to multiple factors[4]. The major reason is that xenografts of human tumors grow primarily in immune-deficient mice as homogenous masses of tumor cells with limited stromal infiltration. This may be particularly relevant for PC, since PC tumors are predominantly comprised of a stromal compartment consisting of an acellular extracellular matrix and a variety of non-neoplastic cell types, such as cancer-associated fibroblasts, immune cells, and vascular cells[12]. To overcome these challenges, more robust animal models are needed.

Accumulating evidence demonstrates that Syrian hamsters (*Mesocricetus auratus*) have advantages as models for various diseases due to the high similarities in anatomy, physiology, and pathology between Syrian hamsters and humans[13,14]. The Syrian hamster is the only rodent species that develops PC in an almost identical manner to the respective human disease regarding such features as clinical symptoms, tumor morphology, tumor biology, metabolic abnormality, and molecular genetic alterations[15]. In addition, we recently found that human interleukin (IL)-12 is effective in stimulating both human and hamster peripheral blood mononuclear cells. Human IL-12 effectively stimulates interferon-gamma and tumor necrosis factor-alpha expression in activated hamster splenocytes *ex vivo* and demonstrates toxicity *in vivo* in Syrian hamsters bearing PC[16]. However, human IL-12 does not function in mouse at all. Similarly, human granulocyte-macrophage colony-stimulating factor functions on hamster cells but not on mouse cells[17]. These observations suggest that human tumor cells may be able to communicate with the host cells of Syrian hamster through human tumor cell secreting molecules that function on Syrian hamster cells. We reasoned that immunocompromised Syrian hamsters might be the most appropriate hosts for human cancer xenografting to model the features of human PC. Recently, we made a technical breakthrough in establishing efficient gene targeting techniques in the Syrian hamster[18]. Here, we report the creation and characterization of an IL-2 receptor subunit gamma (*IL2RG*) gene knockout Syrian hamster model (named ZZU001) and its use as a host for human PC cell xenotransplantation. ZZU001 represents a convenient, cost-effective, and reliable model for recapitulating the progression and multiple-sites metastasis of human PC.

MATERIALS AND METHODS

Animals and ethics statement

Syrian hamsters (4- to 5-wk-old, 80 g in weight) were purchased from Beijing Vital River Laboratory Animal Technology Co. (Beijing, China). B-NDG (NOD-Prkdc^{scid} IL2rg^{tm1}/Bcgen mice deficient in mature T lymphocytes, B lymphocytes, and natural killer cells) mice (4- to 5-wk-old, male, 20 g in weight) were purchased from Beijing Biocytogen Co., Ltd. (Beijing, China). The animals were maintained under specific pathogen-free, 14 h light/10 h dark cycle (room temperature 23 ± 0.5°C, humidity 40%-60%) conditions, and the animals had free access to irradiated chow and water. To ameliorate the suffering of animals observed throughout experimental studies, animals were euthanized by CO_2 inhalation. All surgery was performed under intraperitoneal injection of Avertin (Sigma-Aldrich, St Louis, MO, United States) anesthesia, and all efforts were made to minimize animal suffering. Avertin Stock solution was prepared as follows: 25 g avertin (2, 2, 2-Tribromoethanol) and 15.5 mL tert-Amyl Alcohol (2-methyl-2-butanol) mixed approximately 12 h in a dark bottle at room temperature. Working solution was prepared as follows: 0.5 mL Avertin stock and 39.5 mL 0.9% saline (NaCl) mixed in dark container, filter sterilized, and stored at 4°C. All animal care and experiments were approved by the Ethical Committee of the Zhengzhou University and were in accordance with the Provision and General Recommendation of Chinese Experimental Animals Administration Legislation.

Cell lines and adenovirus

All human pancreatic cell lines listed in Table 1 and A549 cell line were purchased from American Type Culture Collection (ATCC, Manassas, VA, United States). All the cell lines had been short tandem repeat genotyped and confirmed identical to the published deoxyribonucleic acid (DNA) profiles of the American Type Culture Collection. All cells were grown in Dulbecco's modified Eagle's medium (Gibco,

Table 1 Sites and frequency [*n*/*n* (%)] of distant metastasis and local tumor infiltration of MIA-PaCa-2 cells

	MIAPaCa-2 (SC)		MIAPaCa-2 (OrT)	
	B-NDG	ZZU001	B-NDG	ZZU001
Distant metastasis				
Liver	-	-	3/5 (60)	5/5 (100)
Lung	-	5/5 (100)	-	5/5 (100)
Retroperitoneum	-	-	3/5 (60)	5/5 (100)
Mesentery	-	-	3/5 (60)	5/5 (100)
Diaphragm	-	-	2/5 (40)	2/5 (40)
Spleen	-	-	2/5 (40)	-
Stomach	-	-	-	1/5 (20)
Kidney	-	2/5 (40)	-	5/5 (100)
Adrenal gland	-	1/5 (20)	-	2/5 (40)
Local infiltration				
Spleen	-	-	3/5(60)	4/5 (80)
Stomach	-	-	1/5 (20)	3/5 (60)
Liver (hilus)	-	-	3/5 (60)	5/5 (100)
Kidney (hilus)	-	-	-	1/5 (20)
Retroperitoneum	-	-	3/5 (60)	5/5 (100)
Bowel	-	-	3/5 (60)	5/5 (100)
Mesentery (adjacent to pancreas)	-		4/5 (80)	5/5 (100)
Signs of tumor burden				
Ascites	-	-	3/5 (60)	3/5 (60)
Jaundice	-	-	2/5 (40)	3/5 (60)
Ileus	-	-	-	2/5 (40)
Cachexia	-	-	1/5 (20)	3/5 (60)

OrT: Orthotopic; SC: Subcutaneous.

Grand Island, NY, United States) supplemented with 10% fetal bovine serum (PAN, Germany), 50 μg/mL streptomycin, and 50 μg/mL penicillin (Sigma-Aldrich). Cells were maintained at 37°C and 5% CO_2. Human Adenovirus type 5 (Ad5) was made and titrated as previously described[14].

Generation of IL2RG knockout (ZZU001) Syrian hamsters by CRISPR/Cas9

Single-guide ribonucleic acid (sgRNA) design, synthesis, embryo manipulation, and embryo transfer were performed for establishment of *IL2RG*$^{-/-}$ Syrian hamster, as described previously[18]. In brief, sgRNA was designed to target a site-specific sequence within the first exon of *IL2RG* gene (NW_004801714.1). Microinjection was performed under red light, and HECM-9 medium covered by mineral oil was used as injection medium. For cytoplasmic injection, both Cas9 mRNA (100 ng/μL) and sgRNA (50 ng/μL) were co-injected into the cytoplasm of the fertilized eggs. The injected embryos were cultured in HECM-9 medium covered by mineral oil at 37.5˚C under 10% CO_2, 5% O_2, and 85% N_2 for 0.5 h before use. Viable embryos after injection were transferred to each oviduct (15 embryos per oviduct) of pseudo-pregnant females. Genotyping analysis of pups produced from microinjected embryos was performed by Sanger sequence with genomic DNA isolated from toes collected from 2-wk-old pups. Genomic regions flanking the CRISPR targeted sites were amplified by polymerase chain reaction (PCR) using primers; Forward: GAGAGTGGTTCAGGGTTCTGACA, Reverse: TGGGCTGGAGCTCAGAACTG. The PCR products were directly sequenced. Potential off-target effect was analyzed based on the rule that sequences matching the

final 12 nt of the target sequence and protospacer adjacent motif sequence might cause the off-target effect[19]. The off-target fragments were amplified from the founder's genomic DNA and identified by Sanger sequence. The primer sequences are shown in Table S1.

Reverse transcriptase-quantitative PCR (RT-qPCR) and western blotting

Total RNA from spleens or thymus or other organs of 5-wk-old Syrian hamsters was extracted using the TRIzol Reagent (Invitrogen, Carlsbad, CA, United States). First strand cDNA was synthesized from 1 μg of total RNA using PrimeScript RT Master Mix (Takara, Kyoto, Japan). SYBR-green based-qPCR reactions were performed in a StepOnePlus system (Applied Biosystems, Republic of Singapore) thermal cycler. Quantitative PCR reactions were carried out in triplicate, and the specific primers of different immune cell markers were previously described[13]. The mRNA expression was quantitated using the 2-(ΔCt sample–ΔCt control) method. Western blot analyses were performed as previously described[13]. Whole cell protein was isolated from spleens of 5-wk-old Syrian hamsters. Western blotting was performed for detection of the IL2RG protein (A-10 antibody, sc-271060, Santa Cruz Biotechnology, Dallas, TX, United States) while glyceraldehyde 3-phosphate dehydrogenase (60004-1-Ig, Proteintech, Rosemont, IL, United States) expression was used as a loading control.

Infection of hamsters with Ad5 and determination of anti-Ad5 neutralizing antibody (Nab) titers in the serum

The *IL2RG* homozygous Syrian hamsters and wild type (WT) control hamsters were anesthetized with 1.2% working solution avertin (45 mg/kg) and injected with 1×10^{10} plaque forming units /kg of Ad5 by intramuscular injection. Day 14 after prime immunization, the hamsters were boosted using the same dose and route, and the hamsters were sacrificed on day 17. The Nab titer of the samples was determined as described previously[20]. In brief, serum samples were collected and incubated for 30 min at 56°C to inactivate complement. Ad5 was incubated with serially diluted serum samples, and then then the mix (virus-serum) was added to A549 cells and incubated at 37°C. After 10 d, inhibition of cytopathic effects was measured. Nab titer in serum was determined as described previously[14].

Histopathological analysis

Tissues of the Syrian hamsters and immune-deficient mice were harvested, visually inspected, fixed in 10% neutral buffered formalin, and embedded in paraffin. The embedded tissues were stained with hematoxylin and eosin and Masson's trichrome. Immunohistochemistry (IHC) analysis was conducted as described previously[16]. IHC of vimentin and smooth muscle actin (SMA) was performed using paraffin section of the tumors with a primary antibody against vimentin (ZM-0260, ZSGB-BIO, Beijing, China) and SMA antibody (ZM-0003, ZSGB-BIO). The histopathological results were evaluated by two independent pathologists.

Flow cytometry

Five-week-old hamsters were sacrificed, and single cells from the thymus and spleen were prepared for flow cytometric analyses. To obtain single-cell suspensions, tissues were cut to small pieces with scissors and passed through a 70-μm cell strainer (BD Biosciences, Franklin Lakes, NJ, United States) by pressing with plunger. The red blood cells were eliminated by using red blood cell lysis buffer. The prepared cells were stained with a 1:400 dilution of fluorescein isothiocyanate conjugated anti-mouse major histocompatibility complex (MHC) class II (I-Ek; clone 14-4-4S), a 1:300 dilution of antigen presenting cell conjugated anti-mouse CD4 (clone GK1.5) (all from E-Bioscience, San Diego, CA, United States), a 1:100 dilution of anti-CD3 (clone 4F11 developed by us[14]) was followed by incubation with a 1:50 dilution of a goat anti-mouse secondary antibody (ZF-0312, ZSGB-BIO). The samples were analyzed on a BD Accuri C6 (BD Biosciences). The data were acquired using Accuri CFlow software (BD Biosciences) on the LSR II and analyzed using the FlowJo VX software.

Tumor cell xenotransplantation

Subcutaneous injections of 5×10^6 MIA-PaCa2 cells or other cells in the right upper flank were performed on 5-wk-old male ZZU001 Syrian hamsters (n = 14) and same age-matched B-NDG mice (n = 14). Tumor size was measured using calipers twice weekly until tumors reached 2000 mm^3 (for B-NDG mice) or 3500 mm^3 (for ZZU001 Syrian hamster) or tumor ulceration occurred. Tumor volumes (V) were calculated using the formula $V = (\text{length} \times \text{width}^2 \times \pi)/6$). Comparisons were analyzed by

Student's *t*-test. All data were expressed as the mean ± standard deviation.

Orthotopic tumor model establishment

ZZU001 hamsters (n = 5) and B-NDG mice (n = 5) were anesthetized with 1.2% working solution avertin (45 mg/kg). Animals were placed in the dorsal decubitus position, and left subcostal incision was made. The pancreas was carefully exposed. MIA-PaCa2 cells (1×10^6) were suspended in matrigel (Corning, Bedford, MA, United States) (final volume: 50 μL). The cell suspension was orthotopically injected into the tail of the pancreas with a 29-gauge needle. The pancreas was returned to the peritoneal cavity, and the abdominal wall was closed in two layers with 3-0 nylon sutures (Huato, Suzhou, China). The animals were monitored daily for their general condition and sacrificed by CO_2 10 wk after the orthotopic cell injection. Animals had to be killed earlier if one of the following criteria occurred: Formation of ascites with visible abdominal distension; jaundice, cachexia, or both associated with a significant clinical deterioration of the animal.

Statistical analysis

Statistical analyses were conducted using a Student's *t*-test for the comparison between groups. Results were considered significant at $P < 0.05$. The results were analyzed with GraphPad software (La Jolla, CA, United States).

RESULTS

Generation of X-SCID Syrian hamsters by CRISPR/Cas9

To produce *IL2RG* knock-out (KO) Syrian hamster, the CRISPR/Cas9 system with a single guide RNA designed to target the first exon of the hamster *IL2RG* gene (Figure 1A) was employed as described previously[18]. The validated sgRNA and Cas9 mRNA were delivered into Syrian hamster zygotes by cytoplasmic injection. Cytoplasmic injected fertilized eggs were then transferred to pseudopregnant female hamsters (Table S2). Screening of eight newborn pups revealed that three (37.5%) carried targeted mutations. One had a 10 bp deletion that resulted in a reading frameshift in the *IL2RG* gene, leading to a premature stop codon (at 16th amino acid, Figure 1B and C). We established a viable breeding colony from the F0 founder carrying this indel. Because *IL2RG* is located on the X chromosome, the term of "homozygous KO" used herein refers to either female with both of the X chromosome alleles targeted or males with its single X chromosome targeted. The homozygous *IL2RG* KO hamsters were named ZZU001. As shown in Figure 1D, ZZU001 Syrian hamsters with homozygous 10 bp deletion of *IL2RG* had very little mRNA expression of *IL2RG* compared to wild type hamsters in thymus, as revealed by RT-qPCR, and no IL2RG protein expression in ZZU001 spleen was detectable by Western blotting (Figure 1E). In order to determine whether the *IL2RG*-specific sgRNA only induced mutations in the *IL2RG* gene but not in any other genomic loci, we identified six potential off-target sites using Benchling software (Table S3). Off-target analysis showed that no off-target events occurred in the 10 bp deletion of *IL2RG* founder (Figure S1), indicating that the sgRNA used in this study is specific, and all features of ZZU001 are due to defects of the *IL2RG* gene and no other genetic changes.

Abnormal lymphoid cell development and impaired immune function in ZZU001 Syrian hamsters

Gross necropsy and microscopic analyses of ZZU001 Syrian hamsters revealed impaired lymphoid development. The thymuses and spleens were examined at 5 wk of age in WT, heterozygous *IL2RG* KO, and homozygous *IL2RG* KO hamsters. The thymus of homozygous *IL2RG* KO hamsters was extremely hypoplastic and significantly reduced in size (Figure 2A), and consisted of an epithelial rudiment without any lymphocytes compared to WT (Figure 3A and B). The spleen of homozygous *IL2RG* KO hamsters was moderately decreased in size, as seen in Figure 2A. It was also much thinner and more loosely packed than those of heterozygous KO and WT hamsters, while the white pulp was almost completely devoid of lymphocytes compared to WT (Figure 3C and D). The thymus/body and spleen/body weight ratios in homozygous KO Syrian hamsters were lower than those in heterozygous KO and WT (Figure 2B). ZZU001 hamsters had no noticeable lymph nodes compared to WT hamsters (Figure 2C). In addition, *IL2RG* KO Syrian hamsters can survive over 72 wk (1.5 years), with a median survival time that exceeds 89 wk (

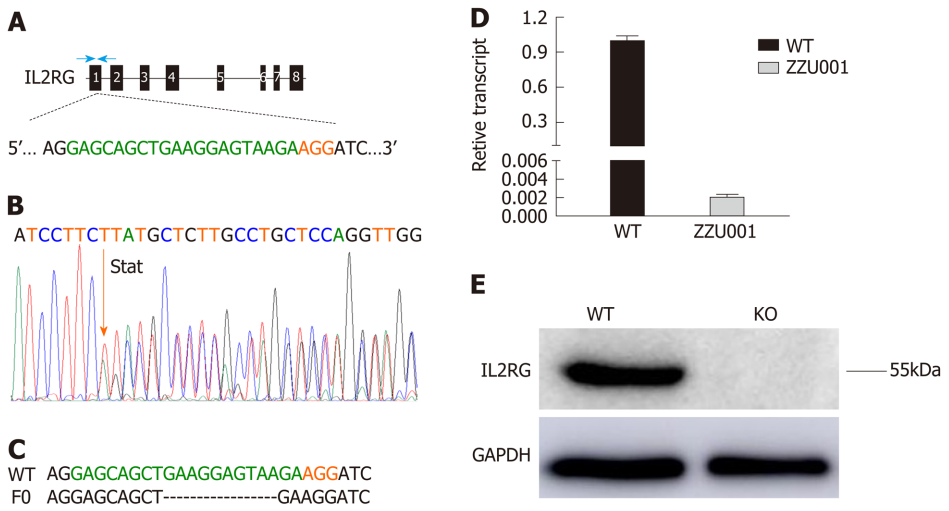

Figure 1 Interleukin 2 receptor subunit gamma knockout Syrian hamsters (ZZU001) generated by CRISPR/Cas9. A: Schematic representation of the Syrian hamster interleukin 2 receptor subunit gamma *(IL2RG)* gene. The single-guide RNA target sequence is shown in green with the protospacer adjacent motif shown in red; B: Polymerase chain reaction product sequencing confirming the founder is shown. "Stat" refers to the mutant site; C: Sequencing assay for single-guide RNA/Cas9-IL2RG-induced mutation in the target region in Syrian hamsters. Multiple deletions are depicted by dashes; D: Quantitative real-time polymerase chain reaction analysis of *IL2RG* mRNA expression in the thymus of wild type and ZZU001 Syrian hamsters. $^{b}P < 0.01$. $n = 3$. Glyceraldehyde 3-phosphate dehydrogenase mRNA expression was used as an internal control; E: Western blotting assay to compare the expression of IL2RG protein in wild type and ZZU001 Syrian hamsters. Glyceraldehyde 3-phosphate dehydrogenase was used as a loading control. KO: Knock-out; sgRNA: Single-guide ribonucleic acid; WT: Wild type.

Figure S2).

RT-qPCR analysis of splenocytes of ZZU001 Syrian hamsters demonstrated that the expression of T lymphocyte-specific genes (CD3γ and CD4), B lymphocyte-specific genes [CD22 and FCMR (immunoglobulin M receptor)], and natural killer cell-specific genes (CD94 and Klrg1) were significantly lower than those in WT hamsters (Figure 3E). Immune cell marker gene expression was also examined in the thymus and bone marrow (Figure S3), showing a similar pattern as in the spleen (Figure 3E). In order to confirm further the deficiency of immune cells in *IL2RG* KO hamsters, flow cytometry analysis of immune molecules in monocytes isolated from thymus and spleen were performed. As shown in Figure S4, there was a clear decrease of the lymphocytes in ZZU001 Syrian hamsters; $CD3^{+}$ or $CD4^{+}$ positive T cells were almost absent from the ZZU001 hamster thymus and spleen. MHC class II positive cells were markedly decreased in ZZU001 Syrian hamster spleen (Figure S4B). There were no MHC class II expressing cells in the thymus. Consistent with the histology, the number of splenocytes and thymocytes was dramatically reduced in ZZU001 Syrian hamster compared with WT hamsters. Analysis of B cell function demonstrated that ZZU001 Syrian hamsters could not produce neutralizing antibodies against Ad5 (Figure 3F) after infection with Ad5. Based on these findings, it is evident that ZZU001 hamsters have a severe immune deficiency in T cell, B cell, and possibly natural killer cells.

Subcutaneous xenotransplantation of human PC cells

Immune-deficient mice can accept transplanted tissues from humans. Having made severely immune-deficient ZZU001 Syrian hamsters, subcutaneous tumors of the human PC cell line MIA-PaCa-2 were established in ZZU001 hamsters and immune-deficient B-NDG mice. It was found that xenografts tumors of the human PC cell line MIA-PaCa-2 developed well in both ZZU001 Syrian hamsters and B-NDG mice (Figure 4A). Consistent with previous reports, no distant metastasis in immune-deficient mice was observed (Table 1, Figure 4B and C). In contrast, all ZZU001 hamsters bearing subcutaneous tumors developed lung metastasis (occurring as early as 29 d after injection of the human PC cell line MIA-PaCa-2), coupled with metastasis in kidneys (40%) and adrenal glands (20%) (Table 1 and Figure 4B). Subcutaneous xenograft tumors from four other human PC cell lines, including Panc-1, SUIT-2, Patu8988T, and Capan-1, were established, and the tumor growth and remote organ metastasis were examined. As shown in Table 2, all four additional PC cell lines developed remote metastasis in lung, liver, and kidney although the remote metastatic frequency and sites varied between different PC cell lines.

Table 2 Sites and frequency [*n*/*n* (%)] of distant metastasis of four different human pancreatic cancer cell lines

	Panc-1 (SC)	SUIT-2 (SC)	Patu8988T (SC)	Capan-1 (SC)
	ZZU001	ZZU001	ZZU001	ZZU001
Distant metastasis				
Liver	-	1/3 (33)	3/5 (60)	-
Lung	5/5 (100)	3/3 (100)	-	5/5 (100)
Retroperitoneum	-	-	-	-
Mesentery	-	-	-	-
Diaphragm	-	-	-	-
Spleen	-	-	-	-
Stomach	-	-	-	-
Kidney	-	1/3 (33)	1/5 (20)	-
Adrenal gland	-	-	-	-

SC: Subcutaneous.

Orthotopic transplantation of human PC cells

Orthotopic transplantation models can mimic the biological behavior of the primary tumor more closely compared with subcutaneous transplantation models, although orthotopic xenotransplantation procedures are technically difficult to perform for PC, with strong potential for complications. In order to assess the potential value of a PC orthotopic model in ZZU001 hamsters, MIA-PaCa-2 cells were injected into pancreas of ZZU001 hamsters and B-NDG mice. Tumor formation rate was 100% (5/5) in the ZZU001 Syrian hamsters that received orthotopic transplantation of Mia-PaCa2 cells (Table 1), and hamsters developed metastasis at multiple-sites after orthotopic implantation, including the liver (100%), lung (100%), retroperitoneum (100%), mesentery (100%), diaphragm (40%), stomach (20%), kidney (100%), and adrenal gland (40%). In comparison, no lung metastasis was detected in the B-NDG mouse orthotopic model, and the frequency of metastasis to other organs was lower (Table 1). The histopathological features of cancer cells in the metastatic nodules presented similar morphological changes as those found in the primary tumors of pancreas, showing epithelial cell morphology. Tumor cells are strikingly heterogeneous within tumors and presented solid growth with nuclear polymorphism and abnormal mitoses while the desmoplastic stromal reaction is less developed in the most of metastatic tumors (Figure 5). Furthermore, ZZU001 Syrian hamster orthotopic models presented similar clinical and pathological features as observed in human patients, such as local infiltration of cancer cells and signs of tumor burden, including ascites, jaundice, ileus, and cachexia (Table 1).

Interaction of PC cells and stroma in xenograft tumors of PC

In order to dissect the possible mechanisms for metastasis of human PC in ZZU001 hamsters, we investigated the alteration of stroma and tumor cells within the xenograft tumors derived from ZZU001 hamsters and B-NDG mice through biochemistry and IHC staining. Of note, desmoplastic reactions that consist of extracellular matrix proteins, including collagen and fibronectin (Figure 4D) and active fibroblasts [SMA-positive staining (Figure 4D)] were readily observed in the stroma of ZZU001 hamster xenograft tumors but not in the xenograft tumors derived from B-NDG mice. Most interestingly, the tumor cells growing in ZZU001 hamsters displayed strong vimentin positive staining, indicative of epithelial to mesenchymal transition (EMT) (Figure 4D), whereas no obviously vimentin-positive tumor cells were observed in B-NDG mice xenograft tumors (Figure 4D). These observations suggest human PC cells could communicate with host cells of ZZU001 hamsters, which results in the improved engraftments and development of human tumor cells in ZZU001 Syrian hamsters. Thus, the ZZU001 hamster bearing PC model can recapitulate more key features of human PC, including metastasis and stromal reaction, compared to severe immune-deficient mice models.

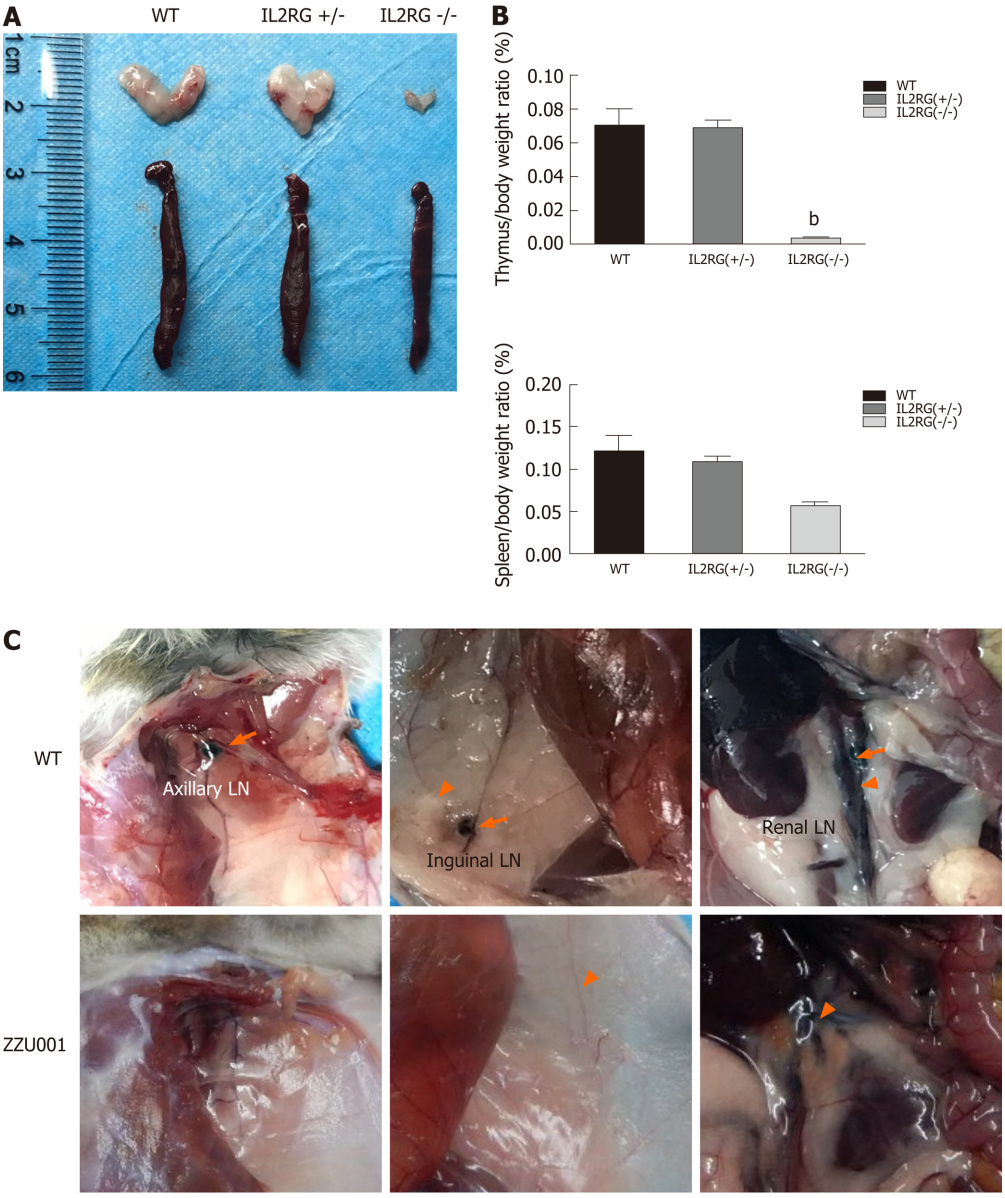

Figure 2 ZZU001 Syrian hamsters demonstrate abnormal lymphoid cell development and impaired immune function. A: The thymus and spleen of interleukin 2 receptor subunit gamma *(IL2RG)* knock-out (KO) hamsters were both evidently smaller than those of age-matched interleukin 2 receptor subunit gamma +/- and wild type (WT) hamsters; B: Comparison of spleen-to-body weight ratio. Each value represents the mean ± standard deviation (n = 3/group), Student's t-test. $^{b}P < 0.01$; and C: Dye labeling of Syrian hamster lymph nodes (LNs) and lymphatic vessels. Efferent lymphatic vessel (orange arrowhead). Axillary LN, Inguinal LN, and Renal LN (orange arrow) are LNs.

DISCUSSION

Implantation of human PC cells subcutaneously into immune-deficient mice has been widely used for the generation of *in vivo* human PC models, largely due to their comparatively low cost, ease and speed of establishment, and predictable tumor growth. However, these models do not faithfully recapitulate the features of human PC, in particular, as they fail to model the multiple-sites of metastasis observed during disease progression[5-7]. In the current study, we created an *IL2RG* KO immune-deficient Syrian hamster (ZZU001) and demonstrated that an array of human PC cell lines, when subcutaneously transplanted, can result in multiple-sites of metastasis, including the lung, liver, kidney, and adrenal glands, although the metastasis frequency in liver is still low compared to observed levels in human patients. In striking contrast, no metastasis from any of these cell lines was observed in severe immune-deficient B-NDG mice. Therefore, the ZZU001 Syrian hamster model provides a novel animal model to recapitulate more accurately metastasis of human PC.

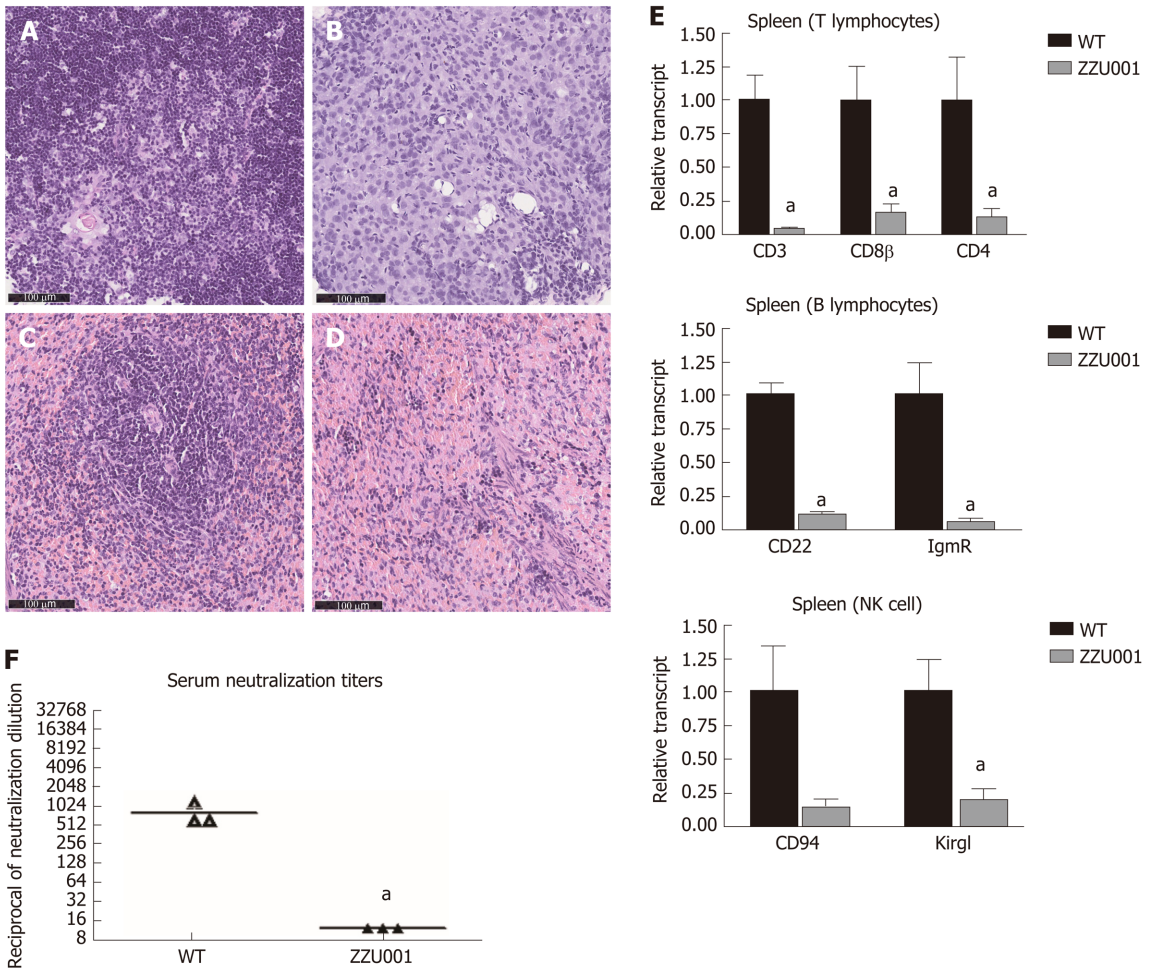

Figure 3 ZZU001 Syrian hamsters demonstrate immune despair cellular abnormalities in lymphoid development. A and C: Representative histology of the wild type (WT) thymus and spleen. Bars = 100 μm; Representative histology of ZZU001 Syrian hamsters thymus B and spleen D and E: The expression of the indicated lymphocyte-specific genes in spleen homogenates was determined by reverse transcriptase quantitative polymerase chain reaction using the 2^ (-ΔΔCt) method. $^{a}P < 0.05$. $n = 3$; F: Development of neutralizing antibodies against AdV-5. $n = 3$. $^{a}P < 0.05$.

Pancreatic metastases can arise in any organ site but are mostly detected in abdominal sites. The liver is the most common organ in which metastasis is detected, followed by the peritoneum, lung and pleura, bones, and adrenal glands[21]. The comparison of MIA-PaCa-2 orthotopic models in B-NDG and ZZU001 (Table 1) demonstrates that the ZZU001 orthotopic tumor model presents a more accurate representation of human PC than the mouse models, particularly with regards to distant metastasis and local infiltration of cancer cells. Interestingly, ZZU001 xenograft models show a high frequency of kidney metastasis (40% in the subcutaneous model and 100% in the orthotopic model), although kidney metastasis of PC in humans has not been extensively reported[22]. This warrants further investigation.

PC progression is complemented by a fibrotic stromal (desmoplastic) reaction characterized by extensive deposition of extracellular matrix components, recruitment and activation of cancer-associated fibroblasts, decreased vasculature patency, and altered immune-surveillance[23]. Stromal remodeling leads to altered interactions between tumor cells and stromal compartments, which can promote tumor progression[24]. Presence of a robust, reactive, and desmoplastic stroma and the crosstalk between cancer cells and stromal cells are critical for PC progression and metastasis[25,26]. An ideal animal model of PC should reflect these important features, but xenografted tumors in mice rarely develop stromal reactions nor the EMT phenotype (Figure 4D). Strikingly, ZZU001 hamster xenograft tumors present a considerable amount of extracellular matrix reaction, as evidenced by diffusive strong Masson staining (Figure 4D) and activation of fibroblasts measured by expression of SMA (Figure 4D). The activated fibroblast may be a key factor affecting distant metastasis in ZZU001 hamster model as cancer-associated fibroblasts promote tumor growth and metastasis in a variety of ways[27]. Importantly, some tumor cells in

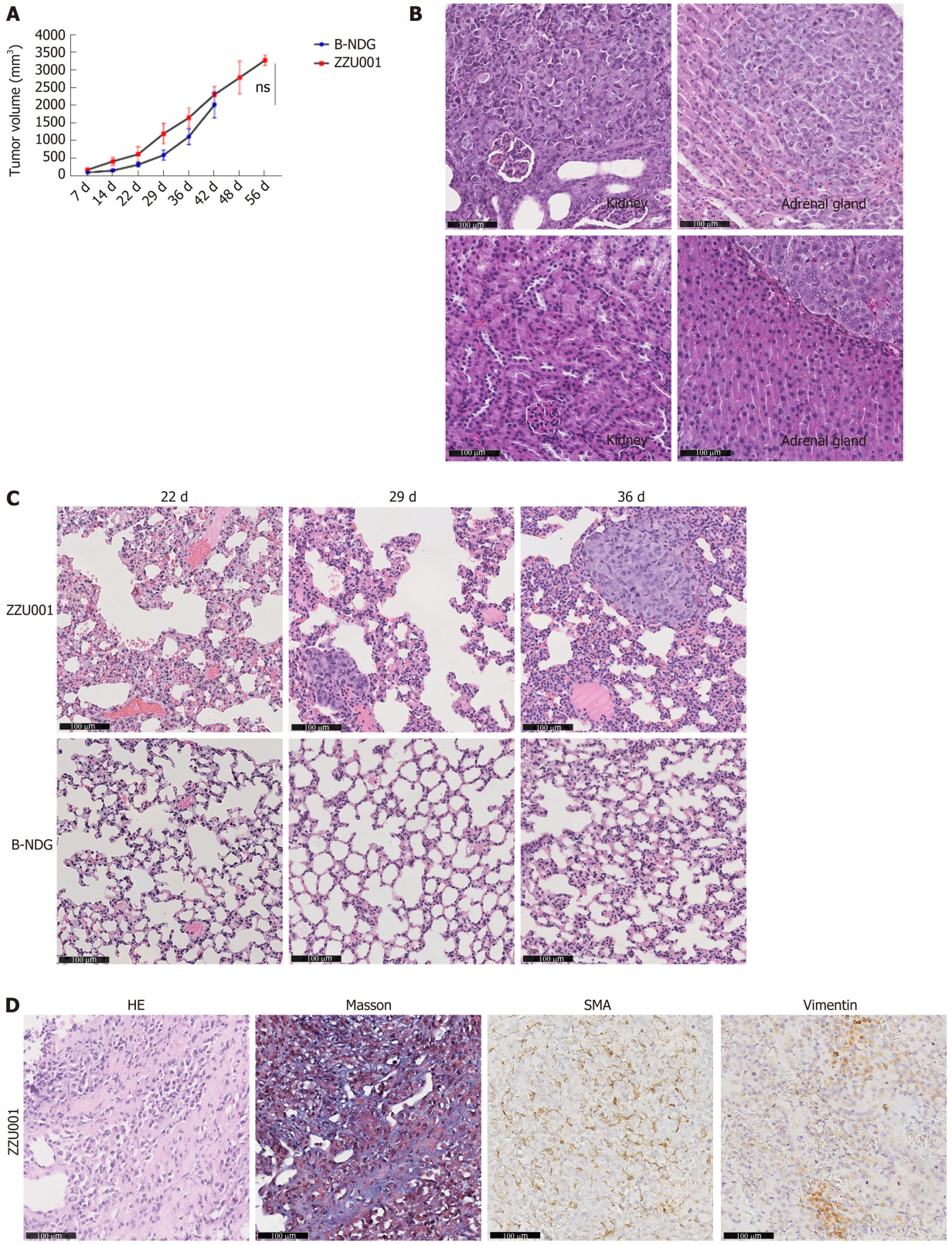
A
Tumor volume (mm3)
4000
3500
3000
2500
2000
1500
1000
500
0
7 d
14 d
22 d
29 d
36 d
42 d
48 d
56 d
B-NDG
ZZU001
ns
B
Kidney
Adrenal gland
Kidney
Adrenal gland
C
22 d
29 d
36 d
ZZU001
B-NDG
D
HE
Masson
SMA
Vimentin
ZZU001

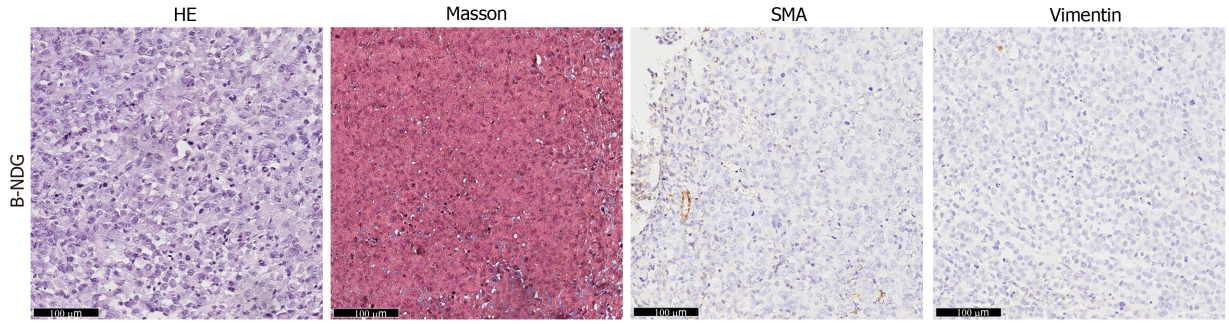

Figure 4 Xenotransplantation of human pancreatic cancer cells into ZZU001 Syrian hamsters recapitulates human pancreatic cancer metastasis. A: Growth curve of human MIA-PaCa-2 pancreatic cancer cells in ZZU01 Syrian hamsters and B-NDG mice. MIAPaCa-2 cells were subcutaneously inoculated into the flank of ZUU001 and B-NDG mice (n = 5/group). Tumors were measured twice weekly and the tumor volume estimated. Mean tumor size ± standard error of the mean is shown. ns: no significance; B: A representative hematoxylin and eosin (HE) stained section of a kidney and adrenal gland with metastatic tumor at the end of the experiment in ZZU001 hamsters (56 d) and B-NDG mice (42 d); C: Representative HE staining of a lung metastasis at 22 d, 29 d, 36 d after the injection of MIA-PaCa-2 cells in ZZU001 hamsters and B-NDG mice; D: Representative HE, Masson, smooth muscle actin (SMA) and vimentin staining of a subcutaneous tumor at 42 d after the injection of the MIA-PaCa-2 cells in ZZU001 hamsters and B-NDG mice. Scale bars = 100 μm.

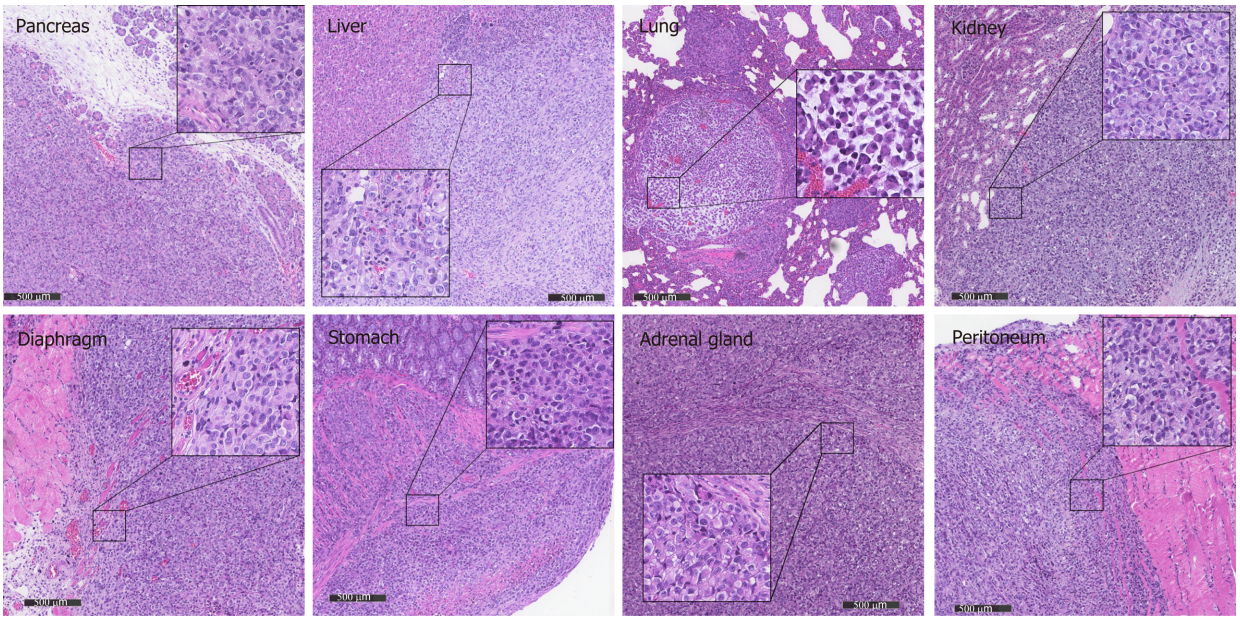

Figure 5 Metastasis in different organs reflects the histology of the primary tumor in ZZZU001 orthotopic xenograft tumor models. The primary tumors were established by injection of 1 × 10^6 of MIA-PaCa-2 cells into the pancreatic tail. The representative tumor in the pancreas, liver, lung, kidney, diaphragm, stomach, adrenal gland, and peritoneum of ZZU001 Syrian hamsters are shown. Inset square shows tumor cells at a magnification 400 ×. Scale bars = 500 μm.

ZZU001 hamster xenograft tumor over-express vimentin, whereas no vimentin positive tumor cells were observed in mouse xenograft tumor. These observations suggest that the EMT of cancer cells in the ZZU001 hamster may be influenced by the stroma, which is highly associated with PC metastasis. The ZZU001 Syrian hamsters described in this study can be a valuable animal model for better understanding of the molecular mechanism of tumorigenesis, in particular for the metastasis of PC and testing novel therapeutics for this most aggressive disease.

ARTICLE HIGHLIGHTS

Research background

Pancreatic cancer (PC) is an extremely aggressive cancer with a poor prognosis. Multiple sites of metastasis from PC remain a significant hurdle in treating this

disease. Reliable animal models that can mimic the clinical features of the disease are needed to study disease progression and develop effective therapies. Xenograft cancer cell transplantation animal models are cost-effective and easily established methods by which to assess tumor progression, metastasis, and pre-clinical efficacy of cancer drugs. However, current xenograft tumor models of human PC in immune-deficient mice rarely develop metastasis. The development of a model that can reflect more accurately human PC progression is therefore required.

Research motivation

Syrian hamsters (*Mesocricetus auratus*) have advantages as models for various diseases due to the high similarities in anatomy, physiology, and pathology between Syrian hamsters and humans. The Syrian hamster is the only rodent species that develop PC in an almost identical manner to the respective human disease regarding such features as clinical symptoms, tumor morphology, tumor biology, metabolic abnormality, and molecular genetic alterations. We reasoned that the immune-deficient Syrian hamster might be a better animal species for establishing xenograft models of human PC and more faithfully recapitulate the features of PC, in particular the multiple sites of metastasis seen during progression of human PC.

Research objectives

This study aimed to create an immune-deficient Syrian hamster by knockout of interleukin 2 (IL-2) receptor subunit gamma (*IL2RG*), characterize the phenotypes of *IL-2RG* knockout (KO) Syrian hamsters, and evaluate whether this animal can present the distinguishing features of human PC.

Research methods

CRISPR/Cas9-mediated genetic editing and cytoplasmic injection into hamster zygotes were employed to create an *IL2RG* KO Syrian hamster. The phenotypes and immune functions of the *IL2RG* KO Syrian hamster were characterized. A panel of human PC cell lines were subcutaneously or orthotopically transplanted into *IL2RG* KO Syrian hamsters or immune-deficient mice. The tumor growth, local invasion of the tumor cells, and remote organ metastasis were compared over time. The histopathology of tumor xenografts, the molecular alterations of tumor cells, and the stroma within the xenograft tumors were investigated by hematoxylin and eosin and immunohistochemistry staining.

Research results

A new immune-deficient Syrian hamster with *IL2RG* gene knockout was created and named ZZU001. We demonstrated that ZZU001 Syrian hamsters have a lymphoid compartment that is greatly reduced in size and diversity and are impaired in their immune function. The comparison studies on xenografting tumors in ZZU001 and severely immune-deficient mice demonstrated that ZZU001 Syrian hamsters engrafted with human tumor cells are a promising animal model, which can recapitulate most of the features of human PC, in particular, the multiple-sites of metastasis. PC tissues derived from ZZU001 hamsters also displayed other key features of human PC, such as desmoplastic reactions in the stroma and epithelial to mesenchymal transition phenotype, whereas PC tissues derived from immune-deficient mice did not present such features.

Research conclusions

This work demonstrates that ZZU001 Syrian hamster can be an extremely valuable animal model for better understanding the molecular mechanisms of tumorigenesis, in particular the metastasis of human PC, and maybe more appropriate in comparison to xenograft mouse models for robust testing of the anti-tumor potential of novel therapeutics.

Research perspectives

Current findings provide a promising xenotransplantation animal model for human PC research. Its wider application requires further evaluation, but the strong similarities between progression of human and Syrian hamster PC may suggest a similarly useful application of this model for more accurately modeling the progression of other human tumors. The model characterized in this study may also provide a useful platform for identification of novel molecules and pathways that control the metastasis of human PC.

REFERENCES

1 **Rahib L**, Smith BD, Aizenberg R, Rosenzweig AB, Fleshman JM, Matrisian LM. Projecting cancer incidence and deaths to 2030: the unexpected burden of thyroid, liver, and pancreas cancers in the United States. *Cancer Res* 2014; **74**: 2913-2921 [PMID: 24840647 DOI: 10.1158/0008-5472.CAN-14-0155]

2 **Oettle H**, Neuhaus P, Hochhaus A, Hartmann JT, Gellert K, Ridwelski K, Niedergethmann M, Zülke C, Fahlke J, Arning MB, Sinn M, Hinke A, Riess H. Adjuvant chemotherapy with gemcitabine and long-term outcomes among patients with resected pancreatic cancer: the CONKO-001 randomized trial. *JAMA* 2013; **310**: 1473-1481 [PMID: 24104372 DOI: 10.1001/jama.2013.279201]

3 **Schnelldorfer T**, Ware AL, Sarr MG, Smyrk TC, Zhang L, Qin R, Gullerud RE, Donohue JH, Nagorney DM, Farnell MB. Long-term survival after pancreatoduodenectomy for pancreatic adenocarcinoma: is cure possible? *Ann Surg* 2008; **247**: 456-462 [PMID: 18376190 DOI: 10.1097/SLA.0b013e3181613142]

4 **Hwang CI**, Boj SF, Clevers H, Tuveson DA. Preclinical models of pancreatic ductal adenocarcinoma. *J Pathol* 2016; **238**: 197-204 [PMID: 26419819 DOI: 10.1002/path.4651]

5 **Qiu W**, Su GH. Challenges and advances in mouse modeling for human pancreatic tumorigenesis and metastasis. *Cancer Metastasis Rev* 2013; **32**: 83-107 [PMID: 23114842 DOI: 10.1007/s10555-012-9408-2]

6 **Hotz HG**, Reber HA, Hotz B, Yu T, Foitzik T, Buhr HJ, Cortina G, Hines OJ. An orthotopic nude mouse model for evaluating pathophysiology and therapy of pancreatic cancer. *Pancreas* 2003; **26**: e89-e98 [PMID: 12717279 DOI: 10.1097/00006676-200305000-00020]

7 **Loukopoulos P**, Kanetaka K, Takamura M, Shibata T, Sakamoto M, Hirohashi S. Orthotopic transplantation models of pancreatic adenocarcinoma derived from cell lines and primary tumors and displaying varying metastatic activity. *Pancreas* 2004; **29**: 193-203 [PMID: 15367885 DOI: 10.1097/00006676-200410000-00004]

8 **Kim JH**, Hilaris B. Iodine 125 source in interstitial tumor therapy. Clinical and biological considerations. *Am J Roentgenol Radium Ther Nucl Med* 1975; **123**: 163-169 [PMID: 1119650 DOI: 10.2214/ajr.123.1.163]

9 **Johnson JI**, Decker S, Zaharevitz D, Rubinstein LV, Venditti JM, Schepartz S, Kalyandrug S, Christian M, Arbuck S, Hollingshead M, Sausville EA. Relationships between drug activity in NCI preclinical in vitro and in vivo models and early clinical trials. *Br J Cancer* 2001; **84**: 1424-1431 [PMID: 11355958 DOI: 10.1054/bjoc.2001.1796]

10 **Van Cutsem E**, van de Velde H, Karasek P, Oettle H, Vervenne WL, Szawlowski A, Schoffski P, Post S, Verslype C, Neumann H, Safran H, Humblet Y, Perez Ruixo J, Ma Y, Von Hoff D. Phase III trial of gemcitabine plus tipifarnib compared with gemcitabine plus placebo in advanced pancreatic cancer. *J Clin Oncol* 2004; **22**: 1430-1438 [PMID: 15084616 DOI: 10.1200/Jco.2004.10.112]

11 **Voskoglou-Nomikos T**, Pater JL, Seymour L. Clinical predictive value of the in vitro cell line, human xenograft, and mouse allograft preclinical cancer models. *Clin Cancer Res* 2003; **9**: 4227-4239 [PMID: 14519650]

12 **Feig C**, Gopinathan A, Neesse A, Chan DS, Cook N, Tuveson DA. The pancreas cancer microenvironment. *Clin Cancer Res* 2012; **18**: 4266-4276 [PMID: 22896693 DOI: 10.1158/1078-0432.CCR-11-3114]

13 **Miao J**, Ying B, Li R, Tollefson AE, Spencer JF, Wold WSM, Song SH, Kong IK, Toth K, Wang Y, Wang Z. Characterization of an N-Terminal Non-Core Domain of RAG1 Gene Disrupted Syrian Hamster Model Generated by CRISPR Cas9. *Viruses* 2018; **10** [PMID: 29734775 DOI: 10.3390/v10050243]

14 **Tysome JR**, Li X, Wang S, Wang P, Gao D, Du P, Chen D, Gangeswaran R, Chard LS, Yuan M, Alusi G, Lemoine NR, Wang Y. A novel therapeutic regimen to eradicate established solid tumors with an effective induction of tumor-specific immunity. *Clin Cancer Res* 2012; **18**: 6679-6689 [PMID: 23091113 DOI: 10.1158/1078-0432.CCR-12-0979]

15 **Pour PM**. Why the Hamster Pancreatic Cancer Model is Still the Most Useful Tool for Clinical Studies? *JOP* 2016; **17**: 566-569

16 **Wang P**, Li X, Wang J, Gao D, Li Y, Li H, Chu Y, Zhang Z, Liu H, Jiang G, Cheng Z, Wang S, Dong J, Feng B, Chard LS, Lemoine NR, Wang Y. Re-designing Interleukin-12 to enhance its safety and potential as an anti-tumor immunotherapeutic agent. *Nat Commun* 2017; **8**: 1395 [PMID: 29123084 DOI: 10.1038/s41467-017-01385-8]

17 **Cho SA**, Park JH, Seok SH, Juhn JH, Kim SJ, Ji HJ, Choo YS, Park JH. Effect of granulocyte macrophage-colony stimulating factor (GM-CSF) on 5-FU-induced ulcerative mucositis in hamster buccal pouches. *Exp Toxicol Pathol* 2006; **57**: 321-328 [PMID: 16414253 DOI: 10.1016/j.etp.2005.09.006]

18 **Li R**, Miao J, Fan Z, Song S, Kong IK, Wang Y, Wang Z. Production of Genetically Engineered Golden Syrian Hamsters by Pronuclear Injection of the CRISPR/Cas9 Complex. *J Vis Exp* 2018 [PMID: 29364218 DOI: 10.3791/56263]

19 **Mali P**, Yang L, Esvelt KM, Aach J, Guell M, DiCarlo JE, Norville JE, Church GM. RNA-guided human genome engineering via Cas9. *Science* 2013; **339**: 823-826 [PMID: 23287722 DOI: 10.1126/science.1232033]

20 **Toth K**, Lee SR, Ying B, Spencer JF, Tollefson AE, Sagartz JE, Kong IK, Wang Z, Wold WS. STAT2 Knockout Syrian Hamsters Support Enhanced Replication and Pathogenicity of Human Adenovirus, Revealing an Important Role of Type I Interferon Response in Viral Control. *PLoS Pathog* 2015; **11**: e1005084 [PMID: 26291525 DOI: 10.1371/journal.ppat.1005084]

21 **Yachida S**, Iacobuzio-Donahue CA. The pathology and genetics of metastatic pancreatic cancer. *Arch Pathol Lab Med* 2009; **133**: 413-422 [PMID: 19260747 DOI: 10.1043/1543-2165-133.3.413]

22 **Malkoç E**, Aktaş Z, Kara K, Haholu A. Renal metastasis from pancreatic adenocarcinoma: a rare case along with literature review. *Turk J Urol* 2015; **41**: 93-95 [PMID: 26328209 DOI: 10.5152/tud.2015.54280]

23 **Sinha S**, Leach SD. New insights in the development of pancreatic cancer. *Curr Opin Gastroenterol* 2016; **32**: 394-400 [PMID: 27454028 DOI: 10.1097/MOG.0000000000000295]

24 **Pickup MW**, Mouw JK, Weaver VM. The extracellular matrix modulates the hallmarks of cancer. *EMBO Rep* 2014; **15**: 1243-1253 [PMID: 25381661 DOI: 10.15252/embr.201439246]

25 **Crawford HC**, Pasca di Magliano M, Banerjee S. Signaling Networks That Control Cellular Plasticity in Pancreatic Tumorigenesis, Progression, and Metastasis. *Gastroenterology* 2019; **156**: 2073-2084 [PMID:

30716326 DOI: 10.1053/j.gastro.2018.12.042]
26 **Thomas D**, Radhakrishnan P. Tumor-stromal crosstalk in pancreatic cancer and tissue fibrosis. *Mol Cancer* 2019; **18**: 14 [PMID: 30665410 DOI: 10.1186/s12943-018-0927-5]
27 **Martinez-Outschoorn UE**, Lisanti MP, Sotgia F. Catabolic cancer-associated fibroblasts transfer energy and biomass to anabolic cancer cells, fueling tumor growth. *Semin Cancer Biol* 2014; **25**: 47-60 [PMID: 24486645 DOI: 10.1016/j.semcancer.2014.01.005]

World Journal of Gastroenterology

Submit a Manuscript: https://www.f6publishing.com

World J Gastroenterol 2020 August 28; 26(32): 4817-4832

DOI: 10.3748/wjg.v26.i32.4817

ISSN 1007-9327 (print) ISSN 2219-2840 (online)

ORIGINAL ARTICLE

Case Control Study

Association between human leukocyte antigen gene polymorphisms and multiple EPIYA-C repeats in gastrointestinal disorders

Suat Saribas, Suleyman Demiryas, Erkan Yilmaz, Omer Uysal, Nuray Kepil, Mehmet Demirci, Reyhan Caliskan, Harika Oyku Dinc, Seher Akkus, Nesrin Gareayaghi, Sahra Kirmusaoglu, Dogukan Ozbey, Hrisi B Tokman, Serdar S Koksal, Ihsan Tasci, Bekir Kocazeybek

ORCID number: Suat Saribas 0000-0002-4549-3887; Suleyman Demiryas 0000-0002-0050-9099; Erkan Yilmaz 0000-0002-5133-4532; Omer Uysal 0000-0002-8833-697X; Nuray Kepil 0000-0001-5494-6422; Mehmet Demirci 0000-0001-9670-2426; Reyhan Caliskan 0000-0002-2764-1823; Harika Oyku Dinc 0000-0003-3628-7392; Seher Akkus 0000-0002-9236-2062; Nesrin Gareayaghi 0000-0002-0812-1128; Sahra Kirmusaoglu 0000-0003-3038-1417; Dogukan Ozbey 0000-0002-0596-1551; Hrisi B Tokman 0000-0002-2205-5120; Serdar S Koksal 0000-0001-7199-2295; Ihsan Tasci 0000-0002-2891-6200; Bekir Kocazeybek 0000-0003-1072-3846.

Author contributions: Saribas S, Demiryas S, Ozbey D and Kocazeybek B designed and coordinated the study; Caliskan R, Tasci I, Demirci M, Dinc HO and Kirmusaoglu S performed the experiments, acquired and analyzed data;Yilmaz E, Kepil N,Uysal O, Akkus S, Gareayaghi N interpreted the data; Koksal SS, Tokman HB, Saribas S, Kocazeybek B wrote the manuscript; all authors approved the final version of the article.

Supported by the Istanbul University Research Fund, No. 45151.

Suat Saribas, Reyhan Caliskan, Harika Oyku Dinc, Seher Akkus, Dogukan Ozbey, Hrisi B Tokman, Bekir Kocazeybek, Department of Medical Microbiology, Istanbul University-Cerrahpasa, Cerrahpasa Medical Faculty, Istanbul 34098, Turkey

Suleyman Demiryas, Ihsan Tasci, Department of General Surgery, Istanbul University-Cerrahpasa, Cerrahpasa Medical Faculty, Istanbul 34098, Turkey

Erkan Yilmaz, Department of Organ Transplantation, HLA Laboratory, Istanbul University-Cerrahpasa, Cerrahpasa Medical Faculty, Istanbul 34098, Turkey

Omer Uysal, Deparment of Biostatistics, Medical School of Bezmialem Vakif University, Istanbul 34093, Turkey

Nuray Kepil, Department of Pathology, Istanbul University-Cerrahpasa, Cerrahpasa Medical Faculty, Istanbul 34098, Turkey

Mehmet Demirci, Department of Medical Microbiology, Beykent University Medical Faculty, Istanbul 34520, Turkey

Nesrin Gareayaghi, Center for Blood, Istanbul Sisli Hamidiye Etfal Training and Research Hospital, University of Health Sciences, Istanbul 34360, Turkey

Sahra Kirmusaoglu, Department of Molecular Biology and Genetics, T.C. Halic University, Faculty of Arts & Sciences, Istanbul 34381, Turkey

Serdar S Koksal, Department of Public Health, Istanbul University-Cerrahpasa, Cerrahpasa Medical Faculty, Istanbul 34098, Turkey

Corresponding author: Bekir Kocazeybek, PhD, Full Professor, Professor, Department of Medical Microbiology, Istanbul University-Cerrahpasa, Cerrahpasa Medical Faculty, Cerrahpasa Street, Istanbul 34098, Turkey. bzeybek@istanbul.edu.tr

Abstract

BACKGROUND

Polymorphisms of human leukocyte antigen (HLA) genes are suggested to increase the risk of gastric cancer (GC).

Institutional review board statement: This study was reviewed and approved by the Ethics Committee of the Istanbul University.

Informed consent statement: Informed written consent was obtained from the patients.

Conflict-of-interest statement: The authors have nothing to disclose.

Data sharing statement: No additional data are available.

STROBE statement: The guidelines of the STROBE Statement have been adopted.

Manuscript source: Invited manuscript

Received: March 12, 2020
Peer-review started: March 12, 2020
First decision: May 15, 2020
Revised: July 2, 2020
Accepted: August 20, 2020
Article in press: August 20, 2020
Published online: August 28, 2020

P-Reviewer: de Melo FF, Du Y, Sun X
S-Editor: Liu M
L-Editor: A
P-Editor: Li JH

AIM

To investigate the HLA allele frequencies of patients with GC relative to a control group in terms of CagA+ multiple (≥ 2) EPIYA-C repeats.

METHODS

The patient group comprised 94 patients [44 GC and 50 duodenal ulcer (DU) patients], and the control group comprised 86 individuals [(50 non-ulcer dyspepsia patients and 36 people with asymptomatic *Helicobacter pylori* (*H. pylori*)]. Polymerase chain reaction was performed for the amplification of the *H. pylori cagA* gene and typing of EPIYA motifs. HLA sequence-specific oligonucleotide (SSO) typing was performed using Lifecodes SSO typing kits (HLA-A, HLA-B HLA-C, HLA-DRB1, and HLA-DQA1-B1 kits).

RESULTS

The comparison of GC cases in terms of CagA+ multiple (≥ 2) EPIYA-C repeats showed that only the HLA-DQB1*06 allele [odds ratio (OR): 0.37, $P = 0.036$] was significantly lower, but significance was lost after correction (Pc = 0.1845). The HLA-DQA1*01 allele had a high ratio in GC cases with multiple EPIYA-C repeats, but this was not significant in the univariate analysis. We compared allele frequencies in the DU cases alone and in GC and DU cases together using the same criterion, and none of the HLA alleles were significantly associated with GC or DU. Also, none of the alleles were detected as independent risk factors after the multivariate analysis. On the other hand, in a multivariate logistic regression with no discriminative criterion, HLA-DQA1*01 (OR = 1.848), HLA-DQB1*06 (OR = 1.821) and HLA-A*02 (OR = 1.579) alleles were detected as independent risk factors for GC and DU.

CONCLUSION

None of the HLA alleles were detected as independent risk factors in terms of CagA+ multiple EPIYA-C repeats. However, HLA-DQA1*01, HLA-DQB1*0601, and HLA-A*2 were independent risk factors with no criterion in the multivariate analysis. We suggest that the association of these alleles with gastric malignancies is not specifically related to cagA and multiple EPIYA C repeats.

Key words: Human leukocyte antigen; *Helicobacter pylori*; Gastric cancer; Duodenal ulcer; EPIYA; CagA

Core tip: The development of gastric cancer (GC) is suggested to be related to the interactions of bacterial virulence and host genetic factors with the immune response of the host. The effects of polymorphisms in the human leukocyte antigen (HLA) gene may regulate the degree of the inflammatory response of the host leading to the gastric malignancies. We could not detect any prominent HLA alleles between the patient and control groups in terms of CagA+ multiple (≥ 2) EPIYA-C repeat numbers. HLA-DQA1*01, HLA-DQB1*06, and HLA-A*02 were detected as independent risk factors for the risk of GC and duodenal ulcer with no criterion in multivariate analyses. We suggest that the association of these alleles with gastric malignancies is not specifically related to cagA and multiple EPIYA C repeats.

Citation: Saribas S, Demiryas S, Yilmaz E, Uysal O, Kepil N, Demirci M, Caliskan R, Dinc HO, Akkus S, Gareayaghi N, Kirmusaoglu S, Ozbey D, Tokman HB, Koksal SS, Tasci I, Kocazeybek B. Association between human leukocyte antigen gene polymorphisms and multiple EPIYA-C repeats in gastrointestinal disorders. *World J Gastroenterol* 2020; 26(32): 4817-4832
URL: https://www.wjgnet.com/1007-9327/full/v26/i32/4817.htm
DOI: https://dx.doi.org/10.3748/wjg.v26.i32.4817

INTRODUCTION

Gastric cancer (GC) is the third most common cause of death among all cancer types (8.2% of all cancers, 2018, World Health Organization)[1]. GC has been closely associated with *Helicobacter pylori* (*H. pylori*) infections, which generally cause mild gastrointestinal symptoms. However, in a few infected patients, they may progress to peptic ulcer (PU) (10%-15%) or GC (1%-3%)[2].

Generally, *H. pylori* infections cause gastric inflammation and a chronic inflammatory response that result in progressive mucosal damage. Eventually, the gastric mucosa transforms into metaplastic and dysplastic epithelia, which leads to gastric adenocarcinomas[3]. The development of GC is suggested to be related to the interactions between bacterial virulence factors, host genetic factors such as the human leukocyte antigen (HLA) gene, the immune response of the host, and environmental factors such as diet and smoking[4]. Some of the host factors may be related to polymorphisms genes such as HLA genes, which regulate the strength of the inflammatory response and influence the probability of specific clinical results[5].

CagA is among the most important virulence factors specific to *H. pylori* and is delivered into the gastric epithelium cells by the type IV secretion system (T4SS) of the bacterium. It is involved with intracellular signal transduction pathways and leads to the malignant transformation of gastric epithelial cells[6]. CagA subtypes are defined by the EPIYA variants (Glu-Pro-Ile-Tyr-Ala) in their C-terminal region, and there are four types of EPIYA motifs: EPIYA-A, -B, -C, and -D[7]. *H. pylori* isolates from East Asia are associated with a higher incidence of GC and contain EPIYA A-B-D motifs. However, in Western countries, GC cases have EPIYA A-B-C motifs. *H. pylori* strains with multiple EPIYA-C repeats have higher phosphorylation capacity and SHP-2 binding affinity and are significantly associated with GC[8].

HLA class I and II proteins bind to bacterial antigen peptides or tumor proteins and present these peptides and proteins to T cells, which leads to the differentiation of T cells into cytotoxic or helper T cells. In HLA gene polymorphism, a variety of alleles may occupy the same locus. A limited number of studies have focused on the relation between gastrointestinal pathologies such as the development of GC risk and HLA polymorphisms in different geographic regions and populations[9,10,11].

In addition to HLA gene polymorphisms, the virulence factors of *H. pylori* strains may also be related to the intensity of the inflammatory response[3]. The limited studies on HLA polymorphisms have focused on MHC class II and specifically the relation of HLA polymorphisms and the development of GC risk[10,12,13]. In these studies, the following HLA class II polymorphisms were suggested to be associated with the development of GC risk: DQB1*03, HLA-DRB1*04, and HLA-DQA1*01/*03[14,15].

Reported HLA allele frequencies related to GC pathologies with *H. pylori* positivity have been contradictory among different ethnic groups. The regional and ethnic differences are very important for the association of HLA gene polymorphism and GC risk. These contradictory results may be attributed to factors such as differences in populations, research designs, environmental factors, *H. pylori* virulence factors, and host genetic factors, such as polymorphisms of HLA alleles. For example, the HLA-DQB1*0301 allele was positively associated with GC in Caucasian populations but negatively associated with it in Taiwanese populations[13,16]. This HLA polymorphism had no effect in Japanese populations[17]. HLA-DQB1*0401 82 and *0602 alleles increase the GC risk in European and Indonesian populations[9,18].

To the best of our knowledge, no studies have compared GC and duodenal ulcer (DU) cases with controls in regard to HLA allele frequencies in terms of differentiation by the CagA+ multiple (≥ 2) EPIYA-C repeat numbers. Therefore, we aimed to investigate the allele frequencies of HLA class I and II in a patient group [*H. pylori* (+) GC and DU patients] and compared the results to those of a control group [*H. pylori* (+) non-ulcer dyspepsia (NUD) and asymptomatic *H. pylori*] in terms of CagA+ multiple EPIYA-C repeats for the first time in a Turkish population.

MATERIALS AND METHODS

Study design and patients

This case–control study was conducted between July 10, 2014 and November 9, 2017. The patient group comprised 94 patients, including 44 (46.8%) GC and 50 (53.2%) DU patients with 58 (61.7%) males, 36 (38.3%) females, a mean age of 49.6 years, and age range of 19–79 years. The control group comprised 86 individuals including 50 (58.1%) NUD patients and 36 (41.9%) people with asymptomatic *H. pylori*. This group had 30

(34.9%) males, 56 (65.1%) females, a mean age of 47.3 years, and age range of 18–86 years. All of the GC + DU patients and the NUD + asymptomatic *H. pylori* members of the control group members had *H. pylori*.

The NUD + Asymptomatic *H. pylori* control group was matched with the GC + DU patient group according to the age and gender distribution of the patient group ($P > 0.05$). Blood samples for the genotyping of HLA alleles were collected when obtaining biopsy samples (from the corpus and antrum) on the same day. The antrum and corpus biopsy specimens were stored and used in molecular studies.

We excluded patient and control group individuals with autoimmune diseases and who were under 18 years old, had previous gastric surgery and *H. pylori* eradication treatment with antibiotics, antisecretory drugs and bismuth salts, in the month prior to sampling. The study was reviewed and approved by the Clinical Research Ethics Board of Istanbul University-Cerrahpasa, Cerrahpasa Faculty of Medicine (No. 83045809/32-38/A-15/2014). The study was also conducted according to the standards of the Declaration of Helsinki. All study participants or their legal guardians provided informed written consent prior to the study.

Polymerase chain reaction analyses

H. pylori DNA extractions were performed using the antrum and corpus biopsy specimens. Genomic DNA extraction (Real Genomics Quality Nucleic Acid/ Purification system; RBC Bioscience Laboratories, Taipei, Taiwan) and QIAamp DNA mini prep kits (Qiagen, Hilden Germany) were used.

UreC gene detection in H. pylori

An *H. pylori*-QLS 1.0 kit (Fluorion, Iontek, Istanbul, Turkey) was used for the detection of 156 bp of the *ureC* gene in *H. pylori* DNA extractions[19].

Amplification of the H. pylori cagA gene

Primers reported in related studies were used for the detection of the *H. pylori cagA* gene (349 bp) (Table 1)[20,21]. The polymerase chain reaction (PCR) cycles were as follows: Denaturation at 95 °C for 2 min, followed by 45 cycles of 95 °C for 30 s, 45 s at 53 °C, and 45 s at 72 °C. The final elongation was done for 5 min at 72 °C.

Molecular studies for the typing of EPIYA motifs

The amplification of *H. pylori* DNA for EPIYA motifs was done using the forward primer cagA28F and reverse primers cagA-P1C, cagA-P2CG, cagA-P2TA, and cagA-P3E (Table 1)[22]. In the PCR assay, the protocol steps were as follows: Initial denaturation step, one cycle at 95 °C for 2 min, 50 cycles at 95 °C for 30 s, 57 °C for 45 s, and 72 °C for 35 s; and a final extension at 72 °C for 5 min. After the PCR amplification, PCR products were sequenced bidirectionally using a Sequence Reagent Mix kit with an ABI Prism (310) analyzer (Applied Biosystems, United States).

Empty-site PCR

An empty-site-positive PCR assay was used to confirm the EPIYA-negative *H. pylori* strains[23]. To confirm cagPAI in all of the strains, amplification was performed with two primers (forward 468 HP519 and reverse 496 HP549 primers of the reference HP519 and HP549 *H. pylori* strains; Table 1, cag empty PCR). In the PCR assay, the protocol steps were as follows: Initial denaturation at 95 °C for 2 min, 40 cycles at 95 °C for 30 s, 57 °C for 30 s, and 72 °C for 20 s; followed by a final extension at 72 °C for 5 min.

Blood collection, DNA extraction, and HLA sequence-specific oligonucleotide typing

Whole blood samples (10 mL) were collected from the patient and control group cases during a biopsy procedure. An EZ1 DNA extraction kit (Qiagen, Germany) was used in a DNA isolation device (Bio Robot EZ1; Qiagen, Germany) for the DNA isolation procedure from 3-mL blood samples collected in tubes containing ethylenediaminetetraacetic acid. Isolated DNA samples were stored at -70 °C until laboratory studies. HLA typing at low levels (2 digits) of HLA-A, HLA-B, HLA-C, and HLA-DQ alleles were done with a Luminex 100/200 instrument with sequence-specific oligonucleotide (SSO) probes bound to color-coded microbeads. LIFECODES SSO HLA typing kits (Lifecodes, Immucor, Germany) were used for the typing of HLA-A HLA-B, HLA-DRB1, and HLA-DQA1/B1. This typing test is a reverse sequence-specific oligonucleotide (rSSO) DNA typing assay using SSO probes and color-coded microspheres.

The PCR mixture was composed of 15 μL of lifecodes Master Mix, 200 ng of

Table 1 PCR primers

Primer	Primer sequence (59R39)	Ref.
cagA-F	GATAACAGGCAAGCTTTTGAGG[1]	[19,20]
cagA-R	CTGCAAAAGATTGTTTGGCAGA[1]	
cagA28F	TTCTCAAAGGAGCAATTGGC[2]	[21]
cagA-P1C	GTCCTGCTTTCTTTTTATTAACTTKAGC[2]	
cagA-P2CG	TTTAGCAACTTGAGCGTAAATGGG[2]	
cagA-P2TA	TTTAGCAACTTGAGTATAAATGGG[2]	
cagA-P3E	ATCAATTGTAGCGTAAATGGG[2]	
"cag empty PCR"	GCTTGCTTGTATTGGCCTTG / GCATGCACATTCCCTAAAGT[3]	[22]

All polymerase chain reactions (PCRs) were performed in a 50 μL final volume with 1.25 U Taq polymerase, 16 μL PCR buffer, 3 μL 2.5 mM $MgCl_2$ and 1 μL dNTP mix (10 mM each) with the described primers using the thermal profiles detailed.
[1]: 95 °C for 2 min initial denaturation, followed by 45 cycles of 30 s at 95 °C, 45 s at 53 °C and 45 s at 72 °C, with a final elongation step performed for 5 min at 72 °C.
[2]: 95 °C for 2 min initial denaturation, followed by 50 cycles of 30 s at 95 °C, 45 s at 57 °C and 35 s at 72 °C, with a final elongation step performed for 5 min at 72 °C.
[3]: 95 °C for 2 min initial denaturation, followed by 40 cycles of 30 s at 95 °C, 30 s at 57 °C, 20 s at 72 °C, with a final elongation step performed for 5 min at 72 °C. PCR: Polymerase chain reaction.

genomic DNA, and 2.5 U Taq polymerase in a final volume of 50 μL. In the PCR assay, the steps were as follows: Initial denaturation step at 95 °C for 5 min; 40 cycles including 8 cycles at 95 °C for 30 s, 60 °C for 45 s, and 72 °C for 45 s, followed by 32 cycles at 95 °C for 30 s, 63 °C for 45 s, and 72 °C for 45 s, and a final extension step at 72 °C for 15 min. The hybridization steps were as follows: Initial step at 97 °C for 5 min followed by 30 min at 47 °C for 30 min and at 56 °C for 10 min with 15 μL of probe mix and 5 μL of PCR product. The obtained samples were diluted with 170 μL of 1:200 pre-diluted streptavidin-phycoerythrin solution and analyzed by a Luminex 200 system (Luminex Corp. United States). The obtained HLA patterns were compared with ah HLA sequence database (Database for IMGT/HLA Sequence, 3.11.0) using the MatchIT DNA program.

Statistical analyses

Hardy-Weinberg (H-W) equilibrium and Linkage Disequilibrium (LD) were examined for HLA-A, HLA-B, HLA-C, HLA-DR1, HLA-DQA1 and HLA-DQB1 allele polymorphisms[24]. Genepop software version 4.7 was used to calculate the Hardy–Weinberg equilibrium and LD. H–W equilibrium was present for *P*-values > 0.05. The allele frequencies of the GC + DU patient and the NUD + Asymptomatic *H. pylori* control groups and subgroups were compared by the chi-squared (χ^2) test and Fisher's exact test (Tables 2-5). Corrected *P* values (*Pc*) were calculated by multiplying with the allele numbers (A = 15, B = 26, DRB1 = 12, DQA1 = 6, and DQB1 = 5) in each locus by Bonferroni correction. Multivariate logistic regression (enter method) was used to assess the relation of HLA alleles and the risk of GC and DU development in terms of CagA+ multiple EPIYA-C repeat numbers (Table 6). $P < 0.05$ was used to determine significance. SPSS 25.0 (IBM Corporation, Armonk, NY, United States) was used for the analyses.

RESULTS

Sixty-four HLA alleles (41 for class I and 23 for class II) were found between the 94 HLA alleles tested in all of the groups (Table 7). The maximum numbers of alleles in the GC + DU patient group were 52 for HLA-A*02 (27.6%), 40 for HLA-B*35 (21.3%), 36 for HLA-DRB1*13 (19%), 76 for HLA-DQA1*01 (40%), and 52 for HLA-DQB1*06 (27.6%) (Figure 1). The maximum numbers of alleles in the NUD + Asymptomatic *H. pylori* control group were 20 for HLA-A*03 (11.6%), 10 for HLA-B*50 (5.81%), 24 for HLA-DRB1*04 (13.95%), 54 for HLA-DQA1*05 (31.4%), and 64 for HLA-DQB1*03 (37.2%) (Figure 2). Among GC cases, the genotype frequencies of HLA- B, DQA1 and DQB1 loci were in H-W equilibrium. Among DU cases, all of the genotype frequencies

Table 2 Comparison of human leukocyte antigen alleles predisposing susceptibility and resistance to gastric cancer/duodenal ulcer in patient and control groups, *n* (%)

HLA alleles	Patient groupGC + DU, *H. pylori* (+) (*n* = 94, alleles = 198)	Control groupNUD + Asymptomatic, *H. pylori* (+) (*n* = 86, alleles = 172)	OR	95%CI		*P* value
				Minimum	Maximum	
HLAs increasing susceptibility to GC/DU						
HLA-A*02	52 (27.6)	38 (22)	1.34	0.833	2.182	0.2239
HLA-B*35	40 (21.3)	26 (15.1)	1.51	0.880	2.615	0.1329
HLA-DRB1*13	36 (19)	24 (14)	1.46	0.831	2.567	0.1880
HLA-DQA1*01	76 (40)	30 (17.4)	3.21	1.968	5.242	0.0001
HLA-DQB1*06	52 (27.6)	20 (11.6)	2.90	1.652	5.139	0.0002
HLAs making resistant to GC/DU						
HLA-A*03	14 (7.4)	20 (11.6)	0.61	0.298	1.252	0.1787
HLA-B*50	0 (0)	10 (5.8)	0.08	0.010	0.680	0.0201
HLA-DRB1*04	16 (8.5)	24 (14)	0.57	0.293	1.120	0.1038
HLA-DQA1*05	28 (14.9)	54 (31.4)	0.38	0.228	0.639	0.0003
HLA-DQB1*03	42 (23)	64 (37.2)	0.48	0.305	0.770	0.0022

HLA: Human leukocyte antigen; *H. pylori*: *Helicobacter pylori*; GC: Gastric cancer; DU: Duodenal ulcer; NUD: Non-ulcer dyspepsia; CI: Confidence interval; OR: Odds ratio.

Table 3 The comparison of human leukocyte antigen alleles which increase or decrease the gastric cancer risk in gastric cancer subgroup cases in terms of CagA+ (≥ 2) EPIYA-C, *n* (%)

	GC (≥ 2) EPIYA-C (*n* = 26, alleles = 52)	GC (< 2) EPIYA-C (*n* = 18, alleles = 36)	OR	95%CI		*P* value
				Minimum	Maximum	
HLA-A*02	12 (23)	10 (27)	0.78	0.29	2.06	0.6170
HLA-B*35	12 (23)	10 (27)	0.78	0.29	2.06	0.6170
HLA-DRB1*13	12 (23)	12 (33)	0.60	0.23	1.54	0.2903
HLA-DQA1*01	24 (46)	16 (44)	1.07	0.45	2.51	0.8742
HLA-DQB1*06	12 (23)	16 (44)	0.37	1.14	2.90	0.0369

HLA: Human leukocyte antigen; GC: Gastric cancer; CI: Confidence interval; OR: Odds ratio.

were in H-W equilibrium. Moreover, Among NUD cases, all of the genotype frequencies in H-W equilibrium except HLA-DQB1 cases and in asymptomatic *H. pylori* control group, all of the genotype frequencies were in H-W equilibrium except HLA-A cases. H-W equilibrium is only valid with a very large sample size and therefore, we suggest that some of our genotype frequencies are not in H-W equilibrium. The deviations from H-W equilibrium is larger at small sample sizes like this study and smaller at large sample sizes. HLA-DR1*13-HLA-DQA1*01-HLA-DQB1*06 haplotype frequency (10/44, 22% for GC; 2/50, 4% for DU, 2/50, 4% for NUD and 0 for NGIS) showed LD and had an odds ratio (OR) value as 6.143 (95%CI: 1.33-28.31, $P = 0.0027$) in the comparison of patient and control group cases. Moreover, HLA-DR1*13-HLA-DQA1*01-HLA-DQB1*06 haplotype frequency compared between GC and DU cases and OR was detected as 10.58 (95%CI: 2.27-49.34).

When comparing the prominent alleles detected, only HLA-DQA1*01 (OR: 3.211, $P = 0.0001$) and HLA-DQB1*06 (OR: 2.906, $P = 0.0002$) were significantly higher in the

Table 4 The comparison of human leukocyte antigen alleles which increase or decrease the duodenal ulcer risk in duodenal ulcer subgroup in terms of CagA+(≥ 2) EPIYA-C, *n* (%)

	DU (≥ 2) EPIYA-C (*n* = 14, alleles = 28)	DU (< 2) EPIYA-C (*n* = 36, alleles = 72)	OR[c]	95%CI		*P* value
				Minimum	Maximum	
HLA-A*02	10 (36)	20 (27)	1.44	0.53	3.62	0.4380
HLA-B*35	4 (14)	14 (19)	0.80	0.24	0.680	0.0201
HLA-DRB1*13	6 (21)	6 (8)	3	0.87	10.26	0.0801
HLA-DQA1*01	10 (36)	26 (36)	0.9	0.39	2.44	0.9704
HLA-DQB1*06	8 (28)	16 (22)	1.4	0.52	3.75	0.5340

HLA: Human leukocyte antigen; DU: Duodenal ulcer; CI: Confidence interval; OR: Odds ratio.

Table 5 The comparison of human leukocyte antigen alleles which increase or decrease the gastric cancer/duodenal ulcer risk in gastric cancer and duodenal ulcer subgroups in terms of CagA+(≥ 2) EPIYA-C, *n* (%)

	GC(≥ 2) EPIYA-C (*n* = 26, alleles=52)	DU(≥ 2) EPIYA-C (*n* = 14, alleles=28)	OR	95%CI		*P* value
				Minimum	Maximum	
HLA-A*02	12 (23)	10 (36)	0.54	0.19	1.47	0.2302
HLA-B*35	12 (23)	4 (14)	1.80	0.52	6.21	0.3527
HLA-DRB1*13	12 (23)	6 (21)	1.10	0.36	3.83	0.8663
HLA-DQA1*01	24 (46)	10 (36)	1.54	0.59	3.97	0.3689
HLA-DRB1*06	12 (23)	8 (28)	0.75	0.26	2.12	0.5889

HLA: Human leukocyte antigen; GC: Gastric cancer; DU: Duodenal ulcer; CI: Confidence interval; OR: Odds ratio.

Table 6 Results of logistic regressions analysis according to the variables in patient group (gastric cancer and duodenal ulcer cases)

	P value	OR	95%CI	
			Lower	Upper
HLA-DQA1*01	0.004	1.848	1.215	2.811
HLA-DQA1*05	0.050			
HLA-DQB1*03	0.061			
HLA-DQB1*06	0.009	1.821	1.163	2.850
HLA-A*02	0.040	1.579	1.021	2.442
HLA-A*25	0.999			

Variable(s) entered on step 1: QA1, QA5, QB3, QB6, A2, A25, B35. HLA: Human leukocyte antigen; CI: Confidence interval; OR: Odds ratio.

GC + DU patient group. The values also stayed significant after Bonferroni correction (DQB1*06: *Pc* = 0.001; DQA1*01: *Pc* = 0.0006). The prominent alleles in the NUD + Asymptomatic *H. pylori* control group were HLA-B*50 (OR: 0.086, *P* = 0.02), HLA-DQA1*05 (OR: 0.384, *P* = 0.0003), and HLA-DQB1*03 (OR: 0.485, *P* = 0.0022), but after Bonferroni correction for multiple comparisons, the changes were statistically significant for only HLA-DQA1*05 (*Pc* = 0.0018) and HLA-DQB1*03 (*Pc* = 0.011) and not HLA-B*50, (*Pc* = 0.52) (Table 2).

Multiple EPIYA-C repeat numbers and CagA positivity were found in 40 (42.5%) subjects in the GC + DU patient group. Multiple EPIYA-C repeats were observed in 26 (59%) GC subgroup cases and 14 (28%) DU subgroup cases in the GC + DU patient group, 2 (2.3%) NUD cases, and no asymptomatic *H. pylori* cases. Other EPIYA motifs and their numbers are shown in Table 8. It was not possible to perform statistical

Table 7 Frequency of detected human leukocyte antigen class I alleles and the class II alleles in patients with cancer and ulcer and in the control groups, *n* (%)

HLA-A	**Allele frequency**		***HLA-B***	**Allele frequency**		***HLA-DRB1***	**Allele frequency**		***HLA-DQA1***	**Allele frequency**		***HLA-DQB1***	**Allele frequency**	
Alleles	Cases (*n* = 94)	Control (*n* = 86)	Alleles	Cases (*n* = 94)	Control (*n* = 86)	Alleles	Cases (*n* = 94)	Control (*n* = 86)	Alleles	Cases (*n* = 94)	Control (*n* = 86)	Alleles	Cases (*n* = 94)	Control (*n* = 86)
01	22 (11.4)	24 (13.9)	07	18 (9.5)	22 (12.8)	01	14 (7.4)	8 (4.6)	01	76 (40)	30 (17.4)	02	20 (10.6)	26 (15.1)
02	52 (27.6)	38 (22)	08	6 (3.2)	6 (3.5)	03	10 (5.3)	10 (5.8)	02	20 (10.6)	20 (11.6)	03	42 (23)	64 (37.2)
03	14 (7.4)	20 (11.6)	13	6 (3.2)	4 (2.3)	04	16 (8.5)	22 (12.7)	03	12 (6.4)	22 (12.8)	04	26 (13.8)	28 (16.2)
11	18 (9.5)	18 (10.4)	14	6 (3.2)	4 (2.3)	07	10 (5.3)	20 (11.6)	04	16 (8.5)	20 (11.6)	05	48 (25.5)	34 (19.8)
23	10 (5.3)	4 (2.3)	15	2 (1)	6 (3.5)	08	4 (2.1)	6 (3.5)	05	28 (14.9)	54 (31.4)	06	52 (27.6)	20 (11.6)
24	26 (13.8)	24 (13.9)	18	10 (5.3)	10 (5.8)	10	6 (3.2)	4 (2.3)	06	36 (19.1)	26 (15.1)			
25	0 (0)	2 (1.1)	27	6 (3.2)	4 (2.3)	11	34 (18)	42 (24.4)						
26	4 (2.1)	4 (2.3)	35	40 (21.3)	26 (15.1)	12	6 (3.2)	2 (1.2)						
29	8 (4.2)	8 (4.6)	37	4 (2.1)	0 (0)	13	36 (19)	24 (14)						
30	4 (2.1)	6 (3.4)	38	8 (4.2)	2 (1.2)	14	18 (9.5)	8 (4.6)						
31	2 (1)	4 (2.3)	39	0 (0)	4 (2.3)	15	28 (14.9)	22 (12.8)						
32	16 (8.5)	10 (5.8)	40	6 (3.2)	6 (3.5)	16	6 (3.2)	4 (2.3)						
33	6 (3.1)	4 (2.3)	41	4 (2.1)	2 (1.2)									
68	4 (2.1)	6 (3.4)	44	8 (4.2)	14 (8.1)									
69	2 (1)	0 (0)	45	0 (0)	2 (1.2)									
			48	2 (1)	2 (1.2)									
			49	6 (3.2)	4 (2.3)									
			50	0 (0)	10 (5.8)									
			51	24 (12)	30 (17.4)									
			52	14 (7.4)	2 (1.2)									
			53	0 (0)	2 (1.2)									
			54	2 (1)	0 (0)									
			55	6 (3.2)	8 (4.6)									
			57	2 (1)	2 (1.2)									
			58	8 (4.2)	0 (0)									

	78	0 (0)	0 (0)

HLA: Human leukocyte antigen.

analysis due to small number of positive cases with CagA+ multiple EPIYA-C repeats in the NUD+ Asymptomatic *H. pylori* control group (n = 2). Instead, we compared two groups without using any criteria with regard to HLA alleles.

Thus, we used the HLA-DQB1*06, HLA-DRB1*13, HLA-B*35, HLA-DQA1 and HLA-A*02 alleles (*i.e.*, the alleles with the maximum numbers in the GC + DU patient group) to investigate their effects on GC/DU in terms of the CagA+ multiple EPIYA-C repeats, which is suitable for our purposes. First, we compared alleles in GC cases in terms of CagA+ multiple EPIYA-C repeat numbers. Only the HLA-DQB1*06 allele (OR: 0.37, 95%CI: 1.149-0.942, P = 0.0369) was significantly associated with GC, but after Bonferroni correction, there was no significant association between DQB1*06 and GC (DQB1*06, Pc = 0.1845).

The HLA-DQA1*01 allele had a high ratio in the multiple EPIYA-C repeat group, but the univariate analysis did not show any significant association. None of the selected alleles were significantly higher in the GC cases in terms of CagA+ multiple EPIYA-C repeats (Table 3). Using the same criterion, we also compared allele frequencies in the DU cases, but none of the HLA alleles were significantly higher (Table 4). When we compared selected allele frequencies in the GC and DU cases together using this criterion, again, none of the HLA alleles were significantly higher (Table 5). HLA-DR1*13-HLA-DQA1*01-HLA-DQB1*06 haplotype frequency was 4/24, 16% and 2/12, 16% for GC and DU cases with multiple EPIYA-C repeat, respectively. No difference was detected between GC and DU cases in terms of multiple EPIYA-C repeat.

Multivariate logistic regression analyses were carried out for the risk of GC and DU development alone and both subcases of the GC + DU patient group combined involving HLA-DQB1*06, HLA-DRB1*13, HLA-A*02, HLA-DQA1*01, and HLA-B*35 alleles, and none of the alleles were detected as independent risk factors for the risk of GC and DU development in terms of CagA+ multiple EPIYA-C repeats. However, a multivariate logistic regression analysis was done without any specific criteria using only the significantly different detected alleles between GC + DU patient and the NUD+Asymptomatic *H. pylori* control groups. The results showed that HLA-DQA1*01 (P = 0.004, OR = 1.848, 95%CI, 1.215-2.811), HLA-DQB1*06 (P = 0.009, OR = 1.821, 95%CI, 1.163-2.850), and HLA-A*02 (P = 0.04, OR = 1.579, 95%CI, 1.021-2.442) were risk factors for the development of GC and DU (Table 6).

Table 8 The distribution of EPIYA motifs for study and control groups, *n* (%)

EPIYA-C repeat patterns	Patient group				Control group				Total (*n* = 140)
	Gastric cancer		Duodenal ulcer		Non-ulcer dyspepsia		Individuals with normal gastrointestinal system		
ABC	12	(27.2)	34	(68)	28	(93.3)	16	(100)	90
AC	2	(4.5)	2	(4)	-		-		4
BC	2	(4.5)	-		-		-		2
ABCC	16	(36.4)	8	(16)	-		-		24
BCC	2	(4.6)	2	(4)	2	(6.7)	-		6
ACCC	-		-		-		-		-
ABCC	8	(18.2)	4	(8)	-		-		12
AB	2	(4.6)	-		-		-		2
Total	44	(100)	50	(100)	30	(100)	16	(100)	140

HLA: Human leukocyte antigen.

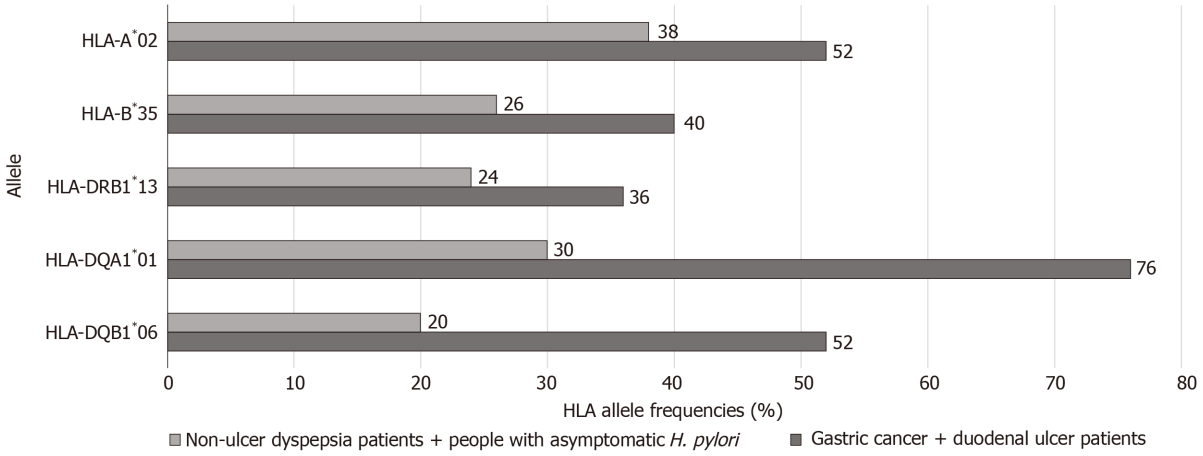

Figure 1 The representations of the highest human leukocyte antigen allele frequencies (%) in the gastric cancer + duodenal ulcer patient group when compared to non-ulcer dyspepsis patients + asymptomatic *Helicobacter pylori* control group. HLA: Human leukocyte antigen; *H. pylori*: *Helicobacter pylori*.

DISCUSSION

The development of GC and PU or DU is influenced by the virulence factors of *H. pylori* along with the host's genetic, epigenetic, and environmental factors. A variety of clinical consequences of *H. pylori* infection may arise depending on the variability of host response to the specific virulence factors of *H. pylori*[7]. For example, genes coding HLA class II molecules (HLA-DP/DQ/DR) may have genetically variable coding loci that lead to HLA gene polymorphisms. Therefore, specific HLA class II alleles were hypothesized to be related to the risks of some gastroduodenal malignancies such as GC and DU or PU development in patients with *H. pylori* infection.

In the literature, there are only traditional comparison studies using only *H. pylori* positivity for the association between HLA gene polymorphisms and the diseases caused by *H. pylori* infections. However, we focused on CagA+ multiple EPIYA-C repeats for the comparison of our study groups for HLA alleles for the first time in Turkey. The incidence of GC in Turkey is higher than in Eastern countries and lower than in Western countries at 5.7 and 9.6 cases per 100000 people for women and men, respectively. The mean age of occurrence is 56 years. It is the second and third leading cause of cancer-related deaths in men and women in Turkey, respectively[25].

The higher incidence in Turkey is mainly associated with dietary factors, and the differences in incidence are especially significant in the central, northeastern, and

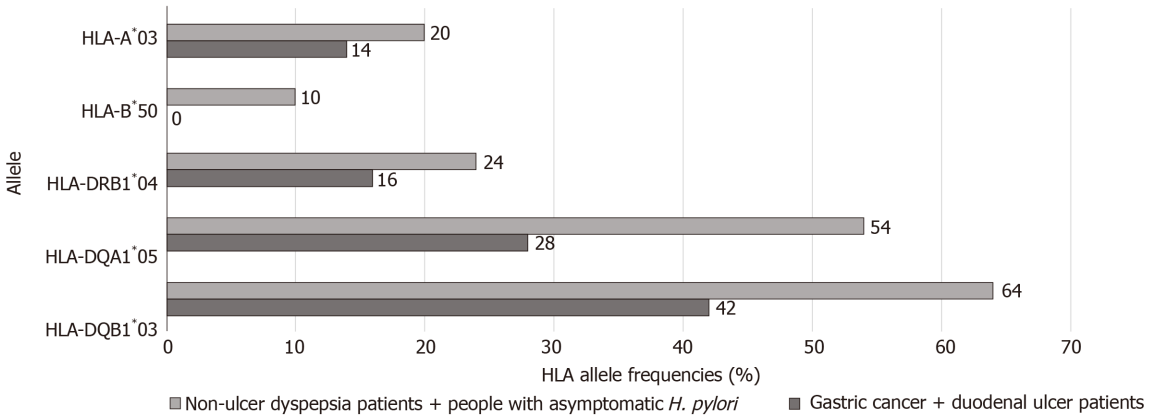

Figure 2 The representations of the highest human leukocyte antigen allele frequencies (%) in the (%) in the non-ulcer dyspepsis patients + Asymptomatic *Helicobacter pylori* control group when compared gastric cancer + duodenal ulcer patient group. HLA: Human leukocyte antigen; *H. pylori*: *Helicobacter pylori*.

eastern regions of the country. Salt is commonly used for food preservation, and wood charcoal with dried cow dung is commonly used for cooking in these regions, which are known to have carcinogenic effects on food. Another important factor for the development of GC is *H. pylori* infections[25].

Studies have shown an association between HLA gene polymorphisms and autoimmune diseases, and in genetically susceptible individuals, persistent bacterial infections can lead to autoimmune responses (*e.g.*, HLA-DR4-restricted autoimmune chronic synovitis following Lyme disease)[26]. While evaluating the effects of *H. pylori* infection on the pathogenesis of GC, the relationship between bacteria and the host should be considered because *H. pylori* infections may cause strong immune responses by causing the secretion of cytokines from the epithelial cells and gastric mucosa infiltration with neutrophils, macrophages, and lymphocytes. After the interaction of *H. pylori* with dendritic cells in luminal and subepithelial regions, dendritic cells may transform naive T cells into immunosuppressive Treg cells, and consequently, developed Th1 and Th17 cells may cause atrophic gastritis, epithelial hyperplasia, and intestinal metaplasia[27]. *H. pylori* infections tend to cause chronic inflammation, which can increase an individual's risk for the development of GC.

A commonly seen (90%) type of GC is adenocarcinoma, which is known to originate from the epithelial cells in chronic inflammation states[28]. Moreover, cytokines, which are the effector cells of inflammatory responses, may regulate a variety of immunologic events, including the inflammation, proliferation, and differentiation of epithelial cells. In the progression of gastric carcinogenesis, initially, *H. pylori* strongly induces specific cytokines, but the immune response generally is not sufficient to clear the *H. pylori* infection completely from the human epithelial cells. As a result, chronic inflammation may occur[29].

Consequently, the tissue damage increases along with parietal cell atrophy and may progress to dysplasia and GC through the combined effects of the various factors of the host and the environment. A subtype of T cells, Th17 cells, and their associated inflammatory cytokines, interleukin (IL)-17A, IL-23, and IL-1β, have important roles in the development of GC, colorectal cancer, ovarian cancer, and hepatocellular carcinoma. Cytokine IL-23 plays a major role in the primary activation of IL-17A. Th17 responses are reported to be increased during *H pylori* infections. The IL-17/IL-23 axis is believed to have an important role in the progression of chronic inflammation and related pathologies like gastric neoplasms[30].

Other than their main roles in chronic inflammation in gastric epithelial cells, cytokines also have specific polymorphisms in their genes. Polymorphisms in cytokine genes may modify the effect of gene-environment interaction and increase the degree of cytokine expression in the promoter regions of the genes. Polymorphisms in genes coding various cytokines such as IL-1β, IL-1Ra, IL-8, IL-10, and tumor necrosis factor-α are also suggested to be associated with the risk of GC. The IL1RN2 allele polymorphism is related to the risk of GC[31]. Wu *et al*[32] found a relation between IL-17F, A7488G and GC, and Felipe *et al*[33] also reported a relation between IL-8 (rs4073)–251A/T gene polymorphism and GC development.

Some virulent factors of *H. pylori* seem to be associated with GC risk, including vacuolating cytotoxin A, cytotoxin associated antigen A, DU promoting gene protein

A, and outer inflammatory protein with blood group antigen binding adhesins. Moreover, the *cagA* gene of *H. pylori* strains with multiple EPIYA-C repeats and EPIYA-D motif in its *cagA* gene are suggested to increase the risk of GC development. However, the role of host polymorphisms and the virulence factors of *H. pylori* in the risk of GC development varies among regions and ethnicities[31].

Several studies suggest that atrophic gastritis and GC risk are increased by CagA-positive *H. pylori* strains. An association has been reported between multiple EPIYA-C phosphorylation sites and GC. In a recent meta-analysis including 23 studies, Li *et al*[8] evaluated the association of EPIYA motifs and gastroduodenal pathologies. They concluded that the EPIYA-D motif was significantly related to GC risk, and multiple EPIYA-C motifs were related to PU and DU in Asia countries.

Conversely, in the United States and Europe, multiple EPIYA-C motifs were commonly associated with GC risk. Multiple EPIYA-C repeats cause stronger binding of CagA to SHP-2 than a single EPIYA-C. Multiple EPIYA C repeats are associated with a higher risk of GC[34,35]. The functionality of CagA is increased with multiple EPIYA-C phosphorylation sites and is involved in cellular phenotypic changes. Therefore, *H. pylori* strains with multiple EPIYA-C sites are related to the risk of GC.

We could not find any studies specifically evaluating the interaction between EPIYA-C repeats, HLA alleles, and gastric pathologies. In our study, there were only two cases in the control group with CagA+ multiple EPIYA-C repeats, and it was not possible to make a comparison as the number was too low and our criteria were not met. HLA-DQA1, HLA-DRB1*13, HLA-A*02, HLA-B*35, and HLA-DQB1*06 alleles were shown to contribute to the susceptibility to GC and DU and were used for a comparison between GC and DU subgroups of patients. However, we did not compare the higher HLA alleles detected in the control group as it was not possible to determine an HLA allele with a protective effect without including a control group.

In the comparison within the GC subgroup, due to our criterion, only the HLA-DQB1*06 allele was significantly low in the GC subgroup without EPIYA C repeats, but the difference was not statistically significant after Bonferroni correction. The higher frequency of the HLA-DQB1*06 allele suggests that this allele remains influential even in GC cases without multiple EPIYA-C repeats. With the presence of the HLA-DQB1*06 allele, we can suggest that mechanisms other than multiple EPIYA-C repeats may contribute to the development of GC. On the other hand, in the GC subgroup, the number of HLA-DQA1*01 alleles was high in the multiple EPIYA-C repeats group, but the result was not significant after the univariate analysis.

In the DU subgroup, none of the alleles were found to be significantly predominant in terms of frequencies. In addition, when the analyses were repeated while including GC and DU subgroups together, none of the HLA alleles were shown to either effective or protective. A multivariate logistic regression analysis was performed for GC and DU subgroups alone and together, and none of the alleles were detected as independent risk factors. We then performed a multivariate logistic regression without including any discriminative criterion and only using the significantly different detected alleles between patient and control groups. As a result, HLA-DQA1*01, HLA-DQB1*0601, and HLA-A*2 alleles were found to be independent risk factors for the risk of GC and DU.

There are no previous studies to compare our results based on the discrimination criteria for the selection of HLA alleles. Our results partly coincided with those of a meta-analysis of Asian populations by Wang *et al*[36]. In that study, the susceptibility genes for *H. pylori* infection were reported as DQB1*0401, DQA1*0103, and DQA1*0301. Garza-González *et al*[37] reported that the HLA-DQA1*0503 allele served as an independent protective factor for GC. In our study, we also detected HLA-DQA1*05 as a protective allele.

Similar to our results, Quintero *et al*[9] reported that the DQB1*0602 allele increased the risk of GC risk in a Southern European population infected with *H. pylori*. On the other hand, the results of several case–control studies conducted with a Japanese population were contradictory. In contrast to our results, Azuma *et al*[38] found that the number of DQA1*0102 alleles was significantly lower in their study group of *H. pylori*-infected patients with GC than in control subjects. However, our data did not support their findings for the DQA1* alleles.

In a study by Herrera-Goepfert *et al*[39], patients with GC displayed a high frequency of HLA-DQA1*0601, similar to our results. After our univariate analysis, DQA1*01 and HLA-DQB1*06 alleles were found to be positively associated with GC and DU, and DQB1*03 was found to be negatively associated with DU. These results are consistent with those of Herrera-Goepfert *et al*[39], Wu *et al*[13], and Quintero *et al*[9] .

The reason for the conflicting results may be the different methods used in HLA typing, ethnicities, and the fact that GC is a heterogeneous disease. Specific HLA

alleles may have the capability to modulate the presentation of peptides derived from *H. pylori* infection to T cells. As a result of this presentation, the type or severity of T cell response may affect the proliferation of a lineage-specific malignant T cell clones[5].

In the study by Li *et al*[10], the HLA-CW*03 ratio was significantly higher in cases with increased risk of GC and *H. pylori*-infected patients. A variety of exogenous stimulations such as toxins of *H. pylori* with gastric and bile juices always affect the gastric mucosa[40]. These stimulations cause epithelial cells to secrete IL-12 and induce natural killer (NK) cells. These NK cells secrete IFN-g, which initiates the Th1 immune response from naive T cells and causes phenotypic changes in epithelial cells, resulting in the upregulation of HLA-DR and HLA-B27 genes[41].

Different mechanisms may be responsible for the synergistic effect of *H. pylori* infection and specific HLA genotypes. Specific HLA genotypes may influence the immune response and lead to carcinogenesis after the initial infection[17]. However, the common consensus is that genetically different host responses against the virulence factors of *H. pylori* may cause inflammation with varying intensities, as well as gastric epithelial erosions with different stages.

Genetic and epigenetic factors may also influence the severity of inflammation and thereby contribute to different clinical outcomes. Upregulation of significant MHC class II type genes in epithelial cells may be related to the activation of T cells in the lamina propria and macrophages, as well as the consequent release of cytokines such as interferon-γ. Confirming this hypothesis, upregulated expression of MHC class II genes in gastric epithelial cells had a positive correlation with the T cells in the lamina propria in children with *H. pylori* infections according to Lopes *et al*[42].

We could not detect any HLA allele as an independent risk factor for GC under our criterion, but without any criterion, some HLA alleles may regulate host susceptibility to *H. pylori* infection in the presence of its virulence factors. It can be suggested that some immunogenetic factors of the host may have important effects for *H. pylori*-initiated inflammation leading to carcinogenesis. Although various host or *H. pylori* virulence factors may have a role in the development of GC, specific host factors like HLAs could also modulate GC susceptibility or the resistance of individuals. Individuals who are at risk due to the susceptibility of HLA alleles to GC should be monitored prior to the initiation of carcinogenesis.

We only focused on the association between HLA gene polymorphisms and multiple EPIYA-C repeats of *H. pylori* DNAs isolated from the gastric biopsy specimens. Only two of our control group cases had multiple EPIYA-C repeats, so we compared two subgroups of the study group. We could not find a significant difference between GC and DU subgroups in terms of multiple EPIYA-C repeats. On the other hand, in a simple comparison between study and control groups, HLA-DQA1*01 (OR = 1.848), HLA-DQB1*06 (OR = 1.821), and HLA-A*2 (OR = 1.579) alleles were detected as independent risk factors for GC and DU.

We believe that there is an association between HLA allele polymorphisms and gastric pathologies, but this is not a definite reality because of differences between regions and ethnicities and the virulence factors of *H. pylori*. The same HLA alleles sometimes show a positive correlation and sometimes show a negative association in different regions and ethnicities. We suggest that the role of host polymorphisms of the host and *H. pylori* virulence factors in the risk of GC development varies among countries of different regions and different ethnicities.

This study has some limitations. The resolution of the HLA kits was low, which prevented an exact HLA comparison with other studies. We also did not evaluate some HLA alleles, such as HLA-C. Other important result of our study was that HLA-DR1*13-HLA-DQA1*01-HLA-DQB1*06 haplotype frequency was detected significantly higher in our GC subgroup cases more than both DU and control group cases. This results is similar for the locus type but different for HLA allele types from the study of Ando *et al*[43] They reported DRB1*04:05-DQA1*03:03-DQB1*04:01 haplotype frequency with 10%–30% in Japanese population and the risk of GC development.

CONCLUSION

This is the first study to evaluate the association between HLA alleles with GC and DU and asymptomatic *H. pylori* cases. Even though no HLA alleles were detected in multivariate analysis, HLA-DQB1*06 was significantly less frequent in the GC subgroup with multiple EPIYA repeats in the univariate analysis. However, this HLA allele was not detected as an independent risk factor in the multivariate analysis. In

the multivariate logistic regression analysis using significantly different alleles and no discriminative criteria, HLA-DQA1*01 (OR = 1.848), HLA-DQB1*06 (OR = 1.821), and HLA-A*02 (OR = 1.579) alleles were found to be risk factors for GC and DU. However, we suggest that these HLA alleles make individuals prone to the development of GC without cagA and multiple EPIYA C repeats of the host. To clarify the effects of HLA alleles on the pathogenesis of gastric malignancies, more comprehensive, prospective, large-scale studies with high HLA resolution detection should be performed in the future.

ARTICLE HIGHLIGHTS

Research background

The development of gastric cancer (GC) is suggested to be related to the interactions between bacterial virulence factors, host genetic factors such as the human leukocyte antigen (HLA) gene, the immune response of the host, and environmental factors. Some of the host factors may be polymorphisms in the host genes such as HLA genes, which regulate the strength of the inflammatory response and influence the probability of a specific clinical outcome.

Research motivation

We seek to determine which HLA class I and II alleles differ in gastrointestinal pathologies such as GC and duodenal ulcer (DU) in Turkey.

Research objectives

We investigated the allele frequencies of HLA class I and II in a patient group [*Helicobacter pylori (H. pylori)*-positive GC and DU patients] and compared the results to a control group (*H. pylori*-positive non-ulcer dyspepsia patients and asymptomatic individuals with *H. pylori*) in terms of CagA+ multiple (≥ 2) EPIYA-C repeats for the first time in a Turkish population.

Research methods

In this case-control study, amplification of the *H. pylori cagA* gene and typing of EPIYA motifs were performed by PCR. HLA allele types were identified by sequence-specific oligonucleotide typing kits (HLA-A, HLA-B HLA-C, HLA-DRB1, and HLA-DQA1/B1 kits).

Research results

None of the alleles were detected as independent risk factors after multivariate analysis in terms of CagA+ multiple (≥ 2) EPIYA-C repeats. On the other hand, in a multivariate logistic regression with no discriminative criterion, HLA-DQA1*01 [odds ratio (OR) = 1.848], HLA-DQB1*06 (OR = 1.821), and HLA-A*02 (OR = 1.579) alleles were detected as independent risk factors for GC and DU.

Research conclusions

We suggest that the association of these alleles with gastric malignancies is not specifically related to cagA and multiple EPIYA C repeats.

Research perspectives

Specific HLA alleles maybe related to the gastric malignancies and could be for the indication of GCs in order to scan populations before the development of GC. The alleles may also be cost-effective to find individuals with a higher risk for GC development.

ACKNOWLEDGEMENTS

We thank Assoc. Prof. Dr. Murat Telli from the Department of Biology in Bolu Abant Izzet Baysal University, Turkey for the calculation of H-W equilirum and LD.

REFERENCES

1 **Ferlay J**, Colombet M, Soerjomataram I, Mathers C, Parkin DM, Piñeros M, Znaor A, Bray F. Estimating the global cancer incidence and mortality in 2018: GLOBOCAN sources and methods. *Int J Cancer* 2019; **144**: 1941-1953 [PMID: 30350310 DOI: 10.1002/ijc.31937]

2 **Malvehy Rovira J**, Barranco Peña F, Terradas Mercader P. [Serratia marcescens and neonatal sepsis]. *An Esp Pediatr* 1988; **29**: 23-25 [PMID: 3056142 DOI: 10.23750/abm.v89i8-S.7947]

3 **Koulis A**, Buckle A, Boussioutas A. Premalignant lesions and gastric cancer: Current understanding. *World J Gastrointest Oncol* 2019; **11**: 665-678 [PMID: 31558972 DOI: 10.4251/wjgo.v11.i9.665]

4 **Burkitt MD**, Duckworth CA, Williams JM, Pritchard DM. Helicobacter pylori-induced gastric pathology: insights from in vivo and ex vivo models. *Dis Model Mech* 2017; **10**: 89-104 [PMID: 28151409 DOI: 10.1242/dmm.027649]

5 **Crux NB**, Elahi S. Human Leukocyte Antigen (HLA) and Immune Regulation: How Do Classical and Non-Classical HLA Alleles Modulate Immune Response to Human Immunodeficiency Virus and Hepatitis C Virus Infections? *Front Immunol* 2017; **8**: 832 [PMID: 28769934 DOI: 10.3389/fimmu.2017.00832]

6 **Ansari S**, Yamaoka Y. *Helicobacter pylori* Virulence Factors Exploiting Gastric Colonization and its Pathogenicity. *Toxins (Basel)* 2019; **11**: 677 [PMID: 31752394 DOI: 10.3390/toxins11110677]

7 **Chang WL**, Yeh YC, Sheu BS. The impacts of H. pylori virulence factors on the development of gastroduodenal diseases. *J Biomed Sci* 2018; **25**: 68 [PMID: 30205817 DOI: 10.1186/s12929-018-0466-9]

8 **Li Q**, Liu J, Gong Y, Yuan Y. Association of CagA EPIYA-D or EPIYA-C phosphorylation sites with peptic ulcer and gastric cancer risks: A meta-analysis. *Medicine (Baltimore)* 2017; **96**: e6620 [PMID: 28445260 DOI: 10.1097/MD.0000000000006620]

9 **Quintero E**, Pizarro MA, Rodrigo L, Piqué JM, Lanas A, Ponce J, Miño G, Gisbert J, Jurado A, Herrero MJ, Jiménez A, Torrado J, Ponte A, Díaz-de-Rojas F, Salido E. Association of Helicobacter pylori-related distal gastric cancer with the HLA class II gene DQB10602 and cagA strains in a southern European population. *Helicobacter* 2005; **10**: 12-21 [PMID: 15691311 DOI: 10.1111/j.1523-5378.2005.00287.x]

10 **Li Z**, Chen D, Zhang C, Li Y, Cao B, Ning T, Zhao Y, You W, Ke Y. HLA polymorphisms are associated with Helicobacter pylori infected gastric cancer in a high risk population, China. *Immunogenetics* 2005; **56**: 781-787 [PMID: 15650879 DOI: 10.1007/s00251-004-0723-9]

11 **Watanabe Y**, Aoyama N, Sakai T, Shirasaka D, Maekawa S, Kuroda K, Wambura C, Tamura T, Nose Y, Kasuga M. HLA-DQB1 locus and gastric cancer in Helicobacter pylori infection. *J Gastroenterol Hepatol* 2006; **21**: 420-424 [PMID: 16509868 DOI: 10.1111/j.1440-1746.2005.04112.x]

12 **Magnusson PKE**, Enroth H, Eriksson I, Held M, Nyrén O, Engstrand L, Hansson LE, Gyllensten UB. Gastric cancer and human leukocyte antigen: distinct DQ and DR alleles are associated with development of gastric cancer and infection by Helicobacter pylori. *Cancer Res* 2001; **61**: 2684-2689 [PMID: 11289148]

13 **Wu MS**, Hsieh RP, Huang SP, Chang YT, Lin MT, Chang MC, Shun CT, Sheu JC, Lin JT. Association of HLA-DQB1*0301 and HLA-DQB1*0602 with different subtypes of gastric cancer in Taiwan. *Jpn J Cancer Res* 2002; **93**: 404-410 [PMID: 11985790 DOI: 10.1111/j.1349-7006.2002.tb01271.x]

14 **Yoshitake S**, Okada M, Kimura A, Sasazuki T. Contribution of major histocompatibility complex genes to susceptibility and resistance in Helicobacter pylori related diseases. *Eur J Gastroenterol Hepatol* 1999; **11**: 875-880 [PMID: 10514120 DOI: 10.1097/00042737-199908000-00011]

15 **Ohtani M**, Azuma T, Yamazaki S, Yamakawa A, Ito Y, Muramatsu A, Dojo M, Yamazaki Y, Kuriyama M. Association of the HLA-DRB1 gene locus with gastric adenocarcinoma in Japan. *Dig Liver Dis* 2003; **35**: 468-472 [PMID: 12870731 DOI: 10.1016/s1590-8658(03)00218-4]

16 **Lee JE**, Lowy AM, Thompson WA, Lu M, Loflin PT, Skibber JM, Evans DB, Curley SA, Mansfield PF, Reveille JD. Association of gastric adenocarcinoma with the HLA class II gene DQB10301. *Gastroenterology* 1996; **111**: 426-432 [PMID: 8690208 DOI: 10.1053/gast.1996.v111.pm8690208]

17 **Ohmori M**, Yasunaga S, Maehara Y, Sugimachi K, Sasazuki T. DNA typing of HLA class I (HLA-A) and class II genes (HLA-DR, -DQ and -DP) in Japanese patients with gastric cancer. *Tissue Antigens* 1997; **50**: 277-282 [PMID: 9331950 DOI: 10.1111/j.1399-0039.1997.tb02871.x]

18 **Zhao Y**, Wang J, Tanaka T, Hosono A, Ando R, Soeripto S, Ediati Triningsih FX, Triono T, Sumoharjo S, Astuti EY, Gunawan S, Tokudome S. Association between HLA-DQ genotypes and haplotypes vs Helicobacter pylori infection in an Indonesian population. *Asian Pac J Cancer Prev* 2012; **13**: 1247-1251 [PMID: 22799313 DOI: 10.7314/apjcp.2012.13.4.1247]

19 **He Q**, Wang JP, Osato M, Lachman LB. Real-time quantitative PCR for detection of Helicobacter pylori. *J Clin Microbiol* 2002; **40**: 3720-3728 [PMID: 12354871 DOI: 10.1128/jcm.40.10.3720-3728.2002]

20 **van Doorn LJ**, Figueiredo C, Rossau R, Jannes G, van Asbroek M, Sousa JC, Carneiro F, Quint WG. Typing of Helicobacter pylori vacA gene and detection of cagA gene by PCR and reverse hybridization. *J Clin Microbiol* 1998; **36**: 1271-1276 [PMID: 9574690]

21 **Erzin Y**, Koksal V, Altun S, Dobrucali A, Aslan M, Erdamar S, Dirican A, Kocazeybek B. Prevalence of Helicobacter pylori vacA, cagA, cagE, iceA, babA2 genotypes and correlation with clinical outcome in Turkish patients with dyspepsia. *Helicobacter* 2006; **11**: 574-580 [PMID: 17083380 DOI: 10.1111/j.1523-5378.2006.00461.x]

22 **Argent RH**, Zhang Y, Atherton JC. Simple method for determination of the number of Helicobacter pylori CagA variable-region EPIYA tyrosine phosphorylation motifs by PCR. *J Clin Microbiol* 2005; **43**: 791-795 [PMID: 15695681 DOI: 10.1128/JCM.43.2.791-795.2005]

23 **Occhialini A**, Marais A, Urdaci M, Sierra R, Muñoz N, Covacci A, Mégraud F. Composition and gene expression of the cag pathogenicity island in Helicobacter pylori strains isolated from gastric carcinoma and gastritis patients in Costa Rica. *Infect Immun* 2001; **69**: 1902-1908 [PMID: 11179371 DOI: 10.1128/IAI.69.3.1902-1908.2001]

24 **Rousset F**. genepop'007: a complete re-implementation of the genepop software for Windows and Linux. *Mol Ecol Resour* 2008; **8**: 103-106 [PMID: 21585727 DOI: 10.1111/j.1471-8286.2007.01931.x]

25 **Tural D**, Selçukbiricik F, Akar E, Serdengeçti S, Büyükünal E. Gastric cancer: a case study in Turkey. *J Cancer Res Ther* 2013; **9**: 644-648 [PMID: 24518710 DOI: 10.4103/0973-1482.126466]

26 **Arvikar SL**, Crowley JT, Sulka KB, Steere AC. Autoimmune Arthritides, Rheumatoid Arthritis, Psoriatic Arthritis, or Peripheral Spondyloarthritis Following Lyme Disease. *Arthritis Rheumatol* 2017; **69**: 194-202 [PMID: 27636905 DOI: 10.1002/art.39866]

27 **Rezalotfi A**, Ahmadian E, Aazami H, Solgi G, Ebrahimi M. Gastric Cancer Stem Cells Effect on Th17/Treg Balance; A Bench to Beside Perspective. *Front Oncol* 2019; **9**: 226 [PMID: 31024835 DOI: 10.3389/fonc.2019.00226]

28 **Bockerstett KA**, DiPaolo RJ. Regulation of Gastric Carcinogenesis by Inflammatory Cytokines. *Cell Mol Gastroenterol Hepatol* 2017; **4**: 47-53 [PMID: 28560288 DOI: 10.1016/j.jcmgh.2017.03.005]

29 **Blogowski W**, Madej-Michniewicz A, Marczuk N, Dolegowska B, Starzyńska T. Interleukins 17 and 23 in patients with gastric neoplasms. *Sci Rep* 2016; **6**: 37451 [PMID: 27869179 DOI: 10.1038/srep37451]

30 **Dixon BREA**, Hossain R, Patel RV, Algood HMS. Th17 Cells in Helicobacter pylori Infection: a Dichotomy of Help and Harm. *Infect Immun* 2019; **87**: e00363-19 [PMID: 31427446 DOI: 10.1128/IAI.00363-19]

31 **de Brito BB**, da Silva FAF, de Melo FF. Role of polymorphisms in genes that encode cytokines and Helicobacter pylori virulence factors in gastric carcinogenesis. *World J Clin Oncol* 2018; **9**: 83-89 [PMID: 30254963 DOI: 10.5306/wjco.v9.i5.83]

32 **Wu X**, Zeng Z, Chen B, Yu J, Xue L, Hao Y, Chen M, Sung JJ, Hu P. Association between polymorphisms in interleukin-17A and interleukin-17F genes and risks of gastric cancer. *Int J Cancer* 2010; **127**: 86-92 [PMID: 19904747 DOI: 10.1002/ijc.25027]

33 **Felipe AV**, Silva TD, Pimenta CA, Kassab P, Forones NM. Interleukin-8 gene polymorphism and susceptibility to gastric cancer in a Brazilian population. *Biol Res* 2012; **45**: 369-374 [PMID: 23558993 DOI: 10.4067/S0716-97602012000400007]

34 **Batista SA**, Rocha GA, Rocha AM, Saraiva IE, Cabral MM, Oliveira RC, Queiroz DM. Higher number of Helicobacter pylori CagA EPIYA C phosphorylation sites increases the risk of gastric cancer, but not duodenal ulcer. *BMC Microbiol* 2011; **11**: 61 [PMID: 21435255 DOI: 10.1186/1471-2180-11-61]

35 **El Khadir M**, Alaoui Boukhris S, Benajah DA, Ibrahimi SA, Chbani L, Bouguenouch L, El Rhazi K, El Abkari M, Nejjari C, Mahmoud M, Bennani B. Helicobacter pylori CagA EPIYA-C motifs and gastric diseases in Moroccan patients. *Infect Genet Evol* 2018; **66**: 120-129 [PMID: 30244090 DOI: 10.1016/j.meegid.2018.09.015]

36 **Wang J**, Zhang Q, Liu Y, Han J, Ma X, Luo Y, Liang Y, Zhang L, Hu Y. Association between HLA-â…¡gene polymorphism and Helicobacter pylori infection in Asian and European population: A meta-analysis. *Microb Pathog* 2015; **82**: 15-26 [PMID: 25773770 DOI: 10.1016/j.micpath.2015.03.011]

37 **Garza-González E**, Bosques-Padilla FJ, Pérez-Pérez GI, Flores-Gutiérrez JP, Tijerina-Menchaca R. Association of gastric cancer, HLA-DQA1, and infection with Helicobacter pylori CagA+ and VacA+ in a Mexican population. *J Gastroenterol* 2004; **39**: 1138-1142 [PMID: 15622476 DOI: 10.1007/s00535-004-1462-2]

38 **Azuma T**, Ito S, Sato F, Yamazaki Y, Miyaji H, Ito Y, Suto H, Kuriyama M, Kato T, Kohli Y. The role of the HLA-DQA1 gene in resistance to atrophic gastritis and gastric adenocarcinoma induced by Helicobacter pylori infection. *Cancer* 1998; **82**: 1013-1018 [PMID: 9506344 DOI: 10.1002/(sici)1097-0142(19980315)82:6<1013::aid-cncr2>3.0.co;2-f]

39 **Herrera-Goepfert R**, Zúñiga J, Hernández-Guerrero A, Rodríguez-Reyna T, Osnalla N, Ruíz-Morales J, Vargas-Alarcón G, Yamamoto-Furusho JK, Mohar-Betancourt A, Hernández-Pando R, Granados J. [Association of the HLA-DQB*0501, allele of the major histocompatibility complex with gastric cancer in Mexico]. *Gac Med Mex* 2004; **140**: 299-303 [PMID: 15259342]

40 **Kitamura H**, Honma I, Torigoe T, Asanuma H, Sato N, Tsukamoto T. Down-regulation of HLA class I antigen is an independent prognostic factor for clear cell renal cell carcinoma. *J Urol* 2007; **177**: 1269-72; discussion 1272 [PMID: 17382705 DOI: 10.1016/j.juro.2006.11.082]

41 **Engstrand L**, Scheynius A, Påhlson C, Grimelius L, Schwan A, Gustavsson S. Association of Campylobacter pylori with induced expression of class II transplantation antigens on gastric epithelial cells. *Infect Immun* 1989; **57**: 827-832 [PMID: 2645211]

42 **Lopes AI**, Victorino RM, Palha AM, Ruivo J, Fernandes A. Mucosal lymphocyte subsets and HLA-DR antigen expression in paediatric Helicobacter pylori-associated gastritis. *Clin Exp Immunol* 2006; **145**: 13-20 [PMID: 16792668 DOI: 10.1111/j.1365-2249.2006.03100.x]

43 **Ando T**, Ishikawa T, Kato H, Yoshida N, Naito Y, Kokura S, Yagi N, Takagi T, Handa O, Kitawaki J, Nakamura N, Hasegawa G, Fukui M, Imamoto E, Nakamura C, Oyamada H, Isozaki Y, Matsumoto N, Nagao Y, Okita M, Nakajima Y, Kurokawa M, Nukina M, Ohta M, Mizuno S, Ogata M, Obayashi H, Park H, Kitagawa Y, Nakano K, Yoshikawa T. Synergistic effect of HLA class II loci and cytokine gene polymorphisms on the risk of gastric cancer in Japanese patients with Helicobacter pylori infection. *Int J Cancer* 2009; **125**: 2595-2602 [PMID: 19544559 DOI: 10.1002/ijc.24666]

World Journal of Gastroenterology

Submit a Manuscript: https://www.f6publishing.com

World J Gastroenterol 2020 August 28; 26(32): 4833-4845

DOI: 10.3748/wjg.v26.i32.4833

ISSN 1007-9327 (print) ISSN 2219-2840 (online)

ORIGINAL ARTICLE

Retrospective Study

Features of extrahepatic metastasis after radiofrequency ablation for hepatocellular carcinoma

Jae H Yoon, Young J Goo, Chae-Jun Lim, Sung K Choi, Sung B Cho, Sang S Shin, Chung H Jun

ORCID number: Jae H Yoon 0000-0002-4993-2496; Young J Goo 0000-0002-5747-1212; Chae-Jun Lim 0000-0001-7373-7167; Sung K Choi 0000-0002-6878-3385; Sung B Cho 0000-0001-9816-3446; Sang S Shin 0000-0002-5752-7431; Chung H Jun 0000-0002-7136-8350.

Author contributions: Yoon JH and Jun CH designed and performed the research and wrote the paper; Choi SK designed the research and supervised the report; Lim CJ and Goo YJ contributed to the analysis; Cho SB and Shin SS provided clinical advice.

Supported by the Research Supporting Program of The Korean Association for the Study of the Liver and the Korean Liver Foundation, No. KASLKLF2019-06.

Institutional review board statement: The study protocol was approved by the Institutional Review Board of Chonnam National University Hospital (CNUH-2019-203). Research was conducted in accordance with the 1964 Declaration of Helsinki and its later amendments.

Informed consent statement: Informed consent requirement was waived because the patient data were de-identified.

Jae H Yoon, Young J Goo, Chae-Jun Lim, Sung K Choi, Department of Gastroenterology, Chonnam National University Hospital and Medical School, Gwangju 61469, South Korea

Sung B Cho, Department of Gastroenterology, Hwasun Chonnam National University Hospital and Medical School, Hwasun 58128, South Korea

Sang S Shin, Department of Radiology, Chonnam National University Hospital and Medical School, Gwangju 61469, South Korea

Chung H Jun, Department of Internal Medicine, Mokpo Hankook Hospital, Mokpo 58643, South Korea

Corresponding author: Chung H Jun, MD, Doctor, Professor, Department of Internal Medicine, Mokpo Hankook Hospital, 483 Yeongsan-ro, Mokpo 58643, South Korea. estevanj@naver.com

Abstract

BACKGROUND

Extrahepatic metastasis (EHM) of hepatocellular carcinoma (HCC) is associated with poor outcomes. However, the clinical features and risk factors of EHM of HCC after radiofrequency ablation (RFA) remain unclear.

AIM

To elucidate the characteristics and risk factors of EHM after RFA for HCC.

METHODS

From January 2008 to December 2017, we retrospectively enrolled 661 patients who underwent RFA as first-line treatment for HCC at 2 tertiary hospitals. The inclusion criteria were age ≥ 18 years, a diagnosis of HCC, and treatment-naivety. Abdominal computed tomography (CT) or magnetic resonance imaging (MRI) and alpha-fetoprotein measurements were routinely performed at 1 mo after RFA and followed-up at intervals of 3-6 mo. Univariate analyses were performed using the chi-squared test or Student's *t*-test, and univariate and multivariate analyses were performed *via* logistic regression, as appropriate.

RESULTS

EHM was diagnosed in 44 patients (6.7%) during a median follow-up period of 1204 days. The 10-year cumulative rate of HCC recurrence and EHM was 92.7% and 33.7%, respectively. Initial recurrence was most often intrahepatic, and the

Conflict-of-interest statement: The authors have no conflicts of interest to declare.

Data sharing statement: No additional data are available.

Manuscript source: Unsolicited manuscript

Received: April 2, 2020
Peer-review started: April 2, 2020
First decision: April 29, 2020
Revised: May 4, 2020
Accepted: August 12, 2020
Article in press: August 12, 2020
Published online: August 28, 2020

P-Reviewer: Aurello P
S-Editor: Gong ZM
L-Editor: A
P-Editor: Zhang YL

rate of extrahepatic recurrence at initial recurrence was only 1.2%. The median time to the diagnosis of EHM was 2.68 years, and 68.2% of patients developed EHM within 2 years of the first recurrence, regardless of recurrence-free survival and 75.0% of patients developed EHM within 5 years after first recurrence. EHM was mostly diagnosed *via* abdominal CT/MRI in 33 (75.0%) and 38 of 44 patients (86.4%) with EHM had either positive abdominal CT scan results or serum AFP level elevation. In multivariate analysis, recurrence-free survival < 2 years, ablation zone/tumor size < 2, and alpha-fetoprotein level > 400 IU/mL were associated with a high EHM risk.

CONCLUSION
EHM occurs following multiple intrahepatic recurrences after RFA and combined contrast-enhanced abdominal CT and serum AFP were useful for surveillance. Patients especially with high-risk factors require close follow-up for EHM.

Key words: Hepatocellular carcinoma; Metastasis; Radiofrequency ablation; Surveillance; Risk factor

Core tip: Extrahepatic metastasis (EHM) after radiofrequency ablation (RFA) of hepatocellular carcinoma (HCC) takes place in substantial clinical situations and EHM of HCC is related with dismal prognosis. Our study provides characteristics and risk factors for EHM after RFA of HCC. EHM after RFA at the time of the first recurrence is rare; however, cumulative EHM frequently occurs following multiple intrahepatic recurrences. Most of the patients (86.4%) had either positive contrast-enhanced computed tomography scan results or serum alpha-fetoprotein level elevation at EHM. EHM turned out to be related with recurrence-free survival < 2 years, ablation zone/tumor size < 2, and alpha-fetoprotein level > 400 IU/mL.

Citation: Yoon JH, Goo YJ, Lim CJ, Choi SK, Cho SB, Shin SS, Jun CH. Features of extrahepatic metastasis after radiofrequency ablation for hepatocellular carcinoma. *World J Gastroenterol* 2020; 26(32): 4833-4845
URL: https://www.wjgnet.com/1007-9327/full/v26/i32/4833.htm
DOI: https://dx.doi.org/10.3748/wjg.v26.i32.4833

INTRODUCTION

Hepatocellular carcinoma (HCC) is the sixth most commonly diagnosed cancer and the fourth leading cause of cancer-related death[1]. Unlike other cancers that cause distant metastasis during progression, HCC has unique characteristics of loco-regional progression with an increase in size, intrahepatic metastasis, and vascular invasion. Therefore, current guidelines in Korea suggest follow-up surveillance after curative HCC treatment using abdominal imaging focusing on the liver and tumor marker such as serum alpha-fetoprotein (AFP) level[2]. Although enrolled subjects of previous studies represented all stages of HCC, the incidence of extrahepatic metastasis (EHM) of HCC ranged from 14%-37% and the presence of EHM was associated with poor clinical outcomes[3]. The reported median survival duration of patients with EHM is less than 6 (range, 4.9-5.9) mo, and the 1-year survival rate was reported as 24.9%[3,4]. Natsuizaka *et al*[3] suggested that the lung was the most common site of metastasis, and screening tests for lung metastases, as well as abdominal imaging, should be performed periodically for HCC patients. Lam *et al*[5] reported that when EHM is identified early and surgical resection is possible, the prognosis may be improved. Therefore, early diagnosis of EHM of HCC may help improve the prognosis.

Radiofrequency ablation (RFA) for the treatment of small HCC lesions (tumor diameter < 3 cm) has shown favorable clinical outcomes with less invasiveness and a low complication rate. RFA is recommended as one of the first-line treatment modalities for the management of HCC along with liver transplantation and surgery[6,7]. However, the recurrence-free survival (RFS) varies substantially (3.2%-38.2%) between studies, and cumulative extrahepatic recurrence rates were reported as

19.1% and 38.2% at 5 and 10 years, respectively[8,9]. Hence, careful monitoring for intra- and extrahepatic HCC recurrence after RFA is essential, but there is a lack of data regarding the effect of post-treatment surveillance on the prognosis of recurred HCC[10]. Moreover, few studies have been conducted on individualized post-treatment surveillance for EHM after RFA according to risk factors[11].

Therefore, we aimed to assess the characteristics and risk factors of EHM among patients who had undergone RFA as initial treatment for HCC and to investigate the appropriate surveillance tool for EHM detection.

MATERIALS AND METHODS

Patients

From January 2008 to December 2017, 1421 patients who underwent RFA for hepatic tumors at 2 tertiary hospitals were assessed. The inclusion criteria for this study were age ≥ 18 years, a diagnosis of HCC, and treatment-naivety. After excluding patients with hepatic tumors other than HCC or a history of HCC treatment, 661 patients were finally enrolled (Figure 1). Baseline clinical and tumor characteristics, complications of RFA, the status of recurrence, RFS, and rescue treatment methods for HCC recurrence were assessed retrospectively. The study protocol was approved by the Institutional Review Board of Chonnam National University Hospital (CNUH-2019-203). The research was conducted in accordance with the 1964 Declaration of Helsinki and its later amendments.

The indications of RFA for HCC in our institutes were as follows: (1) Ineligible for surgical resection/liver transplantation or patient refusal for surgery; (2) Single nodular HCC < 5 cm in maximum diameter or multinodular HCC (3 in number, each < 3 cm in maximum diameter); (3) No EHM or vascular invasion; and (4) Prothrombin time ratio > 50% (international normalized ratio < 1.7).

Baseline staging and work-up

HCC was diagnosed according to the guidelines proposed by the Korean Liver Cancer Study Group and the National Cancer Center[12]. HCC was staged at diagnosis according to the modified Union for International Cancer Control (mUICC) staging system[13] and the Barcelona Clinic Liver Cancer (BCLC) classification system[14]. The initial tumor size was based on planning ultrasonography performed before RFA, and ablation size was measured *via* computed tomography (CT) scan performed immediately after RFA. All measurements were reviewed by board-certified radiologists who were experts in abdominal imaging.

Abdominal CT or magnetic resonance imaging (MRI) and AFP measurements were routinely performed at 1 month after RFA and followed-up at intervals of 3-6 mo. Positron emission tomography (PET)-CT, bone scanning, spinal MRI, and chest CT were also performed in cases of clinically suspected metastasis or as intermittent routine follow-up based on the decision of the treating physician.

Diagnosis of extrahepatic metastasis

The time of EHM diagnosis was defined as the date on which EHM was detected *via* imaging study for the first time. Most cases of EHM were diagnosed during routine follow-up studies while few patients were diagnosed during the evaluation of new symptoms or significant AFP/serial AFP elevation without definite intrahepatic lesions. An increase in AFP > 15 ng/mL compared to the previous value within less than 6 months was considered significant; this was regarded as a feasible cutoff point for the prediction of long-term outcome among patients with HCC[15]. An AFP level that showed an increasing tendency more than twice was considered as serial elevation of AFP.

Statistical analysis

The data are expressed as means ± standard deviations or medians with ranges. Univariate analyses were performed using the chi-squared test or Student's *t*-test, and univariate and multivariate analyses were performed *via* logistic regression, as appropriate. Variables with *P* values ≤ 0.05 in the univariate analysis were included in the multivariate logistic regression analysis. All statistical analyses were performed using SPSS version 22.0 (IBM Corp., Armonk, NY, United States). All analyses items with $P < 0.05$ were considered statistically significant.

The statistical methods of this study were reviewed by Ja Young Baek from

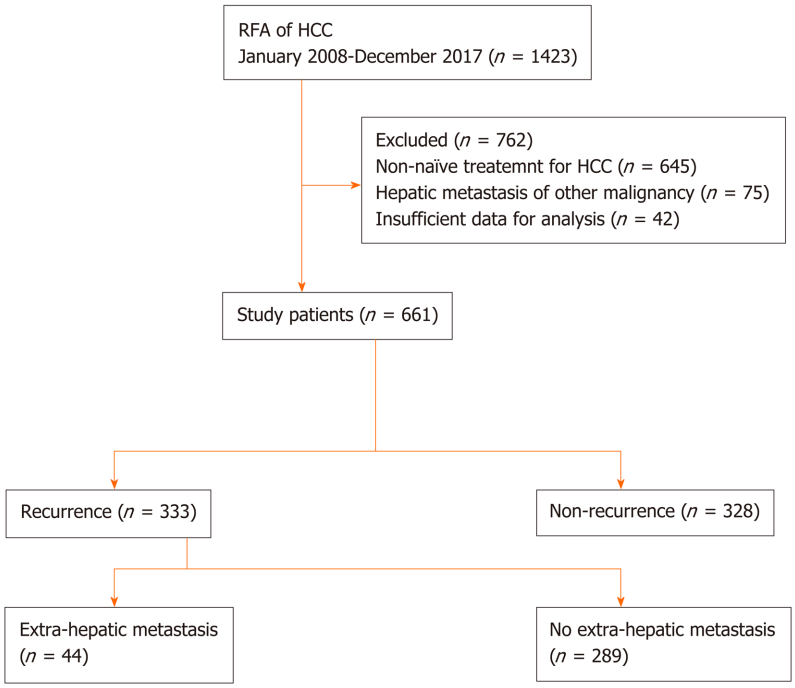

Figure 1 Flowchart indicating the method of patient enrollment. HCC: Hepatocellular carcinoma; RFA: Radiofrequency ablation.

Biomedical Research Institute, Hwasun Chonnam National University Hospital.

RESULTS

Baseline characteristics of enrolled patients

We identified 661 patients who underwent RFA as initial treatment for newly diagnosed HCC, and EHM occurred among 44 patients during the study period. We compared the baseline characteristics between the groups with and without EHM among the enrolled patients (Table 1). The mean age was 66.9 years, and 75.2% of the patients were male. The serum albumin level was lower among patients with EHM (4.3 mg/dL *vs* 3.9 mg/dL, $P = 0.015$). A higher proportion of patients in the EHM group had initial BCLC stage A and mUICC stage II disease compared to patients in the group without EHM who had a higher prevalence of BCLC stage 0 and mUICC stage I disease. There were no differences in tumor size and numbers between the 2 groups; however, the ratio of the ablation zone to tumor size was smaller in the group with EHM (2.07 *vs* 1.57, $P = 0.001$). There were no significant differences in the initial HCC recurrence site and mUICC tumor stage. The median follow-up duration of the enrolled patients was 1204 d.

Characteristics of first recurrence following RFA

Among 661 enrolled patients, 289 (43.7%) developed recurrent lesions without EHM, and 44 (6.7%) were diagnosed with EHM during the follow-up period. The median AFP level was higher at diagnosis of EHM than before the diagnosis of EHM in 79.0% of patients. The 10-year cumulative rates of HCC recurrence and EHM were 92.7% and 33.7%, respectively (Figure 2). Among the 661 patients, the median time to the detection of first HCC recurrence after RFA was 1.75 years, and the median duration to the development of EHM was 2.68 years. In addition, 68.2% of patients developed EHM within 2 years after the first recurrence regardless of RFS, and 75.0% of patients developed EHM within 5 years of the first recurrence (Figure 3). The most common site of initial recurrence was intrahepatic; initial extrahepatic recurrence occurred in only 1.2% (8/661) of patients. Most cases of EHM occurred after multiple intrahepatic recurrences, and the HCC stages at first recurrence are shown in Table 2. In addition, the peritoneum was the most common site of first EHM among 8 patients with EHM (5/8, 62.5%) followed by the lymph nodes (3/8, 37.5%). There was no case of pulmonary metastasis as the first recurrence in this study. Transcatheter arterial chemoembolization and RFA were mostly used as rescue treatment modalities (45.9%

Table 1 Baseline characteristics of enrolled patients

	Total (*n* = 661)	Patients without extrahepatic metastasis (*n* = 617)	Patients with extrahepatic metastasis (*n* = 44)	*P* value
Age (yr)	66.9 ± 10.20	66.8 ± 10.2	68.4 ± 9.98	0.301
Male, *n* (%)	497 (75.2)	469 (76.0)	28 (63.6)	0.066
Etiology of liver cirrhosis, *n* (%)				0.084
Alcohol	137 (20.7)	131 (21.2)	6 (13.6)	
HBV	351 (53.1)	322 (52.2)	29 (65.9)	
HCV	111 (16.8)	108 (17.5)	3 (6.8)	
Combined	40 (6.1)	38 (6.2)	2 (4.5)	
Others	22 (3.3)	18 (2.9)	4 (9.1)	
Platelet (× 10^3/μL)	127.8 ± 55.1	127 ± 54.7	141.2 ± 63.1	0.304
AST (IU/mL)	49.0 ± 45.6	48.6 ± 43.2	54.7 ± 72.1	0.40
ALT (IU/mL)	37.2 ± 46.8	36.7 ± 44.9	43.0 ± 69.2	0.392
ALP (U/L)	97.4 ± 38.6	96.7 ± 38.7	107.4 ± 35.2	0.076
Albumin (mg/dL)	4.3 ± 2.9	4.3 ± 3.0	3.9 ± 0.6	0.015
Total bilirubin (mg/dL)	0.93 ± 0.83	0.92 ± 0.84	1.04 ± 0.67	0.378
Serum AFP (IU/mL)	209.7 ± 1558.3	185.5 ± 1503.8	548.3 ± 2179.0	0.283
PIVKA-II (mAU/mL)	331.9 ± 2901.4	336.3 ± 2973.6	246.1 ± 542.6	0.907
BCLC stage, *n* (%)				0.034
0	257 (39.0)	248 (40.2)	9 (20.5)	
A	378 (57.1)	345 (55.8)	33 (75.0)	
B	26 (3.9)	24 (3.9)	2 (4.5)	
mUICC stage, *n* (%)				0.096
I	298 (45.0)	28 (46.0)	13 (29.5)	
II	316 (47.7)	288 (46.6)	28 (63.6)	
III	48 (7.3)	45 (7.3)	3 (6.8)	
Tumor size (cm)	2.42 ± 1.02	2.41 ± 1.02	2.62 ± 1.05	0.18
Ablation size/tumor size ratio	2.04 ± 0.97	2.07 ± 0.97	1.57 ± 0.74	0.001
Tumor number	1.19 ± 0.45	1.19 ± 0.46	1.16 ± 0.37	0.356
Encapsulated tumor, *n* (%)	157 (23.7)	146 (24.2)	11 (25.6)	0.840
Subcapsular tumor, *n* (%)	263 (39.7)	240 (39.4)	23 (53.5)	0.069
Follow-up duration, d (median, range)	1204 (183-5016)	1175 (183-5016)	1379 (187-4541)	0.270

Values are presented as mean ± SD. SD: Standard deviation; HBV: Hepatitis B virus; HCV: Hepatitis C virus; AST: Aspartate transaminase; ALT: Alanine transaminase; ALP: Alkaline phosphatase; AFP: Alpha-fetoprotein; PIVKA-II: Protein induced by vitamin K absence or antagonist-II; BCLC: Barcelona Clinic Liver Cancer; mUICC: Modified Union for International Cancer Control.

and 36.9%, respectively) for recurrent HCC (Table 2).

Clinical features of patients with extrahepatic metastasis

Forty-four patients with EHM were assessed for clinical features related to metastasis (Table 3). The location of metastasis was distributed evenly in the lymph nodes, bone, lung, and peritoneum. In 68.2% of patients, abdominal CT was used for the diagnosis of EHM (12 patients with lymph node, 11 patients with peritoneum, 6 patients with lung, and 5 patients with bone metastasis including 3 patients with multiple EHM), and 3 (6.8%) patients were diagnosed *via* chest X-rays during routine follow-up

Table 2 Characteristics of patients with first recurrence following radiofrequency ablation (*n* = 333)

	Patients without extrahepatic metastasis (*n* = 289)	Patients with extrahepatic metastasis (*n* = 44)	*P* value
AFP level			
Initial (median, range)	8.13 (0.70-30000.0)	21.750 (0.836-13148.0)	0.291
1st recurrence (median, range)	7.08 (0.93-50000.0)	28.15 (0.73-70000.0)	0.274
CTP score, *n* (%)			0.044
A	277 (95.8)	39 (88.6)	
B	12 (4.2)	5 (11.4)	
Recurrence free survival, d (median, range)	821 (49-3944)	389 (79-2041)	< 0.001
First recurred site, *n* (%)			< 0.001
RFA site	53 (18.3)	7 (15.3)	
Same hepatic lobe	145 (50.2)	20 (45.5)	
Different hepatic lobe	60 (20.8)	8 (18.2)	
Both hepatic lobe	31 (10.7)	1 (3.1)	
Extrahepatic area	0 (0.0)	8 (18.2)	
Peritoneum		5	
Lymph nodes		3	
mUICC stage at 1st recurrence, *n* (%)			< 0.001
I	140 (48.4)	17 (38.6)	
II	101 (34.9)	13 (29.5)	
III	38 (13.1)	4 (9.1)	
IVa	5 (1.7)	2 (4.5)	
IVb	0 (0.0)	8 (18.2)	
Rescue Treatment modalities, *n* (%)			0.003
TACE	138 (47.7)	15 (34.1)	
RFA	110 (38.2)	13 (29.5)	
Sorafenib	1 (0.3)	-	
Surgery	8 (2.8)	3 (6.8)	
Radiotherapy	1 (0.3)	3 (6.8)	
Liver transplantation	1 (0.3)	-	
TACE	11 (3.8)	3 (6.8)	
RFA PEIT	1 (0.3)	-	
None	9 (3.1)	5 (11.4)	
Follow-up loss	9 (3.1)	2 (4.5)	

RFA: Radiofrequency ablation; AFP: Alpha-fetoprotein; CTP: Current procedural terminology; mUICC: Modified Union for International Cancer Control; TACE: Transarterial chemoembolization; PEIT: Percutaneous ethanol injection therapy.

examinations. Three patients (6.8%) were diagnosed *via* abdominal MRI: 1 patient during HCC surveillance and 2 patients while evaluating elevated tumor marker levels without definite HCC recurrence on abdominal CT. Spine MRI was used for the diagnosis of spinal metastasis among 3 patients who presented with new-onset back pain. Five patients (11.4%) underwent PET-CT for re-staging of HCC without signs of intrahepatic recurrence, and EHM was detected in the lung, lymph nodes, and bone.

Table 3 Clinical features of patients with extrahepatic metastasis (*n* = 44), *n* (%)

Clinical features	Value
Location of metastasis[1]	
Lymph nodes	16 (36.3)
Bone	12 (27.3)
Lung	13 (29.5)
Solitary/multiple	4 (30.7)/9 (69.2)
Unilateral/Bilateral	4 (30.7)/9 (69.2)
Lower lobe/non-lower lobe/all lobes	2 (15.4)/9 (69.2)/2 (15.4)
Peritoneum	12 (27.3)
Diagnostic modality	
Abdomen enhanced CT	30 (68.2)
Abdomen enhanced MRI	3 (6.8)
Spine MRI	3 (6.8)
PET-CT	5 (11.4)
Chest X-ray	3 (6.8)
Chest enhanced CT	3 (6.8%)
Tumor marker increment (AFP, PIVKA)	
Both	14 (36.8)
Either	17 (44.7)
AFP/PIVKA	15 (39.5)/2 (5.3)
None	7 (18.4)
N/A	6
Patients diagnosed of EHM with either of abdomen enhanced CT or serum AFP elevation (> 15 IU/mL)	38 (86.4)
Time to extrahepatic metastasis (years, median, range)	2.68 (0.38-10.6)
Intra-hepatic HCC status at diagnosis of EHM (mUICC T stage)	
T0/T1/T2	19 (43.2)/5 (11.4)/7 (15.9)
T3/T4a	2 (4.5)/11 (25.0)

[1]Nine patients had multiple EHM occurrences (3 patients: lymph node and bone, 3 patients: Lymph node and lung, 1 patient: bone and lung, and 1 patient: Bone and peritoneum). CT: Computed tomography; MRI: Magnetic resonance imaging; PET: Positron emission tomography; AFP: Alpha-fetoprotein; PIVKA-II: Protein induced by vitamin K absence or antagonist-II; N/A: Not applicable; EHM: Extrahepatic metastasis; HCC: Hepatocellular carcinoma; mUICC: Modified Union for International Cancer Control.

In detail, 9 patients (20.5%) had multiple sites of EHM at first diagnosis. Among 13 patients with pulmonary metastasis, 7 (53.8%) were diagnosed *via* abdominal CT, 3 (23.1%) *via* chest X-ray, and 3 (23.1%) *via* chest CT.

Thirty-one patients (31/38, 81.5%) had increased tumor marker levels at the time of diagnosis of EHM. A diagnosis of EHM was made in most patients (86.4%) based on either contrast-enhanced CT findings or elevated serum AFP levels. Intrahepatic tumor status categorized according to the mUICC T stage at the time of EHM diagnosis was assessed; 43.2% of patients had no findings of intrahepatic HCC remnant tumor (T0), and 25.0% of patients had stage T4a disease.

Factors associated with extrahepatic metastasis

Multiple factors that might be relevant to EHM were assessed (Table 4). In the univariate analysis, more advanced stage, the presence of intrahepatic recurrence, serum alkaline phosphatase level > 97 U/L, first RFS within less than 2 years, ablation zone/tumor size > 2, and AFP level > 400 IU/mL at first HCC recurrence were

Table 4 Univariate and multivariate analysis of factors associated with extrahepatic metastasis

	Univariate analysis		Multivariate analysis	
	OR (95%CI)	*P* value	OR (95%CI)	*P* value
BCLC stage (0 *vs* A, B)	2.93 (1.38–6.20)	0.003		
mUICC stage (I *vs* II, III)	2.04 (1.04–3.96)	0.034		
Post-RFA complication (fever, abscess)	2.78 (1.31–5.92)	0.050		
Presence of intra-hepatic recurrence	48.8 (6.68–356.63)	0.000		
ALP > 97 U/L	2.29 (1.23-4.26)	0.008		
1st recurrence free survival < 2 yr	2.88 (1.54-5.38)	0.001	2.44 (1.16-5.14)	0.019
Ratio of ablation zone and tumor size < 2	3.84 (1.76-8.39)	0.001	3.33 (1.34-8.27)	0.010
Presence of tumoral thrombosis	2.57 (1.13-5.84)	0.024		
AFP > 400 IU/mL at 1st recurrence	4.52 (2.03-10.07)	0.000	3.35 (1.33-8.43)	0.010
mUICC stage > 2 at 1st recurrence	2.49 (1.22-5.06)	0.012		

OR: Odds ratio; CI: Confidence interval; BCLC: Barcelona Clinic Liver Cancer; mUICC: Modified Union for International Cancer Control; RFA: Radiofrequency ablation; ALP: Alkaline phosphatase; AFP: Alpha-fetoprotein.

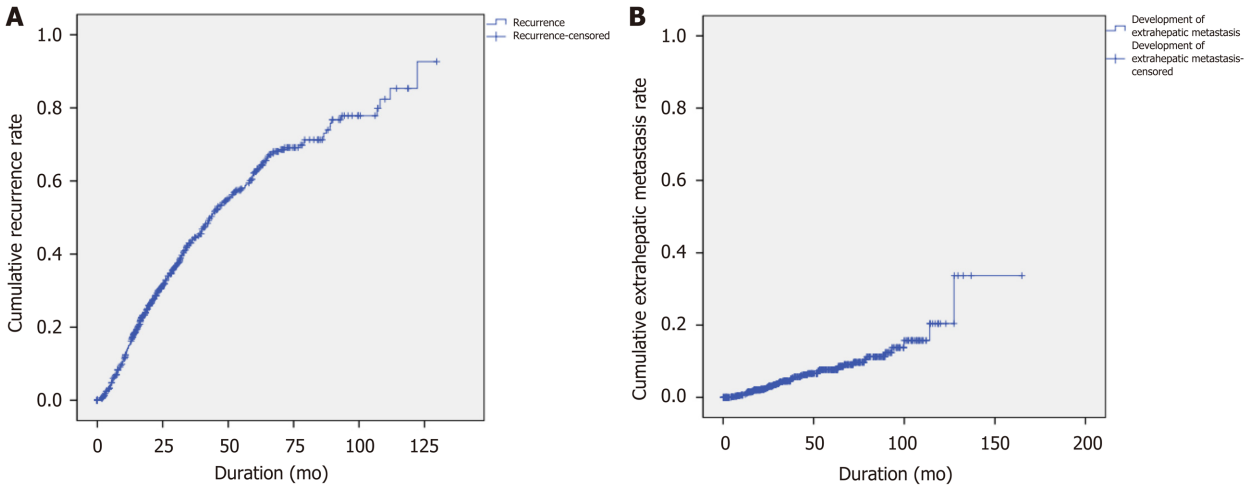

Figure 2 Recurrence curves of 661 patients with hepatocellular carcinoma treated with radiofrequency ablation. A: Cumulative rates of recurrence. The 1-, 3-, 5-, 8-, and 10-year cumulative rates of recurrence were 15.1%, 43.8%, 62.5%, 77.9%, and 92.7%, respectively; B: Cumulative rates of extrahepatic metastasis. The 1-, 3-, 5-, 8-, and 10-year cumulative rates of extrahepatic metastasis were 1.0%, 2.9%, 8.1%, 15.7%, and 33.7%, respectively.

associated with a high risk of EHM. Among these factors, a first HCC RFS < 2 years [odds ratio (OR), 2.44; $P = 0.019$], ablation zone/tumor size < 2 (OR, 3.33; $P = 0.01$), and AFP > 400 IU/mL at first recurrence (OR, 3.35; $P = 0.01$) were identified as significant factors in the multivariate analysis. We stratified the patients who had recurrence after RFA by numbers of risk factors related to EHM occurrence, and in proportion to the numbers of risk factors, the cumulative occurrence of EHM showed an increase (Figure 4).

DISCUSSION

Although RFA is one of the most effective curative treatment modalities for HCC along with surgical resection and liver transplantation, our study and previous studies showed that there is a substantial possibility of EHM even if intrahepatic lesions are stable[8,16,17]. Most other studies showed that the most common initial site of recurrence is intrahepatic and that most cases of EHM occur after multiple intrahepatic recurrences with several treatments[8]. This study focused on the characteristics and

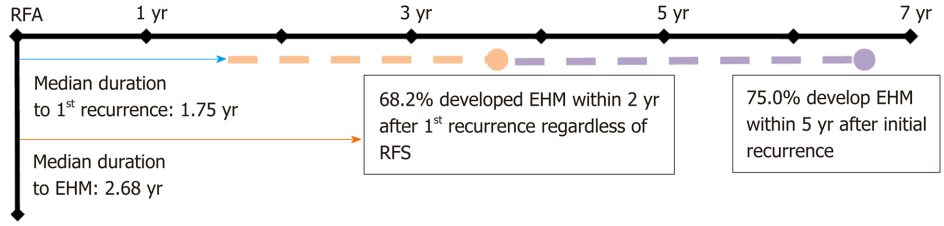

Figure 3 Timelines of recurrence of extrahepatic metastasis after radiofrequency ablation for hepatocellular carcinoma. RFA: Radiofrequency ablation; EHM: Extrahepatic metastasis; RFS: Recurrence-free survival.

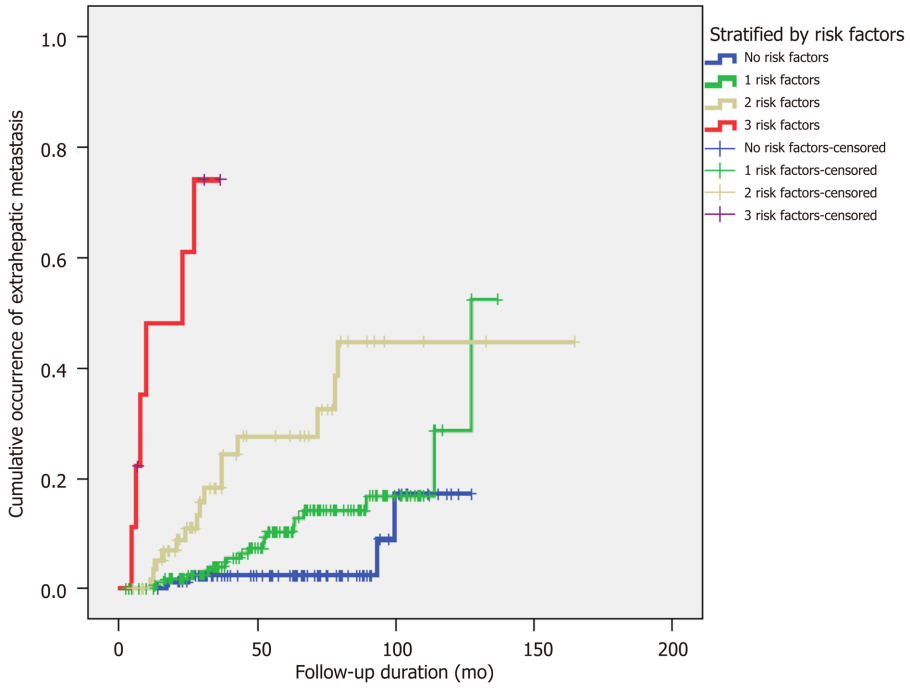

Figure 4 Cumulative occurrence of extrahepatic metastasis in patients with recurrence of hepatocellular carcinoma after radiofrequency ablation: Stratified by numbers of risk factors.

risk factors of extrahepatic recurrence after RFA and whether regular surveillance for EHM is needed. The results are of particular interest because data on the pattern of EHM in HCC after RFA and the role of regular surveillance for EHM are limited, and there have been no reports regarding surveillance methods for EHM in HCC.

In the present study, 289 patients experienced tumor recurrence without EHM, and 44 experienced EHM during a median follow-up period of 1204 d. The 1-, 3-, 5-, 8-, and 10-year cumulative rates of HCC recurrence and EHM development were concordant with the results of previous studies[8,9], but only 1.2% of the enrolled patients presented with EHM as the first recurrence of HCC. The median time to the detection of EHM was 2.68 years, and 68.2% of patients developed EHM within 2 years after the first recurrence regardless of RFS. Furthermore, 75% of patients developed EHM within 5 years of the first recurrence (Figure 3).

Other studies that reported the locations of EHM showed predominance in the lung (39%-54%), lymph nodes (34%-40%), and bone (25%-39%)[3,11,18]. In the present study, the location of EHM was relatively evenly distributed among the intra-abdominal lymph nodes (36.3%), bone (25.0%), lung (29.5%), and peritoneum (27.3%). The proportions of extrahepatic metastatic sites in our study may have differed from those identified in previous studies as our population comprised post-RFA patients who had early-stage disease, while the other studies included patients with diverse stages of HCC ranging from early to terminal. The median duration of peritoneal seeding was 883 d (range: 138–3878); however, in 3 patients, the time from RFA to EHM was less than 1 year, suggesting the possibility that peritoneal dissemination occurred *via* RFA in some patients. There was no case of pulmonary metastasis as the first recurrence in

this study. Most pulmonary metastases occurred after intrahepatic recurrences.

The spread pattern of lung metastasis at the initial diagnosis of recurrent HCC is important because of the possible value of metastectomy, which was reported to yield favorable outcomes in some studies[19,20]. We found that at the time of HCC recurrence 69.2% of patients had multiple lung metastatic lesions, and 69.2% had bilateral lung metastasis for which metastectomy was not indicated. Thus, the option of metastectomy after RFA may be of limited value in the group we studied.

Regarding the detection method, EHM was diagnosed *via* abdominal imaging (CT/MRI) in most patients (75.0%). The backbone of surveillance after RFA for HCC is abdominal imaging, and only 14/661 patients (2.1%) required other diagnostic modalities such as PET-CT, spine MRI, chest CT, or chest X-ray. Considering the small proportion of diagnostic modalities other than abdominal imaging and the low incidence (1.2%) of EHM as the first recurrence of HCC, the need for regular surveillance tools other than abdominal imaging may not be very high. In particular, 38/44 patients (86.4%) with EHM had either positive abdominal CT scan results or serum AFP elevation, which we currently use as surveillance tools for HCC after RFA in clinical practice. Considering the high cost of spine MRI, PET-CT, and chest CT in general, the cost-effectiveness of routine surveillance using these modalities may be high however, an individualized approach in accordance with each country's reimbursement policy is needed.

A correlation between serum PIVKA-II levels and EHM was reported previously[21,22]. In our study, 31/38 patients (81.5%) had increasing tumor marker levels (serum AFP or protein induced by vitamin K absence-II [PIVKA-II]), and serum AFP levels were elevated in 29/38 (76.3%) which showed correlation with the development of EHM, as reported in other studies[23]. Although the PIVKA-II level was only assessed in 24 patients, 16 (66.7%) showed elevated serum levels at EHM development. Regarding the pattern of HCC recurrence, the most common initial site of recurrence was intrahepatic. Although the rate of extrahepatic initial recurrences in our population was only 1.2%, 43.2% of the patients had no sign of intrahepatic HCC at the time of diagnosis of EHM. This implies that even if loco-regionally managed HCC lesions are stable, close surveillance for possible EHM is warranted. In particular, when tumor marker levels increase without definite aggravation of previous HCC lesions, additional examination for EHM development should be considered. Refaat *et al*[17] reported that among 65 patients who underwent loco-regional therapy for HCC and had elevated serum AFP levels, 10 (15.4%) had EHM without intrahepatic tumor recurrence. In addition, Chen *et al*[16] reported that among 26 patients who had elevated serum AFP levels without findings of recurrence on conventional imaging studies, 8 (30.8%) experienced EHM.

Recurrence of HCC after curative treatment is reported to occur mostly within 2 years[24]; therefore, guidelines suggest surveillance for HCC recurrence within a short interval of 2-6 mo until the second year after treatment[25-27]. In the present study, the 1-, 3-, 5-, 8-, and 10-year cumulative rates of HCC recurrence were 15.1%, 43.8%, 62.5%, 77.9%, and 92.7% respectively, and those of EHM development were 1.0%, 2.9%, 8.1%, 15.7%, and 33.7%, respectively. Our results also showed a 1.75-year median time to first recurrence after RFA, a median time to the development of EHM of 2.68 years regardless of RFS, and 75.0% of patients experiencing EHM within 5 years after RFA. Thus, we suggest that it is prudent to pay attention to possible EHM occurrence for at least 5 years after RFA, and patients who experience tumor recurrence may require close observation for the development of EHM, particularly within 2 years after the first recurrence (Figure 3).

In the multivariate analysis of potential risk factors for EHM, first RFS < 2 years, ablation zone/tumor size < 2, and serum AFP level > 400 IU/mL at first recurrence were factors relevant to EHM development. Some studies have suggested that early recurrence is associated with vascular invasion, initial tumor staging, and poor prognosis, and our findings are consistent with these reports[28,29]. Other studies have assessed the risk of local tumor progression in relation to insufficiently ablated margins after RFA in liver malignancies, a minimal margin of < 2-5 mm being reported as an independent factor for local tumor progression[30-32]. Our study showed that ablation zone/tumor size was associated with the risk of EHM development. Most patients (97.9%) had minimal margins of > 5 mm, and the margin length between the tumor and ablation zones showed no relevance in the occurrence of EHM. Some studies have reported that higher AFP levels are associated with increased recurrence following liver transplantation for HCC, as well as worse disease-free survival and overall survival[33,34]. By stratifying patients according to the number of risk factors associated with EHM, the cumulative occurrence of EHM showed an increasing trend related to the number (≥ 2) of risk factors (Figure 4). Therefore, we suggest close

surveillance for EHM after RFA, especially in these high-risk patients.

Our study had some limitations. First, this was a retrospective study based on medical records. Thus, there was no uniform post-treatment or surveillance schedule, and the surveillance modality used for each patient was at the physician's discretion. Second, until the development of EHM, patients underwent different treatment modalities for local HCC recurrence depending on the tumor and patient's status. There may be diverse statuses regarding tumor stage, liver reserve function, and patients' physical performance status. However, we tried to overcome these limitations by using a considerable number of patients with a long-term follow-up duration in multiple tertiary centers.

In conclusion, EHM as the first recurrence after RFA was rare, but cumulative EHM occurred frequently following multiple intrahepatic recurrences. Thus, optimal surveillance for EHM after RFA for HCC is essential according to stratified risk factors (RFS < 2 years, ablation zone/tumor size < 2, and AFP level > 400 IU/mL) related to EHM, and combined contrast-enhanced abdominal CT and serum AFP level have been found useful for this purpose.

ARTICLE HIGHLIGHTS

Research background

Extrahepatic metastasis (EHM) of hepatocellular carcinoma (HCC) is related to dismal prognosis.

Research motivation

The characteristics and risk factors of EHM of HCC after radiofrequency ablation are not elucidated.

Research objectives

To investigate the clinical features and risk factors of EHM after radiofrequency ablation for HCC.

Research methods

Patients who underwent radiofrequency ablation for HCC were identified from the two tertiary hospitals in South Korea from 2008 to 2017. Univariate analyses were performed using the chi-squared test or Student's *t*-test, and univariate and multivariate analyses were performed *via* logistic regression, as appropriate.

Research results

During a median follow-up period of 1,204 days, EHM was diagnosed in 44 patients (6.7%). The 10-year cumulative rate of HCC recurrence and EHM was 92.7% and 33.7%, respectively. The median time to the diagnosis of EHM was 2.68 years, and 68.2% of patients developed EHM within 2 years of the first recurrence, regardless of recurrence-free survival. EHM was mostly diagnosed *via* abdominal CT/MRI in 33 (75.0%) and 38 of 44 patients (86.4%) with EHM had either positive abdominal CT scan results or serum alpha-fetoprotein (AFP) level elevation. In multivariate analysis, recurrence-free survival < 2 years, ablation zone/tumor size < 2, and alpha-fetoprotein level > 400 IU/mL were associated with a high EHM risk.

Research conclusions

EHM occurs following multiple intrahepatic recurrences after radiofrequency ablation and combined contrast-enhanced abdominal CT and serum AFP were useful for surveillance.

Research perspectives

Patients especially with high-risk factors such as recurrence-free survival < 2 years, ablation zone/tumor size < 2, and alpha-fetoprotein level > 400 IU/mL, require close follow-up for EHM.

REFERENCES

1 **Bray F**, Ferlay J, Soerjomataram I, Siegel RL, Torre LA, Jemal A. Global cancer statistics 2018:

GLOBOCAN estimates of incidence and mortality worldwide for 36 cancers in 185 countries. *CA Cancer J Clin* 2018; **68**: 394-424 [PMID: 30207593 DOI: 10.3322/caac.21492]
2 **Korean Liver Cancer Association (KLCA)**; National Cancer Center (NCC), Goyang, Korea. 2018 Korean Liver Cancer Association-National Cancer Center Korea Practice Guidelines for the Management of Hepatocellular Carcinoma. *Korean J Radiol* 2019; **20**: 1042-1113 [PMID: 31270974 DOI: 10.3348/kjr.2019.0140]
3 **Natsuizaka M**, Omura T, Akaike T, Kuwata Y, Yamazaki K, Sato T, Karino Y, Toyota J, Suga T, Asaka M. Clinical features of hepatocellular carcinoma with extrahepatic metastases. *J Gastroenterol Hepatol* 2005; **20**: 1781-1787 [PMID: 16246200 DOI: 10.1111/j.1440-1746.2005.03919.x]
4 **Lee JI**, Kim JK, Kim DY, Ahn SH, Park JY, Kim SU, Kim BK, Han KH, Lee KS. Prognosis of hepatocellular carcinoma patients with extrahepatic metastasis and the controllability of intrahepatic lesions. *Clin Exp Metastasis* 2014; **31**: 475-482 [PMID: 24496959 DOI: 10.1007/s10585-014-9641-x]
5 **Lam CM**, Lo CM, Yuen WK, Liu CL, Fan ST. Prolonged survival in selected patients following surgical resection for pulmonary metastasis from hepatocellular carcinoma. *Br J Surg* 1998; **85**: 1198-1200 [PMID: 9752858 DOI: 10.1046/j.1365-2168.1998.00846.x]
6 **European Association for the Study of the Liver**. EASL Clinical Practice Guidelines: Management of hepatocellular carcinoma. *J Hepatol* 2018; **69**: 182-236 [PMID: 29628281 DOI: 10.1016/j.jhep.2018.03.019]
7 **Marrero JA**, Kulik LM, Sirlin CB, Zhu AX, Finn RS, Abecassis MM, Roberts LR, Heimbach JK. Diagnosis, Staging, and Management of Hepatocellular Carcinoma: 2018 Practice Guidance by the American Association for the Study of Liver Diseases. *Hepatology* 2018; **68**: 723-750 [PMID: 29624699 DOI: 10.1002/hep.29913]
8 **Kim YS**, Lim HK, Rhim H, Lee MW, Choi D, Lee WJ, Paik SW, Koh KC, Lee JH, Choi MS, Gwak GY, Yoo BC. Ten-year outcomes of percutaneous radiofrequency ablation as first-line therapy of early hepatocellular carcinoma: analysis of prognostic factors. *J Hepatol* 2013; **58**: 89-97 [PMID: 23023009 DOI: 10.1016/j.jhep.2012.09.020]
9 **Shiina S**, Tateishi R, Arano T, Uchino K, Enooku K, Nakagawa H, Asaoka Y, Sato T, Masuzaki R, Kondo Y, Goto T, Yoshida H, Omata M, Koike K. Radiofrequency ablation for hepatocellular carcinoma: 10-year outcome and prognostic factors. *Am J Gastroenterol* 2012; **107**: 569-77; quiz 578 [PMID: 22158026 DOI: 10.1038/ajg.2011.425]
10 **Hyder O**, Dodson RM, Weiss M, Cosgrove DP, Herman JM, Geschwind JH, Kamel IR, Pawlik TM. Trends and patterns of utilization in post-treatment surveillance imaging among patients treated for hepatocellular carcinoma. *J Gastrointest Surg* 2013; **17**: 1774-1783 [PMID: 23943387 DOI: 10.1007/s11605-013-2302-6]
11 **Uchino K**, Tateishi R, Shiina S, Kanda M, Masuzaki R, Kondo Y, Goto T, Omata M, Yoshida H, Koike K. Hepatocellular carcinoma with extrahepatic metastasis: clinical features and prognostic factors. *Cancer* 2011; **117**: 4475-4483 [PMID: 21437884 DOI: 10.1002/cncr.25960]
12 **Llovet JM**, Di Bisceglie AM, Bruix J, Kramer BS, Lencioni R, Zhu AX, Sherman M, Schwartz M, Lotze M, Talwalkar J, Gores GJ; Panel of Experts in HCC-Design Clinical Trials. Design and endpoints of clinical trials in hepatocellular carcinoma. *J Natl Cancer Inst* 2008; **100**: 698-711 [PMID: 18477802 DOI: 10.1093/jnci/djn134]
13 **Kudo M**, Kitano M, Sakurai T, Nishida N. General Rules for the Clinical and Pathological Study of Primary Liver Cancer, Nationwide Follow-Up Survey and Clinical Practice Guidelines: The Outstanding Achievements of the Liver Cancer Study Group of Japan. *Dig Dis* 2015; **33**: 765-770 [PMID: 26488173 DOI: 10.1159/000439101]
14 **Forner A**, Reig ME, de Lope CR, Bruix J. Current strategy for staging and treatment: the BCLC update and future prospects. *Semin Liver Dis* 2010; **30**: 61-74 [PMID: 20175034 DOI: 10.1055/s-0030-1247133]
15 **Hsu CY**, Liu PH, Lee YH, Hsia CY, Huang YH, Lin HC, Chiou YY, Lee FY, Huo TI. Using serum α-fetoprotein for prognostic prediction in patients with hepatocellular carcinoma: what is the most optimal cutoff? *PLoS One* 2015; **10**: e0118825 [PMID: 25738614 DOI: 10.1371/journal.pone.0118825]
16 **Chen YK**, Hsieh DS, Liao CS, Bai CH, Su CT, Shen YY, Hsieh JF, Liao AC, Kao CH. Utility of FDG-PET for investigating unexplained serum AFP elevation in patients with suspected hepatocellular carcinoma recurrence. *Anticancer Res* 2005; **25**: 4719-4725 [PMID: 16334166]
17 **Refaat R**, Basha MAA, Hassan MS, Hussein RS, El Sammak AA, El Sammak DAEA, Radwan MHS, Awad NM, Saad El-Din SA, Elkholy E, Ibrahim DRD, Saleh SA, Montasser IF, Said H. Efficacy of contrast-enhanced FDG PET/CT in patients awaiting liver transplantation with rising alpha-fetoprotein after bridge therapy of hepatocellular carcinoma. *Eur Radiol* 2018; **28**: 5356-5367 [PMID: 29948070 DOI: 10.1007/s00330-018-5425-z]
18 **Uka K**, Aikata H, Takaki S, Shirakawa H, Jeong SC, Yamashina K, Hiramatsu A, Kodama H, Takahashi S, Chayama K. Clinical features and prognosis of patients with extrahepatic metastases from hepatocellular carcinoma. *World J Gastroenterol* 2007; **13**: 414-420 [PMID: 17230611 DOI: 10.3748/wjg.v13.i3.414]
19 **Kuo TM**, Chang KM, Cheng TI, Kao KJ. Clinical Factors Predicting Better Survival Outcome for Pulmonary Metastasectomy of Hepatocellular Carcinoma. *Liver Cancer* 2017; **6**: 297-306 [PMID: 29234633 DOI: 10.1159/000477134]
20 **Mizuguchi S**, Nishiyama N, Izumi N, Tsukioka T, Komatsu H, Iwata T, Tanaka S, Takemura S, Kubo S. Clinical Significance of Multiple Pulmonary Metastasectomy for Hepatocellular Carcinoma. *World J Surg* 2016; **40**: 380-387 [PMID: 26306890 DOI: 10.1007/s00268-015-3213-3]
21 **Bae HM**, Lee JH, Yoon JH, Kim YJ, Heo DS, Lee HS. Protein induced by vitamin K absence or antagonist-II production is a strong predictive marker for extrahepatic metastases in early hepatocellular carcinoma: a prospective evaluation. *BMC Cancer* 2011; **11**: 435 [PMID: 21985636 DOI: 10.1186/1471-2407-11-435]
22 **Orita K**, Sakamoto A, Okamoto T, Matsuda S. Solitary Muscle Metastasis of Hepatocellular Carcinoma to the Biceps Femoris Muscle with Only Elevated Serum PIVKA-II: A Case Report. *Am J Case Rep* 2019; **20**: 306-309 [PMID: 30846677 DOI: 10.12659/AJCR.913730]
23 **Yokoo T**, Patel AD, Lev-Cohain N, Singal AG, Yopp AC, Pedrosa I. Extrahepatic metastasis risk of hepatocellular carcinoma based on α-fetoprotein and tumor staging parameters at cross-sectional imaging. *Cancer Manag Res* 2017; **9**: 503-511 [PMID: 29081671 DOI: 10.2147/CMAR.S147097]
24 **Poon RT**. Differentiating early and late recurrences after resection of HCC in cirrhotic patients: implications

on surveillance, prevention, and treatment strategies. *Ann Surg Oncol* 2009; **16**: 792-794 [PMID: 19190964 DOI: 10.1245/s10434-009-0330-y]

25 **He XX**, Li Y, Ren HP, Tian DA, Lin JS. [2010 guideline for the management of hepatocellular carcinoma recommended by the American Association for the Study of Liver Diseases]. *Zhonghua Gan Zang Bing Za Zhi* 2011; **19**: 249-250 [PMID: 21805732]

26 **European Association for the Study of the Liver**; European Organisation For Research And Treatment Of Cancer. EASL-EORTC clinical practice guidelines: management of hepatocellular carcinoma. *J Hepatol* 2012; **56**: 908-943 [PMID: 22424438 DOI: 10.1016/j.jhep.2011.12.001]

27 **Liu D**, Chan AC, Fong DY, Lo CM, Khong PL. Evidence-Based Surveillance Imaging Schedule After Liver Transplantation for Hepatocellular Carcinoma Recurrence. *Transplantation* 2017; **101**: 107-111 [PMID: 28009758 DOI: 10.1097/TP.0000000000001513]

28 **Yamamoto Y**, Ikoma H, Morimura R, Konishi H, Murayama Y, Komatsu S, Shiozaki A, Kuriu Y, Kubota T, Nakanishi M, Ichikawa D, Fujiwara H, Okamoto K, Sakakura C, Ochiai T, Otsuji E. Optimal duration of the early and late recurrence of hepatocellular carcinoma after hepatectomy. *World J Gastroenterol* 2015; **21**: 1207-1215 [PMID: 25632194 DOI: 10.3748/wjg.v21.i4.1207]

29 **Shimada M**, Takenaka K, Gion T, Fujiwara Y, Kajiyama K, Maeda T, Shirabe K, Nishizaki T, Yanaga K, Sugimachi K. Prognosis of recurrent hepatocellular carcinoma: a 10-year surgical experience in Japan. *Gastroenterology* 1996; **111**: 720-726 [PMID: 8780578 DOI: 10.1053/gast.1996.v111.pm8780578]

30 **Jiang C**, Liu B, Chen S, Peng Z, Xie X, Kuang M. Safety margin after radiofrequency ablation of hepatocellular carcinoma: precise assessment with a three-dimensional reconstruction technique using CT imaging. *Int J Hyperthermia* 2018; **34**: 1135-1141 [PMID: 29392978 DOI: 10.1080/02656736.2017.1411981]

31 **Kim YS**, Lee WJ, Rhim H, Lim HK, Choi D, Lee JY. The minimal ablative margin of radiofrequency ablation of hepatocellular carcinoma (> 2 and < 5 cm) needed to prevent local tumor progression: 3D quantitative assessment using CT image fusion. *AJR Am J Roentgenol* 2010; **195**: 758-765 [PMID: 20729457 DOI: 10.2214/AJR.09.2954]

32 **Wang X**, Sofocleous CT, Erinjeri JP, Petre EN, Gonen M, Do KG, Brown KT, Covey AM, Brody LA, Alago W, Thornton RH, Kemeny NE, Solomon SB. Margin size is an independent predictor of local tumor progression after ablation of colon cancer liver metastases. *Cardiovasc Intervent Radiol* 2013; **36**: 166-175 [PMID: 22535243 DOI: 10.1007/s00270-012-0377-1]

33 **Mahmud N**, John B, Taddei TH, Goldberg DS. Pre-transplant alpha-fetoprotein is associated with post-transplant hepatocellular carcinoma recurrence mortality. *Clin Transplant* 2019; **33**: e13634 [PMID: 31177570 DOI: 10.1111/ctr.13634]

34 **Hakeem AR**, Young RS, Marangoni G, Lodge JP, Prasad KR. Systematic review: the prognostic role of alpha-fetoprotein following liver transplantation for hepatocellular carcinoma. *Aliment Pharmacol Ther* 2012; **35**: 987-999 [PMID: 22429190 DOI: 10.1111/j.1365-2036.2012.05060.x]

World Journal of Gastroenterology

Submit a Manuscript: https://www.f6publishing.com

World J Gastroenterol 2020 August 28; 26(32): 4846-4856

DOI: 10.3748/wjg.v26.i32.4846

ISSN 1007-9327 (print) ISSN 2219-2840 (online)

ORIGINAL ARTICLE

Retrospective Study

Current status of *Helicobacter pylori* eradication and risk factors for eradication failure

Tian-Lian Yan, Jian-Guo Gao, Jing-Hua Wang, Dan Chen, Chao Lu, Cheng-Fu Xu

ORCID number: Tian-Lian Yan 0000-0003-2322-5029; Jian-Guo Gao 0000-0002-9414-5395; Jing-Hua Wang 0000-0003-2198-2659; Dan Chen 0000-0001-7910-9161; Chao Lu 0000-0002-1265-0903; Cheng-Fu Xu 0000-0002-6172-1253.

Author contributions: Yan TL and Gao JG contributed equally to this work; Xu CF, Yan TL, and Lu C designed the research; Yan TL, Gao JG, and Chen D performed the research; Wang JH analyzed the data; Yan TL and Xu CF drafted and revised the manuscript. All authors approved the final draft of this manuscript for submission.

Supported by the National Natural Science Foundation of China, No. 81600447.

Institutional review board statement: This study was reviewed and approved by the Clinical Research Ethics Committee of the First Affiliated Hospital, Zhejiang University School of Medicine.

Informed consent statement: Because of the retrospective and anonymous nature of this study, the need for informed consent was exempted by the institutional review board.

Conflict-of-interest statement: All

Tian-Lian Yan, Jian-Guo Gao, Jing-Hua Wang, Dan Chen, Chao Lu, Cheng-Fu Xu, Department of Gastroenterology, The First Affiliated Hospital, Zhejiang University School of Medicine, Hangzhou 310003, Zhejiang Province, China

Corresponding author: Cheng-Fu Xu, MD, Doctor, Department of Gastroenterology, The First Affiliated Hospital, Zhejiang University School of Medicine, No. 79 Qingchun Road, Hangzhou 310003, Zhejiang Province, China. xiaofu@zju.edu.cn

Abstract

BACKGROUND

The *Helicobacter pylori* (*H. pylori*) eradication rate is decreasing in the general population of China.

AIM

To evaluate the *H. pylori* eradication status in real-world clinical practice and to explore factors related to eradication failure.

METHODS

Patients with *H. pylori* infection who were treated with standard 14-d quadruple therapy and received a test of cure at a provincial medical institution between June 2018 and May 2019 were enrolled. Demographic and clinical data were recorded. Eradication rates were calculated and compared between regimens and subgroups. Multivariate analysis was performed to identify predictors of eradication failure.

RESULTS

Of 2610 patients enrolled, eradication was successful in 1999 (76.6%) patients. Amoxicillin-containing quadruple regimens showed a higher eradication rate than other quadruple therapy regimens (83.0% *vs* 69.0%, $P < 0.001$). The quadruple therapy containing amoxicillin plus clarithromycin achieved the highest eradication rate (83.5%). Primary therapy had a higher eradication rate than rescue therapy (78.3% *vs* 66.5%, $P < 0.001$). In rescue therapy, the amoxicillin- and furazolidone-containing regimens achieved the highest eradication rate (80.8%). Esomeprazole-containing regimens showed a higher eradication rate than those containing other proton pump inhibitors (81.8% *vs* 74.9%, $P = 0.001$). Multivariate regression analysis found that older age, prior therapy, and use of omeprazole or pantoprazole were associated with an increased risk of eradication failure.

of the authors declare that they have no conflicts of interest to disclose.

Data sharing statement: No additional data are available.

Manuscript source: Unsolicited manuscript

Received: April 24, 2020
Peer-review started: April 24, 2020
First decision: June 13, 2020
Revised: July 18, 2020
Accepted: July 30, 2020
Article in press: July 30, 2020
Published online: August 28, 2020

P-Reviewer: Gavriilidis P, Sezgin O
S-Editor: Wang DM
L-Editor: Wang TQ
P-Editor: Zhang YL

CONCLUSION

The total eradication rate is 76.6%. Amoxicillin-containing regimens are superior to other regimens. Age, prior therapy, and use of omeprazole or pantoprazole are independent risk factors for eradication failure.

Key words: *Helicobacter pylori*; Eradication; Quadruple therapy; Proton pump inhibitor; Retrospective study

Core tip: The *Helicobacter pylori* eradication rate is decreasing worldwide, and there is a lack of recent data from China. The current study of 14-d quadruple regimens in Eastern China revealed an eradication rate of 76.6%. Amoxicillin-containing regimens had the highest eradication rate in primary therapy, and amoxicillin- and furazolidone-containing regimens showed superiority in rescue therapy. Age, prior therapy, and use of omeprazole or pantoprazole were independent risk factors for eradication failure. This study can improve the choice of antibiotics and proton pump inhibitors and indicates that in clinical practice, attention should be paid to elderly patients and rescue therapy.

Citation: Yan TL, Gao JG, Wang JH, Chen D, Lu C, Xu CF. Current status of *Helicobacter pylori* eradication and risk factors for eradication failure. *World J Gastroenterol* 2020; 26(32): 4846-4856
URL: https://www.wjgnet.com/1007-9327/full/v26/i32/4846.htm
DOI: https://dx.doi.org/10.3748/wjg.v26.i32.4846

INTRODUCTION

Helicobacter pylori (*H. pylori*) is a widespread bacterium that typically infects the human gastric mucosa. The infection may induce numerous gastrointestinal diseases, including gastritis, peptic ulcer, gastric carcinoma, and gastric lymphoma[1-3], and it is also associated with significant extragastric diseases, such as idiopathic thrombocytopenic purpura, idiopathic iron deficiency anemia, and vitamin B12 deficiency[4]. Epidemical studies reported that *H. pylori* affects 24%-50% of people in industrialized nations and up to 79% of those in less-developed countries. *H. pylori* infection is a worldwide threat to public health[5].

Currently, *H. pylori* infection is considered the most important (yet controllable) risk factor for intestinal gastric cancer, as it accounts for the vast majority of cases of gastric cancer, which generally develops from a normal gastric mucosa to superficial gastritis and pre-neoplastic lesions[6]. A large number of studies have confirmed that *H. pylori* screening and treatment strategies could prevent gastric cancer in a cost-effective way, especially before the appearance of pre-neoplastic lesions and in high-risk areas[7-9]. In recent decades, the urea breath test has been widely used to detect *H. pylori* infection not only in specialized hospitals but also in physical examination centers and community hospitals in China. This has led to large numbers of asymptomatic patients being referred to specialized clinics for treatment[10].

However, *H. pylori* eradication therapies are facing decreasing eradication rates, mainly owing to antimicrobial resistance, and are partially influenced by the efficacy of acid-suppressive drugs[11]. Recent guidelines recommend 14-d combination therapies with two types of antibiotics, a proton pump inhibitor (PPI) and bismuth[12,13]. Studies using susceptibility tests based on *H. pylori* strains cultured *in vitro* and prospective studies with relatively small sample sizes reported increasing resistance rates to clarithromycin, metronidazole, and levofloxacin, while resistance rates to amoxicillin, tetracycline, and furazolidone were low[14,15]. However, there is a scarcity of eradication data from large-sample size studies of real-world practice, which are important for formulating future guidelines and conducting clinical work in China. Moreover, it remains uncertain whether the acidic environment in the stomach during therapy, prior therapy, and demographic characteristics are related to eradication failure.

In this study, we reviewed the medical records of a large series of *H. pylori*-positive patients from the First Affiliated Hospital, Zhejiang University School of Medicine. We

evaluated the *H. pylori* eradication status in the local population of Eastern China in real clinical practice and explored factors related to therapy failure.

MATERIALS AND METHODS

Study design and research subjects

All of the patients diagnosed with *H. pylori* infection in the electronic medical records obtained from the First Affiliated Hospital, Zhejiang University School of Medicine (Hangzhou, China) between June 2018 and May 2019 were included. In addition, separate databases of laboratory test, endoscopy, and pathology results were searched. Anonymized information of each patient was linked to a unique identification number. Two clinicians checked the therapy regimens independently.

The inclusion criteria were the following: (1) The general and clinical information and the prescription records were complete and available; (2) The *H. pylori* infection status before treatment was directly determined by one or more of the standard detection methods (urea breath test, histologic staining, and/or bacterial culture); (3) Patients received quadruple therapy for *H. pylori* infection according to the standard antibiotic combinations and dosages of the "Fifth Chinese National Consensus Report on the management of *H. pylori* infection," which highlights bismuth-containing quadruple therapy (PPI, bismuth, and two antibiotics) as the main empirical therapy for *H. pylori* eradication[12]; (4) The treatment lasted 14 d; and (5) Test of cure: The *H. pylori* status was confirmed by urea breath test 4-8 wk after the end of treatment.

The exclusion criteria were the following: (1) Patients who were lost to follow-up or changed the therapy regimen; and (2) Therapies that included other drugs, such as probiotics and/or Chinese traditional medicines.

The study protocol was approved by the Clinical Research Ethics Committee of the First Affiliated Hospital, Zhejiang University School of Medicine.

Statistical analysis

Statistical analyses were performed using SPSS version 22.0 (IBM SPSS Statistics, IBM Corporation, Armonk, NY, USA). Categorical variables are displayed as frequencies and proportions (%). Continuous variables are presented as the mean and standard deviation (SD) unless otherwise stated. Continuous variables were compared by Student's *t*-test or one-way ANOVA. Categorical variables were compared using the χ^2 test. The Cochran-Armitage trend test was used to analyze *H. pylori* eradication rates in the different age groups. A stepwise logistic regression analysis was performed to examine the relationship between *H. pylori* eradication failure and risk factors (probability to enter = 0.05 and probability to remove = 0.10). Two-tailed *P* values < 0.05 were considered to indicate statistical significance.

RESULTS

Patient selection and clinical characteristics

A total of 2652 *H. pylori*-positive patients received 14-d quadruple therapy between June 2018 and May 2019 and took the urea breath test 4-8 wk later. We excluded 34 patients because the therapy regimens were changed due to drug intolerance. We also excluded another five patients who received amoxicillin plus metronidazole-based therapy and three patients who received levofloxacin plus metronidazole-based therapy owing to the small sample sizes. Finally, 2610 patients (1088 men and 1522 women) with a mean age of 44.53 ± 14.43 years were included in the analyses (Figure 1).

Of the 2610 patients, 373 (14.3%) had a prior history of *H. pylori* treatment, and 2237 (85.7%) did not (Table 1). One or more symptoms were observed in 1301 (49.8%) patients, including upper abdominal pain (15.6%), abdominal distension (24.6%), nausea (5.3%), acid regurgitation or heartburn (9.6%), bitter taste in the mouth (6.0%), belching (8.6%), increased stool frequency (5.5%), and others (5.8%). A total of 1390 (53.3%) patients underwent gastroscopy before or after therapy, 244 had at least one peptic ulcer, 416 had atrophy, intestinal metaplasia, or dysplasia, as determined by biopsy histology, and 17 were diagnosed with MALT lymphoma or gastric cancer (Table 1).

Table 1 Demographic and clinical characteristics of patients with *Helicobacter pylori* infection

Variable	Cases (*n*)	Percentage
Overall cases	2610	
Gender		
Male	1088	41.70%
Female	1522	58.30%
Age, range (yr)		
< 30	582	22.30%
30-40	576	22.10%
40-50	478	18.30%
50-60	528	20.20%
> 60	446	17.10%
Chief complaint		
Upper abdominal pain	406	15.60%
Abdominal distension	643	24.60%
Nausea	138	5.30%
Acid regurgitation or heartburn	250	9.60%
Bitter taste in mouth	157	6.00%
Belching	224	8.60%
Increased stool frequency	143	5.50%
Others	152	5.80%
No symptoms	1309	50.20%
Received gastroscopy	1390	53.30%
Endoscopic and pathological findings		
Peptic ulcer	244	9.30%
Pre-neoplastic lesions	416	15.90%
MALT lymphoma or gastric cancer	17	0.70%
Eradication attempts		
Primary	2237	85.70%
Rescue	373	14.30%

Helicobacter pylori eradication rates

Of the 2610 patients, eradication was successful in 1999 (76.6%) patients. The eradication rate of each antibiotic combination is illustrated in Figure 2. Amoxicillin-based therapy showed a significantly higher eradication rate than other regimens (83.0% *vs* 69.0%, $P < 0.001$). Therapy consisting of amoxicillin plus clarithromycin achieved the highest eradication rate (83.5%; 95%CI: 81.4%-85.5%), followed by therapy that consisted of amoxicillin plus furazolidone (79.4%; 95%CI: 69.4%-89.4%), amoxicillin plus levofloxacin (78.9%; 95%CI: 69.8%-88.1%), clarithromycin plus levofloxacin (72.1%; 95%CI: 69.3%-74.9%), levofloxacin plus furazolidone (63.2%; 95%CI: 41.5%-84.8%), clarithromycin plus metronidazole (54.7%; 95%CI: 46.7%-62.7%), and clarithromycin plus furazolidone (44.1%; 95%CI: 27.4%-60.8%). The eradication rate was not significantly different among the three different amoxicillin-based therapies (Figure 2).

We also found that the choice of PPI is a factor that influenced the eradication rate (Table 2). Therapy with esomeprazole achieved the highest eradication rate (81.8%; 95%CI: 78.2%-84.0%), followed by therapies with rabeprazole (78.6%; 95%CI: 75.8%-81.4%), lansoprazole (78.2%; 95%CI: 67.3%-89.1%), pantoprazole (74.0%; 95%CI: 70.5%-77.5%), and omeprazole (68.6%; 95%CI: 64.1%-73.1%). Eradication rates of therapies

Table 2 Eradication rates of specific *Helicobacter pylori* regimens classified by proton pump inhibitor

PPI	Successful eradication (*n*)	Total (*n*)	Eradication rate (%)	95%CI (%)
Esomeprazole	566	698	81.1	78.2-84.0
Non-esomeprazole PPIs	1433	1912	74.9	73.0-76.8
Rabeprazole	657	836	78.6	75.8-81.4
Lansoprazole	43	55	78.2	67.3-89.1
Pantoprazole	449	607	74.0	70.5-77.5
Omeprazole	284	414	68.6	64.1-73.1

The following PPI dosages were prescribed: Esomeprazole, 20 mg bid; rabeprazole, 20 mg bid; omeprazole, 20 mg bid; lansoprazole, 30 mg bid; pantoprazole, 40 mg bid. PPI: Proton pump inhibitor.

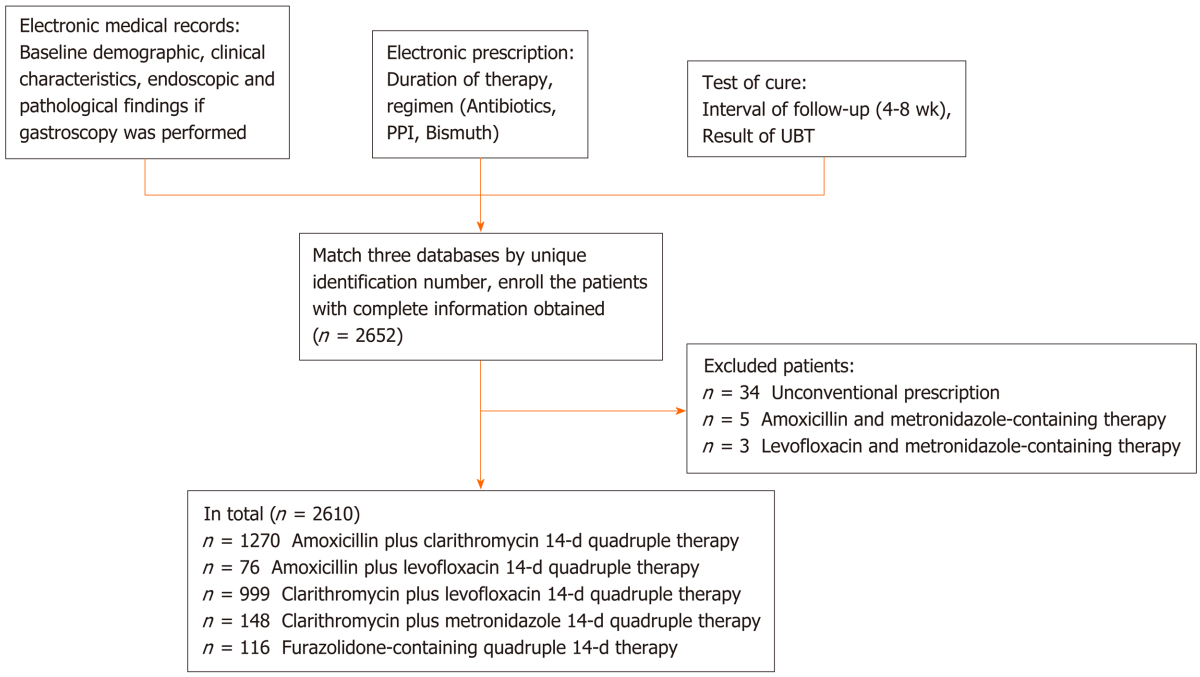

Figure 1 Study flowchart.

with omeprazole and pantoprazole were significantly lower than that of therapy with esomeprazole ($P < 0.005$). Eradication rates of therapies with rabeprazole and lansoprazole were lower than that of therapy with esomeprazole, but the difference was not statistically significant. Therapies with esomeprazole showed a significantly higher overall eradication rate than those with other PPIs (81.8% *vs* 74.9%, $\chi^2 = 10.755$, $P = 0.001$).

In addition, we found that the eradication rate showed a significant decreasing trend with increase in age (Figure 3). The eradication rates were 84.0%, 79.3%, 74.5%, 70.8%, and 72.4% in patients aged < 30, 30-39, 40-49, 50-59, and ≥ 60 years, respectively (P for trend < 0.001).

Subgroup analysis

The eradication rates for primary and rescue therapies were 78.3% (95%CI: 76.6%-80.0%) and 66.5% (95%CI: 61.7%-71.3%), respectively. Primary therapy showed a higher eradication rate than rescue therapy ($P < 0.001$). The amoxicillin-containing regimens showed superiority in primary therapy, and amoxicillin- and furazolidone-containing regimens achieved the highest eradication rate (80.8%; 95%CI: 70.1%-91.5%) in rescue therapy, followed by amoxicillin- and clarithromycin-containing regimens (77.1%; 95%CI: 69.1%-85.2%).

The regimens containing amoxicillin plus levofloxacin, clarithromycin plus

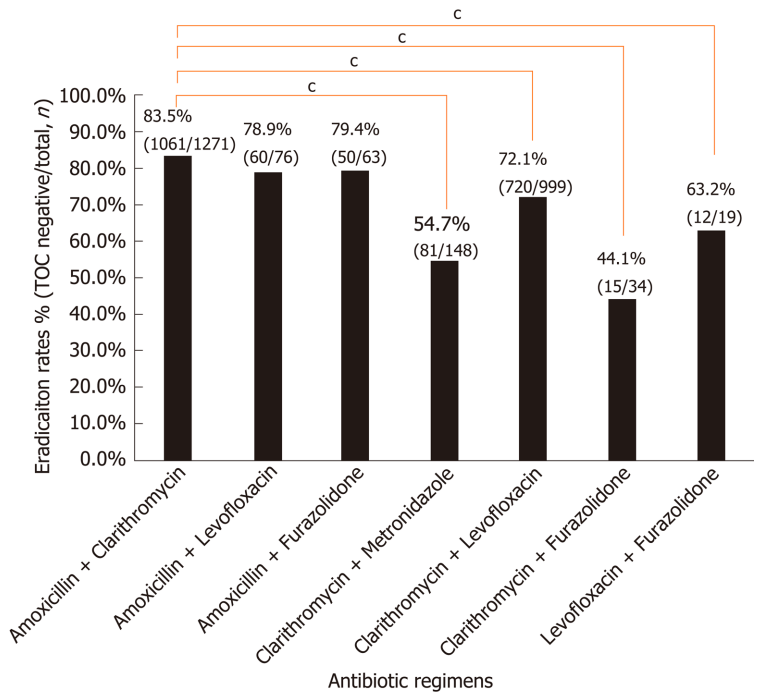

Figure 2 Eradication rates of Helicobacter pylori treatment regimens classified by antibiotic combination. °$P < 0.001$ compared with the regimen containing amoxicillin plus clarithromycin.

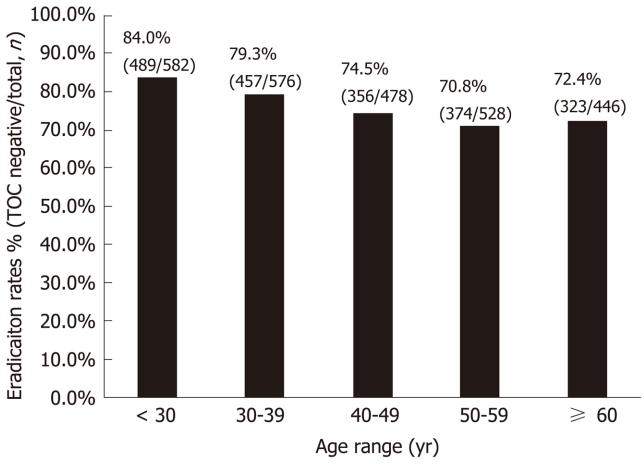

Figure 3 Eradication rates in specific patient age ranges.

levofloxacin, and clarithromycin plus metronidazole showed lower eradication rates in rescue therapy than in primary therapy ($P < 0.05$). The regimens containing amoxicillin plus clarithromycin, amoxicillin plus furazolidone, clarithromycin plus furazolidone, and levofloxacin plus furazolidone showed no significant difference in eradication rates between primary and rescue therapy (Table 3).

Risk factors for eradication failure

We performed stepwise logistic regression analyses to explore factors associated with eradication failure. The univariate analysis showed that age, prior therapy, antibiotic regimen, and choice of PPI were significantly associated with the risk of eradication failure, while gender and chief complaint were not. The multivariate logistic regression analysis confirmed that older age and prior therapy were significantly associated with an increased risk of eradication failure ($P < 0.001$). Setting the regimen containing amoxicillin plus clarithromycin as the reference group, regimens containing clarithromycin plus levofloxacin, clarithromycin plus metronidazole, and clarithromycin plus furazolidone all showed a higher odds of eradication failure ($P <$

Table 3 Subgroup comparison of eradication rates

	Antibiotic regimen	Successful eradication (*n*)	Total (*n*)	Eradication rate (%)	95%CI (%)
Primary	Total	1751	2237	78.3	76.6-80.0
	Amoxicillin plus clarithromycin	980	1166	84.0	81.9-86.1
	Amoxicillin plus levofloxacin	47	54	87.0	78.1-96.0
	Amoxicillin plus furazolidone	8	11	72.7	46.4-99.0
	Clarithromycin plus metronidazole	61	112	54.5	45.2-63.7
	Clarithromycin plus levofloxacin	647	871	74.3	71.4-77.2
	Clarithromycin plus furazolidone	7	20	35.0	14.1-55.9
	Levofloxacin plus furazolidone	1	3	33.3	0.0-86.7
Rescue	Total	248	373	66.5	61.7-71.3
	Amoxicillin plus clarithromycin	81	105	77.1	69.1-85.2
	Amoxicillin plus levofloxacin	13	22	59.1	38.5-79.6
	Amoxicillin plus furazolidone	42	52	80.8	70.1-91.5
	Clarithromycin plus metronidazole	20	36	55.6	39.3-71.8
	Clarithromycin plus levofloxacin	73	128	57.0	48.5-65.6
	Clarithromycin plus furazolidone	8	14	57.1	31.2-83.1
	Levofloxacin plus furazolidone	11	16	68.8	46.0-91.5

The following antibiotic dosages were prescribed: Amoxicillin, 1000 mg bid; clarithromycin, 500 mg bid; levoflaxacin, 500 mg qd or 200 mg bid; furazolidone, 100 mg bid; metronidazole, 200 mg bid, 400 mg bid, or 200 mg tid.

0.001). Other regimens were not significantly associated with eradication failure. Setting regimens containing esomeprazole as the reference group, the regimens containing omeprazole and pantoprazole showed a significantly higher risk of eradication failure ($P < 0.05$), whereas rabeprazole and lansoprazole were not significantly associated with eradication failure (Table 4).

DISCUSSION

In this large-sized retrospective study, we evaluated the efficiency of various standard 14-d quadruple regimens recommended for *H. pylori* treatment. We found that amoxicillin-based quadruple therapy was superior, and amoxicillin- and furazolidone-based therapy showed a high eradication rate in rescue therapy. Our multivariate analysis showed that older age, prior therapy, and application of omeprazole or pantoprazole increased the risk of eradication failure.

This study reports an unsatisfactory eradication rate of 76.6%, even though prescription was in strict accordance with guidelines. In a single-center retrospective study performed by another hospital in Eastern China, 992 patients received 10 to 14 d of quadruple therapy for *H. pylori* infection based on furazolidone and amoxicillin between January and December 2015. The eradication rate of rescue therapy was 91.3%[16]. However, in our study, the eradication rate of 14-d quadruple rescue therapy based on amoxicillin and furazolidone was only 80.8%. One possible reason for this discrepancy is that *H. pylori* resistance rates to antibiotics have increased during the past years. However, antibiotic resistance of *H. pylori* cultures was not investigated for all of the enrolled patients. Because of its cost and relatively low sensitivity, *H. pylori* culture is not recommended for routine diagnosis of *H. pylori* infection[17]. Another reason might be the lack of tetracycline-containing regimens and the low proportion of furazolidone-containing regimens, the resistance rates of which are relatively low in China[18]. Unfortunately, most hospitals in China are facing shortages of tetracycline, which yielded effective anti-*H. pylori* results in the USA[19]. Moreover, the potentially severe side effects of furazolidone limit its widespread application in initial empiric

Table 4 Univariate and multivariate analyses of risk factors for eradication failure

Variable		Univariate analysis			Multivariate analysis		
		OR	95%CI	*P* value	OR	95%CI	*P* value
Gender	Male	1 (Reference)					
	Female	1.202	0.998-1.447	0.052			
Age		1.018	1.011-1.024	< 0.001	1.014	1.008-1.021	< 0.001
Eradication attempts	Primary	1 (Reference)			1 (Reference)		
	Rescue	1.816	1.432-2.302	< 0.001	1.538	1.179-2.007	0.002
Antibiotic regimens	Amoxicillin plus clarithromycin	1 (Reference)			1 (Reference)		
	Amoxicillin plus levofloxacin	1.347	0.761-2.385	0.306	1.167	0.654-2.084	0.601
	Amoxicillin plus furazolidone	1.314	0.701-2.461	0.394	0.982	0.505-1.911	0.958
	Clarithromycin plus metronidazole	4.179	2.928-5.966	< 0.001	3.139	2.125-4.637	< 0.001
	Clarithromycin plus levofloxacin	1.958	1.599-2.397	< 0.001	1.863	1.517-2.287	< 0.001
	Clarithromycin plus furazolidone	6.4	3.200-12.797	< 0.001	5.748	2.834-11.655	< 0.001
	Levofloxacin plus furazolidone	2.947	1.147-7.574	0.025	2.115	0.798-5.605	0.132
PPIs	Esomeprazole	1 (Reference)			1 (Reference)		
	Rabeprazole	1.168	0.909-1.502	0.225	1.138	0.879-1.473	0.327
	Lansoprazole	1.197	0.614-2.332	0.598	1.262	0.638-2.496	0.504
	Pantoprazole	1.509	1.161-1.961	0.002	1.398	1.067-1.831	0.015
	Omeprazole	1.963	1.482-2.600	< 0.001	1.513	1.113-2.056	0.008

therapy. Therefore, furazolidone-containing regimens are more frequently used for patients with refractory *H. pylori* infection[20].

In this study, we also observed that only half of the patients had symptoms, and the other half were asymptomatic. As more asymptomatic patients are referred to the hospital for *H. pylori* therapy, we predict that antibiotic resistance of *H. pylori* will increase in the near future. It is, therefore, worthwhile to explore methods to improve the eradication rate. A previous study reported that patient compliance is an indispensable factor influencing treatment results[21]. In addition, high-dose PPI and amoxicillin dual therapy could decrease the use of unnecessary antibiotics, which is a promising alternative approach[22,23]. Adjuvant therapy, including specific probiotics or vitamins, also showed good results, although more evidence will be needed[24].

Consistent with previous studies, our results also suggest that acid-suppressive drugs play an important role in eradication therapy. A previous meta-analysis reported that regimens containing new-generation PPIs (esomeprazole or rabeprazole) showed a significantly higher eradication rate than those containing first-generation PPIs (omeprazole, lansoprazole, or pantoprazole)[25]. In this study, we also found a significantly lower eradication rate for omeprazole- or pantoprazole-containing regimens than for those containing new-generation PPIs. However, the difference in eradication rates between regimens containing lansoprazole and new-generation PPIs was not significant. Due to the relatively small size of the lansoprazole group, this result needs to be confirmed in future studies. The main role of PPIs in the treatment of *H. pylori* infections is to elevate the gastric pH, leading to an increase in the population of dividing *H. pylori*. Subsequently, the bacteria become more susceptible to antibiotics, such as amoxicillin and clarithromycin[26]. Selecting a PPI with a stable effect and high efficacy that is weakly influenced by CYP2C19 genotypes can improve the eradication rate[12]. In addition to the modification of dual therapy by high-dose PPI mentioned above, vonoprazan, a first-in-class potassium-competitive acid blocker, was recently reported to be an independent factor for successful *H. pylori* eradication in both primary and rescue therapy[27].

In this study, a significant trend of decreasing eradication rates was observed with increasing age, which is consistent with previous reports[27,28]. Possible reasons include lower tolerance to and compliance with therapy, more potential complications, increased risks of drug side effects, and increased antibiotic resistance because of higher accumulated antibiotic consumption[29]. In contrast, no significant difference in

the eradication rate or frequency of adverse effects between the elderly group and the younger group was found in other studies[30,31].

Several limitations should be considered when explaining the results of this study. First, because of its retrospective nature, the classification of primary or rescue therapy was completely dependent on the electronic medical records. The percentage of rescue therapy might be underestimated if the patients' medical histories were not fully recorded, and some rescue therapy cases might be misclassified as primary therapy, resulting in a relatively low eradication rate in the primary therapy group. Second, patient compliance was not analyzed in this study. However, all of the patients enrolled in this study completed the urea breath test 4-8 wk after finishing treatment, indicating a relatively high compliance. Third, similar to previous reports of *H. pylori* eradication, the data used in this study were extracted from a single center. The results may not be extrapolated to other areas, especially if resistance rates vary geographically. In addition, the small sample sizes of some regimens, such as the furazolidone-containing regimens in subgroup analysis of primary therapy and lansoprazole-containing regimens, limit the reliability of the corresponding results.

In conclusion, this study revealed an unsatisfactory *H. pylori* eradication rate of 76.6% in Eastern China. Amoxicillin-containing 14-d quadruple regimens have the highest eradication rate in primary therapy, and amoxicillin- and furazolidone-containing regimens show superiority in rescue therapy. An inferiority of omeprazole and pantoprazole is also observed. These findings may be helpful to improve the eradication rate of anti-*H. pylori* therapy.

ARTICLE HIGHLIGHTS

Research background

Helicobacter pylori (*H. pylori*) is a widespread bacterium that affects approximately 50% of the world's population and induces numerous gastrointestinal and extragastric diseases. Currently, *H. pylori* infection is considered the most important (yet controllable) risk factor for gastric cancer. To date, there are limited data in clinical practice regarding eradication rate and factors related to therapy failure.

Research motivation

In recent years, *H. pylori* eradication therapies are facing decreasing eradication rates. However, risk factors related to therapy failure are still uncertain. In addition, there is a lack of recent eradication rate from China. Study in this aspect will certainly be helpful to improve the effectiveness of anti-*H. pylori* therapy in the future.

Research objectives

This study aimed to evaluate the *H. pylori* eradication status in the local population of Eastern China and to explore factors related to eradication failure.

Research methods

Medical records for patients with *H. pylori* infection who underwent standard 14-d quadruple therapy and received urea breath test after treatment were retrospectively reviewed. Eradication rates were calculated and compared between regimens and subgroups. Multivariate analysis was performed to identify predictors of eradication failure.

Research results

Of 2610 patients enrolled, eradication was successful in 1999 (76.6%) patients. Amoxicillin-containing quadruple regimens showed a higher eradication rate than other quadruple therapy regimens (83.0% *vs* 69.0%, $P < 0.001$). The quadruple therapy containing amoxicillin plus clarithromycin achieved the highest eradication rate (83.5%). Primary therapy had a higher eradication rate than rescue therapy (78.3% *vs* 66.5%, $P < 0.001$). In rescue therapy, amoxicillin- and furazolidone-containing regimens achieved the highest eradication rate (80.8%). Esomeprazole-containing regimens showed a higher eradication rate than those containing other proton pump inhibitors (81.8% *vs* 74.9%, $P = 0.001$). Multivariate regression analysis found that older age, prior therapy, and use of omeprazole or pantoprazole were associated with an increased risk of eradication failure.

Research conclusions

This study confirmed that the total eradication rate is 76.6% in eastern China. Amoxicillin-containing regimens are superior to other regimens. Age, prior therapy, and use of omeprazole or pantoprazole are independent risk factors for eradication failure.

Research perspectives

This study can improve the choice of antibiotics and proton pump inhibitors and indicates that in clinical practice, attention should be paid to elderly patients and rescue therapy. Further prospective research focusing on optimizing the treatment strategies considering these factors is required.

REFERENCES

1 **Boltin D**, Niv Y, Schütte K, Schulz C. Review: Helicobacter pylori and non-malignant upper gastrointestinal diseases. *Helicobacter* 2019; **24** Suppl 1: e12637 [PMID: 31486237 DOI: 10.1111/hel.12637]
2 **Sugano K**. Effect of Helicobacter pylori eradication on the incidence of gastric cancer: a systematic review and meta-analysis. *Gastric Cancer* 2019; **22**: 435-445 [PMID: 30206731 DOI: 10.1007/s10120-018-0876-0]
3 **Venerito M**, Vasapolli R, Rokkas T, Delchier JC, Malfertheiner P. Helicobacter pylori, gastric cancer and other gastrointestinal malignancies. *Helicobacter* 2017; **22** Suppl 1 [PMID: 28891127 DOI: 10.1111/hel.12413]
4 **Franceschi F**, Covino M, Roubaud Baudron C. Review: Helicobacter pylori and extragastric diseases. *Helicobacter* 2019; **24** Suppl 1: e12636 [PMID: 31486239 DOI: 10.1111/hel.12636]
5 **Sjomina O**, Pavlova J, Niv Y, Leja M. Epidemiology of Helicobacter pylori infection. *Helicobacter* 2018; **23** Suppl 1: e12514 [PMID: 30203587 DOI: 10.1111/hel.12514]
6 **Rugge M**, Genta RM, Di Mario F, El-Omar EM, El-Serag HB, Fassan M, Hunt RH, Kuipers EJ, Malfertheiner P, Sugano K, Graham DY. Gastric Cancer as Preventable Disease. *Clin Gastroenterol Hepatol* 2017; **15**: 1833-1843 [PMID: 28532700 DOI: 10.1016/j.cgh.2017.05.023]
7 **Lansdorp-Vogelaar I**, Sharp L. Cost-effectiveness of screening and treating Helicobacter pylori for gastric cancer prevention. *Best Pract Res Clin Gastroenterol* 2013; **27**: 933-947 [PMID: 24182612 DOI: 10.1016/j.bpg.2013.09.005]
8 **Han Y**, Yan T, Ma H, Yao X, Lu C, Li Y, Li L. Cost-Effectiveness Analysis of Helicobacter pylori Eradication Therapy for Prevention of Gastric Cancer: A Markov Model. *Dig Dis Sci* 2020; **65**: 1679-1688 [PMID: 31673902 DOI: 10.1007/s10620-019-05910-1]
9 **Bae SE**, Choi KD, Choe J, Kim SO, Na HK, Choi JY, Ahn JY, Jung KW, Lee J, Kim DH, Chang HS, Song HJ, Lee GH, Jung HY. The effect of eradication of Helicobacter pylori on gastric cancer prevention in healthy asymptomatic populations. *Helicobacter* 2018; **23**: e12464 [PMID: 29345408 DOI: 10.1111/hel.12464]
10 **Du Y**, Zhu H, Liu J, Li J, Chang X, Zhou L, Chen M, Lu N, Li Z. Consensus on eradication of Helicobacter pylori and prevention and control of gastric cancer in China (2019, Shanghai). *J Gastroenterol Hepatol* 2020; **35**: 624-629 [PMID: 31788864 DOI: 10.1111/jgh.14947]
11 **Suzuki S**, Gotoda T, Kusano C, Ikehara H, Ichijima R, Ohyauchi M, Ito H, Kawamura M, Ogata Y, Ohtaka M, Nakahara M, Kawabe K. Seven-day vonoprazan and low-dose amoxicillin dual therapy as first-line *Helicobacter pylori* treatment: a multicentre randomised trial in Japan. *Gut* 2020; **69**: 1019-1026 [PMID: 31915235 DOI: 10.1136/gutjnl-2019-319954]
12 **Liu WZ**, Xie Y, Lu H, Cheng H, Zeng ZR, Zhou LY, Chen Y, Wang JB, Du YQ, Lu NH; Chinese Society of Gastroenterology, Chinese Study Group on Helicobacter pylori and Peptic Ulcer. Fifth Chinese National Consensus Report on the management of Helicobacter pylori infection. *Helicobacter* 2018; **23**: e12475 [PMID: 29512258 DOI: 10.1111/hel.12475]
13 **Malfertheiner P**, Megraud F, O'Morain CA, Gisbert JP, Kuipers EJ, Axon AT, Bazzoli F, Gasbarrini A, Atherton J, Graham DY, Hunt R, Moayyedi P, Rokkas T, Rugge M, Selgrad M, Suerbaum S, Sugano K, El-Omar EM; European Helicobacter and Microbiota Study Group and Consensus panel. Management of Helicobacter pylori infection-the Maastricht V/Florence Consensus Report. *Gut* 2017; **66**: 6-30 [PMID: 27707777 DOI: 10.1136/gutjnl-2016-312288]
14 **Hu Y**, Zhu Y, Lu NH. Primary Antibiotic Resistance of Helicobacter pylori in China. *Dig Dis Sci* 2017; **62**: 1146-1154 [PMID: 28315035 DOI: 10.1007/s10620-017-4536-8]
15 **Zhang W**, Chen Q, Liang X, Liu W, Xiao S, Graham DY, Lu H. Bismuth, lansoprazole, amoxicillin and metronidazole or clarithromycin as first-line Helicobacter pylori therapy. *Gut* 2015; **64**: 1715-1720 [PMID: 26338726 DOI: 10.1136/gutjnl-2015-309900]
16 **Zhang YW**, Hu WL, Cai Y, Zheng WF, Du Q, Kim JJ, Kao JY, Dai N, Si JM. Outcomes of furazolidone- and amoxicillin-based quadruple therapy for *Helicobacter pylori* infection and predictors of failed eradication. *World J Gastroenterol* 2018; **24**: 4596-4605 [PMID: 30386109 DOI: 10.3748/wjg.v24.i40.4596]
17 **Atkinson NS**, Braden B. Helicobacter Pylori Infection: Diagnostic Strategies in Primary Diagnosis and After Therapy. *Dig Dis Sci* 2016; **61**: 19-24 [PMID: 26391269 DOI: 10.1007/s10620-015-3877-4]
18 **Zhang YX**, Zhou LY, Song ZQ, Zhang JZ, He LH, Ding Y. Primary antibiotic resistance of Helicobacter pylori strains isolated from patients with dyspeptic symptoms in Beijing: a prospective serial study. *World J Gastroenterol* 2015; **21**: 2786-2792 [PMID: 25759550 DOI: 10.3748/wjg.v21.i9.2786]
19 **Alsamman MA**, Vecchio EC, Shawwa K, Acosta-Gonzales G, Resnick MB, Moss SF. Retrospective Analysis Confirms Tetracycline Quadruple as Best Helicobacter pylori Regimen in the USA. *Dig Dis Sci* 2019; **64**: 2893-2898 [PMID: 31187323 DOI: 10.1007/s10620-019-05694-4]

20 **Nijevitch AA**, Shcherbakov PL, Sataev VU, Khasanov RSh, Al Khashash R, Tuygunov MM. Helicobacter pylori eradication in childhood after failure of initial treatment: advantage of quadruple therapy with nifuratel to furazolidone. *Aliment Pharmacol Ther* 2005; **22**: 881-887 [PMID: 16225499 DOI: 10.1111/j.1365-2036.2005.02656.x]

21 **Wang T**, Yang X, Li Y, Li L, Liu J, Ji C, Sun Y, Li Y, Zuo X. Twice daily short-message-based re-education could improve Helicobacter pylori eradication rate in young population: A prospective randomized controlled study. *Helicobacter* 2019; **24**: e12569 [PMID: 30848868 DOI: 10.1111/hel.12569]

22 **Yang J**, Zhang Y, Fan L, Zhu YJ, Wang TY, Wang XW, Chen DF, Lan CH. Eradication Efficacy of Modified Dual Therapy Compared with Bismuth-Containing Quadruple Therapy as a First-Line Treatment of Helicobacter pylori. *Am J Gastroenterol* 2019; **114**: 437-445 [PMID: 30807294 DOI: 10.14309/ajg.0000000000000132]

23 **Tai WC**, Liang CM, Kuo CM, Huang PY, Wu CK, Yang SC, Kuo YH, Lin MT, Lee CH, Hsu CN, Wu KL, Hu TH, Chuah SK. A 14 day esomeprazole- and amoxicillin-containing high-dose dual therapy regimen achieves a high eradication rate as first-line anti-Helicobacter pylori treatment in Taiwan: a prospective randomized trial. *J Antimicrob Chemother* 2019; **74**: 1718-1724 [PMID: 30768161 DOI: 10.1093/jac/dkz046]

24 **Hu Y**, Zhu Y, Lu NH. Recent progress in Helicobacter pylori treatment. *Chin Med J (Engl)* 2020; **133**: 335-343 [PMID: 31929363 DOI: 10.1097/CM9.0000000000000618]

25 **McNicholl AG**, Linares PM, Nyssen OP, Calvet X, Gisbert JP. Meta-analysis: esomeprazole or rabeprazole vs. first-generation pump inhibitors in the treatment of Helicobacter pylori infection. *Aliment Pharmacol Ther* 2012; **36**: 414-425 [PMID: 22803691 DOI: 10.1111/j.1365-2036.2012.05211.x]

26 **Hu Y**, Zhu Y, Lu NH. Novel and Effective Therapeutic Regimens for *Helicobacter pylori* in an Era of Increasing Antibiotic Resistance. *Front Cell Infect Microbiol* 2017; **7**: 168 [PMID: 28529929 DOI: 10.3389/Fcimb.2017.00168]

27 **Mori H**, Suzuki H, Omata F, Masaoka T, Asaoka D, Kawakami K, Mizuno S, Kurihara N, Nagahara A, Sakaki N, Ito M, Kawamura Y, Suzuki M, Shimada Y, Sasaki H, Matsuhisa T, Torii A, Nishizawa T, Mine T, Ohkusa T, Kawai T, Tokunaga K, Takahashi S. Current status of first- and second-line *Helicobacter pylori* eradication therapy in the metropolitan area: a multicenter study with a large number of patients. *Therap Adv Gastroenterol* 2019; **12**: 1756284819858511 [PMID: 31320930 DOI: 10.1177/1756284819858511]

28 **Kim BJ**, Yang CH, Song HJ, Jeon SW, Kim GH, Kim HS, Kim TH, Shim KN, Chung IK, Park MI, Choi IJ, Kim JH, Kim BW, Baik GH, Han SW, Seo HE, Jung WT, Hwan Oh J, Kim SG, Lee JH, Park SK, Park BJ, Yang BR, Lee J, Kim JG. Online registry for nationwide database of Helicobacter pylori eradication in Korea: Correlation of antibiotic use density with eradication success. *Helicobacter* 2019; **24**: e12646 [PMID: 31368629 DOI: 10.1111/hel.12646]

29 **Boyanova L**, Gergova G, Markovska R, Kandilarov N, Davidkov L, Spassova Z, Mitov I. Primary Helicobacter pylori resistance in elderly patients over 20 years: A Bulgarian study. *Diagn Microbiol Infect Dis* 2017; **88**: 264-267 [PMID: 28506722 DOI: 10.1016/j.diagmicrobio.2017.05.001]

30 **Kobayashi S**, Joshita S, Yamamoto C, Yanagisawa T, Miyazawa T, Miyazawa M, Kubota D, Sato J, Umemura T, Tanaka E. Efficacy and safety of eradication therapy for elderly patients with helicobacter pylori infection. *Medicine (Baltimore)* 2019; **98**: e16619 [PMID: 31348311 DOI: 10.1097/MD.0000000000016619]

31 **Nishizawa T**, Suzuki H, Fujimoto A, Kinoshita H, Yoshida S, Isomura Y, Toyoshima A, Kanai T, Yahagi N, Toyoshima O. Effects of patient age and choice of antisecretory agent on success of eradication therapy for *Helicobacter pylori* infection. *J Clin Biochem Nutr* 2017; **60**: 208-210 [PMID: 28584402 DOI: 10.3164/jcbn.16-86]

World Journal of Gastroenterology

Submit a Manuscript: https://www.f6publishing.com

World J Gastroenterol 2020 August 28; 26(32): 4857-4865

DOI: 10.3748/wjg.v26.i32.4857

ISSN 1007-9327 (print) ISSN 2219-2840 (online)

ORIGINAL ARTICLE

Retrospective Study

Development of a novel score for the diagnosis of bacterial infection in patients with acute-on-chronic liver failure

Su Lin, Yan-Yan Yan, Yin-Lian Wu, Ming-Fang Wang, Yue-Yong Zhu, Xiao-Zhong Wang

ORCID number: Su Lin 0000-0001-7517-9859; Yan-Yan Yan 0000-0003-2720-8058; Yin-Lian Wu 0000-0001-9298-8367; Ming-Fang Wang 0000-0001-7306-955X; Yue-Yong Zhu 0000-0002-0746-4911; Xiao-Zhong Wang 0000-0003-1756-6775.

Author contributions: Lin S designed the study; Wang MF and Yan YY collected and analyzed the data; Lin S, Yan YY and Wu YL drafted the manuscript; Zhu YY and Wang XZ contributed to critical comments of the manuscript; all authors approved the final version of the manuscript prior to submission.

Supported by the Chinese National Science and Technology Projects, No. 2017ZX10202201.

Institutional review board statement: The study was approved by the Ethics Committee of the First Affiliated Hospital of Fujian Medical University.

Informed consent statement: All patients hospitalized in the First Affiliated Hospital of Fujian Medical University sign a written consent for anonymous use of digital data for scientific research. We are not able to present each document of the included 386 cases. An example of the consent is shown below.

Su Lin, Xiao-Zhong Wang, Department of Gastroenterology, Union Hospital of Fujian Medical University, Fuzhou 350000, Fujian Province, China

Yan-Yan Yan, Yin-Lian Wu, Ming-Fang Wang, Yue-Yong Zhu, Liver Research Center, The First Affiliated Hospital of Fujian Medical University, Fuzhou 350000, Fujian Province, China

Yan-Yan Yan, Clinical Liver Center, The 180th Hospital of People's Liberation Army, Quanzhou Fujian Province, 362100, China

Corresponding author: Xiao-Zhong Wang, MD, PhD, Chief Doctor, Department of Gastroenterology, Union Hospital of Fujian Medical University, No. 29 Shengmiao Road, Gulou, Fuzhou 350000, Fujian Province, China. drwangxz@163.com

Abstract

BACKGROUND

The diagnosis of bacterial infection is difficult in patients with acute-on-chronic liver failure (ACLF).

AIM

To evaluate the diagnostic accuracy of widely used parameters for bacterial infection in ACLF and to develop a simple scoring system to improve diagnostic efficiency.

METHODS

This was a retrospective study. Procalcitonin (PCT), white blood cells (WBC), proportion of neutrophils (N%), and C-reactive protein (CRP) were examined. Logistic regression was used to select variables for the scoring models and receiver operating characteristic curve (ROC) analysis was used to evaluate the diagnostic value of different indices.

RESULTS

This study included 386 patients with ACLF, 169 (43.78%) of whom had bacterial infection on admission. The area under the ROC (AUROC) of PCT, CRP, WBC and N% for the diagnosis of bacterial infection ranged from 0.637 to 0.692, with no significant difference between them. Logistic regression showed that only N%, PCT, and CRP could independently predict infection. A novel scoring system (infection score) comprised of N%, PCT and CRP was developed. The AUROC of the infection score was 0.740, which was significantly higher than that for the

Conflict-of-interest statement: The authors have no conflict of interest to declare.

Data sharing statement: Not available.

Manuscript source: Invited manuscript

Received: May 23, 2020
Peer-review started: May 23, 2020
First decision: June 12, 2020
Revised: June 18, 2020
Accepted: July 30, 2020
Article in press: July 30, 2020
Published online: August 28, 2020

P-Reviewer: El-Shabrawi MHF
S-Editor: Yan JP
L-Editor: Webster JR
P-Editor: Ma YJ

other four indices (infection score *vs* N%, PCT, CRP, and WBC, P = 0.0056, 0.0001, 0.0483 and 0.0008, respectively). The best cutoff point for the infection score was 4 points, with a sensitivity of 78.05%, a specificity of 55.29%, a positive predictive value of 57.91% and a negative predictive value of 76.16%.

CONCLUSION
The infection score is a simple and useful tool for discriminating bacterial infection in ACLF.

Key words: Acute on chronic liver failure; Bacterial infection; Score

Core tip: This is a retrospective study evaluating the diagnostic value of widely used biomarkers for infection, including procalcitonin (PCT), white blood cells, proportion of neutrophils (N%), and C-reactive protein (CRP) for bacterial infection in ACLF. The results showed that all four parameters did not perform well in ACLF, with no significant difference found among them. A novel scoring system was developed comprised of N%, PCT and CRP which demonstrated higher accuracy for bacterial infection in ACLF than the indicators used alone. Further validation of this scoring system is required in prospective studies.

Citation: Lin S, Yan YY, Wu YL, Wang MF, Zhu YY, Wang XZ. Development of a novel score for the diagnosis of bacterial infection in patients with acute-on-chronic liver failure. *World J Gastroenterol* 2020; 26(32): 4857-4865
URL: https://www.wjgnet.com/1007-9327/full/v26/i32/4857.htm
DOI: https://dx.doi.org/10.3748/wjg.v26.i32.4857

INTRODUCTION

Acute-on-chronic liver failure (ACLF) is a severe syndrome characterized by the loss of hepatocyte function and consequent multiple organ failure[1,2]. Patients with ACLF are usually vulnerable to infection[3,4]. On the other hand, bacterial infection can lead to deterioration of liver function or even death in such populations[5-8]. Thus, early detection of bacterial infection and timely treatment are crucial in the management of ACLF. However, compared with the general population or cases with liver cirrhosis, patients with ACLF demonstrate different clinico-pathophysiological features[9]. For example, significant systemic inflammation is commonly observed in ACLF[10-13], which makes the diagnosis of infection more difficult in the ACLF population than in other populations.

Routine blood testing is the preferred method for detecting infection in the general population. However, its value is not satisfactory in ACLF as leucopenia resulting from hypersplenism is common in patients with chronic liver disease. Serum C-reactive protein (CRP) and serum procalcitonin (PCT) level are widely used as diagnostic indicators for bacterial infection[14]. Previous studies have shown that CRP level decreases with the severity of liver failure[15,16]; therefore, the diagnostic capacity of CRP is interfered by hepatocyte dysfunction[17]. We previously demonstrated that the threshold of PCT should be elevated in ACLF when it is used for the diagnosis of bacterial infection[18], and this view was supported by several other studies[19-22]. Therefore, it is important to identify a new biomarker or to develop a model to improve diagnostic efficiency. This retrospective study aimed to develop a novel scoring system containing common biomarkers for the identification of bacterial infection in ACLF.

MATERIALS AND METHODS

Patients

This study included ACLF patients who were hospitalized in the First Affiliated

Hospital of Fujian Medical University from January 2014 to March 2019. The First Affiliated Hospital of Fujian Medical University is a teaching hospital that receives patients referred from other hospitals. Many of these patients may have previously been treated for some time in other hospitals and have developed nosocomial infection; therefore, the infection rate on admission in this cohort is relatively higher than reported. We excluded patients without a PCT test on admission and those with severe trauma, acute pancreatitis, malignancy, fungal infection, and those who had undergone major surgery.

Diagnostic criteria

ACLF was diagnosed based on the guideline of the Asian Pacific Association for the Study of the Liver (2014)[23], which are the most widely used criteria in Asia[24]. ACLF was confirmed in patients with chronic liver disease who had a total serum bilirubin ≥ 5 mg/dL or an international normalized ratio of ≥ 1.5 within 4 wk, complicated by encephalopathy and/or ascites[23].

Data collection

The following data were collected from all patients on admission: Sex, age, the etiology of liver diseases, etiologies, infection source, PCT, CRP, white blood cell count (WBC), proportion of neutrophils (N%), liver and kidney function tests. The normal ranges of the four parameters were as follows: WBC 3.5-9.5 × 109/L, N% 40%-75%, CRP 0-8 mg/L, and PCT 0-0.05 ng/mL.

Statistical analysis

Continuous variables are expressed as the mean ± standard deviation and were compared using the Student's *t* test in the case of normal distribution or the Mann-Whitney test in the remaining cases. Categorical variables are expressed as counts (percentages) and were compared by the Chi-squared test or Fisher's exact test[25]. The diagnostic accuracy of PCT and the other parameters were examined by the receiver operating characteristic curve (ROC curve). The best cut-off value of each indicator was chosen based on Youden's index. The sensitivity, specificity, negative predictive value (NPV), and positive predictive value (PPV) were calculated based on the cut-off point. Statistical analyses were performed using SPSS software, version 18.0 (SPSS, Chicago, IL, United States). The ROC curves were compared using MedCalc software version15.2.2 (MedCalc Software, Mariakerke, Belgium). A P value < 0.05 was considered statistically significant.

Ethics

This study was in compliance with the Declaration of Helsinki. All patients signed a written consent form for use of their clinical data. The study was approved by the Institutional Ethics Committee of the First Affiliated Hospital of Fujian Medical University.

RESULTS

Baseline characteristics of the patients

This study included 386 patients with ACLF, 169 (43.78%) of whom had bacterial infection on admission and 217 (56.22%) did not (Figure 1). The baseline characteristics of these patients are shown in Table 1. Hepatitis B virus-related ACLF was the predominant etiology of liver disease in this population (75%). Patients with infection were older (52.18 ± 14.70 years *vs* 45.96 ± 13.94 years, P < 0.001) and had significantly higher MELD scores (22.24 ± 7.36 *vs* 18.94 ± 4.39, P < 0.001) than non-infected cases. Sex and etiologies were similar between the two groups.

The most common infection in this ACLF cohort was pneumonia, accounting for 55.62%. The proportions of spontaneous bacterial peritonitis (SBP) (13.60%) and both pneumonia and SBP (12.43%) were similar. The remaining infections were from an unidentified source (7.69%), biliary tract infection (7.10%), urinary tract infection (5.92%) and blood stream infection (1.78%).

Comparison of the four parameters between infected and non-infected patients with ACLF

The PCT levels were increased in patients with ACLF even in the absence of bacterial infection (0.75 ± 0.60 ng/mL), which was demonstrated in our previous study[18]. This

Table 1 Baseline characteristics of the patients

	Non-infected (*n* = 217)	Infected (*n* = 169)	*P* value
Age (yr)	45.96 ± 13.94	52.18±14.70	< 0.001
Male, *n* (%)	177 (81.6)	126 (74.6)	0.096
Etiology, *n* (%)			0.051
HBV infection	173 (79.7)	114 (67.5)	
Alcohol	17 (7.8)	23 (13.6)	
HBV and alcohol	8 (3.7)	8 (4.7)	
Others	19 (8.8)	24 (14.2)	
MELD score	18.94 ± 4.39	22.24 ± 7.36	< 0.001
PT (s)	21.97 ± 6.52	26.22 ± 9.90	< 0.001
INR	1.90 ± 0.56	2.35 ± 1.16	< 0.001
Total bilirubin (μmol/L)	272.56 ± 127.41	317.70 ± 153.10	0.001
Albumin (g/L)	31.34 ± 4.76	28.81 ± 5.36	< 0.001
ALT (U/L)	663.30 ± 694.59	524.97 ± 800.98	0.070
AST (U/L)	463.18 ± 494.97	477.25 ± 662.96	0.811
GGT (U/L)	159.74 ± 160.13	141.85 ± 143.03	0265
Creatinine (μmol/L)	61.67 ± 19.37	81.71 ± 56.61	< 0.001
PCT (ng/mL)	0.75 ± 0.60	1.46 ± 1.81	< 0.001
CRP (mg/L)	15.86 ± 9.61	25.59 ± 17.50	< 0.001
WBC (× 10^9/L)	6.67 ± 3.11	9.01 ± 5.62	< 0.001
N%	66.80 ± 10.57	73.03 ± 11.56	< 0.001

PT: Prothrombin time; INR: International normalized ratio; ALT: Alanine aminotransferase; AST: Aspartate transaminase; GGT: Gamma-glutamyl transferase; PCT: Procalcitonin; CRP: C-reactive protein; WBC: White blood cell count; N%: Proportion of neutrophils.

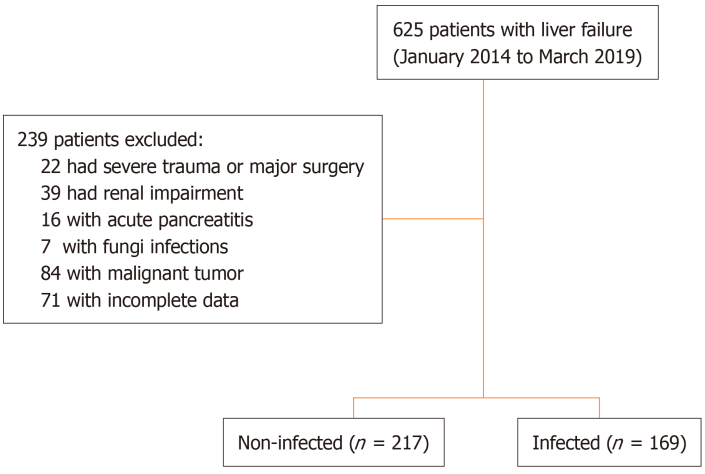

Figure 1 Flowchart of patient selection.

increase was nearly 15 times higher than the normal range (0.05 ng/mL). However, the PCT levels in the infected group were still significantly higher than those in the non-infected group (1.46 ± 1.81 ng/mL, $P < 0.05$, Table 1). In the group with infection, CRP levels differed significantly with infection site, while PCT, WBC and N% levels showed no significant differences regarding the infection site (Table 2).

Table 2 Procalcitonin levels in relation to different infection sites

	PCT (ng/mL)	CRP (mg/L)	WBC (× 10^9/L)	N%
Overall (n = 169)	1.46 ± 1.81	25.59 ± 17.50	9.01 ± 5.62	73.03 ± 11.56
Pneumonia (n = 94)	1.35 ± 1.77	25.26 ± 17.80	8.87 ± 5.98	71.77 ± 11.23
SBP (n = 23)	1.29 ± 0.83	18.55 ± 9.19	8.46 ± 3.88	72.05 ± 14.06
Pneumonia and SBP (n = 21)	2.30 ± 2.83	37.71 ± 24.00	11.30 ± 6.72	77.26 ± 13.85
Infection without identified source (n = 13)	2.12 ± 2.04	29.26 ± 11.98	9.35 ± 4.81	75.57 ± 10.87
Biliary tract (n = 12)	0.59 ± 0.37	14.61 ± 8.12	7.92 ± 4.66	73.42 ± 10.25
Urinary (n = 10)	0.74 ± 0.54	19.72 ± 5.90	5.38 ± 2.43	67.43 ± 9.25
Bloodstream (n = 3)	1.02 ± 0.42	32.65 ± 17.90	8.21 ± 1.13	74.67 ± 5.80
P value	0.084	0.001	0.203	0.406

SBP: Spontaneous bacterial peritonitis; PCT: Procalcitonin; CRP: C-reactive protein; WBC: White blood cell count; N%: Proportion of neutrophils.

Diagnostic value of the four parameters for bacterial infection in patients with ACLF

Figure 2 shows the ROC curves of PCT, CRP, WBC, and N% for the diagnosis of bacterial infection. Table 3 shows the best cutoff points and the area under the ROC (AUROC) of these parameters. There were no significant differences in multiple comparisons of the AUROCs (all P values > 0.05).

Infection score for the diagnosis of bacterial infection in ACLF

The results of logistic regression showed that PCT, CRP and N% could independently predict infection, with an odds ratio (OR) of 1.595 (95%CI: 1.202-2.116), 1.047 (95%CI: 1.025-1.069) and 1.030 (95%CI: 1.005-1.055), respectively, while the WBC was not an independent indicator for infection (OR = 1.063, 95%CI: 0.993-1.137).

According to the variables selected for logistic regression analysis and the cut-offs defined by ROC analysis, we developed a scoring system that contained three components, N%, PCT, and CRP (Table 4). For example, the OR of PCT for infection was 1.595, which meant that each additional unit (1 ng/mL) increment in PCT increased the risk of infection by 59%. The baseline level of PCT in the non-infected group was approximately 0.75 ng/mL and the optimal cutoff point of PCT for discriminating infection and non-infection was 1 ng/mL. After combining the above information and making the scoring system more user-friendly, PCR < 0.5 ng/mL was assigned 0 point, 1 > PCT ≥ 0.5 was assigned 1 point, and 2 > PCT ≥ 1 was assigned 2 points. The AUROC of this infection score for the diagnosis of bacterial infection in patients with ACLF was 0.740, which was significantly higher than the other four biomarkers (infection score *vs* N%, PCT, CRP, and WBC, P = 0.0056, 0.0001, 0.0483 and 0.0008, respectively). The best cutoff value of the infection score was 4 points, with a sensitivity of 78.05%, specificity of 55.29%, PPV of 57.91%, and NPV of 76.16%. Cases with an infection score of 0-2 points were not likely to have a bacterial infection (NPV was 94.10%). On the other hand, cases with an infection score of 8 points and greater were largely considered infected and empiric antibiotics were strongly recommended (PPV was 91.68%) (Table 5).

DISCUSSION

The early diagnosis of bacterial infection is crucial for the management of liver failure. This study firstly demonstrated that common indicators of infection, including WBC, N%, CRP, and PCT, did not perform well in ACLF as all the AUROCs were less than 0.7 and no differences were found between these indicators. A novel scoring system was developed in this study and the results showed that this infection score had better accuracy than those four parameters alone for the diagnosis of bacterial infection in ACLF.

This infection score comprised three commonly used indicators, the N%, PCT and CRP. Neutrophils are known to be the first immune cells in the response to infection[26]. The N% is independent of the WBC, which means that hypersplenism might not significantly influence the N%. In this cohort, the N% alone was not an

Table 3 Diagnostic accuracy of procalcitonin, C-reactive protein, white blood cells, and proportion of neutrophils for the diagnosis of infection in liver failure

	Cut offs	Sensitivity (%)	Specificity (%)	PLR	NLR	PPV (%)	NPV (%)	*P* value	AUROC
PCT	≥ 1.01	42.60	78.80	2.01	0.73	61.01	63.81	< 0.0001	0.637
CRP	≥ 17.5	63.91	67.28	1.95	0.54	60.33	70.54	< 0.0001	0.692
WBC	≥ 7.90	47.93	79.72	2.36	2.36	64.79	66.28	< 0.0001	0.638
N%	≥ 73.8	55.03	76.50	2.34	0.59	64.58	68.60	< 0.0001	0.674

PCT: Procalcitonin; CRP: C-reactive protein; WBC: White blood cell count; N%: Proportion of neutrophils; PLR: Positive likelihood ratio; NLR: Negative likelihood ratio; PPV: Positive predictive value; NPV: Negative predictive value; AUROC: Area under the receiver operating characteristic curve.

Table 4 The infection scoring system

Items	Definition	Score
N%	< 60	0
	70 > N ≥ 60	1
	80 > N ≥ 70	2
	≥ 80	3
PCT	< 0.5	0
	1 > PCT ≥ 0.5	1
	2 > PCT ≥ 1	2
	≥ 2	3
CRP	< 10	0
	20 >N ≥ 10	1
	≥ 20	2

PCT: Procalcitonin; CRP: C-reactive protein; N%: Proportion of neutrophils.

Table 5 Diagnostic value of the infection score

Score	Sensitivity (%)	Specificity (%)	PPV (%)	NPV (%)	PLR	NLR
≥ 2	98.22	22.12	49.55	94.10	1.26	0.08
≥ 4	78.05	55.29	57.91	76.16	1.75	0.40
≥ 6	26.63	91.24	70.30	61.49	3.04	0.80
≥ 8	6.51	99.54	91.68	57.76	14.12	0.94

PPV: Positive predictive value; NPV: Negative predictive value; PLR: Positive likelihood ratio; NLR: Negative likelihood ratio.

excellent biomarker of bacterial infection as the AUROC was only 0.674 and its best cutoff value was still within the normal range. However, when combined with other biomarkers, the diagnostic value was greatly improved.

PCT has been questioned as an index of bacterial infection in patients with liver diseases as several studies have demonstrated elevated PCT levels in the absence of bacterial infection in such patients[18,27,28]. We previously showed that PCT was not the best parameter of infection in cirrhotic patients following the onset of sepsis[29]. Mallet *et al*[21] showed that the diagnostic value of PCT for infections was related to the etiology of liver failure. PCT has also been shown to be a better biomarker for liver cell injury than a biomarker for bacterial infection in patients with acute liver failure[20]. A study from China suggested adjusting the threshold of PCT according to liver function[19]. The results of this study showed that the diagnostic value of PCT alone

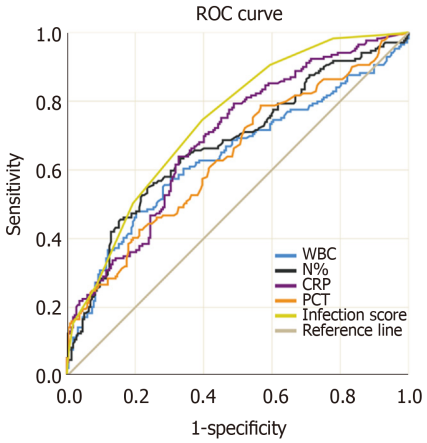

Figure 2 Receiver operating characteristic curves of procalcitonin, C-reactive protein, white blood cells, and proportion of neutrophils for the diagnosis of infections in acute-on-chronic liver failure. ROC: Receiver operating characteristic curve; WBC: White blood cells; CRP: C-reactive protein; PCT: Procalcitonin; N%: Proportion of neutrophils.

was similar to that of WBC, N% and CRP even though the threshold for PCT was increased to 20 times greater than the upper limit of the normal range. This result was supported by the aforementioned studies.

Similar to PCT and N%, the diagnostic value of CRP alone was not satisfactory. Inflammation and bacterial translocation in liver cirrhosis may lead to an increase in the synthesis of CRP[30]. On the other hand, a previous study showed that CRP levels will remain high even when bacterial infections are resolved[31]. The CRP might partially reflect systemic inflammation in ACLF in addition to bacterial infection.

With the combination of these three widely used parameters, the performance of the infection score was better in diagnosing bacterial infection. The AUROC values were significantly higher than any of the other indicators used alone. When the infection score was equal to or less than 2 points, the NPV was 90%, suggesting that infection can be ruled out and antibiotics should not be administered. When the score was 8 points, the PPV was 90%, suggesting that anti-infective therapy was required. The variables in this model are widely used in clinical practice and the score is easy to compute. This novel scoring system might be a useful tool for early detection of infection in patients with ACLF and help to improve the outcome of this population.

The limitation of this research is that it is a retrospective study performed in a single medical center. As ACLF is an uncommon disease, we were unable to include sufficient cases to validate this model. Studies regarding the diagnosis of infection in liver failure are still limited, thus studies with a large sample size are needed to validate this scoring system.

In conclusion, a novel scoring system comprised of N%, CRP and PCT is useful for the diagnosis of bacterial infection in ACLF.

ARTICLE HIGHLIGHTS

Research background

Patients with acute-on-chronic liver failure (ACLF) are prone to have bacterial infection. However, the diagnosis of infection is difficult in the ACLF population due to their specific clinico-pathophysiological features.

Research motivation

Early detection of bacterial infection and timely treatment are crucial in the management of ACLF. Therefore, it is important to identify a new biomarker or to develop a model to improve diagnostic efficiency.

Research objectives

This retrospective study aimed to develop a novel scoring system containing common biomarkers for the identification of bacterial infection in ACLF.

Research methods

This was a retrospective study. Procalcitonin (PCT), white blood cells (WBC), proportion of neutrophils (N%), and C-reactive protein (CRP) were examined. Logistic regression was used to select variables for the scoring models and receiver operating characteristic curve (ROC) analysis was used to evaluate the diagnostic value of different indices.

Research results

This study included 386 patients with ACLF, 169 (43.78%) of whom had bacterial infection on admission. The area under the ROC (AUROC) of PCT, CRP, WBC and N% for the diagnosis of bacterial infection ranged from 0.637 to 0.692, with no significant difference between them. Logistic regression showed that only N%, PCT, and CRP could independently predict infection. A novel scoring system (infection score) comprised of N%, PCT and CRP was developed. The AUROC of the infection score was 0.740, which was significantly higher than that for the other four indices (infection score *vs* N%, PCT, CRP, and WBC, P = 0.0056, 0.0001, 0.0483 and 0.0008, respectively). The best cutoff point for the infection score was 4 points, with a sensitivity of 78.05%, a specificity of 55.29%, a positive predictive value of 57.91% and a negative predictive value of 76.16%.

Research conclusions

The common indicators of infection, including WBC, N%, CRP, and PCT, did not perform well in ACLF as all the AUROCs were less than 0.7 and no differences were found between these indicators. A novel scoring system comprised of N%, PCT and CRP demonstrated higher accuracy for bacterial infection in ACLF than the indicators used alone.

Research perspectives

Further validation of this scoring system is required in prospective studies.

REFERENCES

1 **Lange CM**, Bechstein WO, Berg T, Engelmann C, Bruns T, Canbay A, Moreau R, Trebicka J. Acute-on-Chronic Liver Failure. *Visc Med* 2018; **34**: 296-300 [PMID: 30345288 DOI: 10.1159/000491406]

2 **Chen T**, Yang Z, Choudhury AK, Al Mahtab M, Li J, Chen Y, Tan SS, Han T, Hu J, Hamid SS, Huei LG, Ghazinian H, Nan Y, Chawla YK, Yuen MF, Devarbhavi H, Shukla A, Abbas Z, Sahu M, Dokmeci AK, Lesmana LA, Lesmana CRA, Xin S, Duan Z, Guo W, Ma K, Zhang Z, Cheng Q, Jia J, Sharma BC, Sarin SK, Ning Q. Complications constitute a major risk factor for mortality in hepatitis B virus-related acute-on-chronic liver failure patients: a multi-national study from the Asia-Pacific region. *Hepatol Int* 2019; **13**: 695-705 [PMID: 31650510 DOI: 10.1007/s12072-019-09992-x]

3 **Fernández J**, Acevedo J, Wiest R, Gustot T, Amoros A, Deulofeu C, Reverter E, Martínez J, Saliba F, Jalan R, Welzel T, Pavesi M, Hernández-Tejero M, Ginès P, Arroyo V; European Foundation for the Study of Chronic Liver Failure. Bacterial and fungal infections in acute-on-chronic liver failure: prevalence, characteristics and impact on prognosis. *Gut* 2018; **67**: 1870-1880 [PMID: 28847867 DOI: 10.1136/gutjnl-2017-314240]

4 **Engelmann C**, Berg T. Management of Infectious Complications Associated with Acute-on-Chronic Liver Failure. *Visc Med* 2018; **34**: 261-268 [PMID: 30345283 DOI: 10.1159/000491107]

5 **Grgurevic I**, Trkulja V, Bozin T, Madir A, Miletic M, Marusic S, Skrlin J, Sestan Crnek S, Dobrovic K. Infection as a predictor of mortality in decompensated liver cirrhosis: exploring the relationship to severity of liver failure. *Eur J Gastroenterol Hepatol* 2019 [PMID: 31895905 DOI: 10.1097/MEG.0000000000001667]

6 **Li B**, Gao Y, Wang X, Qian Z, Meng Z, Huang Y, Deng G, Lu X, Liu F, Zheng X, Li H, Chen J. Clinical features and outcomes of bacterascites in cirrhotic patients: A retrospective, multicentre study. *Liver Int* 2020; **40**: 1447-1456 [PMID: 32128975 DOI: 10.1111/liv.14418]

7 **Cao Z**, Liu Y, Wang S, Lu X, Yin S, Jiang S, Chen L, Cai M, Zeng B, Yao Y, Tang W, Zhao G, Xiang X, Wang H, Cai W, Zhu C, Li H, Xie Q. The impact of HBV flare on the outcome of HBV-related decompensated cirrhosis patients with bacterial infection. *Liver Int* 2019; **39**: 1943-1953 [PMID: 31206235 DOI: 10.1111/liv.14176]

8 **Mücke MM**, Rumyantseva T, Mücke VT, Schwarzkopf K, Joshi S, Kempf VAJ, Welsch C, Zeuzem S, Lange CM. Bacterial infection-triggered acute-on-chronic liver failure is associated with increased mortality. *Liver Int* 2018; **38**: 645-653 [PMID: 28853199 DOI: 10.1111/liv.13568]

9 **Moreau R**, Jalan R, Gines P, Pavesi M, Angeli P, Cordoba J, Durand F, Gustot T, Saliba F, Domenicali M, Gerbes A, Wendon J, Alessandria C, Laleman W, Zeuzem S, Trebicka J, Bernardi M, Arroyo V; CANONIC Study Investigators of the EASL–CLIF Consortium. Acute-on-chronic liver failure is a distinct syndrome that develops in patients with acute decompensation of cirrhosis. *Gastroenterology* 2013; **144**: 1426-1437, 1437.e1-1437.e9 [PMID: 23474284 DOI: 10.1053/j.gastro.2013.02.042]

10 **Hensley MK**, Deng JC. Acute on Chronic Liver Failure and Immune Dysfunction: A Mimic of Sepsis. *Semin Respir Crit Care Med* 2018; **39**: 588-597 [PMID: 30485889 DOI: 10.1055/s-0038-1672201]

11 **Clària J**, Stauber RE, Coenraad MJ, Moreau R, Jalan R, Pavesi M, Amorós À, Titos E, Alcaraz-Quiles J,

Oettl K, Morales-Ruiz M, Angeli P, Domenicali M, Alessandria C, Gerbes A, Wendon J, Nevens F, Trebicka J, Laleman W, Saliba F, Welzel TM, Albillos A, Gustot T, Benten D, Durand F, Ginès P, Bernardi M, Arroyo V; CANONIC Study Investigators of the EASL-CLIF Consortium and the European Foundation for the Study of Chronic Liver Failure (EF-CLIF). Systemic inflammation in decompensated cirrhosis: Characterization and role in acute-on-chronic liver failure. *Hepatology* 2016; **64**: 1249-1264 [PMID: 27483394 DOI: 10.1002/hep.28740]

12 **Yang D**, Xie Y, Pan H, Huang Y, Dai Y, Tong Y, Chen M. Clinical characteristics and prognostic factors of liver cirrhosis patients with systemic inflammatory response syndrome. *Hepatol Res* 2017; **47**: 1174-1185 [PMID: 28249358 DOI: 10.1111/hepr.12886]

13 **Laleman W**, Claria J, Van der Merwe S, Moreau R, Trebicka J. Systemic Inflammation and Acute-on-Chronic Liver Failure: Too Much, Not Enough. *Can J Gastroenterol Hepatol* 2018; **2018**: 1027152 [PMID: 30155448 DOI: 10.1155/2018/1027152]

14 **Pfäfflin A**, Schleicher E. Inflammation markers in point-of-care testing (POCT). *Anal Bioanal Chem* 2009; **393**: 1473-1480 [PMID: 19104782 DOI: 10.1007/s00216-008-2561-3]

15 **Park WB**, Lee KD, Lee CS, Jang HC, Kim HB, Lee HS, Oh MD, Choe KW. Production of C-reactive protein in Escherichia coli-infected patients with liver dysfunction due to liver cirrhosis. *Diagn Microbiol Infect Dis* 2005; **51**: 227-230 [PMID: 15808312 DOI: 10.1016/j.diagmicrobio.2004.11.014]

16 **Mackenzie I**, Woodhouse J. C-reactive protein concentrations during bacteraemia: A comparison between patients with and without liver dysfunction. *Intensive Care Med* 2006; **32**: 1344-1351 [PMID: 16799774 DOI: 10.1007/s00134-006-0251-1]

17 **Fernández J**, Gustot T. Management of bacterial infections in cirrhosis. *J Hepatol* 2012; **56** Suppl 1: S1-12 [PMID: 22300459 DOI: 10.1016/S0168-8278(12)60002-6]

18 **Lin S**, Yan Y, Wu Y, Van Poucke S, Wang M, Zhu Y, Wang X. Procalcitonin as a biomarker for diagnose of bacterial infection in patients with acute-on-chronic liver failure. *Clin Res Hepatol Gastroenterol* 2020; **44**: e32-e34 [PMID: 31303532 DOI: 10.1016/j.clinre.2019.06.011]

19 **Qu J**, Feng P, Luo Y, Lü X. Impact of hepatic function on serum procalcitonin for the diagnosis of bacterial infections in patients with chronic liver disease: A retrospective analysis of 324 cases. *Medicine (Baltimore)* 2016; **95**: e4270 [PMID: 27472699 DOI: 10.1097/MD.0000000000004270]

20 **Rule JA**, Hynan LS, Attar N, Sanders C, Korzun WJ, Lee WM; Acute Liver Failure Study Group. Procalcitonin Identifies Cell Injury, Not Bacterial Infection, in Acute Liver Failure. *PLoS One* 2015; **10**: e0138566 [PMID: 26393924 DOI: 10.1371/journal.pone.0138566]

21 **Mallet M**, Haq M, Tripon S, Bernard M, Benosman H, Thabut D, Rudler M. Elevated procalcitonin is associated with bacterial infection during acute liver failure only when unrelated to acetaminophen intoxication. *Eur J Gastroenterol Hepatol* 2017; **29**: 811-816 [PMID: 28272093 DOI: 10.1097/MEG.0000000000000862]

22 **Sugihara T**, Koda M, Okamoto T, Miyoshi K, Matono T, Oyama K, Hosho K, Okano JI, Isomoto H. Serum Procalcitonin in Patients with Acute Liver Failure. *Yonago Acta Med* 2017; **60**: 40-46 [PMID: 28331420]

23 **Sarin SK**, Kedarisetty CK, Abbas Z, Amarapurkar D, Bihari C, Chan AC, Chawla YK, Dokmeci AK, Garg H, Ghazinyan H, Hamid S, Kim DJ, Komolmit P, Lata S, Lee GH, Lesmana LA, Mahtab M, Maiwall R, Moreau R, Ning Q, Pamecha V, Payawal DA, Rastogi A, Rahman S, Rela M, Saraya A, Samuel D, Saraswat V, Shah S, Shiha G, Sharma BC, Sharma MK, Sharma K, Butt AS, Tan SS, Vashishtha C, Wani ZA, Yuen MF, Yokosuka O; APASL ACLF Working Party. Acute-on-chronic liver failure: consensus recommendations of the Asian Pacific Association for the Study of the Liver (APASL) 2014. *Hepatol Int* 2014; **8**: 453-471 [PMID: 26202751 DOI: 10.1007/s12072-014-9580-2]

24 **Lin S**, Zhang K, Zhang J, Wang M, Velani B, Zhu Y. Long-term outcomes of patients with hepatitis B virus-related acute on chronic liver failure: An observational cohort study. *Liver Int* 2019; **39**: 854-860 [PMID: 30753752 DOI: 10.1111/liv.14072]

25 **Zhang Z**. Univariate description and bivariate statistical inference: the first step delving into data. *Ann Transl Med* 2016; **4**: 91 [PMID: 27047950 DOI: 10.21037/atm.2016.02.11]

26 **Lawrence SM**, Corriden R, Nizet V. The Ontogeny of a Neutrophil: Mechanisms of Granulopoiesis and Homeostasis. *Microbiol Mol Biol Rev* 2018; **82**: e00057-17 [PMID: 29436479 DOI: 10.1128/mmbr.00057-17]

27 **Woźnica E**, Łysenko L. Procalcitonin in liver dysfunction - Dr Jekyll or Mr Hyde? *Anaesthesiol Intensive Ther* 2018; **50**: 226-229 [PMID: 29995971 DOI: 10.5603/AIT.a2018.0023]

28 **Dong R**, Wan B, Lin S, Wang M, Huang J, Wu Y, Wu Y, Zhang N, Zhu Y. Procalcitonin and Liver Disease: A Literature Review. *J Clin Transl Hepatol* 2019; **7**: 51-55 [PMID: 30944820 DOI: 10.14218/JCTH.2018.00012]

29 **Lin S**, Huang Z, Wang M, Weng Z, Zeng D, Zhang Y, Zhu Y, Jiang J. Interleukin-6 as an early diagnostic marker for bacterial sepsis in patients with liver cirrhosis. *J Crit Care* 2015; **30**: 732-738 [PMID: 25891645 DOI: 10.1016/j.jcrc.2015.03.031]

30 **Jalan R**, Fernandez J, Wiest R, Schnabl B, Moreau R, Angeli P, Stadlbauer V, Gustot T, Bernardi M, Canton R, Albillos A, Lammert F, Wilmer A, Mookerjee R, Vila J, Garcia-Martinez R, Wendon J, Such J, Cordoba J, Sanyal A, Garcia-Tsao G, Arroyo V, Burroughs A, Ginès P. Bacterial infections in cirrhosis: a position statement based on the EASL Special Conference 2013. *J Hepatol* 2014; **60**: 1310-1324 [PMID: 24530646 DOI: 10.1016/j.jhep.2014.01.024]

31 **Cervoni JP**, Thévenot T, Weil D, Muel E, Barbot O, Sheppard F, Monnet E, Di Martino V. C-reactive protein predicts short-term mortality in patients with cirrhosis. *J Hepatol* 2012; **56**: 1299-1304 [PMID: 22314431 DOI: 10.1016/j.jhep.2011.12.030]

World Journal of Gastroenterology

Submit a Manuscript: https://www.f6publishing.com

World J Gastroenterol 2020 August 28; 26(32): 4866-4877

DOI: 10.3748/wjg.v26.i32.4866

ISSN 1007-9327 (print) ISSN 2219-2840 (online)

ORIGINAL ARTICLE

Observational Study

Inactive matrix Gla protein is elevated in patients with inflammatory bowel disease

Darko Brnic, Dinko Martinovic, Piero Marin Zivkovic, Daria Tokic, Marino Vilovic, Doris Rusic, Ivana Tadin Hadjina, Christian Libers, Sandro Glumac, Daniela Supe-Domic, Ante Tonkic, Josko Bozic

ORCID number: Darko Brnic 0000-0002-2925-0463; Dinko Martinovic 0000-0003-2060-5130; Piero Marin Zivkovic 0000-0001-5649-698X; Daria Tokic 0000-0001-9508-4160; Marino Vilovic 0000-0002-5433-5063; Doris Rusic 0000-0002-7018-4947; Ivana Tadin Hadjina 0000-0002-4443-5896; Christian Libers 0000-0002-2856-9245; Sandro Glumac 0000-0002-9533-1261; Daniela Supe-Domic 0000-0002-5584-3182; Ante Tonkic 0000-0002-3217-6890; Josko Bozic 0000-0003-1634-0635.

Author contributions: Brnic D, Martinovic D and Bozic J were involved in the study conceptualization, methodology design, funding acquisition and manuscript drafting and writing; Zivkovic PM, Tokic D, Vilovic M, Tadin H and Libers C were involved in the literature investigation, software statistical analysis and manuscript visualization and editing; Supe-Domic D, Rusic D and Glumac S were involved in patient sampling, laboratory analysis and manuscript editing; Tonkic A was involved in supervision and project administration.

Institutional review board statement: The study was reviewed and approved by the University Hospital of Split

Darko Brnic, Piero Marin Zivkovic, Ivana Tadin Hadjina, Department of Gastroenterology, University Hospital of Split, Split 21000, Croatia

Dinko Martinovic, Daria Tokic, Department of Emergency Medicine, Institute of Emergency Medicine of Split-Dalmatia County, Split 21000, Croatia

Marino Vilovic, Christian Libers, Josko Bozic, Department of Pathophysiology, University of Split School of Medicine, Split 21000, Croatia

Doris Rusic, Department of Pharmacy, University of Split School of Medicine, Split 21000, Croatia

Sandro Glumac, Department of Anesthesiology and Intensive Care, University Hospital of Split, Split 21000, Croatia

Daniela Supe-Domic, Department of Medical Laboratory Diagnostics, University Hospital of Split, Split 21000, Croatia

Ante Tonkic, Department of Internal Medicine, University of Split School of Medicine, Split 21000, Croatia

Corresponding author: Josko Bozic, MD, PhD, Associate Professor, Department of Pathophysiology, University of Split School of Medicine, Soltanska 2, Split 21000, Croatia. josko.bozic@mefst.hr

Abstract

BACKGROUND

Matrix Gla protein (MGP) is a vitamin K dependent peptide which has an established role in suppression of vascular calcification. Recent studies have pointed to a possible link between immunomodulatory effect of MGP and inflammatory bowel disease (IBD).

AIM

To compare plasma levels of dephosphorylated and uncarboxylated MGP (dp-ucMGP) between IBD patients and controls.

METHODS

This cross-sectional study was conducted on 70 patients with IBD (30 patients

Institutional Review Board (Approval No. 2181-147-01/06/M.S.-17-2).

Conflict-of-interest statement: There are no conflicts of interest to report.

Data sharing statement: Data set is available from the corresponding author at email: josko.bozic@mefst.hr.

Manuscript source: Unsolicited manuscript

Received: May 30, 2020
Peer-review started: May 30, 2020
First decision: June 12, 2020
Revised: July 30, 2020
Accepted: August 15, 2020
Article in press: August 15, 2020
Published online: August 28, 2020

P-Reviewer: Poullis A
S-Editor: Wang DM
L-Editor: A
P-Editor: Zhang YL

with ulcerative colitis and 40 patients with Crohn's disease) and 60 age and gender matching healthy controls. Plasma dp-ucMGP levels were analyzed from blood samples by CLIA method using IDS-iSYS InaKtif MGP (Immunodiagnostic Systems, Frankfurt, Germany) according to the manufacturer's instructions. fecal calprotectin (FC) levels were determined from stool samples by turbidimetric immunoassay method using Bühlmann fecal calprotectin turbo assay (Bühlmann Laboratories Aktiengesellschaft, Schonenbuch, Switzerland). Other parameters were analyzed according to the standard laboratory procedures.

RESULTS

Plasma levels of dp-ucMGP were significantly higher in patients with IBD compared to the healthy control group (629.83 ± 124.20 pmol/mL *vs* 546.7 ± 122.09 pmol/mL, $P < 0.001$), and there was no significant difference between patients with Crohn's disease and patients with ulcerative colitis (640.02 ± 131.88 pmol/mL *vs* 616.23 ± 113.92 pmol/mL, $P = 0.432$). Furthermore, a significant positive correlation of plasma dp-ucMGP levels was found with both FC levels ($r = 0.396$, $P < 0.001$) and high sensitivity C-reactive protein (hsCRP) levels ($r = 0.477$, $P < 0.001$). Moreover, in the total study population a significant positive correlation was found between dp-ucMGP with age ($r = 0.210$, $P = 0.016$) and waist circumference ($r = 0.264$, $P = 0.002$). Multiple linear regression analysis showed that dp-ucMGP levels retained significant association with FC (β ± SE, 0.06 ± 0.02, $P = 0.003$).

CONCLUSION

Study results support experimental data of MGP immunomodulatory IBD effect and indicate potential involvement in the pathophysiology of the disease, and possibly extraintestinal manifestations.

Key words: Matrix Gla protein; Inflammatory bowel disease; Fecal calprotectin; Ulcerative colitis; Crohn's disease

Core tip: Matrix Gla protein (MGP) is well-established as a protector against vascular calcification. Recent studies pointed to a possible link between MGP and inflammatory bowel disease (IBD). Our study found significantly higher inactive plasma MGP levels in patients with IBD compared to the healthy controls and there were no differences between patients with ulcerative colitis and Crohn's disease. Furthermore, there was a significant positive correlation between inactive plasma MGP levels with both fecal calprotectin and high sensitivity C-reactive protein levels. These results imply that MGP is somehow involved in complex IBD pathophysiology.

Citation: Brnic D, Martinovic D, Zivkovic PM, Tokic D, Vilovic M, Rusic D, Tadin Hadjina I, Libers C, Glumac S, Supe-Domic D, Tonkic A, Bozic J. Inactive matrix Gla protein is elevated in patients with inflammatory bowel disease. *World J Gastroenterol* 2020; 26(32): 4866-4877
URL: https://www.wjgnet.com/1007-9327/full/v26/i32/4866.htm
DOI: https://dx.doi.org/10.3748/wjg.v26.i32.4866

INTRODUCTION

Inflammatory bowel disease (IBD) is a chronic, intermittent inflammatory disorder with an unstable course[1]. While the exact etiology of the disease is unknown, it is currently considered to be a complex interaction between genetics, environmental factors, immunological disorders and microbial disturbances[2]. Although the globally highest prevalence of IBD has been reported to be in Europe and North America, incidence in these regions appears to be stable or even on the decline. Yet it is important to stress that the incidence of IBD is rising in newly developing countries in Africa, South America and Asia[3]. A phenotypical classification approach put forward by the Montreal Working Group in 2003 encompasses the forms and the extents of IBD

and classifies them as ulcerative colitis (UC), Crohn´s disease (CD) and indeterminate colitis[4]. It is well established that IBD has numerous extraintestinal manifestations which can affect the joints, eyes, kidneys, liver, skin, blood circulation and neurocognitive performance[5,6]. Furthermore, there is an increased risk of ischemic heart disease that had been reported in patients with IBD[7,8]. Previous studies compared endothelial-dependent dilatation assessed *via* reactive hyperemia and compared it to endothelial-independent dilatation elicited by sublingual isosorbide dinatrate in a set of UC patients with variable disease severity. The endothelial dependent dilatation was significantly worse in patients with severe UC compared to its milder forms. It can be assumed that the systemic inflammatory state evoked by IBD drives the impairment of endothelial function[9,10].

Matrix Gla protein (MGP) is a 12-kDa vitamin K–dependent extracellular matrix protein synthesized mostly by vascular smooth muscle cells and chondrocytes. With high binding affinity to hydroxyapatite crystals, it is considered as one of the most important biological agents in the prevention of vascular calcification[11-13]. Furthermore, increased levels of its inactive dephosphorylated and uncarboxylated form, designated as dp-ucMGP, have been associated with number of different cardiovascular consequences and complications, including endothelial dysfunction, retinal arteriolar narrowing, atherosclerosis, increased aortic stiffness, and higher overall cardiovascular, non-cancer and total mortality[14-17].

However, aside from its cardiovascular importance, experimental studies indicate that MGP might be a novel important mediator of mesenchymal stromal cell-mediated immunomodulation in treating experimental Crohn´s disease in mice. In a recent experiment, lentiviral transfected short hairpin RNA (shRNA) targeting the MGP gene in mesenchymal stromal cells (MSC) of mice was introduced, decreasing MGP secretion compared to insert-free mice. MSCs are known to inhibit the secretion mediated by T-cells of proinflammatory cytokines such as TNF-α and INF-γ. By comparing the inhibition proinflammatory cytokine secretion of T-cells in insert-free mice MSCs to the shRNA modified MSCs, it has been proposed that higher levels of MSC-derived MGP are likely to be the reason for suppressed cytokine production and a possible alleviation of experimental colitis in mice[18].

The possible immunomodulatory role of MGP and its inactive counterpart stresses the importance of further necessary research in this field. However, while experimental studies showed the potential that MGP could bring in managing IBD, clinical studies are still lacking. Therefore, the aim of this study was to investigate plasma dp-ucMGP levels in patients with IBD in comparison with the control group and evaluate the difference of dp-ucMGP levels between UC and CD patients. The additional goal was to investigate the association of plasma dp-ucMGP levels with the anthropometric, clinical and laboratory parameters.

MATERIALS AND METHODS

Study design and ethical considerations

This cross-sectional study was performed at the University Hospital of Split during the period from January 1, 2018 to September 1, 2018.

The study was approved by the Ethics Committee of University Hospital of Split, and was conducted in accordance with all ethical principles of the Helsinki Declaration from 2013. Prior to the commencement of the study, every participant was informed about the procedures, course and purpose of this research, and they individually signed an informed written agreement.

Subjects

The study included 70 adult patients with pre-diagnosed IBD (30 patients with ulcerative colitis and 40 patients with Crohn's disease) and 60 healthy control subjects. IBD was diagnosed in accordance with the European Consensus on Crohn's Disease and Ulcerative Colitis (ECCO)[19]. The control group consisted of healthy volunteers, matched with the age and gender of the investigated group. Inclusion criteria for participation were: At least one year of disease duration and age between 18 and 65 years. Exclusion criteria were: Malignancies; diabetes mellitus; chronic cardiovascular, renal, endocrine and pulmonary diseases; therapy with corticosteroids during 3 mo prior to study onset. Detailed medical records of the control subjects were checked relating to gastrointestinal conditions and additional screening was performed regarding the presence of symptoms according to Rome IV criteria for irritable bowel syndrome[20], as well as any other indications which could suggest gluten and lactose

intolerance. If any of these disorders were found, the subject was excluded from the control group.

Clinical and laboratory evaluation

All participants were subjected to detailed physical examination and measurements of anthropometric traits while relevant clinical information was collected from patient's medical records while anamnestic data were taken directly from all study participants.

Disease severity was evaluated by the same experienced gastroenterologist according to the latest recommendations and the colonoscopy used for the assessment was performed within 2 wk of blood sampling. Disease activity in patients with UC was assessed using Ulcerative colitis endoscopic index of severity (UCEIS) while disease activity in patients with CD was assessed using Simple endoscopic score for Crohn's disease (SES-CD)[21-23].

UCEIS is a grading system used for scoring mucosal inflammation based on the specific endoscopic findings. Three parameters are graded: Vascular pattern; bleeding; erosions and ulcers. Depending on the score there are four possible grades for disease activity: ≤ 1 remission; 2-4 mild activity; 5-6 moderate activity; and ≥ 7 severe disease[22].

SES-CD is a grading system used for endoscopic evaluation of CD activity based on four parameters: Ulcers; extent of affected surface; extent of ulcerated surface; presence and type of narrowing. According to the majority of studies the threshold values for interpretation of the results are: ≤ 2 remission; 3-7 mild activity; 7-15 moderate activity; and ≥ 16 severe disease[23].

Blood samples were collected after 12-h fasting in test tubes with anticoagulant and after extraction were centrifuged and stored at -80°C for further analysis. Blood samples were handled by the same, qualified medical biochemist, who was blinded to the subject's group in the study. Plasma dp-ucMGP levels were analyzed by CLIA method using IDS-iSYS InaKtif MGP (Immunodiagnostic Systems, Frankfurt, Germany) according to the manufacturer's instructions. Minimum limit of detection was 200 pmol/L. Intra-assay coefficient of variability (CV) was 4.5% and inter-assay CV of 7.9%. Plasma high sensitivity C-reactive protein (hs-CRP) levels were determined using a latex turbidimetric method (Abbott Laboratories, Chicago, USA).

Stool samples were collected within 3 d of sampling. FC levels were determined by turbidimetric immunoassay method using Bühlmann fecal calprotectin turbo assay (Bühlmann Laboratories Aktiengesellschaft, Schonenbuch, Switzerland).

Statistical analysis

Statistical analysis was performed using MedCalc for Microsoft Windows (MedCalc Software, Ostend, Belgium, version 17.4.1). Data distribution was analyzed with D'Agostino-Pearson test, and according to results quantitative data was expressed as mean ± standard deviation or median and interquartile range. Qualitative data was expressed as whole number and percentage, with Chi-squared test used for comparison between such variables. Comparison of dp-ucMGP levels and anthropometrics between groups was performed with t-test for independent samples, while Mann-Whitney U test was used to test differences in hsCRP concentrations between IBD and control group. Correlation analysis of dp-ucMGP levels with FC, disease duration and hsCRP was estimated with Spearman rank correlation, while Pearson's correlation coefficient was used to test association between dp-ucMGP levels and age, BMI and waist circumference. Furthermore, multiple linear regression analysis adjusted for age and anthropometric measurements was used to determine significant independent predictors of plasma dp-ucMGP levels. From these analyses, we reported respective *P* values with unstandardized β-coefficients, standard error and *t*-values. In addition, independent predictors for positive IBD status were analyzed with multivariable logistic regression, with OR (odds ratio), 95%CI (95% confidence interval) and *P* value reported. Finally, FC and hsCRP concentrations were divided into tertiles, and according dp-ucMGP levels were calculated and compared using one-way ANOVA with *post hoc* Sceffé test. Statistical significance was set at *P* value < 0.05.

RESULTS

There was no statistically significant difference regarding age, gender and anthropometric features between the patients with IBD and the control group ($P > 0.05$; for all analysis) (Table 1). Endoscopic scores determined that 8 patients were in

Table 1 Baseline characteristics of inflammatory bowel disease patients and healthy controls

Parameter	IBD group (*n* = 70)	Control group (*n* = 60)	*P* value
Men (*n*, %)	46 (65.7)	38 (63.3)	0.778[1]
Women (*n*, %)	24 (34.3)	22 (36.7)	
Age (yr)	40.8 ± 14.9	38.7 ± 12.6	0.390[2]
Body weight (kg)	77.7 ± 12.5	81.3 ± 13.2	0.111[2]
Body height (cm)	177.7 ± 8.2	180.1 ± 9.1	0.132[2]
Body mass index (kg/m^2)	24.6 ± 3.5	25.0 ± 2.8	0.493[2]
Waist circumference (cm)	88.1 ± 12.6	88.0 ± 12.1	0.997[2]
hsCRP (mg/L)	2.65 (1.0-7.8)	0.75 (0.4-1.75)	< 0.001[3]
Fecal calprotectin (μg/g)	235 (56.0-658)	-	-
Disease duration (yr)	8.5 (3.5-13.0)	-	-
UCEIS score	6.0 (5.0-7.0)	-	-
SES-CD	10.3 (5.2-13.6)	-	-
mAb therapy (*n*, %)	48 (68.5%)	-	-

Data are presented as mean ± standard deviation or median or *n* (%).
[1]Chi-squared test.
[2]*t*-test for independent samples.
[3]Mann-Whitney *U* test. UCEIS: Ulcerative Colitis Endoscopic Index of Severity; SES-CD: Simple Endoscopic Score for Crohn's Disease; mAb: Monoclonal antibody; hsCRP: High sensitivity C-reactive protein.

remission, 9 had mild disease, 33 moderate and 20 severe form of disease. Laboratory analysis showed significantly higher hsCRP levels in IBD patients compared to the control group [2.65 (1.0-7.8) mg/L *vs* 0.75 (0.4-1.75) mg/L, $P < 0.001$] (Table 1).

Plasma dp-ucMGP levels were significantly higher in patients with IBD compared with the control group (629.83 ± 124.20 pmol/mL *vs* 546.7 ± 122.09 pmol/mL, $P < 0.001$) and there was no significant difference between patients with CD and patients with UC (640.02 ± 131.88 pmol/mL *vs* 616.23 ± 113.92 pmol/mL, $P = 0.432$) (Figure 1).

A significant positive correlation was found in patients with IBD between dp-ucMGP and fecal calprotectin (FC) levels ($r = 0.396$, $P < 0.001$), but there was no significant correlation between dp-ucMGP and the disease duration ($r = -0.190$, $P = 0.115$) (Figure 2). Moreover, in the total study population a significant positive correlation was found between dp-ucMGP and hsCRP ($r = 0.477$, $P < 0.001$), age ($r = 0.210$, $P = 0.016$) and waist circumference ($r = 0.264$, $P = 0.002$) (Figure 3).

Comparison of hsCRP tertiles in patients with IBD (F-ratio = 11.22, $P = 0.004$) showed a significantly higher dp-ucMGP plasma levels in the 3rd tertile compared to both the 2nd and the 1st tertiles ($P < 0.05$) (Figure 4). Moreover, comparison of FC tertiles in patients with IBD (F-ratio = 7.81, $P = 0.014$) also showed a significantly higher levels of plasma dp-ucMGP in the 3rd tertile compared to both the 2nd and the 1st tertiles ($P < 0.05$) (Figure 4).

Multiple linear regression analysis showed that dp-ucMGP levels retained significant association with FC (β ± SE, 0.06 ± 0.02, $P = 0.003$) and waist circumference (4.35 ± 1.72, $P = 0.013$) after model adjustment for BMI, age and disease duration, with plasma dp-ucMGP levels as a dependent variable (Table 2). Furthermore, multivariable logistic regression showed that plasma dp-ucMGP was a significant predictor of positive IBD status when computed along with baseline characteristics (OR 1.006, 95%CI: 1.002-1.009, $P < 0.001$). There was no significant difference in plasma dp-ucMGP levels between patients with IBD who are using mAb therapy and those who are not using mAb therapy (621.37 ± 115.03 pmol/L *vs* 648.27 ± 143.36 pmol/L, $P = 0.404$).

DISCUSSION

This cross-sectional study showed that plasma dp-ucMGP levels are significantly

Table 2 Multiple linear regression model of independent predictors for dephosphorylated and uncarboxylated matrix Gla protein concentration

Variable	β[1]	SE	*t* value	*P* value
Fecal calprotectin (μg/g)	0.06	0.02	3.08	0.003
hsCRP (mg/L)	0.66	0.47	1.41	0.162
Body mass index (kg/m^2)	-11.15	5.82	-1.92	0.058
Age (years)	1.87	1.13	1.65	0.102
Waist circumference (cm)	4.35	1.72	2.54	0.013
Disease duration (yr)	-3.96	1.81	-1.84	0.062

[1]Unstandardized coefficient β. SE: Standard error; hsCRP: High sensitivity C-reactive protein.

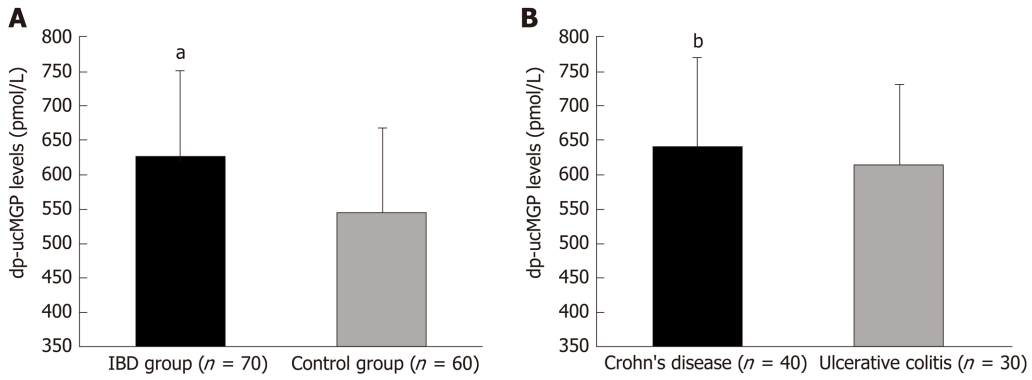

Figure 1 Plasma dephosphorylated and uncarboxylated matrix Gla protein levels in inflammatory bowel disease patients and control group (A) and between patients with Crohn's disease and ulcerative colitis (B). [a]*P* < 0.001 *vs* control group; [b]*P* = 0.432 *vs* ulcerative colitis group. dp-ucMGP: Dephosphorylated and uncarboxylated matrix Gla protein.

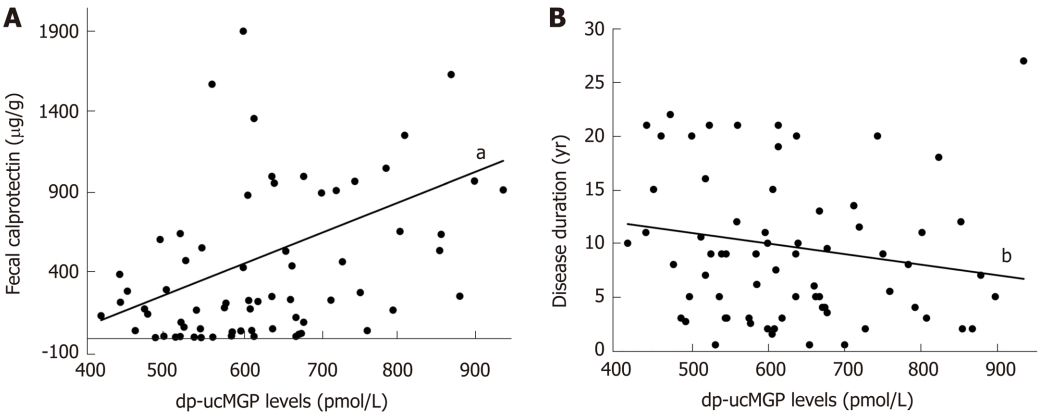

Figure 2 Correlation analysis between plasma dephosphorylated and uncarboxylated matrix Gla protein levels and fecal calprotectin (A) and disease duration (B) in patients with inflammatory bowel disease (*n* = 70). [a]*P* < 0.001, *r* = 0.396; [b]*P* = 0.115, *r* = -0.190. dp-ucMGP: Dephosphorylated and uncarboxylated matrix Gla protein.

higher in patients with IBD compared to the healthy control group, while there was no significant difference between UC and CD patients. Furthermore, there was a significant positive correlation between dp-ucMGP with both hsCRP and FC levels. As far as we know, this is the first clinical study that investigated plasma dp-ucMGP levels in patients with IBD.

Given results are in line with the outcomes of a recent study conducted on human patients with UC and on mice with dextran sulfate sodium (DSS) induced colitis[24].

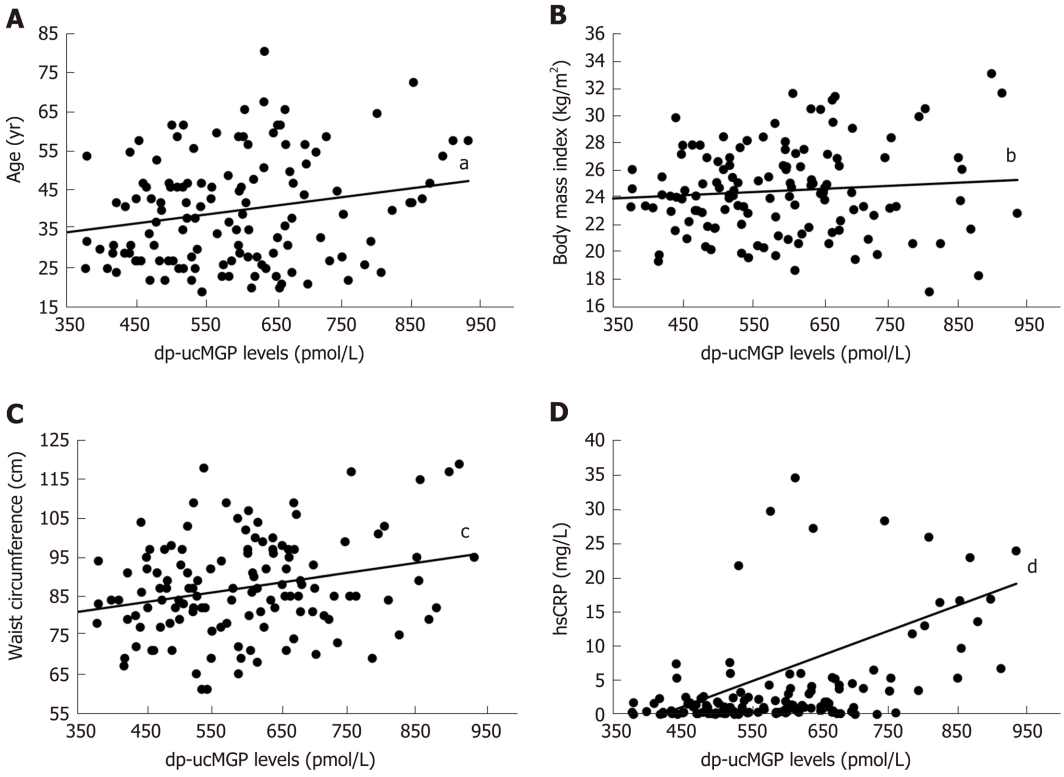

Figure 3 Correlation analysis between plasma dephosphorylated and uncarboxylated matrix Gla protein levels and age (A), body Mass Index (B) waist circumference (C) and hsCRP (D) in total study population (n = 130). [a]P = 0.016, r = 0.210; [b]P = 0.289, r = 0.094; [c]P = 0.002, r = 0.264; [d]P < 0.001, r = 0.477.

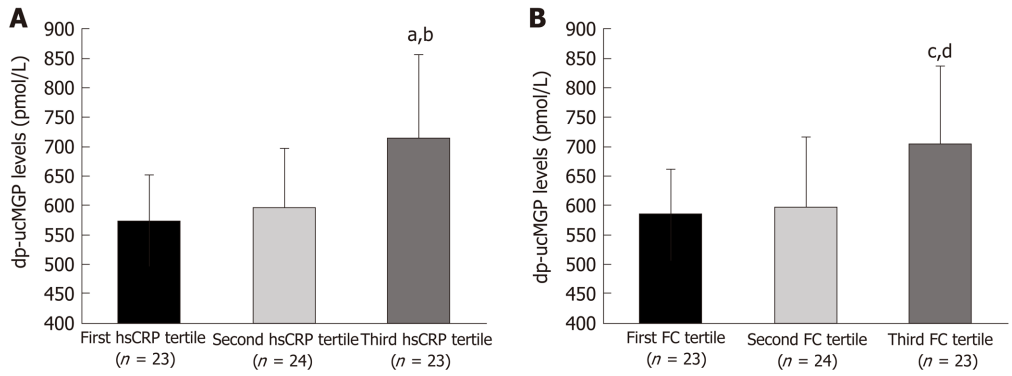

Figure 4 Dephosphorylated and uncarboxylated matrix Gla protein concentrations between tertiles of high sensitivity C-reactive protein (A) and FC levels (B). Tested with one-way analysis of variance with *post hoc* Sceffé test to examine differences between each of the groups; [a]P < 0.05 *vs* first hsCRP tertile; [b]P < 0.05 *vs* second hsCRP tertile ; [c]P < 0.05 *vs* first FC tertile; [d]P < 0.05 *vs* second FC tertile; hsCRP: High sensitivity C-reactive protein; FC: Fecal calprotectin.

They showed that MGP mRNA levels are significantly higher in both UC patients and DSS-induced colitis mice compared to their control groups. Additionally, they showed that the expression of MGP mRNA increases with the disease severity while patients in remission had a similar MGP mRNA expression as the healthy controls. Feng Y *et al*[18] in their study conducted on MSC reported an immunomodulatory effect of MGP by showing that *in vitro* MGP reduces proliferation and production of proinflammatory cytokines in T-cells. Furthermore, by using mouse models with experimentally induced colitis, they compared results from intraperitoneal injection of MSC with knockout MGP and those with insert free MSC. The results showed that MGP improved the clinical and histopathological severity of colonic inflammation, alleviated the T-cells infiltration and suppressed the production of pro-inflammatory cytokines in colon tissues. These results indicate that MGP could play an important

role in IBD inflammation and it could even have a therapeutic effect.

Another common feature that could link higher dp-ucMGP in IBD patients and positive association with inflammatory markers is endothelial dysfunction. It is well-established that intestinal inflammation leads to functional and structural changes of the vascular endothelium, which can consequently lead to increased cardiovascular risk in IBD patients[25,26]. Moreover, as disease severity and inflammation rise, greater endothelial dysfunction accompanies these changes. On the other hand, studies have also linked higher dp-ucMGP concentrations with markers of endothelial dysfunction in patients on hemodialysis *via* brachial artery flow-mediated dilation (FMD)[27], and in healthy postmenopausal women *via* biochemical markers (Vascular Cell Adhesion Molecule, VCAM; E-selectin; Advanced Glycation Endproducts, AGEs)[28]. According to these data, it is evident that dp-ucMGP concentration could easily be increased due to combined features of its ameliorative effect on active inflammatory process, increased endothelial dysfunction present in such process, but also due to vitamin K deficiency as well.

It is known that MGP depends on vitamin K for its full activation through carboxylation of Gla residues, followed by phosphorylation of serine residues. Furthermore, its inactive form has been acknowledged as a direct marker of vitamin K deficiency, due to its inability to be contained in artery wall, and consequent plasmatic accumulation[29]. Moreover, there is a well-established connection between IBD and vitamin K deficiency, with malnutrition stated as a leading cause of disorder[30,31]. Due to exacerbation of abdominal pain, patients tend to avoid food entirely, or they are using parenteral nutrition without administrating proper supplements[32]. Additionally, due to ulcerations, erosions and surgical resections they have a reduction of the intestinal absorptive surface and consequently vitamin K malabsorption[33]. However, in a recent RCT study, IBD patients were given daily supplementation of 1000 μg of vitamin K_1 (phylloquinone) during a 12-mo period, with results showing no significant effect of the indices of their bone health[34]. Those results imply that although the patients were taking a large supplementation dose of vitamin K_1, there was no significant beneficial effect coming along with the improvement of their vitamin K status. It is possible that vitamin K_2 (menaquinone) deficiency is the main reason for such results due to a recent study showing vitamin K_2 as a more potent and effective bone and vascular protector than vitamin K_1[35]. Furthermore, two large scale studies showed that an adequate dietary intake of vitamin K_2 significantly correlates with better cardiovascular and bone health, while they failed to prove that vitamin K_1 demonstrates any protective value against vascular calcification and osteoporosis[36,37]. Interestingly, patients with IBD have a higher risk of coronary heart disease and heart failure[38], while the prevalence of high BMI, diabetes, hyperlipidemia, obesity, hypertension, lack of physical activity and other traditional cardiovascular risk factors is fairly lower in comparison with the general population[39,40]. Possible reason for cumulative increase in cardiovascular risks could lie in accelerated promotion of vascular calcification, one of the most prominent risk factors for cardiovascular diseases, due to inability of dp-ucMGP to fully activate in vitamin K_2 deficiency. Furthermore, several studies already confirmed significant association of elevated dp-ucMGP concentrations with promotion of vascular calcification[41,42]. Knapen *et al*[28] conducted an RCT study that further confirms these results. They showed that three years of vitamin K_2 supplementation in healthy postmenopausal women significantly improved arterial stiffness parameters, and decreased dp-ucMGP concentrations by 50% in comparison with placebo. Additionally, a recent study conducted on mice with DSS induced colitis reported that mice supplemented with vitamin K_2 showed reduced symptoms of colitis along with a decrease of IL-6 expression[43]. Nevertheless, MGP and vitamin K_2 are tightly related, and all these evidence stresses the need of addressing their involvement and possible therapeutic admission for IBD in future studies.

Another interesting finding of this study is the positive correlation of plasma dp-ucMGP levels with both FC and hsCRP. A recent study showed that MGP is synthesized and carboxylated in the majority of human immune system cells which are either involved in innate or adaptive immune reactions[44]. Furthermore, it showed that stimulation of monocytes and macrophages with LPS or hydroxyapatite triggered an inflammatory response which up regulated MGP expression following the up-regulation pattern of IL-1β. These results indicate that MGP is somehow involved in the inflammatory response mechanisms of monocytes and macrophages. Inflammation is considered as a potential leading cause in promotion of vascular calcification, and it is closely associated with endothelial dysfunction, with both conditions being hallmarks of IBD. Both FC and CRP are established and used as markers of IBD activity and severity[45] while several studies showed a significant correlation between

CRP and coronary artery calcification[46-48]. Our findings could be implying that increased IBD activity up regulates MGP through complex inflammatory mechanisms, but due to possible vitamin K deficiency, the peptide cannot be fully activated and therefore loses its inhibitory effect on vascular calcification. This would be in line with the results of a Danish cohort study, which reported that flares and persistent IBD activity increases the risk of myocardial infarction, stroke and cardiovascular death[49], and the previously mentioned study on UC patients which showed that the expression of MGP mRNA increases with the disease severity[24]. Moreover, after division of patients with IBD into tertiles depending on hsCRP levels and FC levels our study showed in both cases significantly higher plasma levels of dp-ucMGP in the 3rd tertile compared to the 1st and 2nd tertiles which further indicates the possible association of dp-ucMGP with the IBD activity. However, additional research is needed to give us a better insight of the relationship between MGP and IBD activity.

The limitation of our study was its cross-sectional design and a relatively small sample size. Additionally, due to technical reasons we were not able to determine vitamin K_2 levels in patients with IBD.

CONCLUSION

This is the first study that proved higher plasma dp-ucMGP levels in patients with IBD and showed a significant positive correlation between dp-ucMGP with both hsCRP and FC levels. Overall, our results support previous experimental data of MGP involvement in IBD pathophysiology through inflammation process and disease activity. However, these findings should be addressed in future larger studies.

ARTICLE HIGHLIGHTS

Research background

Several recent studies have pointed to a possible link between immunomodulatory effect of matrix Gla protein (MGP) and inflammatory bowel disease (IBD). Their results showed that MGP improved the clinical and histopathological severity of colonic inflammation, alleviated the T-cells infiltration and suppressed the production of pro-inflammatory cytokines in colon tissues.

Research motivation

While experimental studies showed the potential that MGP could bring in managing IBD, clinical studies are still lacking.

Research objectives

The aim of this study was to compare plasma levels of inactive dephosphorylated and uncarboxylated (dp-ucMGP) between patients with IBD and healthy controls. The additional goal was to investigate the association of plasma dp-ucMGP levels with the anthropometric, clinical and laboratory parameters.

Research methods

This cross-sectional study was conducted on 70 patients with IBD (30 patients with ulcerative colitis and 40 patients with Crohn's disease) and 60 age and gender matching healthy controls. Plasma dp-ucMGP levels were analyzed from blood samples by CLIA method using IDS-iSYS InaKtif MGP (Immunodiagnostic Systems, Frankfurt, Germany) according to the manufacturer's instructions. Other parameters were analyzed according to the standard laboratory procedures.

Research results

Plasma levels of dp-ucMGP were significantly higher in patients with IBD compared to the control group ($P < 0.001$), and there was no significant difference between patients with Crohn's disease and patients with ulcerative colitis ($P = 0.432$). Furthermore, a significant positive correlation of plasma dp-ucMGP levels was found with both fecal calprotectin levels ($P < 0.001$) and hsCRP levels ($P < 0.001$).

Research conclusions

Our clinical results support previous experimental data of MGP involvement in IBD

pathophysiology through inflammation process and disease activity.

Research perspectives

The potential MGP immunomodulatory effect should be addressed with larger scale studies in the future.

REFERENCES

1 **Kim DH**, Cheon JH. Pathogenesis of Inflammatory Bowel Disease and Recent Advances in Biologic Therapies. *Immune Netw* 2017; **17**: 25-40 [PMID: 28261018 DOI: 10.4110/in.2017.17.1.25]

2 **Zhang YZ**, Li YY. Inflammatory bowel disease: pathogenesis. *World J Gastroenterol* 2014; **20**: 91-99 [PMID: 24415861 DOI: 10.3748/wjg.v20.i1.91]

3 **Ng SC**, Shi HY, Hamidi N, Underwood FE, Tang W, Benchimol EI, Panaccione R, Ghosh S, Wu JCY, Chan FKL, Sung JJY, Kaplan GG. Worldwide incidence and prevalence of inflammatory bowel disease in the 21st century: a systematic review of population-based studies. *Lancet* 2018; **390**: 2769-2778 [PMID: 29050646 DOI: 10.1016/s0140.6736(17)32448-0]

4 **Satsangi J**, Silverberg MS, Vermeire S, Colombel JF. The Montreal classification of inflammatory bowel disease: controversies, consensus, and implications. *Gut* 2006; **55**: 749-753 [PMID: 16698746 DOI: 10.1136/gut.2005.082909]

5 **Vavricka SR**, Schoepfer A, Scharl M, Lakatos PL, Navarini A, Rogler G. Extraintestinal Manifestations of Inflammatory Bowel Disease. *Inflamm Bowel Dis* 2015; **21**: 1982-1992 [PMID: 26154136 DOI: 10.1097/mib.0000000000000392]

6 **Tadin Hadjina I**, Zivkovic PM, Matetic A, Rusic D, Vilovic M, Bajo D, Puljiz Z, Tonkic A, Bozic J. Impaired neurocognitive and psychomotor performance in patients with inflammatory bowel disease. *Sci Rep* 2019; **9**: 13740 [PMID: 31551482 DOI: 10.1030/s41598-019-50192-2]

7 **Singh S**, Singh H, Loftus EV Jr, Pardi DS. Risk of cerebrovascular accidents and ischemic heart disease in patients with inflammatory bowel disease: a systematic review and meta-analysis. *Clin Gastroenterol Hepatol* 2014; **12**: 382-93.e1: quiz e22 [PMID: 23978350 DOI: 10.1016/j.cgh.2013.08.023]

8 **Schicho R**, Marsche G, Storr M. Cardiovascular complications in inflammatory bowel disease. *Curr Drug Targets* 2015; **16**: 181-188 [PMID: 25642719 DOI: 10.2174/1389450116666502021615 00]

9 **Kocaman O**, Sahin T, Aygun C, Senturk O, Hulagu S. Endothelial dysfunction in patients with ulcerative colitis. *Inflamm Bowel Dis* 2006; **12**: 166-171 [PMID: 16534416 DOI: 10.1097/01.mib.0000217764.88980.74]

10 **Principi M**, Mastrolonardo M, Scicchitano P, Gesualdo M, Sassara M, Guida P, Bucci A, Zito A, Caputo P, Albano F, Ierardi E, Di Leo A, Ciccone MM. Endothelial function and cardiovascular risk in active inflammatory bowel diseases. *J Crohns Colitis* 2013; **7**: e427-e433 [PMID: 23473915 DOI: 10.1016/j.crohns.2013.02.001]

11 **Hackeng TM**, Rosing J, Spronk HM, Vermeer C. Total chemical synthesis of human matrix Gla protein. *Protein Sci* 2001; **10**: 864-870 [PMID: 11274477 DOI: 10.1110/ps.44701]

12 **Barrett H**, O'Keeffe M, Kavanagh E, Walsh M, O'Connor EM. Is Matrix Gla Protein Associated with Vascular Calcification? A Systematic Review. *Nutrients* 2018; **10** [PMID: 29584693 DOI: 10.3390/nu10040415]

13 **Vilovic M**, Dogas Z, Ticinovic Kurir T, Borovac JA, Supe-Domic D, Vilovic T, Ivkovic N, Rusic D, Novak A, Bozic J. Bone metabolism parameters and inactive matrix Gla protein in patients with obstructive sleep apnea†. *Sleep* 2020; **43** [PMID: 31631227 DOI: 10.1093/sleep/zsz243]

14 **Wei FF**, Huang QF, Zhang ZY, Van Keer K, Thijs L, Trenson S, Yang WY, Cauwenberghs N, Mujaj B, Kuznetsova T, Allegaert K, Struijker-Boudier HAJ, Verhamme P, Vermeer C, Staessen JA. Inactive matrix Gla protein is a novel circulating biomarker predicting retinal arteriolar narrowing in humans. *Sci Rep* 2018; **8**: 15088 [PMID: 30305657 DOI: 10.1038/s41598-018-33257-6]

15 **Liu YP**, Gu YM, Thijs L, Knapen MH, Salvi E, Citterio L, Petit T, Carpini SD, Zhang Z, Jacobs L, Jin Y, Barlassina C, Manunta P, Kuznetsova T, Verhamme P, Struijker-Boudier HA, Cusi D, Vermeer C, Staessen JA. Inactive matrix Gla protein is causally related to adverse health outcomes: a Mendelian randomization study in a Flemish population. *Hypertension* 2015; **65**: 463-470 [PMID: 25421980 DOI: 10.1161/hypertensionaha.114.04494]

16 **Mayer O Jr**, Seidlerová J, Wohlfahrt P, Filipovský J, Vaněk J, Cífková R, Windrichová J, Topolčan O, Knapen MH, Drummen NE, Vermeer C. Desphospho-uncarboxylated matrix Gla protein is associated with increased aortic stiffness in a general population. *J Hum Hypertens* 2016; **30**: 418-423 [PMID: 26016598 DOI: 10.1038/jhh.2015.55]

17 **Yao J**, Guihard PJ, Blazquez-Medela AM, Guo Y, Liu T, Boström KI, Yao Y. Matrix Gla protein regulates differentiation of endothelial cells derived from mouse embryonic stem cells. *Angiogenesis* 2016; **19**: 1-7 [PMID: 26364300 DOI: 10.1007/s10456-015-9484-3]

18 **Feng Y**, Liao Y, Huang W, Lai X, Luo J, Du C, Lin J, Zhang Z, Qiu D, Liu Q, Shen H, Xiang AP, Zhang Q. Mesenchymal stromal cells-derived matrix Gla protein contribute to the alleviation of experimental colitis. *Cell Death Dis* 2018; **9**: 691 [PMID: 29880866 DOI: 10.1038/s41419-018-0734-3]

19 **Magro F**, Gionchetti P, Eliakim R, Ardizzone S, Armuzzi A, Barreiro-de Acosta M, Burisch J, Gecse KB, Hart AL, Hindryckx P, Langner C, Limdi JK, Pellino G, Zagorowicz E, Raine T, Harbord M, Rieder F, European Crohn's and Colitis Organisation [ECCO]. Third European Evidence-based Consensus on Diagnosis and Management of Ulcerative Colitis. Part 1: Definitions, Diagnosis, Extra-intestinal Manifestations, Pregnancy, Cancer Surveillance, Surgery, and Ileo-anal Pouch Disorders. *J Crohns Colitis* 2017; **11**: 649-670 [PMID: 28158501 DOI: 10.1093/ecco-jcc/jjx008]

20 **Schmulson MJ**, Drossman DA. What Is New in Rome IV. *J Neurogastroenterol Motil* 2017; **23**: 151-163 [PMID: 28274109 DOI: 10.5056/jnm16214]

21 **Sturm A**, Maaser C, Calabrese E, Annese V, Fiorino G, Kucharzik T, Vavricka SR, Verstockt B, van Rheenen P, Tolan D, Taylor SA, Rimola J, Rieder F, Limdi JK, Laghi A, Krustins E, Kotze PG, Kopylov U, Katsanos K, Halligan S, Gordon H, Gonzalez Lama Y, Ellul P, Eliakim R, Castiglione F, Burisch J, Borralho Nunes P, Bettenworth D, Baumgart DC, Stoker J, European Crohn's and Colitis Organisation [ECCO] and the European Society of Gastrointestinal and Abdominal Radiology [ESGAR]. ECCO-ESGAR Guideline for Diagnostic Assessment in IBD Part 2: IBD scores and general principles and technical aspects. *J Crohns Colitis* 2019; **13**: 273-284 [PMID: 30137278 DOI: 10.1093/ecco-jcc/jjy114]

22 **Travis SP**, Schnell D, Krzeski P, Abreu MT, Altman DG, Colombel JF, Feagan BG, Hanauer SB, Lichtenstein GR, Marteau PR, Reinisch W, Sands BE, Yacyshyn BR, Schnell P, Bernhardt CA, Mary JY, Sandborn WJ. Reliability and initial validation of the ulcerative colitis endoscopic index of severity. *Gastroenterology* 2013; **145**: 987-995 [PMID: 23891974 DOI: 10.1053/j.gastro.2013.07.024]

23 **Daperno M**, D'Haens G, Van Assche G, Baert F, Bulois P, Maunoury V, Sostegni R, Rocca R, Pera A, Gevers A, Mary JY, Colombel JF, Rutgeerts P. Development and validation of a new, simplified endoscopic activity score for Crohn's disease: the SES-CD. *Gastrointest Endosc* 2004; **60**: 505-512 [PMID: 15472670 DOI: 10.1016/s0016-5107(04)01878-4]

24 **Dong XY**, Wu MX, Zhang HM, Lyu H, Qian JM, Yang H. Association between matrix Gla protein and ulcerative colitis according to DNA microarray data. *Gastroenterol Rep (Oxf)* 2020; **8**: 66-75 [PMID: 32257220 DOI: 10.1093/gastro/goz038]

25 **Cibor D**, Domagala-Rodacka R, Rodacki T, Jurczyszyn A, Mach T, Owczarek D. Endothelial dysfunction in inflammatory bowel diseases: Pathogenesis, assessment and implications. *World J Gastroenterol* 2016; **22**: 1067-1077 [PMID: 26811647 DOI: 10.3748/wjg.v22.i3.1067]

26 **Zivkovic PM**, Matetic A, Tadin Hadjina I, Rusic D, Vilovic M, Supe-Domic D, Borovac JA, Mudnic I, Tonkic A, Bozic J. Serum Catestatin Levels and Arterial Stiffness Parameters Are Increased in Patients with Inflammatory Bowel Disease. *J Clin Med* 2020; **9** [PMID: 32110996 DOI: 10.3390/jcm9030628]

27 **Fain ME**, Kapuku GK, Paulson WD, Williams CF, Raed A, Dong Y, Knapen MHJ, Vermeer C, Pollock NK. Inactive Matrix Gla Protein, Arterial Stiffness, and Endothelial Function in African American Hemodialysis Patients. *Am J Hypertens* 2018; **31**: 735-741 [PMID: 29635270 DOI: 10.1093/ajh/hpy049]

28 **Knapen MH**, Braam LA, Drummen NE, Bekers O, Hoeks AP, Vermeer C. Menaquinone-7 supplementation improves arterial stiffness in healthy postmenopausal women. A double-blind randomised clinical trial. *Thromb Haemost* 2015; **113**: 1135-1144 [PMID: 25694037 DOI: 10.1160/th14-08-0675]

29 **Dalmeijer GW**, van der Schouw YT, Magdeleyns E, Ahmed N, Vermeer C, Beulens JW. The effect of menaquinone-7 supplementation on circulating species of matrix Gla protein. *Atherosclerosis* 2012; **225**: 397-402 [PMID: 23062766 DOI: 10.1016/j.atherosclerosis.2012.09.019]

30 **Fabisiak N**, Fabisiak A, Watala C, Fichna J. Fat-soluble Vitamin Deficiencies and Inflammatory Bowel Disease: Systematic Review and Meta-Analysis. *J Clin Gastroenterol* 2017; **51**: 878-889 [PMID: 28858940 DOI: 10.1097/mcg.0000000000000911]

31 **Kuwabara A**, Tanaka K, Tsugawa N, Nakase H, Tsuji H, Shide K, Kamao M, Chiba T, Inagaki N, Okano T, Kido S. High prevalence of vitamin K and D deficiency and decreased BMD in inflammatory bowel disease. *Osteoporos Int* 2009; **20**: 935-942 [PMID: 18825300 DOI: 10.1007/s00198-008-0764-2]

32 **Zallot C**, Quilliot D, Chevaux JB, Peyrin-Biroulet C, Guéant-Rodriguez RM, Freling E, Collet-Fenetrier B, Williet N, Ziegler O, Bigard MA, Guéant JL, Peyrin-Biroulet L. Dietary beliefs and behavior among inflammatory bowel disease patients. *Inflamm Bowel Dis* 2013; **19**: 66-72 [PMID: 22467242 DOI: 10.1002/ibd.22965]

33 **Lucendo AJ**, De Rezende LC. Importance of nutrition in inflammatory bowel disease. *World J Gastroenterol* 2009; **15**: 2081-2088 [PMID: 19418580 DOI: 10.3748/wjg.15.]

34 **O'Connor EM**, Grealy G, McCarthy J, Desmond A, Craig O, Shanahan F, Cashman KD. Effect of phylloquinone (vitamin K1) supplementation for 12 months on the indices of vitamin K status and bone health in adult patients with Crohn's disease. *Br J Nutr* 2014; **112**: 1163-1174 [PMID: 25181575 DOI: 10.1017/s0007114514001913]

35 **van Ballegooijen AJ**, Beulens JW. The Role of Vitamin K Status in Cardiovascular Health: Evidence from Observational and Clinical Studies. *Curr Nutr Rep* 2017; **6**: 197-205 [PMID: 28944098 DOI: 10.1007/s13668-017-0208-8]

36 **Geleijnse JM**, Vermeer C, Grobbee DE, Schurgers LJ, Knapen MH, van der Meer IM, Hofman A, Witteman JC. Dietary intake of menaquinone is associated with a reduced risk of coronary heart disease: the Rotterdam Study. *J Nutr* 2004; **134**: 3100-3105 [PMID: 15514282 DOI: 10.1093/jn/134.11.3100]

37 **Gast GC**, de Roos NM, Sluijs I, Bots ML, Beulens JW, Geleijnse JM, Witteman JC, Grobbee DE, Peeters PH, van der Schouw YT. A high menaquinone intake reduces the incidence of coronary heart disease. *Nutr Metab Cardiovasc Dis* 2009; **19**: 504-510 [PMID: 19179058 DOI: 10.1016/j.numecd.2008.10.004]

38 **Yarur AJ**, Deshpande AR, Pechman DM, Tamariz L, Abreu MT, Sussman DA. Inflammatory bowel disease is associated with an increased incidence of cardiovascular events. *Am J Gastroenterol* 2011; **106**: 741-747 [PMID: 21386828 DOI: 10.1038/ajg.2011.63]

39 **Jahnsen J**, Falch JA, Mowinckel P, Aadland E. Body composition in patients with inflammatory bowel disease: a population-based study. *Am J Gastroenterol* 2003; **98**: 1556-1562 [PMID: 12873577 DOI: 10.1111/j.1572-0241.2003.07520.x]

40 **Geerling BJ**, Badart-Smook A, Stockbrügger RW, Brummer RJ. Comprehensive nutritional status in recently diagnosed patients with inflammatory bowel disease compared with population controls. *Eur J Clin Nutr* 2000; **54**: 514-521 [PMID: 10878655 DOI: 10.1038/sj.ejcn.1601049]

41 **Dalmeijer GW**, van der Schouw YT, Vermeer C, Magdeleyns EJ, Schurgers LJ, Beulens JW. Circulating matrix Gla protein is associated with coronary artery calcification and vitamin K status in healthy women. *J Nutr Biochem* 2013; **24**: 624-628 [PMID: 22819559 DOI: 10.1016/j.jnutbio.2012.02.012]

42 **Budoff MJ**, Shaw LJ, Liu ST, Weinstein SR, Mosler TP, Tseng PH, Flores FR, Callister TQ, Raggi P, Berman DS. Long-term prognosis associated with coronary calcification: observations from a registry of 25,253 patients. *J Am Coll Cardiol* 2007; **49**: 1860-1870 [PMID: 17481445 DOI: 10.1016/j.jacc.2006.10.079]

43 **Shiraishi E**, Iijima H, Shinzaki S, Nakajima S, Inoue T, Hiyama S, Kawai S, Araki M, Yamaguchi T,

Hayashi Y, Fujii H, Nishida T, Tsujii M, Takehara T. Vitamin K deficiency leads to exacerbation of murine dextran sulfate sodium-induced colitis. *J Gastroenterol* 2016; **51**: 346-356 [PMID: 26314836 DOI: 10.1007/s00535-015-1112-x]

44 **Viegas CSB**, Costa RM, Santos L, Videira PA, Silva Z, Araújo N, Macedo AL, Matos AP, Vermeer C, Simes DC. Gla-rich protein function as an anti-inflammatory agent in monocytes/macrophages: Implications for calcification-related chronic inflammatory diseases. *PLoS One* 2017; **12**: e0177829 [PMID: 28542410 DOI: 10.1371/journal.pone.0177829]

45 **Norouzinia M**, Chaleshi V, Alizadeh AHM, Zali MR. Biomarkers in inflammatory bowel diseases: insight into diagnosis, prognosis and treatment. *Gastroenterol Hepatol Bed Bench* 2017; **10**: 155-167 [PMID: 29118930]

46 **Li JJ**, Zhu CG, Yu B, Liu YX, Yu MY. The role of inflammation in coronary artery calcification. *Ageing Res Rev* 2007; **6**: 263-270 [PMID: 17964226 DOI: 10.1016/j.arr.2007.09.001]

47 **Stompór T**, Pasowicz M, SulÅ‚owicz W, DembiÅ„ska-KieÄ‡ A, Janda K, Wójcik K, Tracz W, Zdzienicka A, Klimeczek P, Janusz-Grzybowska E. An association between coronary artery calcification score, lipid profile, and selected markers of chronic inflammation in ESRD patients treated with peritoneal dialysis. *Am J Kidney Dis* 2003; **41**: 203-211 [PMID: 12500238 DOI: 10.1053/ajkd.2003.50005]

48 **Wang TJ**, Larson MG, Levy D, Benjamin EJ, Kupka MJ, Manning WJ, Clouse ME, D'Agostino RB, Wilson PW, O'Donnell CJ. C-reactive protein is associated with subclinical epicardial coronary calcification in men and women: the Framingham Heart Study. *Circulation* 2002; **106**: 1189-1191 [PMID: 12208790 DOI: 10.1161/01.cir.0000032135.98011.c4]

49 **Kristensen SL**, Ahlehoff O, Lindhardsen J, Erichsen R, Jensen GV, Torp-Pedersen C, Nielsen OH, Gislason GH, Hansen PR. Disease activity in inflammatory bowel disease is associated with increased risk of myocardial infarction, stroke and cardiovascular death--a Danish nationwide cohort study. *PLoS One* 2013; **8**: e56944 [PMID: 23457642 DOI: 10.1371/journal.pone.0056944]

World Journal of Gastroenterology

Submit a Manuscript: https://www.f6publishing.com

World J Gastroenterol 2020 August 28; 26(32): 4878-4888

DOI: 10.3748/wjg.v26.i32.4878

ISSN 1007-9327 (print) ISSN 2219-2840 (online)

ORIGINAL ARTICLE

Prospective Study

Emergency department targeted screening for hepatitis C does not improve linkage to care

Inbal Houri, Noya Horowitz, Helena Katchman, Yael Weksler, Ofer Miller, Liat Deutsch, Oren Shibolet

ORCID number: Inbal Houri 0000-0002-6397-6604; Noya Horowitz 0000-0002-2678-1533; Helena Katchman 0000-0001-8490-1735; Yael Weksler 0000-0003-1143-0498; Ofer Miller 0000-0002-7035-5371; Liat Deutsch 0000-0001-5022-4318; Oren Shibolet 0000-0003-6111-5067.

Author contributions: Shibolet O, Horowitz N and Katchman H designed the research; Weksler Y and Miller O performed the research; Houri I and Deutsch L analyzed the data; Houri I and Shibolet O wrote the paper; Houri I, Katchman H, Deutsch L and Shibolet O critically reviewed the manuscript.

Supported by an Educational Grant from AbbVie Inc. Israel.

Institutional review board statement: The study was reviewed and approved by the Tel-Aviv Medical Center institutional review board (IRB) (0634-16). All study participants screened provided informed consent prior to study enrollment.

Informed consent statement: The informed consent to the study was provided.

Conflict-of-interest statement: O.S received consultation fees from Abbvie Inc. Israel but not

Inbal Houri, Noya Horowitz, Helena Katchman, Yael Weksler, Ofer Miller, Liat Deutsch, Oren Shibolet, Department of Gastroenterology and Hepatology, Tel-Aviv Medical Center, Tel-Aviv 6423906, Israel

Inbal Houri, Helena Katchman, Yael Weksler, Ofer Miller, Liat Deutsch, Oren Shibolet, Sackler Faculty of Medicine, Tel-Aviv University, Tel-Aviv 6997801, Israel

Corresponding author: Oren Shibolet, MD, Professor, Director, Department of Gastroenterology and Hepatology, Tel-Aviv Medical Center, Weizmann 6, Tel-Aviv 6423906, Israel. orensh@tlvmc.gov.il

Abstract

BACKGROUND

Hepatitis C virus (HCV) infection is a leading cause of chronic liver disease worldwide. New treatments for HCV revolutionized management and prompted the world health organization to set the goal of viral elimination by 2030. These developments strengthen the need for HCV screening in order to identify asymptomatic carriers prior to development of chronic liver disease and its complications. Different screening strategies have been attempted, most targeting high-risk populations. Previous studies focusing on patients arriving at emergency departments showed a higher prevalence of HCV compared to the general population.

AIM

To identify previously undiagnosed HCV carriers among high risk emergency room attendees and link them to care for anti-viral treatment.

METHODS

In this single center prospective study, persons visiting the emergency department in an urban hospital were screened by a risk factor-specific questionnaire. The risk factors screened for were exposure to blood products or organ transplantation before 1992; origins from countries with high prevalence of HCV; intravenous drug use; human immunodeficiency virus carriers; men who have sex with men; those born to HCV-infected mothers; prior prison time; and chronic kidney disease. Those with at least one risk factor were tested for HCV by serum for HCV antibodies, a novel oral test from saliva (OraQuick®) or both.

RESULTS

associated to this project. The other authors of this manuscript have no conflicts of interest to disclose.

Data sharing statement: No additional data are available.

CONSORT 2010 statement: The authors have read the CONSORT 2010 Statement, and the manuscript was prepared and revised according to the CONSORT 2010 Statement.

Manuscript source: Unsolicited Manuscript

Received: May 20, 2020
Peer-review started: May 20, 2020
First decision: June 4, 2020
Revised: June 13, 2020
Accepted: August 9, 2020
Article in press: August 9, 2020
Published online: August 28, 2020

P-Reviewer: Asghar K
S-Editor: Zhang H
L-Editor: A
P-Editor: Ma YJ

Five hundred and forty-one participants had at least one risk factor and were tested for HCV. Eighty four percent of all study participants had only one risk factor. Eighty five percent of participants underwent OraQuick® testing, 34% were tested for serum anti-HCV antibodies, and 25% had both tests. 3.1% of patients (17/541) had a positive result, compared to local population incidence of 1.96%. Of these, 82% were people who inject drugs (current or former), and 64% served time in prison. One patient had a negative HCV-RNA, and two patients died from non-HCV related reasons. On review of past medical records, 12 patients were found to have been previously diagnosed with HCV but were unaware of their carrier state. At 1-year follow-up none of the remaining 14 patients had completed HCV-RNA testing, visited a hepatology clinic or received anti-viral treatment.

CONCLUSION
Targeted high-risk screening in the emergency department identified undiagnosed and untreated HCV carriers, but did not improve treatment rates. Other strategies need to be developed to improve linkage to care in high risk populations.

Key words: Screening; Emergency departments; Israel; Saliva; Hepatitis C; Liver

Core tip: Hepatitis C virus (HCV) infection is a leading cause of chronic liver disease. We attempted to identify previously undiagnosed HCV infected patients by screening high-risk populations arriving in the emergency department and link them to care. Although we identified infected persons at a higher rate than the Israeli population prevalence, none have started treatment despite multiple efforts.

Citation: Houri I, Horowitz N, Katchman H, Weksler Y, Miller O, Deutsch L, Shibolet O. Emergency department targeted screening for hepatitis C does not improve linkage to care. *World J Gastroenterol* 2020; 26(32): 4878-4888
URL: https://www.wjgnet.com/1007-9327/full/v26/i32/4878.htm
DOI: https://dx.doi.org/10.3748/wjg.v26.i32.4878

INTRODUCTION

Hepatitis C viral (HCV) infection is a leading cause of liver cirrhosis, hepatocellular carcinoma and liver transplantation worldwide[1]. The heavy burden of disease and the recent marked advances in HCV treatment have led the World Health Organization (WHO) to declare a goal of elimination of viral hepatitis as a major public health threat by 2030[2], and to propose that each country develop a strategy to promote prevention and treatment of viral hepatitis. The goals set were a 30% reduction of new cases of chronic hepatitis B virus (HBV) and HCV and a 10% reduction of viral hepatitis-associated deaths by 2020, and by 2030 - a 90% reduction of new cases and a 65% reduction of deaths. Many countries have begun implementing programs to that end[3-6].

In order to achieve these goals, two main obstacles need to be overcome. The first is to identify HCV infected persons, and the second is to link them to care. Globally, less than 5% of viral hepatitis (HBV and HCV) carriers are aware of their diagnosis[7]. A study in the United States showed that 50% of patients diagnosed with HCV were unaware of their status[8]. Therefore, in order to achieve the WHO goals, we need to integrate viral hepatitis testing into routine health policies and define priority populations for screening.

The benefits of early detection of HCV are significant, as timely treatment decreases the risk for all liver-related complications, as well as the potential for virus transmission.

Different strategies for identifying these patients have been used[9]. Universal screening was implemented in France and was found to be effective[10]. Other screening programs target high-risk populations, as previous studies have shown that 85%-90% of HCV-infected patients had an identifiable risk factor[11,12]. These included people

who inject drugs (PWID), recipients of blood transfusion before 1992 and abnormally elevated liver enzymes. In addition to these risk factors there are population groups with high prevalence of HCV, including dialysis patients, people who have been incarcerated, HIV-infected individuals, men who have sex with men (MSM) and those born in the United Stated between 1945-1965 ("baby-boomers").

Additionally, screening is recommended for patients with high risk of virus transmission, such as pregnant women.

Worldwide, some programs have focused efforts for HCV screening on patients arriving at the emergency department (ED). The reasoning behind this strategy is mainly the over-representation of at-risk groups in this population, including PWID, immigrants, *etc*[13,14]. Studies have shown a higher prevalence of HCV among ED patients compared to the general population[15-17]. Furthermore, HCV-infected patients utilize more medical services than non-HCV carriers[13], and have more ED visits[18,19]. The ED often serves as a "safety net" for these vulnerable populations, providing unique access to them[20].

In a single-center United States based study from 1992, 18% of all patients presenting to an inner-city hospital ED were positive for HCV[21]. A study by Hsieh *et al*[22] from an american urban ED screened all patients arriving at the ED during an 8-wk period. 13.8% of patients had positive anti-HCV antibodies, with 31.3% of them previously undiagnosed. The study estimated that 25% of newly diagnosed patients would not have been screened using risk-/birth-cohort based testing, and suggested a practice of 1-time universal testing for all ED attendees.

A Swiss study from 2007 screened 5000 patients arriving to the ED for various complaints, with an anti-HCV prevalence twice as high as the general population[16]. Finally, a study conducted in tertiary care EDs from Germany screened 28809 patients unselectively for anti-HCV antibodies, with an overall prevalence of positive screening of 2.6%, compared to an estimated 0.4%-0.6% in the German population, and overall positive HCV- polymerase chain reaction (PCR) in 1.6%[17]. Nineteen percent of HCV-RNA positive patients were previously undiagnosed.

All these studies were conducted in the pre-direct acting anti-viral agents (DAA) era and did not assess linkage to care. One study conducted in an urban ED in the United States at 2013 screened "baby boomers" arriving in the ED. Of 102 patients diagnosed with HCV, only 20% attended an initial appointment with a liver specialist[23].

Recently, a study conducted in an ED in Melbourne, Australia was published[24]. In this study, comers to the ED were screened for risk factors and were offered the OraQuick® oral HCV antibody test. Those with positive results had confirmatory testing with HCV-RNA. 34% of participants screened reported at least one risk factor. Of those, 14% had a reactive result on OraQuick®. Among the patients with positive HCV-RNA, 37% commenced treatment and 70% of these obtained a cure.

Data regarding the epidemiology of HCV in Israel is limited. A systematic review by Cornberg *et al*[25] estimated HCV prevalence in Israel at 1.96% of the population, while prevalence among immigrants from the former Union of Soviet Socialist Republics (USSR) was 4%. It was estimated that approximately 27000, or 33% of infected patients were already diagnosed. Risk factors for HCV carrier state in Israel include: immigration from the former USSR; PWID, current or past; reception of blood transfusions before 1992; close contact with infected individuals; and surgery.

In this study, we implemented a screening program in high risk populations attending our ED in order to assess the prevalence of undiagnosed HCV in this population and to analyze linkage to care.

MATERIALS AND METHODS

Patient selection

This was a single-center prospective trial. Patients arriving at the ED in Tel-Aviv Medical Center for any cause and their accompanying parties in selected days during March-August 2018 were screened via questionnaire for risk factors for HCV infection. Inclusion criteria were: Ages 18-75, ability to give consent, clinical stability and at least one positive answer for risk factors on the verbal questionnaire. Exclusion criteria were a known HCV diagnosis (as reported on initial screening) and special populations (pregnant women, children). Patients declaring a known HCV diagnosis were immediately offered a referral to the hepatology clinic for further treatment.

The questionnaires were administered by clinicians from our research team who worked in shifts in the ED, additional to ED personnel. Shifts varied in hours during the day, not including night shifts. Non-critical patients and their accompanying

parties were approached, and those consenting to participate were screened. Initially, verbal screening was conducted to identify those with risk factors. The verbal questions included country of birth, a known HCV diagnosis, and the different risk factors as in the written questionnaire. Those with at least one positive answer were given a written questionnaire.

The written questionnaire included 9 questions for established national and international risk factors for HCV infection. The risk factors screened for were: Exposure to blood transfusion, blood products or organ transplantation before 1992; those born in countries from the former USSR; current/past IV drug use; HIV carriers; MSM; those born to HCV-infected mothers; prior prison time; and chronic kidney disease (CKD). Additionally, participants were asked of prior knowledge of a diagnosis of HCV.

Those with any positive answer for a risk factor on the questionnaire were tested for HCV.

The study was conducted in compliance with the declaration of Helsinki and was approved by the Institutional review board (IRB) (0634-16). All participants screened gave informed consent.

HCV Testing

Two screening methods were used. All participants were planned for OraQuick® testing (based on availability of the kit), that detects HCV antibodies in saliva[26]. The OraQuick® is a highly accurate, rapid, point-of-care test for HCV antibodies, with sensitivity of 98.1% in oral fluid and specificity of 100%[27].

Participants who had blood taken in the ED for other reasons also had serology testing for anti-HCV antibodies.

Patients who tested positive for HCV on either screening test were referred to complete HCV-RNA-PCR and HCV genotype testing *via* healthcare providers.

Patient contacts

Multiple attempts at contacting patients testing positive for HCV were made *via* phone calls to numbers given by the patients at the time of signing informed consent and those in electronic medical records. Contact was also attempted though opioid substitution therapy clinics for 3 patients, and through HIV clinics for 2 patients.

Statistical analysis

Descriptive analyses were performed for all variables. Continuous data are reported as mean ± SD, and categorical data are presented as percentages. Univariate analyses were used for the comparison of variable's distribution between the study groups. To test differences in continuous variables between two groups the independent samples *t*-test was used. To test the differences in categorical variables the Pearson Chi-Square test was performed, $P < 0.05$ was considered statistically significant for all analyses. We used stepwise Logistic Regression analysis for prediction modeling of positive HCV testing according to the risk factors. All statistical analysis was performed using SPSS version 25.0 for Windows (SPSS Inc., Chicago, IL, United States). The statistical methods of this study were reviewed by Dr. Liat Deutsch from Tel-Aviv medical center.

RESULTS

Study population

Five hundred and forty-one participants had at least one positive answer and formed the study group. Fifty three percent of participants were male. The average age was 47.2 ± 15.3 years (range 19-88). Seventy one percent of participants were patients arriving for care in the ED, while 29% were their accompanying party.

As shown in Figure 1A, most participants had only one risk factor for HCV infection. Figure 1B details the risk factors among the participants. The most common risk factor was immigration from the former USSR (76% of participants).

Positive HCV screening

All participants had at least one HCV diagnostic test performed. All were planned for OraQuick® testing, though only 88% (476/541) underwent the test due to kit availability. Thirty six percent (199/541) of all participants who had blood drawn in the ED for other reasons had serology testing. Twenty five percent (134/541

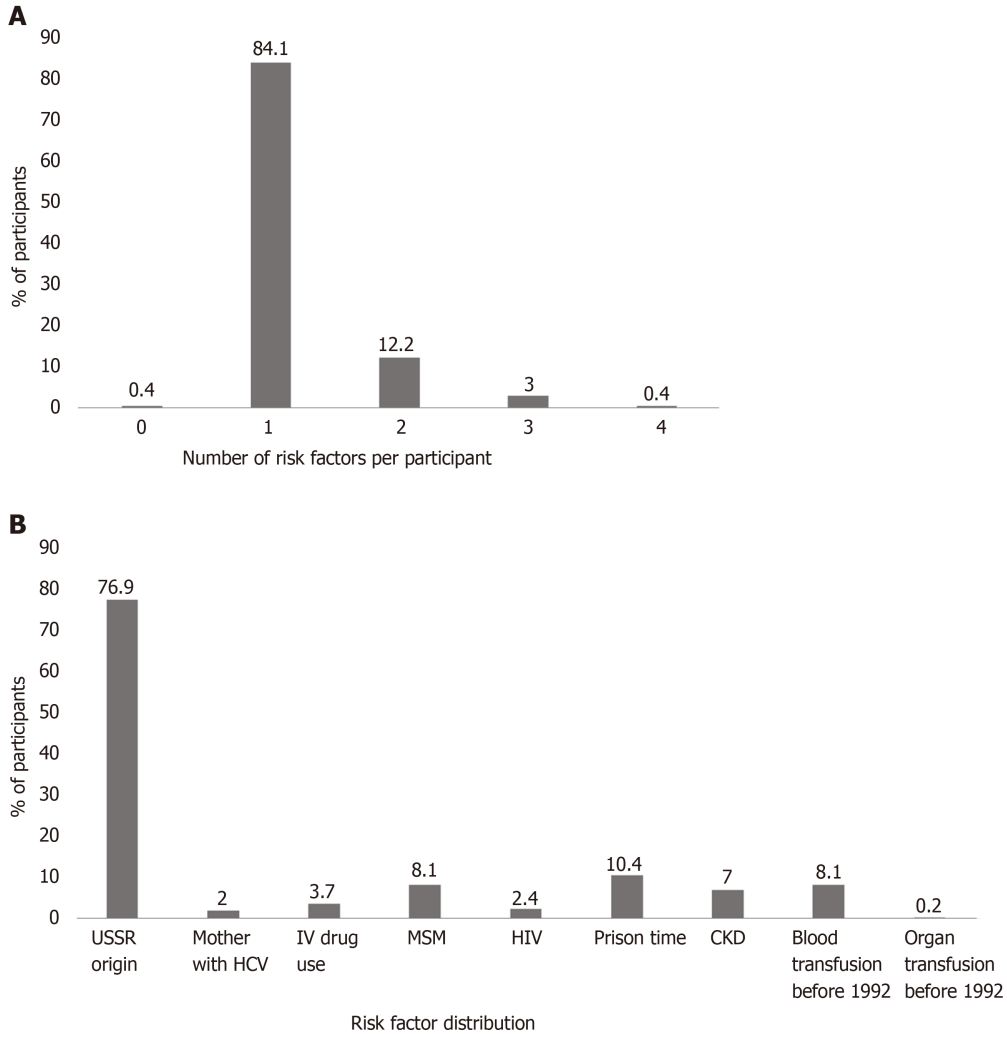

Figure 1 Number of risk factors per participant and distribution of risk factors. A: Number of risk factors per participant. 84% of all study participants had only one risk factor; B: Distribution of risk factors among study participants. The most common risk factor among all study participants was Union of Soviet Socialist Republics origin, accounting for 76.9% of participants. HCV: Hepatitis C virus; USSR: Union of Soviet Socialist Republics; MSM: Men who have sex with men; HIV: Human immunodeficiency virus; CKD: Chronic kidney disease.

participants) underwent both tests.

Seventeen participants (3.1% of all screened, CI: 1.8%-5%) were positive for HCV (Table 1). Two participants who had a negative OraQuick® but positive serum anti-HCV had lower antibody levels than other positive participants. One of the two later completed testing for HCV-RNA-PCR which was negative, coinciding with previous reports indicating the sensitivity of the test from oral fluids is lower in non-viremic patients[27,28].

Twelve of the HCV-positive patients had a previous diagnosis of HCV infection. Five of them answered negatively in the initial screening to the question of a known HCV diagnosis, but later reported a known HCV diagnosis in the written questionnaire. In examining prior medical records, we found 7 additional patients who had a previous diagnosis of HCV but were unaware of it. They all had not received anti-viral treatment and were not followed up by a hepatologist.

Table 2 compares the characteristics of the anti-HCV positive to negative groups. Most of the patients testing positive for HCV had multiple risk factors (Figure 2A), the most common being IV drug use (82%) and serving time in prison (65%) (Figure 2B). Univariate analysis showed that gender, PWID, HIV carriers, and time served in prison were all associated with positive HCV screening. Patients positive for HCV were less likely to have been born in the former USSR, though this is most probably a selection bias, as the participants were screened based on known risk factors. The only risk factor that remained independently associated with positive HCV screening in the multivariate analysis was PWID ($P < 0.001$, Table 3).

Our cohort did not show increased risk for HCV in CKD patients or those who had received blood products/organ transplant prior to 1992, though this may be due to the

Table 1 Screening results of hepatitis C virus-positive patients

Patient ID	OraQuick®	anti-HCV	Anti-HCV levels
84	Positive		
195	Positive		
263	Positive	Positive	11 <
267	Positive	Positive	11 <
333	Positive		
348	Positive	Positive	11 <
373	Positive	Positive	11 <
374	Positive	Positive	11 <
410	Positive	Positive	11 <
413	Negative	Positive	1.35
422	Negative	Positive	9.67
424	Positive	Positive	11 <
426	Positive		
428	Positive	Positive	11 <
435	Positive		
490		Positive	11 <
515		Positive	11 <

Seventeen patients screened positively on either OraQuick® or serum anti-hepatitis C virus antibodies. HCV: Hepatitis C virus.

Table 2 Patient characteristics

	HCV negative (% of patients, *n* = 524)	HCV positive (% of patients, *n* = 17)	*P* value
Males	52	93.8	0.001
Born in the former USSR	77.9	47.1	0.003
PWID	1.1	82.4	< 0.001
Served time in prison	8.6	64.7	< 0.001
HIV	1.7	23.5	< 0.001
MSM	8.4	0.0	0.212
Received blood products prior to 1992	8.4	0.0	0.213
Mother with HCV infection	2.1	0.0	0.546
Received organ transplant prior to 1992	0.2	0.0	0.857
Chronic kidney disease	7.1	5.9	0.85

HCV: Hepatitis C virus; USSR: Union of Soviet Socialist Republics; PWID: People who inject drugs; HIV: Human immunodeficiency virus; MSM: Men who have sex with men.

small sample size. Interestingly, although the study included 8.5% MSMs, none were found to be HCV positive, suggesting that this risk factor might be less significant than previously assumed.

Among all self-reported PWID's in the cohort, anti-HCV prevalence was 70% (14/20), while among participants who served time in prison the prevalence was 19.6% (11/56). These data concur with previous publications where among PWID, HCV prevalence ranged from 35%[29] to 75%[25].

Table 3 Multivariate analysis of risk factors for hepatitis C virus

	Univariate logistic regression			Multivariate logistic regression		
Variable	**Exp (b)**	**95%CI**	***P* value**	**Exp (b)**	**95%CI**	***P* value**
Gender (female *vs* male)	0.072	0.009-0.55	0.011	0.578	0.043-7.71	0.679
PWID (yes *vs* no)	402.889	91.3-1777.1	< 0.001	188.95	33.88-1053.82	< 0.001
Served time in prison (yes *vs* no)	19.515	6.89-55.25	< 0.001	4.076	0.623-26.67	0.143
HIV (yes *vs* no)	17.6	4.8-64.6	< 0.001	5.32	0.242-116.78	0.289
Born in the former USSR (yes *vs* no)	0.25	0.09-0.67	0.006	0.562	0.092-3.42	0.532

Dependent variable: Hepatitis C virus positive. PWID: People who inject drugs; HIV: Human immunodeficiency virus; USSR: Union of Soviet Socialist Republics.

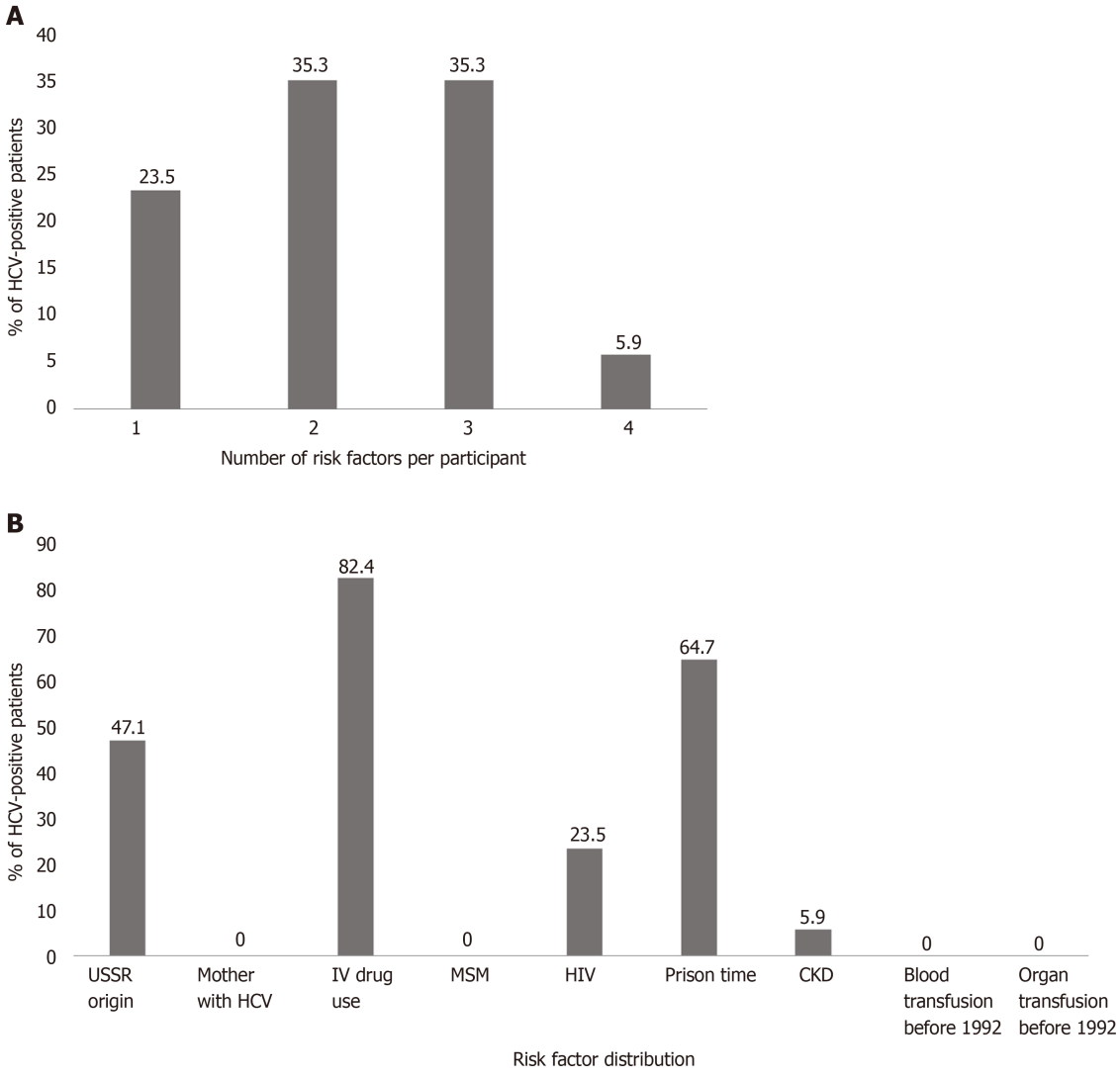

Figure 2 Number of risk factors per hepatitis C virus-positive patient and distribution of risk factors. A: Risk factors per patient. 76.5% of participants with positive hepatitis C virus (HCV) screening had more than one risk factor per patient; B: Distribution of risk factors among HCV-positive patients. The most common risk factors among HCV-positive patients were IV drug use and prior prison time. HCV: Hepatitis C virus; USSR: Union of Soviet Socialist Republics; MSM: Men who have sex with men; HIV: Human immunodeficiency virus; CKD: Chronic kidney disease.

Linkage to care

Multiple attempts were made to contact patients with positive HCV results. Of the 17 patients found positive in this study, none received anti-viral treatment at the end of follow-up. Two of the patients died from non-liver related diseases. One patient

completed a blood test for HCV-RNA-PCR that was negative. Three patients were interested in treatment in initial phone conversations; however, they did not arrive for clinic appointments. Eleven of the patients, mostly PWID or homeless, had no updated contact information and were unreachable.

DISCUSSION

High-risk targeted HCV screening in the ED identified higher rates of HCV, compared to previously published HCV prevalence rates in the Israeli general population (3.1% compared to 1.96%[25]). More than half of the HCV-positive patients identified in our study had a previous diagnosis, but most were unaware of the diagnosis and none were treated or followed-up in a hepatology clinic.

Linkage to care in this population proved difficult, and despite repeated efforts, none have started anti-viral treatment during 1 year of follow up. Many of the HCV-positive patients were homeless and without correct contact information. Since the results of the screening tests were available usually 24 h after the ED visit, patients had already been discharged by that time. Similar issues were described in studies in other countries[30,31]. One study in an American urban hospital targeted PWID's for screening at ED visits. Although HCV prevalence was 26% in the individuals tested, only 1/22 was treated at 1 year follow-up[32].

Additionally, all Israeli citizens have medical insurance and access to medical care, thus the ED serves as a "safety net" for extreme cases only.

These findings suggest that though ED screening in Israel may identify HCV infection in high-risk patients, some of whom are otherwise without regular medical care, this does not improve treatment rates.

Screening with OraQuick® had similar results to anti-HCV serum antibodies. Our study design did not allow to accurately assess the performance of the test, though previous publications and the high correlation with serum antibody levels suggests that this is a good alternative for HCV blood testing and may allow quicker response times and better access to difficult-to-screen populations.

The extremely high prevalence of HCV infection among PWID and people who were incarcerated suggests that these populations are an essential and critical target for intervention in order to achieve viral elimination, as shown also in the Australian study[24].

Future avenues for investigation include targeted screening in high-risk populations, conducted in facilities with long-term follow-up to ensure linkage to care, such as opioid substitution therapy clinics, HIV clinics, prisons *etc*. Additionally, further studies will be needed to address whole-population non-targeted screening in order to assess linkage to care in these populations. Furthermore, efforts are being made to identify previously diagnosed but yet untreated patients and link them to care.

Our study had several limitations. This was a single-center study in an urban city hospital that has a relatively large population of high-risk patients. Thus, the relatively high prevalence of HCV may not be indicative of other EDs in Israel. Additionally, risk factors were patient-reported and thus are prone to biases related to this method. Only patients who were clinically stable and able to give informed consent were included, thus excluding high-risk groups, such as intoxicated patients, those with mental health issues, *etc*. Finally, the number of HCV-positive patients was low.

In conclusion, although we identified more HCV carriers than the expected population rate, ED targeted-screening of high-risk patients did not improve anti-viral treatment rates.

ARTICLE HIGHLIGHTS

Research background

Hepatitis C virus (HCV) infection is a leading cause of chronic liver disease worldwide. In the last few years, new treatments for HCV have revolutionized management of this infection.

Research motivation

A major obstacle to viral elimination is identifying asymptomatic infected patients. Most screening strategies focus on high-risk patients, while others target the general

population. Prior studies showed that HCV prevalence in emergency department attendees is higher than the general population.

Research objectives

A single center prospective study, aimed at identifying undiagnosed HCV carriers among high risk emergency room attendees and linking them to anti-viral treatment.

Research methods

Persons visiting the emergency department were screened by a 9-question risk factor-specific questionnaire. Those with at least one risk factor were tested for HCV with blood and saliva antibody tests.

Research results

Five hundred and forty-one participants were tested for HCV. Eighty five percent of participants underwent saliva testing, 34% were tested for serum antibodies, and 25% had both tests. 17 patients (3.1%) had a positive result, compared to local population incidence of 1.96%. Eighty two percent of patients with positive HCV were people who inject drugs, and 64% served time in prison. Twelve patients were found to have been previously diagnosed with HCV but were unaware of the diagnosis. At 1-year follow-up, only one patient completed HCV-RNA testing and was found negative. None of the remaining patients completed the recommended testing, visited a hepatology clinic or received anti-viral treatment.

Research conclusions

Targeted high-risk screening in the emergency department identified undiagnosed and untreated HCV carriers, but did not improve treatment rates.

Research perspectives

This study suggests that in order to achieve viral elimination, other avenues need to be explored to find a framework that will enable treatment completion for this population.

REFERENCES

1 **Lavanchy D**. Evolving epidemiology of hepatitis C virus. *Clin Microbiol Infect* 2011; **17**: 107-115 [PMID: 21091831 DOI: 10.1111/j.1469-0691.2010.03432.x]

2 **WHO**. Combating hepatitis B and C to reach elimination by 2030. [cited 18 May 2019]. In: World Health Organization [Internet]. Available from: http://www.who.int/hepatitis/publications/hep-elimination-by-2030-brief/en/

3 **Dore GJ**, Ward J, Thursz M. Hepatitis C disease burden and strategies to manage the burden (Guest Editors Mark Thursz, Gregory Dore and John Ward). *J Viral Hepat* 2014; **21** Suppl 1: 1-4 [PMID: 24713003 DOI: 10.1111/jvh.12253]

4 **Wedemeyer H**, Duberg AS, Buti M, Rosenberg WM, Frankova S, Esmat G, Örmeci N, Van Vlierberghe H, Gschwantler M, Akarca U, Aleman S, Balık I, Berg T, Bihl F, Bilodeau M, Blasco AJ, Brandão Mello CE, Bruggmann P, Calinas F, Calleja JL, Cheinquer H, Christensen PB, Clausen M, Coelho HS, Cornberg M, Cramp ME, Dore GJ, Doss W, El-Sayed MH, Ergör G, Estes C, Falconer K, Félix J, Ferraz ML, Ferreira PR, García-Samaniego J, Gerstoft J, Giria JA, Gonçales FL Jr, Guimarães Pessôa M, Hézode C, Hindman SJ, Hofer H, Husa P, Idilman R, Kåberg M, Kaita KD, Kautz A, Kaymakoglu S, Krajden M, Krarup H, Laleman W, Lavanchy D, Lázaro P, Marinho RT, Marotta P, Mauss S, Mendes Correa MC, Moreno C, Müllhaupt B, Myers RP, Nemecek V, Øvrehus AL, Parkes J, Peltekian KM, Ramji A, Razavi H, Reis N, Roberts SK, Roudot-Thoraval F, Ryder SD, Sarmento-Castro R, Sarrazin C, Semela D, Sherman M, Shiha GE, Sperl J, Stärkel P, Stauber RE, Thompson AJ, Urbanek P, Van Damme P, van Thiel I, Vandijck D, Vogel W, Waked I, Weis N, Wiegand J, Yosry A, Zekry A, Negro F, Sievert W, Gower E. Strategies to manage hepatitis C virus (HCV) disease burden. *J Viral Hepat* 2014; **21** Suppl 1: 60-89 [PMID: 24713006 DOI: 10.1111/jvh.12249]

5 **Younossi Z**, Papatheodoridis G, Cacoub P, Negro F, Wedemeyer H, Henry L, Hatzakis A. The comprehensive outcomes of hepatitis C virus infection: A multi-faceted chronic disease. *J Viral Hepat* 2018; **25** Suppl 3: 6-14 [PMID: 30398294 DOI: 10.1111/jvh.13005]

6 **Papatheodoridis GV**, Hatzakis A, Cholongitas E, Baptista-Leite R, Baskozos I, Chhatwal J, Colombo M, Cortez-Pinto H, Craxi A, Goldberg D, Gore C, Kautz A, Lazarus JV, Mendão L, Peck-Radosavljevic M, Razavi H, Schatz E, Tözün N, van Damme P, Wedemeyer H, Yazdanpanah Y, Zuure F, Manns MP. Hepatitis C: The beginning of the end-key elements for successful European and national strategies to eliminate HCV in Europe. *J Viral Hepat* 2018; **25** Suppl 1: 6-17 [PMID: 29508946 DOI: 10.1111/jvh.12875]

7 **WHO**. Global health sector strategy on viral hepatitis 2016-2021. [cited 18 May 2019]. In: World Health Organization [Internet]. Available from: http://www.who.int/hepatitis/strategy2016-2021/ghss-hep/en/

8 **Spradling PR**, Rupp L, Moorman AC, Lu M, Teshale EH, Gordon SC, Nakasato C, Boscarino JA, Henkle EM, Nerenz DR, Denniston MM, Holmberg SD; Chronic Hepatitis Cohort Study Investigators. Hepatitis B

and C virus infection among 1.2 million persons with access to care: factors associated with testing and infection prevalence. *Clin Infect Dis* 2012; **55**: 1047-1055 [PMID: 22875876 DOI: 10.1093/cid/cis616]

9 **Institute of Medicine (US) Committee on the Prevention and Control of Viral Hepatitis Infection**. Hepatitis and Liver Cancer: A National Strategy for Prevention and Control of Hepatitis B and C. Washington (DC): National Academies Press (US). Cited 15 July 2019. Available from: http://www.ncbi.nlm.nih.gov/books/NBK220039/

10 **Deuffic-Burban S**, Huneau A, Verleene A, Brouard C, Pillonel J, Le Strat Y, Cossais S, Roudot-Thoraval F, Canva V, Mathurin P, Dhumeaux D, Yazdanpanah Y. Assessing the cost-effectiveness of hepatitis C screening strategies in France. *J Hepatol* 2018; **69**: 785-792 [PMID: 30227916 DOI: 10.1016/j.jhep.2018.05.027]

11 **Armstrong GL**, Wasley A, Simard EP, McQuillan GM, Kuhnert WL, Alter MJ. The prevalence of hepatitis C virus infection in the United States, 1999 through 2002. *Ann Intern Med* 2006; **144**: 705-714 [PMID: 16702586 DOI: 10.7326/0003-4819-144-10-200605160-00004]

12 **Chou R**, Cottrell EB, Wasson N, Rahman B, Guise JM. Screening for hepatitis C virus infection in adults: a systematic review for the U.S. Preventive Services Task Force. *Ann Intern Med* 2013; **158**: 101-108 [PMID: 23183613 DOI: 10.7326/0003-4819-158-2-201301150-00574]

13 **Minassian A**, Vilke GM, Wilson MP. Frequent emergency department visits are more prevalent in psychiatric, alcohol abuse, and dual diagnosis conditions than in chronic viral illnesses such as hepatitis and human immunodeficiency virus. *J Emerg Med* 2013; **45**: 520-525 [PMID: 23845528 DOI: 10.1016/j.jemermed.2013.05.007]

14 **Woolard R**, Degutis LC, Mello M, Rothman R, Cherpitel CJ, Post LA, Hirshon JM, Haukoos JS, Hungerford DW. Public health in the emergency department: surveillance, screening, and intervention--funding and sustainability. *Acad Emerg Med* 2009; **16**: 1138-1142 [PMID: 20053234 DOI: 10.1111/j.1553-2712.2009.00550.x]

15 **Orkin C**, Leach E, Flanagan S, Wallis E, Ruf M, Foster GR, Tong CY. High prevalence of hepatitis C (HCV) in the emergency department (ED) of a London hospital: should we be screening for HCV in ED attendees? *Epidemiol Infect* 2015; **143**: 2837-2840 [PMID: 25672420 DOI: 10.1017/S0950268815000199]

16 **Russmann S**, Dowlatshahi EA, Printzen G, Habicht S, Reichen J, Zimmermann H. Prevalence and associated factors of viral hepatitis and transferrin elevations in 5036 patients admitted to the emergency room of a Swiss university hospital: cross-sectional study. *BMC Gastroenterol* 2007; **7**: 5 [PMID: 17280611 DOI: 10.1186/1471-230X-7-5]

17 **Vermehren J**, Schlosser B, Domke D, Elanjimattom S, Müller C, Hintereder G, Hensel-Wiegel K, Tauber R, Berger A, Haas N, Walcher F, Möckel M, Lehmann R, Zeuzem S, Sarrazin C, Berg T. High prevalence of anti-HCV antibodies in two metropolitan emergency departments in Germany: a prospective screening analysis of 28,809 patients. *PLoS One* 2012; **7**: e41206 [PMID: 22848445 DOI: 10.1371/journal.pone.0041206]

18 **Thakarar K**, Morgan JR, Gaeta JM, Hohl C, Drainoni M-L. Predictors of Frequent Emergency Room Visits among a Homeless Population. *PLoS One* 2015; **10**: e0124552 [PMID: 25906394 DOI: 10.1371/journal.pone.0124552]

19 **Dibonaventura MD**, Yuan Y, Lescrauwaet B, L'italien G, Liu GG, Kamae I, Mauskopf JA. Multicountry burden of chronic hepatitis C viral infection among those aware of their diagnosis: a patient survey. *PLoS One* 2014; **9**: e86070 [PMID: 24465875 DOI: 10.1371/journal.pone.0086070]

20 **Rhodes KV**, Gordon JA, Lowe RA. Preventive care in the emergency department, Part I: Clinical preventive services--are they relevant to emergency medicine? Society for Academic Emergency Medicine Public Health and Education Task Force Preventive Services Work Group. *Acad Emerg Med* 2000; **7**: 1036-1041 [PMID: 11044001 DOI: 10.1111/j.1553-2712.2000.tb02097.x]

21 **Kelen GD**, Green GB, Purcell RH, Chan DW, Qaqish BF, Sivertson KT, Quinn TC. Hepatitis B and hepatitis C in emergency department patients. *N Engl J Med* 1992; **326**: 1399-1404 [PMID: 1373867 DOI: 10.1056/NEJM199205213262105]

22 **Hsieh YH**, Rothman RE, Laeyendecker OB, Kelen GD, Avornu A, Patel EU, Kim J, Irvin R, Thomas DL, Quinn TC. Evaluation of the Centers for Disease Control and Prevention Recommendations for Hepatitis C Virus Testing in an Urban Emergency Department. *Clin Infect Dis* 2016; **62**: 1059-1065 [PMID: 26908800 DOI: 10.1093/cid/ciw074]

23 **Galbraith JW**, Franco RA, Donnelly JP, Rodgers JB, Morgan JM, Viles AF, Overton ET, Saag MS, Wang HE. Unrecognized chronic hepatitis C virus infection among baby boomers in the emergency department. *Hepatology* 2015; **61**: 776-782 [PMID: 25179527 DOI: 10.1002/hep.27410]

24 **Hutton J**, Doyle J, Zordan R, Weiland T, Cocco A, Howell J, Iser S, Snell J, Fry S, New K, Sloane R, Jarman M, Phan D, Tran S, Pedrana A, Williams B, Johnson J, Glasgow S, Thompson A. Point-of-care Hepatitis C virus testing and linkage to treatment in an Australian inner-city emergency department. *Int J Drug Policy* 2019; **72**: 84-90 [PMID: 31351752 DOI: 10.1016/j.drugpo.2019.06.021]

25 **Cornberg M**, Razavi HA, Alberti A, Bernasconi E, Buti M, Cooper C, Dalgard O, Dillion JF, Flisiak R, Forns X, Frankova S, Goldis A, Goulis I, Halota W, Hunyady B, Lagging M, Largen A, Makara M, Manolakopoulos S, Marcellin P, Marinho RT, Pol S, Poynard T, Puoti M, Sagalova O, Sibbel S, Simon K, Wallace C, Young K, Yurdaydin C, Zuckerman E, Negro F, Zeuzem S. A systematic review of hepatitis C virus epidemiology in Europe, Canada and Israel. *Liver Int* 2011; **31** Suppl 2: 30-60 [PMID: 21651702 DOI: 10.1111/j.1478-3231.2011.02539.x]

26 **Cha YJ**, Park Q, Kang ES, Yoo BC, Park KU, Kim JW, Hwang YS, Kim MH. Performance evaluation of the OraQuick hepatitis C virus rapid antibody test. *Ann Lab Med* 2013; **33**: 184-189 [PMID: 23667844 DOI: 10.3343/alm.2013.33.3.184]

27 **Lee SR**, Kardos KW, Schiff E, Berne CA, Mounzer K, Banks AT, Tatum HA, Friel TJ, Demicco MP, Lee WM, Eder SE, Monto A, Yearwood GD, Guillon GB, Kurtz LA, Fischl M, Unangst JL, Kriebel L, Feiss G, Roehler M. Evaluation of a new, rapid test for detecting HCV infection, suitable for use with blood or oral fluid. *J Virol Methods* 2011; **172**: 27-31 [PMID: 21182871 DOI: 10.1016/j.jviromet.2010.12.009]

28 **Pallarés C**, Carvalho-Gomes Â, Hontangas V, Conde I, Di Maira T, Aguilera V, Benlloch S, Berenguer M, López-Labrador FX. Performance of the OraQuick Hepatitis C virus antibody test in oral fluid and

fingerstick blood before and after treatment-induced viral clearance. *J Clin Virol* 2018; **102**: 77-83 [PMID: 29525634 DOI: 10.1016/j.jcv.2018.02.016]

29 **Loebstein R**, Mahagna R, Maor Y, Kurnik D, Elbaz E, Halkin H, Olchovsky D, Ezra D, Almog S. Hepatitis C, B, and human immunodeficiency virus infections in illicit drug users in Israel: prevalence and risk factors. *Isr Med Assoc J* 2008; **10**: 775-778 [PMID: 19070285]

30 **White DA**, Anderson ES, Pfeil SK, Trivedi TK, Alter HJ. Results of a Rapid Hepatitis C Virus Screening and Diagnostic Testing Program in an Urban Emergency Department. *Ann Emerg Med* 2016; **67**: 119-128 [PMID: 26253712 DOI: 10.1016/j.annemergmed.2015.06.023]

31 **Franco RA**, Overton ET, Tamhane AR, Forsythe JM, Rodgers JB, Schexnayder JK, Guthrie D, Thogaripally S, Zinski A, Saag MS, Mugavero MJ, Wang HE, Galbraith JW. Characterizing Failure to Establish Hepatitis C Care of Baby Boomers Diagnosed in the Emergency Department. *Open Forum Infect Dis* 2016; **3**: ofw211 [PMID: 28066793 DOI: 10.1093/ofid/ofw211]

32 **Anderson ES**, Pfeil SK, Deering LJ, Todorovic T, Lippert S, White DA. High-impact hepatitis C virus testing for injection drug users in an urban ED. *Am J Emerg Med* 2016; **34**: 1108-1111 [PMID: 27037135 DOI: 10.1016/j.ajem.2016.03.004]

Published by **Baishideng Publishing Group Inc**
7041 Koll Center Parkway, Suite 160, Pleasanton, CA 94566, USA
Telephone: +1-925-3991568
E-mail: bpgoffice@wjgnet.com
Help Desk: https://www.f6publishing.com/helpdesk
https://www.wjgnet.com